Molecular Analysis of Olfactory Signal Transduction

Thesis by

Jonathan Christopher Bradley

In Partial Fulfillment of the Requirements

for the Degree of Doctor of Philosophy

California Institute of Technology

Pasadena, CA

1996

(Submitted March 31, 1996)

Defense 2 PM April 4, 1996

Beckman Behavioral Biology Rm3

To my granddmother, Oma mam

ACKNOWLEDGMENTS

Some of my fellow students have asked me what it's like to be finished with graduate school at Caltech. Thinking about it, the way I would like to answer is summed-up well by Lou Reed.

> It's a lot like what my painter friend Donald said to me "Stick a fork in their ass and turn them over, they're done"
>
> *Last Great American Whale, New York*

I feel very lucky to have done my graduate studies at Caltech and am grateful to a number of people for helping me reach this goal. In particular, Eckard Wimmer, my undergraduate research advisor at the State University of New York at Stony Brook has influenced me with his incredible enthusiasm and passion for scientific discovery. Kai Zinn, my graduate advisor at Caltech, has also been a source of inspiration with his fantastic ability to see clearly to the heart of the matter and develop straight forward solutions time after time. I thank Kai for allowing me to take control of much of the projects in this thesis which has given me the valuable training experience of both thinking-up and designing doable experiments, and carrying them out. Kai has been more than just a research advisor and solver of problems with experiments, he has been understanding at both the best and worst of times. I thank the other members of my committee; Mel Simon, Gilles Lauret, Mary Kennedy, and Henry Lester for their encouragement and support.

I have been fortunate to have collaborated with a number of other research groups. The group of Norman Davidson, and Henry Lester at Caltech, and Gabriele Ronnett's group at Johns Hopkins University. I thank Yasuhito Uezono and Mike Quick, electrophysiologists in the Lester/Davidson group, with whom I collaborated with on the characterization and assay of the olfactory receptors. I thank Jun Li, also of the Lester/Davidson group, who did all of the electrophysiological characterization of the second subunit of the cyclic nucleotide-gated channel. Also, I thank Norman and Henry

for their stimulating ideas and interest in the field of olfactory signal transduction. Thanks to Rob Bakin in Gabriele's group who did the immunohistochemistry with the channel antibodies. Finally, Yinong Zhang who also did electrophysiological characterization of the olfactory receptors, and the cyclic nucleotide-gated channels of the cultured hippocampal neurons.

I thank the other members of Kai's group, especially Chand Desai and Sarah Fashena who had to put up with sharing the same room with me. Special thanks to Nirao Shah and Chris Scheonherr for allowing me to whine to them any time, and Paul Mueller who was always able to make the grass seem browner on the other side of the fence.

I thank my family, Laetitia and Jan, Mimi and Mark, and Arvid.

Finally, nothing would have been possible without the love, support, understanding, and patience of Nathalie, Adrien, and Morgane.

ABSTRACT

Olfactory receptor neurons respond to odorant stimulation with a rapid and transient increase in intracellular cAMP that opens cyclic nucleotide-gated (cng) cation channels. Cng channels in rat olfactory neurons are activated by cAMP in the low micromolar range and are outwardly rectifying. The cloned rat olfactory cng channel, (rOCNC1), however, is much less sensitive to cAMP and exhibits very weak rectification. We have investigated this discrepancy between native and cloned channels, and have cloned a new rat cng channel subunit, denoted rOCNC2. rOCNC2 does not form functional channels when expressed alone in HEK 293 cells. When rOCNC1 and rOCNC2 are coexpressed, however, an outwardly rectifying cation conductance with cAMP sensitivity near that of the native channel is observed. *In situ* hybridization with probes specific for the two subunits shows they are coexpressed in olfactory receptor neurons. Further, subunit specific antibodies coimmunoprecipitate the other subunit from olfactory cilia membrane extracts. These data indicate that the native olfactory cng channel is likely to be a hetero-oligomer of the rOCNC1 and rOCNC2 subunits (Bradley *et al.* Proc. Natl. Acad. Sci. USA *91*, 8890-8894 1994).

The olfactory cng channels are also expressed in non sensory neurons in the brain. We have determined by *in situ* hybridization, immunocytochemistry, and Western blot that the olfactory cng channels are expressed in the hippocampus, cerebellum, and cortex of adult rats. Cultured hippocampal neurons from embryonic day 17 rats also express the olfactory cng channels as detected by immunofluorescence. Whole cell and excised inside-out patch recordings indicate that these cells have cng channels sensitive to 10μMcAMP, are outwardly rectifying, and insensitive to block by nickel ions. Consistent with the identification of these channels as the two subunits of the olfactory cng channel.

In order to identify and characterize olfactory receptors for specific odorant chemicals, we have developed a method for generating an electrophysiological signal in response to cAMP elevation in Xenopus oocytes. To do this, we expressed the cystic

fibrosis transmembrane regulator (CFTR), a chloride channel that is controlled via phosphorylation by cAMP-dependent protein kinase A (Uezono *et al.* Receptors and Channels *1*:223-241 1993). Pools of synthetic mRNAs from clones of putative olfactory receptor genes were coinjected into oocytes together with CFTR mRNA and tested with odorant mixtures. We have preliminary data indicating that single clones can mediate odorant responses. These responses are quite variable and we have determined using immunofluorescence that this is likely due to a trafficking problem of the expressed receptor protein inside the cell. We have observed this trafficking problem in both the *Xenopus* oocytes and HEK293 cells. To circumvent this problem we isolated the small fraction (1%) of transfected HEK293 cells that express receptor protein on their surface by fluorescence activated cell sorting (FACS). These cells can then be assayed functionally for odorant interaction using a fura based Ca^{2+} imaging set-up. Here, the reporter is the cng channels which conduct Ca^{2+} into the cell in response the receptor mediated rise in intracellular cAMP.

TABLE OF CONTENTS

FIGURES

Chapter 1.

Chapter 2.

Chapter 1. Introduction

In this introduction I have tried to provide as complete a review of the work to date on olfaction. I have concentrated on work generated concerning olfaction in mammals and discussed much of the earlier electrophysiological data on olfaction. Much of the data concerning the molecular biology has been produced more recently (in the last six years) and gets reviewed rather often so I have not dealt with this aspect of research of olfaction in the same detail.

Olfaction

Although animals are capable of distinguishing very large numbers of different odors the mechanisms involved in olfactory signal transduction are, to date, poorly understood. Little is known about how these transduction events in the periphery contribute to the perception of odors either. Over the past 30 years or so much data has been generated from studies on olfaction, starting with experiments using electrophysiology and more recently (the last six years) molecular biology. From these works a picture is beginning to emerge as to how this processes might be working.

Tissue

The sensory tissue, or olfactory epithelium (OE), is located in the nasal cavity. In mammals the inhaled air first passes over a respiratory epithelium (RE) in the anterior portion of the nasal cavity where it is warmed and moistened. The lateral walls of the posterior portion of the cavity are elaborated into a series of complex folds called turbinal extensions. These have a surface area of a few cm^2 in man, and more than $100cm^2$ in dogs. The OE is located on these ecto and endoturbinals. The OE is divided into two histologically distinct layers isolated by a basement membrane. The deeper layer, or lamina propria, is glandular and contains vascular and connective tissue. The Bowman's glands have ducts that traverse the basement membrane and neuroepithelium to the nasal lumen and secrete components of a protective mucus layer. These include secratory forms of the immunoglobulins type A and M, bacteriostatic and bacteriocidal proteins including lactoferrin and lysozyme and detoxifying enzymes (see below)(Getchell and Getchell, 1991). This layer also contains the nerve fascicles of the receptor neurons, located in the upper neuroepithelial layer. The neuroepithelium is 100-200μm thick and pseudostratifed consisting of three cell types with the nuclei of each cell type in fairly discrete layers (see Fig. 1.1).

Cell types of the neuroepithelium

Receptor cells

The olfactory receptor neurons (ORNs) constitute the predominant cell type in the OE, and have nuclei scattered in a band six or eight nuclei wide through the central portion of the epithelium. There are about 10^6 ORNs in the rat and they constitute 75-80% of all the epithelial cells(Farbman, 1988) ORNs are bipolar with unmyelinated axons which group into fascicles in the lamina propria surrounded by a single Schwann cell and project directly to the CNS, synapsing in the olfactory bulb. A single dendrite terminates at the nasal lumen and ends in a structure referred to as a dendritic knob. Emanating from each dendritic knob, and extending into the lumen of the nasal cavity, are 5-20 immotile cilia 50-200μm in length (in mammals) which taper from 2-3μm at their base to about 0.1μm at their tip. ORNs are a unique neuronal cell type in that they continually turn over on average every 30-60 days and are replenished from a population of mitotic basal cells (see below)(Graziadei and Monti Graziadei, 1979). Although the ORNs are derived from the basal cells, and differentiate into mature sensory neurons, several features classify them as "juvenile" in comparison to neurons elsewhere. First, the time course of death of the ORNs in response to axotomy is rapid in comparison to other neurons. Neurons in adult animals typically survive axotomy, or die over the course of days or weeks, even when the site of axotomy is relatively close to the soma(Berkelaar et al., 1994). In contrast ORNs, like neuronal populations in embryos and neonates(Snider et al., 1992), respond to axotomy with profound and rapid death. Immunohistochemically ORNs also resemble "juvenile" neurons elsewhere in that they retain a pattern of intermediate filament and microtubule-associated protein expression which is characteristic of immature neurons(Ophir, 1988; Schwob et al., 1986; Viereck et al., 1989). Recent *in situ* and *in vitro* experiments suggest that death of the ORNs, as well as of "immature" (keratin$^-$, non process bearing) basal neurons, may be the result of apoptosis as revealed by end-labeling of DNA fragments with biotinylated dUTP

(TUNEL staining)(Holcomb et al., 1995). Consistent with this observation, apoptotic death of both the ORNs and their precursors could be inhibited by aurintricarboxylic acid and cyclic AMP, agents that prevent apoptosis in other cell types, and by certain members of the neurotrophin family of growth factors, specifically brain-derived neurotrophic factor (BDNF), neurotrophin-3 (NT-3), and neurotrophin-5 (NT-5) (but not nerve growth factor (NGF))(Holcomb, et al., 1995). Dovetailing with these results is immunohistochemical localization of neurotrophin receptors trkB and trkC, but not trkA (the NGF receptor), to fractions of the ORNs in the neonatal OE(Holcomb, et al., 1995). Together these results suggest that apoptosis may regulate neuronal number in the OE and that multiple factors, including certain neurotrophins, may be involved in this process.

Sustentacular cells

Supporting or sustentacular cells span the width of the epithelium and have their nuclei most apical, forming a single layer. In the rat, sustentacular cells constitute 10-12% of all the epithelial cells(Farbman, 1988). These cells act to physically protect and electrically isolate the receptor neurons, and also contribute secretions to the mucus(Okano, 1974). Each sustentacular cell is surrounded by the dendrites and somata of 2-8 sensory neurons(Graziadei and Monti Graziadei, 1979). Sustentacular cells have a relatively high resting membrane potential (-80 to -120mV) and a low membrane impedance ($\leq$10MΩ)(Masukawa et al., 1985). Injection of current into these cells fails to generate an action potential, and studies with injection of fluorescent dye indicate they are not electrically coupled(Masukawa, et al., 1985; Okano, 1974). Besides physically protecting the underlying sensory neurons, sustentacular cells contain detoxification enzymes including an olfactory specific isoform of cytochrome P-450 (P-450olf1) (phase I biotransformation enzyme) and UDP-glucuronoysal trasferase (UGT_{olf}) (phase II biotransformation enzyme) at levels that rival their concentration in the liver (Lazard et al., 1991; Nef et al., 1989). In phase I, cytochrome P-450 catalyzes the hydroxylation of

the substrate and in phase II UGT catalyzes transfer of glucuronic acid from UDP-glucuronate to hydroxyl groups, converting a hydrophobic molecule into a hydrophilic, membrane-impenetrable one that is readily excreted. Beyond their obvious role in the destruction of inhaled toxins it has been suggested that these enzymes play a role in the metabolism of odorants. Hydroxyl-containing odorants are substrates for UGT_{olf} and UGT_{olf} is 2-5 fold more active than the liver enzyme on odorants(Lazard, et al., 1991). Moreover, glucuronidation abolishes the activity of odorants in an *in vitro* assay for olfactory signal transduction (see below)(Lazard, et al., 1991). These data suggest a role for these enzymes in chemosensory signal termination by shortening the tissue residence time of odorants and facilitating their removal through chemical modification.

Basal cells

The third basic cell type in the OE are the stem cells or basal cells located at the base of the olfactory epithelium along the basement membrane. In contrast to mature neurons, basal cells do not express the cytoplasmic olfactory marker protein (OMP)(Margolis, 1972) but do express N-CAM(Key and Akeson, 1990). Two types of basal cells have been described, which are referred to as globose basal cells and horizontal basal cells. Globose and horizontal cell can be distinguished ultrastructurally and immunohistochemically. Globose cells, as the name implies, have rounded nuclei. These cells stain lightly with toluidine blue and are located just one cell layer above the basal lamina. Horizontal cells have elongated nuclei, stain darkly with toluidine blue, and lie adjacent to the basal lamina. Horizontal cells are also the only cells in the OE that express cytokeratin(Levey et al., 1991). Evidence that the basal cells are a self-renewing source of receptor neurons comes from the observations that both globose and horizontal cells undergo mitosis and incorporate ^{3}[H]thymydine, with 90% of the labeled cells ending up in the receptor cell zone(Graziadei and Monti Graziadei, 1979). Bulbectomy, (removal of the olfactory bulb, which is the target of the receptor neurons), increases the production of neurons and specifically enhances mitotic activity of the globose

cells(Levey, et al., 1991). These data suggest that the globose cells are the direct precursors of new neurons. Using a replication-incompetent retrovirus that expresses human placental alkaline phosphatase, the fate of cells from both types of basal cells were determined to high resolution(Caggiano et al., 1994). The results show that the globose cells are the major source of new olfactory receptor neurons and that some progeny of the globose cells divide, or transiently amplify, in the globose cell zone of the OE before migrating up to the receptor cell zone and differentiating into mature receptor neurons. This is consistent with observations *in vitro* of an immediate neuronal precursor that is keratin$^-$, N-CAM$^-$, migratory, and non-neurite bearing(Gordon et al., 1995) characterized as a transient amplifying cell dependent on fibroblast growth factors(Dehamer et al., 1994). In primary cultures *in vitro* there is also a population of OE cells that express the mammalian *achaete-scute* homologue 1 (MASH1) gene(Gordon, et al., 1995), a basic helix-loop-helix (bHLH) transcription factor expressed in neuronal precursors(Johnson et al., 1990), Guillemot, 1993 #673. Mice engineered homozygous for a null allele of the MASH1 have almost no neural progenitors in the embryonic OE, either horizontal or globose type, resulting in few mature receptor neurons, but do have nonneuronal supporting cells(Guillemot et al., 1993). The MASH1 expressing cells in the wild type adult OE need to be characterized in order to determine in which of the basal cell types MASH1 is acting. This could clarify the role of the horizontal cells. These cells do divide but, in contrast to the globose cells don't appear to populate any layers other than their own and don't alter their numbers in response bulbectomy(Caggiano, et al., 1994).

Electrophysiology

Field recordings

The electroolfactogram (EOG) was one of the early electrophysiological experiments done with the OE(Ottoson, 1956). EOG studies showed that the cilia, which are bathed in a thin layer of mucus, are the site of interaction with volatile odorants and

that cAMP plays a role in olfactory transduction(Minor and Sakina, 1973). An EOG is essentially a field recording done with an electrode near the cilia during the transient application of odorants or other compounds. It represents a summation of the receptor neuron generator potentials and shows a monophasic negative voltage transient involving sodium but unaffected by tetrodotoxin, and a requirement for extracellular calcium. An EOG cannot be recorded from respiratory epithelium, and is abolished when the epithelium is lesioned with zinc sulfate or Triton X-100 to remove the cilia(Horn and Marty, 1988). Killing the receptor neurons by transection of the olfactory nerve also abolishes the EOG(Molday et al., 1991). Recovery of the EOG is accompanied by repopulation of the epithelium with receptor neurons and regrowth of cilia. A brief latency precedes the onset of the EOG and may reflect partitioning of the odorant in the mucus followed by diffusion to the cilia, perhaps mediated by odorant binding proteins (OBPs)(see below). In addition a component of this latency likely involves activation of a second messenger pathway(see below). The EOG amplitude is dependent on the concentration of odorant applied, with a larger amplitude for higher concentrations. However, when odorant is repeatedly applied there is a reduction in the relative amplitude. This is thought to reflect adaptation and also involves calcium(see below). Analysis of electroolfactogram responses indicate that many regions of the epithelium can respond to a given odorant, although some areas are activated to a greater extent than others(Duchamp et al., 1974; Gesteland et al., 1965; Getchell and Shepherd, 1978; Sicard and Holey, 1984). Thus, it seems unlikely that each molecular receptor species is found only on a precisely located group of neurons (see below).

In order to look at the activity of individual receptor neurons, spike frequencies in response to odorants were measured with extracellular electrodes . In this configuration individual cells respond to more than one odorant but not to all, and different cells show only partial agonist overlap. Interestingly, the firing frequencies varied from 0 to a maximum of 20-25 over a narrow range of less than one log unit of

concentration(Getchell and Shepherd, 1978). This suggests that a particular odorant can excite, or in some cases inhibit, a unique population of cells and produce a distinct pattern of activity(Duchamp, et al., 1974; Gesteland, et al., 1965; Getchell and Shepherd, 1978; Sicard and Holey, 1984).

Cellular recordings

Intracellular recording from olfactory neurons showed that these cells have a low resting potential (~-50mV) and a high membrane impedance (~200MΩ), and therefore require only picoamperes of current to depolarize to threshold and fire an action potential. These properties likely allow these cells to have a tight electrical coupling between the initial transduction events in the cilia, and the site of action potential generation at the axon hillock (see Fig 1.2). How does the biochemical process of an odorant interaction on the surface of the cilia change the membrane potential of the sensory neuron and get converted into an electrical signal sent to the brain? Several events came together to answer this question. Electrophysiologically it had been observed that cAMP played a role in olfaction(Minor and Sakina, 1973) . In these early, rather crude, experiments Minor and Sakina recorded EOGs from explants of frog OE that they could place in a tube or gutter and over which Ringer's solution flowed. They were able to record slow (odorant like) depolarizations of the ORNs when cAMP or it's dibutyryl derivatives were introduced into the flow of the Ringer's. In addition they could see odorant potentiating effects with phosphodiesterase inhibitors and odorant depressing effects with phosphodiesterase activators. Minor and Sakina even proposed what we now call a "signal transduction pathway" for odorant detection.

"Cyclic 3', 5'- AMP is considered to play the role of mediator in the mechanism of excitation of the olfactory receptor; during interaction between an odiferous substance and the receptor, adenyl cyclase is activated and the concentration of 3', 5'-AMP increases; this, in turn, causes depolarization of the receptor cell membrane"(Minor and Sakina, 1973).

Patch recordings

More than ten years later, a cGMP gated conductance mediating phototransduction in rod and cone outer segments was discovered(Fesenko et al., 1985; Haynes and Yau, 1985). These data led Nakamura and Gold(Nakamura and Gold, 1987)to do patch clamp experiments on the cilia of olfactory neurons and look for a cAMP gated conductance. In excised patches their results directly demonstrated an outwardly rectifying, nonselective cation conductance with little sensitivity to voltage (in the absence of divalent cations) that could be gated by cAMP (affinity of 2.4μM). Unexpectedly all the patches also showed a 1.7x higher affinity to cGMP (affinity 1.6μM). The Hill coefficients were 1.8 for cAMP and 1.7 for cGMP, indicating cooperativity of ligand binding. Interestingly two of five patches had ~10 times lower affinity for the cyclic nucleotides suggesting some channel heterogeneity and perhaps different classes of channels(see next chapter). They proposed that an odorant stimulated increase in cyclic nucleotide has a direct effect on a cation conductance which initiates a depolarizing response to odorants. Nakamura and Gold added the caveat that this model does not apply to odorants which do not appear to stimulate AC(Sklar et al., 1986)or to those that stimulate polyphosphoinositide turnover(Huque and Bruch, 1986).

The significance of the conductance's sensitivity to cGMP is less clear. Based on the relatively slow time scale of formation (50ms delay) and it's persistence after the primary response (more than 1s) cGMP production has been implicated in mechanisms of olfactory adaptation(Breer et al., 1992; Leinders-Zufall et al., 1995). It has been suggested the mechanism(s) of odor induced production of cGMP is the activation of a soluble form of guanylyl cyclase (sGC) by either, or both, of the diffusible messenger molecules (for review see (Dawson and Snyder, 1994)nitric oxide (NO)(Breer, et al., 1992) or carbon monoxide (CO)(Leinders-Zufall, et al., 1995) to produce cGMP. The sources of CO and NO have not been firmly established. It appears that nitric oxide synthetase (NOS), the enzyme that generates NO, is down regulated in the adult OE and

has its principal functions instead in activity-dependent establishment of connections in both the developing and regenerating olfactory neurons(Roskams et al., 1994). CO is produced by heme oxygenase (HO) during the degradation of heme to biliverdin(Maines, 1988). There is a constitutive isoform of HO (HO-2) abundantly expressed in the OE that colocalizes with sGC and produces CO in cultured olfactory neurons(Ingi and Ronnett, 1995). Unclear is the mechanism by which HO-2 activity is regulated.

Following the pioneering work of Nakamura and Gold several whole cell and excised patch recording studies were conducted (Firestein et al., 1991b; Firestein et al., 1991a; Frings et al., 1992; Zufall et al., 1991a) to further characterize the cAMP gated channel in terms of its pharmacology and activation behavior. Greatly facilitating these studies were the observations that the channels also existed in the much more accessible membranes of the dendrites and at a much lower density than in the cilia. By noise analysis it was shown that toad ciliary membranes have a cyclic nucleotide-gated (cng) channel density of 2,400/μm^2 while the density in the dendritic membrane and soma is 6/μm^2(Kurahashi and Kaneko, 1991). One of the most detailed studies(Frings, et al., 1992)characterized the cng channels in the dendritic knob, dendritic stalk and soma of ORNs from rats and toads. The characteristics determined were rectification, activation by cyclic nucleotides, selectivity for monovalent cations, inhibition by cytosolic acidification, and inhibition by organic blockers.

Their results established that the single channel conductances, in the absence of divalent cations, were 12-15pS. There was a graded increase in patch current with the application of cAMP or cGMP to the cytosolic face of the membrane, saturating at 10-30μM. In agreement with Nakamura and Gold(Nakamura and Gold, 1987), the concentration for half-maximal activation (EC_{50}) for cAMP at +50mV was 2.5μM and 4μMat -50mV with a Hill coefficient (HC) of 1.8 for rat ORNs. For cGMP the values were (rat) EC_{50} 1.0μM(+50mV); 1.8μM(-50mV), HC 1.3. There was weak outward rectification strongly dependent on cyclic nucleotide concentration and influenced by

membrane voltage. A rectification ratio (RR=I_{+V}/I_{-V}) of 7.5 on their 100mV curve translates to a 7.5x greater cAMP gated current at +100mV than at -100mV. There was no rundown of the current with conductances remaining constant over the course of ~30min. The selectivity for monovalent cations was determined by applying voltage ramps in the presence or absence of saturating concentrations of cAMP(40μM) with an extracellular concentration of Na^+ in the pipet of 150mM and successive exposure of the intracellular membrane to similar concentrations of either Na^+, K^+, Li^+, Rb^+, or Cs^+. The difference revealed the *I-V* relationship under each biionic condition and yielded the following sequence of permeation ratios relative to Na^+, $Na^+(1):K^+(0.81):Li^+(0.74):Rb^+(0.74):Cs^+(0.52)$. The fact that the current carried by Li^+ is smaller than the Na^+ current, despite the equilibrium selectivity for Li^+, is an anomalous permeation property that has also been observed for the cGMP-gated channel in rod photoreceptors(Menini, 1990). Mole-fraction behavior of ion currents can be used to detect the presence of several binding sites(Almers and McCleskey, 1984; Hess and Tsien, 1984). The presence of several binding sites is indicated when the current passes through a distinct minimum, as one ion is progressively replaced by another (anomalous mole-fraction). The fractional current carried by various mixtures of Na^+ and Li^+ was found to decline monotonically with increasing Li^+ mole-fraction implying one binding site within the channel.

Reducing the pH of the solution on the cytosolic side of the inside-out patch from 7.0 to 5.0 inhibited the cAMP-induced current by 60% and completely blocked it at pH4 in 18s (solution change <100ms). This effect was titrated (at +60mV) and found to have a pK of 5.0 but showed no voltage dependence and was reversible. No such effect was observed when the solution on the outside of outside-out patches was acidified, and the effect was independent of cAMP concentration indicating that the titratable group interacts with residues involved in permeation rather than in ligand binding. It is unlikely that acidification of this magnitude occurs in the ORNs (in photoreceptor cells cytosolic

pH does not change by more than 0.002 units during light excitation)(Yoshikami and Hagins, 1985) but these results indicate the presence of negatively charged residues near the channel mouth, with possible effects on ion permeation.

When the effects of several organic blockers (amiloride, the phenylalkylamine D 600 (methoxyverapamil), and the benzothiazepine diltiazem) were assessed it was found that all could block to some degree from the inside. Some data suggest that amiloride can block from the outside(Frings and Lindemann, 1988). There is a question if this effect might actually be due to amiloride getting to the inside via the basolateral membrane of the cell (based on the long latency of effect). Similarly, data on block of the retinal rod and cone cng channels by extracellular and intracellular *l-cis*-diltiazem is consistent with a single binding site on the cytoplasmic side of the channel(Haynes, 1992). There is no data on external block of the olfactory cng channel by phenylalkylamines or benzothiazepines. In excised patches from rat or frog ORNs the compounds showed a voltage dependent block, with 10-12x higher sensitivity at more positive membrane potentials, presumably due to the positively charged compound being driven into the channel. In patches from frog ORNs the K*i* decreased from 400μM at -100mV to 17μM at +100mV. Interestingly, 2 out of 11 membrane patches taken from the dendritic knob of rat ORNs did not show sensitivity to amiloride (300μM) perhaps indicating some heterogeneity in the cng channel population. It would be interesting to know the cAMP sensitivity of the channels in those patches and whether it correlates with the earlier observation of Nakamura & Gold who found channels with two classes of sensitivity to cAMP. The K*i* at +60mV for amiloride on the rat channels was 71μM. This is two orders of magnitude higher than that of Na^+ epithelial channels(Benos, 1982) (K*i* 0.1-0.5μM) but similar to Na^+/H^+ exchangers(Zhuang, 1984) and T-type Ca^{2+} channels(Tang, 1988) (3-80μM). On the other hand the olfactory cng channels are more sensitive to amiloride than are other Na transporters. For instance the Na/Ca exchanger K*i* is 1mM(Bielefeld, 1986), Na/K-ATPase K*i* is 3mM(Soltoff and Mandel, 1983), Na-

glucose transporter K*i* is 2mM(Kleyman and Cragoe, 1988), and voltage sensitive Na channels K*i* is 0.6mM(Kleyman and Cragoe, 1988). In parallel with their similar sensitivity to amiloride both the cng channel(Nicol et al., 1987) and the T-type Ca^{2+} channel(Bielefeld, 1986) have an even higher sensitivity to the amiloride derivative 3'-4'-dichlorobenzamil, suggesting a possible relationship between these channels. D 600 and diltiazem, other Ca^{2+} channel blockers, also block the olfactory cng channels in a voltage dependent manner but have K*i* values up to two orders of magnitude higher than on Ca^{2+} channels. Frings *et al.* determined K*i* s for D 600 of 200μM at -20mV and 12μM at +100mV for the cng channels from frog ORNs. The ability of diltiazem to block the cng channels showed a stereospecificity with the *l-cis* enantiomer being more potent (K*i* 70μM) than *d-cis* diltiazem (K*i*200μM) at +50mV. This same stereospecificity is also true for the photoreceptor cng channel(Stern et al., 1986) . Ca^{2+}channels also show stereospecific diltiazem block but with the *d-cis* enantiomer being more potent than the *l-lcis* one. The diltiazem stereoselectivity implies that this block of the cng channels is not "nonspecific" but involves interaction with a binding site on the cytoplasmic side of the channel. For photoreceptor channels diltiazem binding and interaction with cGMP appear to involve separate domains, when purified photoreceptor channels incorporated into artificial membranes are digested with trypsin (producing a 63kDa product) they retain activation by cGMP but lose sensitivity to *l-cis* diltiazem(Hurwitz and Holcombe, 1991).

Odorant response kinetics

Temporal evidence for a second messenger mediated mechanism of cng channel activation came from kinetic studies of odorant induced currents using whole patch-clamp techniques(Firestein and Werblin, 1989). Here ORNs from salamander were recorded from the cell body and dendritic knob, either in a slice preparation of the OE or as mechanically dissociated cells, stimulating with an odorant cocktail delivered as a pressure pulse (35ms) from a second pipet 10-25μ from the cilia. By making the odorant

solution also elevated in K^+ concentration an inward potassium transient was induced within 20ms, which decayed exponentially with a time constant of 200ms. This transient preceded the odorant response, which had a latency of more than 100ms (range 150-600ms, mean 320ms;n=19) and activated along a sigmoidal time course reaching a peak in 300-500ms (peak amplitude 30-700pA). The odorant response decayed exponentially with time constant of nearly 2s.(Firestein and Shepherd, 1991c; Firestein et al., 1990). Thus the two currents could be measured independently. Assuming that odorants and potassium diffuse at equal rates, the magnitude of the potassium current recorded in response to a pulse of 100mM-K^+ can be used as a measure of the concentrations of both K^+ and odorants delivered to the cell. In order to construct dose-response curves the pressure of the pulse was changed to deliver different concentrations of stimulus. The lowest concentration that gave a response was 6μM and the mean concentration that elicited a half-maximal response was 28μM. The curves for six cells are shifted a bit along the concentration axis but their sigmoidal shape remains constant. In all cases, the response curves rise steeply and saturate over less than a log unit of concentration, indicating that these cells have limited dynamic range(Firestein and Werblin, 1989)(see Fig. 1.3). The same concentration range for responses was seen previously in extracellular recordings of spike frequencies (Getchell and Shepherd, 1978). Although the responses reported were to lower concentrations, these were in preparations with an intact mucus layer and odorant stimulus was as vapor pulses lasting one to several seconds. Here the mucus may act to concentrate the odorants which is favored by their air-mucus partition coefficients(Amoore and Buttery, 1978). From the recordings of Firestein and Werblin(Firestein, et al., 1990; Firestein and Werblin, 1989) it was suggested that the latency of the odorant response supports the idea of a signal transduction system involving a second messenger. The response latencies for odorants are at least an order of magnitude slower than that of the current directly gated by nicotinic acetylcholine receptors (latencies of 1-10ms). The sigmoidal shape of the dose-

response curves imply cooperativity in the response (Hill coefficient; HC=2.7 for five cells). The HC for cAMP of the cng channel is only 1.8 which argues for cooperativity at one or more steps in this transduction pathway.

In the experiments described above Firestein *et al.*(Firestein, et al., 1990; Firestein and Werblin, 1989) used brief pulses of odorant to avoid complications due to effects of adaptation. By varying the pressure of the pulse they obtained different concentrations of stimulus. To examine the responses to maintained stimuli, either the duration of the pulse was increased for a given pressure(Firestein, et al., 1990), or the cell, firmly attached at the tip of the patch pipet, was moved in front of one of several adjacent perfusion tubes by a computer controlled stepping motor that drove the perfusion chamber(Firestein et al., 1993). When cells unresponsive to the brief pulses of stimulus were exposed to steps of up to 500ms responses were observed. This was striking because the maximum concentration of stimulus reached during the brief pulse was greater than that for the longer step. To determine if this signal was in response to stimulus duration as well as intensity, the duration of the odor pulses were varied (50, 200, 500ms) while the pressure was adjusted to maintain the same maximum concentration of stimulus. Under these conditions the amplitude of the K^+ currents were the same, therefore the stimulus concentrations were also the same, but the integrals of the K^+ responses were different for the three pulses. The amplitude of the odor elicited currents on the other hand followed the integral and not the peak concentration of the stimulus, giving larger amplitudes with increased exposure time. This result suggests that the ORNs integrate concentration information over time, or expressed another way, ORNs can evaluate flux. Maintained stimulus to longer steps of 7-10s produced transient responses representing adaptation that appeared to have two phases. The first being an initial rise to plateau amplitude lasting 1-2s followed by an exponential decay. These recording experiments indicate that there is roughly a 50% chance of finding a cell responsive to a mix of three odorants, and 50% of those cells will respond to more than one of the three odorants.

This indicates the ORNs are not very selective. Although they appear broadly tuned they do show specificity even when tested with high or low concentrations of an ineffective odorant.

These characteristics, of being responsive to more than one stimulus, having a relatively low affinity and narrow dynamic range, and integration of stimulus over 1-2s differ strikingly from those of photoreceptors and hormone receptors which have dynamic ranges of up to three orders of magnitude and $K_{1/2}$ values in the nmolar range. These distinctions likely reflect fundamental differences between these superficially similar systems. This is to say, without devoting an entire genome to encoding several million receptor proteins, and not invoking a model of somatic rearrangement to generate a complex receptor repertoire, perhaps the OE acts as a broad detector array. This is accomplished with a relatively low number of receptors, (see below) relative to the number of potential ligands, that are not high specificity or high affinity. Odor intensity then is not encoded at the ligand receptor step per se but is gained by the integration of inputs from cells with overlapping response ranges by high convergence of afferent input to the olfactory bulb (see below). In this way temporal and intensity information, at the detector level, is sacrificed by using broad affinity receptors that have as a consequence given up some resolution. The OE therefore sacrifices temporal information in order to maximize sampling. Further refinement of the signal from the OE may occur by lateral inhibition in the olfactory bulb(Buonviso and Chaput, 1990). In the bulb granule cells appear to mediate lateral inhibition of mitral cell responses to sharpen the peaks of activity. This is thought to occur through the reciprocal inhibitory GABAergic synapses that granule cells make to mitral cells(Mori et al., 1992b). This is not to say all receptors are low affinity and broadly specific. There probably are high affinity receptors for temporally important cues like smoke, survival cues like rotten food, and reproductive cues like pheromones.

cAMP transduction pathway

To show direct involvement of cng channels in olfactory transduction, recording was done from on-cell patches in response to extracellulary applied odorant(Firestein, et al., 1991a). 13 of 21 successfully patched cells responded to pulsed odor stimulation with bursts of channel openings. 10 of those 13 were single channel openings and in 9 of 13 patches if the pipet potential went more negative than 0mV (i.e. depolarizing Vm) then voltage-dependent channels were activated. To avoid interference from voltage-gated channels the extracellular Na^+ was replaced by the impermeant cationic compound choline, after establishing a seal on the cell. Either with or without choline, the latency of odorant response ranged between 1500 and 750ms with increasing pulse duration (increasing odorant concentration). When a single channel was activated with a short pulse, more than one was often activated with a long pulse, consistent with macroscopic results(Firestein, et al., 1990). That these odorant activated channels were the same as the previously identified cng channels of the cilia was shown by comparison, in the same patch, of the single channel odorant response to the single channel response due to treatments that directly increase intracellular cAMP. For these experiments IBMX, a phosphodiesterase inhibitor, and 8-bromo cGMP, a membrane permeable cyclic nucleotide were exogenously applied and it was found that these agents affects mimicked that of odorant at the single channel level.

Hormonal stimulation of adenylyl cyclase is known to occur by the binding of agonist to a serpentine receptor, or seven helix receptor, in the cells' plasma membrane. Occupancy of the receptor triggers activation of a guanine nucleotide binding protein (G protein) which translocates along the inner surface of the plasma membrane to stimulate the plasma membrane associated adenylyl cyclase. Receptor occupancy promotes exchange of GTP for GDP on the G protein, which is required for G-protein activation. The G protein in turn stimulates the cyclase, and also has an intrinsic GTPase activity that hydrolyzes the bound GTP to GDP resulting in recycling of the G protein (Levitski,

1988). One mechanism of cAMP production to open the cng channel could be the use of such a pathway. To investigate the potential role of an adenylyl cyclase stimulating G protein in olfactory transduction the effects of pharmacological agents known to interact with distinct enzymes in the proposed pathway were assessed on isolated ORNs under whole-cell patch clamp conditions (Firestein, et al., 1991b).

Pretreatment with the membrane-permeable phosphodiesterase inhibitor IBMX generates a small (25-30pA) basal current and prolongs the odorant response by allowing accumulation of cyclic nucleotide. This IBMX effect showed concentration dependence; the time constant (2.1, 2.2, 5.8, and 12.3s) for decay of the odor-induced current increased with IBMX concentration (0, 5, 50, and 200μM) but always fit a single exponential suggesting that PDE activity is a major mechanism for turning off the odor-induced current. Consistent with the idea that the PDE controls the decay and not onset of the odor-induced current, IBMX had almost no effect on the rate of current to rise between 0.2 and 0.8 of the peak amplitude. An additional effect of IBMX treatment was a 35-50% reduction in the peak amplitude of the odorant response. This might be due to activation of negative feedback processes mediated by protein kinase A and/or an increase in Ca^{2+}(see below). PKA would be activated by the increase in basal cAMP, and Ca^{2+} would enter through the cng channels. At even higher concentrations (500μM) IBMX could induce a current of 300-500pA in the absence of odorant. This current was transient but reduced the subsequent responses to odorant by as much as 90%, again suggesting the activation of negative feedback perhaps through cAMP, Ca^{2+}, or other desensitization mechanisms.

To look more directly at the interplay between odorant-induced cyclic nucleotide production and cyclicnucleotide gating of the channel the levels of intracellular cyclic nucleotide were manipulated while recording responses to odorant in the whole cell configuration. To do this membrane permeable analogs of cyclic nucleotides (8-bromo-cGMP or cAMP) were perfused on to the cell, or on cell patches were ruptured with

pipets filled with cyclic nucleotide. Results from these experiments show that perfusion of 8-bromo-cGMP on to the cell caused a large inward conductance that occluded the odorant-induced response and was reversible. 8-bromo-cAMP had no effect on membrane conductance but reduced the odorant response by 25%. cAMP and 8-bromo-cGMP do appear to act on the same conductance because cAMP applied intracellulary occludes the 8-bromo-cGMP response. Therefore is seems that the cAMP and its 8-bromo analog do not activate the channel equally, or that 8-bromo-AMP is not as permeable as 8-bromo-cGMP. Support for the former comes from the use of other permeant analogs of cAMP like dibutyryl cAMP and para-chloro-phenyl-thio-cAMP, which also fail to activate the channel. Moreover, it does appear that 8-bromo-cAMP enters the cell because it can reduce the odorant-induced current by 25%, perhaps by activating a cAMP sensitive desensitizing pathway like PKA. Further support for the idea that cAMP participates in a desensitization pathway comes from comparison of the time courses of cAMP and cGMP evoked currents. Here a patch pipet was filled with 500μM cAMP or cGMP (different cells). After the patch was ruptured, in the case of cGMP, a large inward current was induced that remained steady over several minutes of recording. A very different time course was seen for cAMP, where after patch rupture the same type of current seen for cGMP developed and reached a peak in a few hundred milliseconds but then the current began to decay in 5-15s, returning to between 0 and 30% of maximum within 35s to 2min. In all cases cells remained refractory to odorant stimulation. Thus it appears there is a process of desensitization dependent on a process mediated by cAMP.

G-proteins

With a role for cyclic nucleotides in olfactory transduction established, evidence for G proteins that could couple a receptor to effectors that produce second messengers like cAMP was examined. To do this Firestein *et al.*(Firestein, et al., 1991b) made use of nonhydrolyzable analogs of GTP and GDP which uncouple the G protein from its

receptor. GTP-γ-S acts to lock the G protein in an activated conformation, while GDP-β-S locks the G protein in an inactive state. In the context of olfactory signal trasduction GTP-γ-S would be expected to prolong an odorant response, even in the absence of further odorant stimulation, assuming no other downstream controls. GDP-β-S would act in olfaction to block the odorant response by preventing exchange of GDP for GTP, once bound to the G protein. When included in the patch pipet, and after rupture of the patch, both compounds did in fact uncouple the receptor from the response. As expected both analogs required prior stimulus-driven activation of the G protein to have an effect. Successive rounds of odorant stimulation in the presence of GTP-γ-S generated responses that lasted longer and longer, eventually never returning to baseline and becoming refractive to odorant after four sitmulations. The effect of GTP-γ-S was on the decay of the odorant response only, consistent with the G protein population shifting to a constitutively active one. The decay with GTP-γ-S was biphasic, with an initial fast component (see Fig. 1.4 ,upper). This is in contrast to the inhibition of the PDE with IBMX described earlier which consistently lengthened the exponential time constant. This suggests that the hydrolysis of cAMP (PDE activity) sets the rate for the decline of the odorant-induced current. On the other hand, with GDP-β-S in the pipet odorant responses became smaller with each stimulus and disappeared after the fourth. GDP-β-S appears to affect the rate of the latency of the response onset while not altering the slope of the response rise. This suggests that activation of the G protein is rate limiting for the onset of the odorant response. This could be governed at the level of receptor activation, through its affinity for ligand and/or the affinity of occupied receptors for the G protein. Either, or both of these parameters could govern the G proteins exchange rate of GDP for GTP and would be consistent with the idea that integration of the stimulus occurs, perhaps at the level of "loading" the G protein.

Cl^- component of depolarization; a role for Ca^{2+}

The cng channel turns out not to be the sole source of the odorant-induced depolarizing current. Careful comparison of the cng-gated single channel recordings from excised patches and the odorant-induced currents from whole cell recordings reveals an anomaly(Kleene, 1993; Kurahashi and Yau, 1993). The cng conductance in excised patches was sensitive to extracellular divalent cations, which can block the inward cation current causing strong outward rectification of the current-voltage (I-V)relation(Zufall and Firestein, 1993b). The odor-induced currents in contrast show little rectification, even in the presence of external divalent cations. The explanation appears to be that the depolarizing current has two components, an initial inward cationic conductance followed by an inward anionic Cl^- conductance(Kleene, 1993; Kurahashi and Yau, 1993; Lowe and Gold, 1993). To prove this, the two odor-induced currents were separated by recording in the presence of low extracellular Cl^- ($[Cl^-]_o$, 34mM). At +24mV the odor-induced current becomes biphasic, consisting of an outward component followed by an inward component(Kurahashi and Yau, 1993). In this case Ca^{2+}, which enters the cell (cilia) through the cng channel, triggers a Ca^{2+} activated Cl- channel known to be in the olfactory cilia membrane(Kleene and Gesteland, 1991). The equilibrium potential for Cl^- in these cells must be sufficiently high (near 0mV in the newt(Kurahashi and Yau, 1993))and away from the resting potential in order to participate in depolarization. Experiments with excised frog cilia indicate that this Cl^- channel is activated with a $K_{1/2}$ of 5μM Ca^{2+} with a HC of ~2, and that the secondary Cl^- current is absent without external $Ca2^+$. If the cytoplasmic $Ca2^+$ buffering capacity is reduced in this preparation the latency of the Cl^- current is reduced and its amplitude increased in response to cAMP. The steady state of this Cl^- conductance is reached at 20μM $Ca2^+$. In the presence of a Cl^- channel blocker the total current is reduced and does not rise as steeply. In other words the total current is larger and rises faster with cAMP concentration than the cationic component alone. In amphibians the Cl^- current contributes ~40% to the total,

and in rats this increases to ~85% of the total inward current. The Cl^- current therefore is a nonlinear function of cAMP concentration and increases the cooperativity of the cng current from ~1.5 to ~3.5 in amphibians and from ~1.5 to ~4.7 in rats, resulting in nonlinear amplification of the receptor occupancy that triggers this pathway(Lowe and Gold, 1993) . The nonlinear activation of the Cl^- current is likely a function of its own cooperativity and of any intracellular Ca^{2+} buffering which would combine to produce a threshold for activation of this conductance. Interestingly, even in the absence of cAMP, a reduction in Ca^{2+} buffering can induce the Cl^- current. Consistent with the observation that olfactory cilia have a small basal conductance to Na^+, K^+, and also Ca^{2+} (Kleene, 1993).but not to Cl^-(Kleene, 1992). This basal conductance is inhibited by l-cis-diltiazem, an inhibitor of the cng channel, and exists because the cng channel does not show any sort of run down or desensitization. In fact the olfactory adenylyl cyclase (AC type III) has very little basal activity when expressed in 293 cells (see below) so it would be interesting to know if this basal current is mediated not by cAMP but by cGMP, the other agonist for the cng-channel. This would be analogous to the constitutive level of cGMP maintained in the outer segment of rod photoreceptors in the vertebrate retina. Here cGMP gates the dark current which is turned off by the light-induced activation of a PDE. Perhaps in ORNs there may be a GC enzyme with an intrinsically high basal activity that is inhibited by Ca^{2+}. This is the case in the vertebrate retina where the cloned GC (retGC-1) has a 25 fold greater basal activity than the natriuretic peptide receptor A (NPR-A), a receptor linked GC, when expressed in 293 cells(Shyjan et al., 1992)and is inhibited by Ca^{2+}(Dizhoor, 1994). Biochemical data on the basal level of cGMP support this idea. Cohen and Blazynski have determined that the resting level of cGMP in the retina is ~50-75pmol/mg protein(Cohen and Blazynski, 1993). According to Breer *et al.* (Breer, et al., 1992)the level of cGMP in the olfactory cilia is 5-7pmol/mg protein. This is lower than in the retina but the olfactory cng channel has more than 30 fold greater sensitivity to cGMP than the rod cGMP-gated channel. To examine this idea

further, one could assay if GTP-β-S can hyperpolarize the ORN in the absence of any stimulus. This would happen if GC was the source of constitutive cGMP and gradual loading of GTP-β-S would turn off the cyclase and the cng channel would close.

In any case, the ORN has a highly cooperative pathway for amplification of a stimulus and this pathway is set almost to threshold. Perhaps this configuration is necessary in order to have a functional detector with receptors that may have sacrificed high affinity for broad specificity. This sacrifice is in order to detect an overwhelming number of odorants with a limited repertoire of candidate receptors. The extreme convergence of signal from the OE to the olfactory bulb (see below) may allow the addition of a large number of isolated events to produce a significant response.

A second role for Ca^{2+}

Ca^{2+} appears to control at least one other process during the odorant response. Olfactory cilia contain the Ca^{2+} binding protein calmodulin at a concentration of ~1μM(Anholt and Rivers, 1990). In retinal rod photoreceptors it has been shown that Ca^{2+} bound to calmodulin reduces the cGMP affinity of the rod cng channel from 19μM to 32μM at low concentrations of cGMP, effectively reducing the cation influx by two to six fold(Hsu and Molday, 1993). Therefore when light stimulates hydrolysis of cGMP and the channel closes, intracellular Ca2+ falls. This relieves the inhibitory binding of calmodulin and promotes recovery by stimulating the channels to rebind cGMP. A similar Ca^{2+} effect occurs with the olfactory cng channel(Zufall et al., 1991b). In this case the odorant-induced intracellular elevation of Ca^{2+} is thought to promote adaptation because Ca^{2+}/calmodulin can reduce the affinity of the cng channel for cAMP by ~20 fold, shifting the $K_{1/2}$ from 3.2μM to 63μM (Chen and Yau, 1994). In addition to adaptation this mechanism may operate in the turning off of the odorant response. Extracellular Ca^{2+} is absolutely required for the decay phase of the odorant-induced whole cell current, which in the absence of extracellular $Ca2^{+}$ remains at a steady state (Kurahashi and Shibuya, 1990).

Quantal responses vs. noise

Recently a controversy has developed(Gold and Lowe, 1995) over the suggestion that odorants induce quantal events (currents) in the ORNs(Menini et al., 1995). Menini *et al.* recorded in whole cell configuration from salamander ORNs with low concentrations of odorant (0.5μM cineole) for long periods of time (>30min). Their claim that small current responses seen during these recordings correspond to quantal evoked odor activation of the above outlined transduction cascade is not substantiated by the data. The biggest problem with their interpretation of this data as representing quantal responses is this type of analysis assumes a linear relationship between current and the number of quantal events. As outlined above the transduction current is highly non linear and undermines their estimating quantal-event amplitude from their histograms.

Biochemistry and molecular biology

Biochemical evidence for second messengers in olfaction

About the time of the patch clamp recordings of Nakamura and Gold there was biochemical evidence for an odorant-stimulated adenylyl cyclase (AC) in olfactory cilia(Pace et al., 1985; Sklar, et al., 1986). These cell free fractions enriched for cilia, prepared by Ca^{2+} shock of the ORNs(Rhein and Cagan, 1980), from rats, frogs, or toads had very high levels of AC. It was calculated that the cilia contain ~40% of the total OE cyclase protein but only 3% of the total OE protein. The specific activity of the cilia AC was 10-15 times that of whole OE or membranes from brain and had a basal activity of ~5nmol cAMP/mg protein/min(Pace, et al., 1985). Since then this number has been reported to be a bit lower, 50-100pmole/mg protein/min(Breer et al., 1990; Sklar, et al., 1986), this is due to differences in the respective methods of determining protein concentration. All parties agree on this revised value(Sklar, et al., 1986). Odorants alone have no effect on AC activity alone but GTP stimulates about 2 fold over basal and micro molar concentrations of Ca^{2+} inhibit this stimulation. Consistent with this ion being a

physiologic regulator of hormone sensitive AC(Robison et al., 1971). The addition of odorants plus GTP enhanced cAMP production 4-6 fold over basal, arguing that a G protein is also involved in vertebrate olfactory signal transduction(Pace and Lancet, 1986). Interestingly some odorants were refractile in this assay prompting Sklar *et al.* to propose an alternative pathway involving phosphatidylinositol turnover mediated by $G_{\alpha o}$.

Biochemical evidence for G proteins in olfaction

G proteins are substrates for ADP-ribosylation. The AC stimulating G protein $G_{\alpha s}$ is ADP-ribosylated by cholera toxin and the AC inhibiting G protein $G_{\alpha i}$ is ADP-ribosylated by pertussis toxin(Gilman, 1984), as is the phospholipase C activating G protein $G_{\alpha o}$. Pace and Lancet(Pace and Lancet, 1986)were able to biochemically identify a G_s like G protein in OE cilia membranes 0.5kDa larger than the liver $G_{\alpha s}$ using cholera toxin and ^{32}P labeled ADP-ribose. Pretreatment of the cilia membranes with cholera toxin decreased the odorant stimulation of AC in a dose dependent manner, establishing a relation between a G_s like G protein and odorant stimulation of AC. Unlike the cholera toxin catalyzed ADP-ribosylated protein, the three proteins ADP-ribosylated by pertussis toxin were not OE specific.

Cloning of G proteins expressed in the OE

These data, and the previously described electrophysiological data, directed molecular studies to clone and characterize members of a signal transduction pathway in which receptors of the seven helix class could activate a G_s like G-protein which would stimulate AC increasing cAMP levels. The cAMP would then in turn gate a cation channel, initiating depolarization of the receptor neuron. The influx of Ca^{2+} through the cng channel triggers the Cl^- conductance amplifying the depolarization and bring the cell to threshold. This pathway is diagrammed in figure 1.5.

To clone cDNAs for G proteins expressed in the OE, a library was screened with an oligonucleotide against a portion of an 18 amino acid sequence common to all known

G protein at the time. Clones for five different G proteins were isolated. The majority of clones were $G_{\alpha s}$, the rest were $G_{\alpha o}$, $G_{\alpha i1}$, $G_{\alpha i2}$, and a new species $G_{\alpha i3}$(Jones and Reed, 1987). In order to determine if these cDNA clones encoded proteins expressed in the ORNs northern blots were done on RNA from rats that had, or had not been bulbectomized. The results showed that none of the G proteins had their signal reduced due to bulbectomy, which results in death of the ORNs by removal of their target, suggesting non sensory cell expression of these genes in the OE(Jones et al., 1988). A second screen done at low stringency was initiated using a mixture of the five G proteins plus a degenerate sequence against a conserved region of the GTP binding domain. Re-isolates of the original five were identified by high stringency hybridization, resulting in one class of clones weakly hybridizing to $G_{\alpha s}$. This new G protein, named $G_{\alpha olf}$, is 88% identical at the amino acid level to $G_{\alpha s}$ and shows robust expression in the OE. $G_{\alpha olf}$ can activate AC in S49 cyc^- kin^- cells, a cell line devoid of $G_{\alpha s}$, by incubation with GTP-γ-S or AlF_4^-, potent activators of G proteins. Not surprisingly $G_{\alpha olf}$ is also activated as potently as $G_{\alpha s}$ by cholera toxin. $G_{\alpha olf}$ can also couple to the β2 adrenergic receptor in transfected S49 cyc^- kin^- cells about as well as $G_{\alpha s}$(Jones et al., 1990). Bulbectomy results in loss of $G_{\alpha olf}$ message and peptide specific antisera against $G_{\alpha olf}$ stains the OE cilia and axon bundles(Jones and Reed, 1989). It would have been important for these researchers to look at the staining pattern with $G_{\alpha s}$ antisera as well. Ultrastructural/immunohistochemical EM studies using rapid freezing followed by rapid freeze-etching or freeze-substitution localize both $G_{\alpha olf}$ and $G_{\alpha s}$ to the long thin distal portions of the cilia(Menco, 1994). These data suggest that $G_{\alpha olf}$ and possibly $G_{\alpha s}$ are the AC stimulating G protein mediating olfaction. The exclusive expression of $G_{\alpha olf}$ to the OE has been challenged with the report of $G_{\alpha olf}$ expression in the basal ganglia(Drinnan et al., 1991) and its implication in dopamine D_1 receptor signaling through AC(Herve et al., 1993).

Kinetic analysis of second messenger production

In order to demonstrate temporal production of second messengers on a time scale relevant for signal transduction, i.e. faster than the channel the cAMP is supposed to open in the proposed pathway, subsecond kinetics of odorant-induced changes were analyzed with a rapid quench device(Boekhoff et al., 1990; Breer, et al., 1990). Here three syringes containing 1) cilia membranes, 2) odorant, and 3) stop solution of 10% perchloric acid are computer controlled to mix and quench samples at intervals ranging from 8-500ms. The neutralized supernatants then can be analyzed by radioimmuneassay for the production of second messenger. The results indicate second messengers are indeed produced rapidly and transiently. The peak of concentration increase, typically 10 fold over the basal level, was within 50ms of odor addition and declined with a time constant of ~100ms. Monitoring of the odorant-induced second messenger formation over a large concentration range revealed biphasic dose response curves prompting these authors to suggest the existence of two systems (receptors) which have different affinities for a single stimulant. For citralva one system has K_{m1} 50nM and the second K_{m2} 6.2μM. These authors also found some odors do not influence the level of cAMP at all. Instead these odors can rapidly increase the concentration of inositol 1,4,5-trisphosphate (IP_3) (peak concentration within 25ms) which transiently declined with a time constant of ~100ms. Like the dose response curve for citralva, the IP_3 generating odorant pyrizine has a biphasic dose response curve (K_{m1} 18nM, K_{m2} 2.2μM). The potential involvement of G proteins was addressed by showing cAMP or IP3 production with GTP-γ-S and block of odorant induced second messenger production with GDP-β-S. The above mentioned bacterial toxins, cholera toxin and pertussis toxin, were used to dissect which G proteins participate in production of a specific second messenger. Cholera toxin will activate Gαs, pertussis toxin inactivates Gαo and Gαi(Gilman, 1987),. Addition of cholera toxin to the cilia membranes induced accumulation of cAMP but had no effect on IP_3 concentration while pertussis toxin blocked production of IP_3 by pyrizine. These

observations suggest the involvement of a pertussis toxin sensitive G protein in the IP_3 response to pyrizine and that a $G_{\alpha s}$ like G protein may mediate the production of cAMP in the response to citralva. Another compound which could have been used is mastoparan(Mousli et al., 1990). This activates both $G_{\alpha o}$ and $G_{\alpha i}$ and therefore should inhibit the citralva response and reveal the $G_{\alpha o}$ mediated component of the IP_3 response to GTP-γ-S. By analysis of many more odorants in this assay, Breer and colleagues determined that seven of the odorants found to be nonresponsive in the cAMP assay (from the Skalr *et al.*) stimulated the production of IP_3. No one class of odor tested (fruity, floral, herbaceous, or putrid) exclusively stimulated production of cAMP or IP3 . For example, four of five fruity odors (citralva, citraldimethylactal, citronellal, and citronellylacetate) produced only cAMP with one, lyral, producing only IP_3.

The characterization of odorant-induced second messenger responses in ORNs is controversial. Most agree on one important point. The fact that odorant can induce the production and degradation of a second messenger on a time scale meaningful to the electrophysiological results with ORNs i.e. within 100ms. If in fact a single odorant exclusively induces phosphatidylinositol turnover or production of cAMP is in question. The results of Breer and colleagues, using cilia membrane preparations, are outlined above and argue for a distinction between odorant and the second messenger. On the other hand, using metabolic labeling of intact cells in culture with ^{3}H-myo-inositol, all odorants were found to stimulate phospholipase C (PLC) activity, as well as AC activity(Ronnett et al., 1993). An example in particular concerns the odorants citralva and isovaleric acid. In contrast to the findings of Breer and colleagues, Ronnett *et al.* determined that both these odorants were able to stimulate the production of both cAMP and IP_3. This may be a simple case of apples and oranges because one group used the cilia membrane preparation from fresh tissue while the other groups measurements were done on 5-7 day old neuronal cultures.

There is reasonable evidence for a plasma membrane localized IP_3 sensitive cation channel in lobster ORNs(Fadool and Ache, 1992).. There have not been any electrophysiology experiments done in mammals to corroborate the biochemical results of Breer. One could imagine titrating out the AC stimulatory G proteins with GDP-β-S and odorants which produce cAMP as shown in figure 1.4. Then challenging the neuron with an odorant like lyral to see if there is any attenuation of the "IP_3" response.

Cloning of an adenylyl cyclase expressed in the OE

To clone an adenylyl cyclase from the rat OE Bakalyar and Reed (Bakalyar and Reed, 1990) screened a rat olfactory cDNA library at low stringency with a mixture of coding sequence from the type I and type II adenylyl cyclase enzymes. Two overlapping clones were combined to generate a cDNA with an open reading frame that encodes 1144 amino acids. This enzyme is referred to as adenylyl cyclase type III (AC III). The deduced amino acid sequence appears topologically similar to the 1134 amino acid type I enzyme. Both proteins have two hydrophobic regions: one near the NH_2 terminus and the other between amino acid residues 600and 850. Each hydrophobic region contains six potential transmembrane regions. Northern blot analysis indicates that AC III mRNA is enriched in the OE and AC III mRNA disappeared after bulbectomy. Similarly, protein expression on the cilia reduced concomitantly with bulbectomy as detected by staining with a polyclonal antibody. When expressed stabely in HEK293 cells AC III had almost no basal activity (4.7±0.1 pmol/min/mg protein) as compared to control (4.0±0.3 pmol/min/mg protein). In contrast AC I has a relatively high basal activity (125.6±8.8 pmol/min/mg protein). A similar level of basal activity is observed for AC II under these conditions. When the isoforms were stimulated with forskolin, AC III proved to be most active. The authors use this *ex vivo* result to argue that in the ORNs, AC III activity could modulate considerably the intracellular cAMP concentration.

Cloning of a cng channel expressed in the OE

Cloning of the rat olfactory cng channel (rOCNC1)(Dhallan et al., 1990)was facilitated by the earlier cloning of the bovine retinal rod cng channel (bRCNC1) which followed a biochemical approach of purification and amino acid sequencing of protein from bovine retina(Kaupp et al., 1989). To isolate clones of the olfactory cng channel Dhallan *et al.* screened an olfactory cDNA library at low stringency with bRCNC1. Much of this thesis concerns properties of this channel so they won't be reiterated here. Suffices to say rOCNC1 was shown to be a non-specific cation channel gated by cAMP or cGMP. There was a discrepancy in the rectification properties and sensitivity to cAMP relative to the native channel which the authors attributed to heterologous expression. Chapter 2 proves this incorrect and argues that the native channel is a heterooligomer of rOCNC1 and a new subunit, refereed to as rOCNC2(Bradley et al., 1994; Liman and Buck, 1994). Importantly, Frings *et al.* (Frings et al., 1995) have shown by simultaneous whole cell recording and fura based Ca^{2+} imaging that the olfactory cng channel functions as a Ca^{2+} channel in the presence of physiological levels of extracellular Ca^{2+} with $\gtrsim$70% of the fractional conductance (P_f) being Ca^{2+} mediated at $[Ca^{2+}]_o$ =3mM.

Receptors

A very large gene family of closely related olfactory-specific seven helix receptors has been identified using a polymerase chain reaction (PCR) probe. The probe was generated by amplification of olfactory epithelial cDNA with oligonucleotides based on seven helix receptor sequences from transmembrane regions (TM) II and VII from the angiotensin receptor and the lutropin-choriogonadotropin hormone receptor, respectively (Buck and Axel, 1991). Ten complete cDNA sequences and 8 partial sequences have been published thus far. Southern blotting data with probes derived from these cDNAs provides direct evidence for 70 genes belonging to the family. Estimates for the size of the family in humans and mice range from 500 to 1000(Ressler et al., 1994b). It has not,

however, been shown convincingly that any of these receptors actually interact with odorants.

Much progress has been made, not in functional analysis of these receptors, but patterns of mRNA expression as analyzed by *in situ* hybridization, for review see (Buck, 1996; Ressler, et al., 1994b). Several main points come from these expression studies. In the rat, the OE can be divided into a number of "zones" and that individual receptor mRNA expression is confined to a particular zone. In its' particular zone the receptors' pattern of expression appears to be random. Zones of receptor expression are conserved between different rats and even between rats and mice. The pattern of receptor expression is also bilaterally symmetric in the animal, with a mirror image of expression pattern on the other side of the nasal septum. In the fish the story seems a little simpler in terms of expression. In catfish there do not appear to be any zones of expression and receptors are expressed randomly throughout the OE. Likewise the repertoire of receptors is estimated to be around 100 genes, which fits with the more limited number of waterborne odorants the fish would sample. Therefore it is generally assumed that the fish nose is a "1x" detector and the rat nose is a zonal multiple of the fish.

Sullivan et al. (Sullivan et al., 1996) have shown by chromosomal localization of these genes (mouse) that olfactory receptor (OR) genes expressed in the same zone map to numerous loci; moreover, a single locus can contain genes expressed in different zones. These findings lead the authors to propose the possibility that OR gene choice may be locus-independent or involve consecutive stochastic choices. The choice of OR gene expression has been analyzed at the level of the individual allele (Chess et al., 1994) with the conclusion that only one allele of a particular OR is expressed in an individual cell. The mechanism and significance of this result is unclear except to say that there is some sort of stochastic choice of OR gene expression going on in ORNs. The only data on transcriptional control in the OE is work showing that a transcription factor, OLF-1, can bind an element found upstream of several olfactory expressed genes(Wang and Reed,

1993). Namely, rOCNC1, AC III, G_{olf} and OMP. It was determined that Olf-1 is identical to a previously characterized transcription factor called EBF published as a novel regulator of B lymphocyte-specific gene expression (Hagman et al., 1993). Since, it has been shown that mice lacking EBF show failure in B-cell differentiation(Lin and Grosschedl, 1995). The fact that these same mice appear to express OMP and G_{olf} and the OE is morphologically normal suggests that EBF/Olf-1 may be functionally redundant in the OE.

One of the most interesting recent studies on OR expression was done on *Xenopus laevis*(Freitag et al., 1995). The authors determined that *Xenopus laevis* possess an OR gene repertoire encoding two distinct classes of olfactory receptors: one class related to receptors of fish and one class similar to receptors of mammals. The fish-like receptor genes are exclusively expressed in the lateral diverticulum of the frog's nose, specialized for detecting water-soluble odorants, where as mammalian-like receptors are expressed in sensory neurons of the main diverticulum, responsible for the reception of volatile odors. This data provide strong anatomical evidence for this family of genes encoding odorant receptors.

Olfactory bulb

It is also unclear how information about odor identity is organized in the olfactory bulb. The olfactory receptor neurons project axons to the glomeruli of the olfactory bulb, where they synapse on single primary dendrites of mitral and tufted cells. These neurons project directly to olfactory cortical regions. Two other classes of bulb neurons, the periglomerular cells and the inhibitory granule cells, also synapse within the glomeruli. There are about 1,000-3,000 glomeruli in an adult rat, so each glomerulus receives input from thousands of primary sensory neurons.

By mapping of activity in the bulb using single-unit recordings from mitral/tufted cells in the rabbit it was shown that individual mitral/tufted cells are activated by a range of odors with similar sereochemical structure or conformation(Imamura et al., 1992; Mori

et al., 1992a). It was found that individual neurons were activated selectively by a range of odors with a similar hydrocarbon chain length, similar functional groups, or with the functional group in the same position.

A similar type of odorant specific segregation of input has been shown in the moth pheromone pathway. Here the female pheromone that drives the male mate-seeking behavior is a mixture of two compounds, (E,Z)-10,12-hexadecadienal and (E,E,Z)-10,12,14-hexadecatrienal. Information about the first is sent to a compartment of macroglomerular complex called the toroid and information about the second is sent to a compartment called the cumulus(Hansson et al., 1992).

Odor evoked response maps in the olfactory bulb have also been obtained using 2-deoxyglucose uptake(Shepherd, 1994) and analysis of mRNA expression of the immediate early gene c-Fos(Guthrie et al., 1993). All these studies show that single odor molecules elicit specific spacial patterns of glomerular activation and suggests glomerular convergence of information.

Support for a such a hypothesis comes from *in situ* hybridization studies using sections of olfactory bulb(Ressler et al., 1994a; Vassar et al., 1994). In these studies it was shown that olfactory receptor axons do indeed converge on specific glomeruli. It is possible to demonstrate this by *in situ* hybridization with OR probes because apparently there is mRNA for the OR in the axon and therefore the glomeruli. A second method used to demonstrate OR axon targeting was to express a DNA construct that produces a form of β-galactosidase fused to the axonal targeted protein tau. In this way the axons of the cells that expresses the construct can be visualized by staining for β-galactosidase activity. When targeted to the coding sequence of receptor X the axons of ORNs that express receptor X can be visualized. The results show typical dispersed localization of the ORNs in an expression zone in the OE with their axons all converging to a single glomerulus (see Fig 1.6).

This presents an interesting problem in axon guidance, since the olfactory neurons die and are regenerated from the basal cells(Graziadei et al., 1979). If there is topographic specificity in their connections to specific glomeruli in the bulb, one has to explain how the axons of the regenerated neurons can reconnect to the same sites. It has been proposed that the ORs might mediate this function serving as guidance molecules(Singer et al., 1995). This is an interesting, but untested idea.

References

W. Almers and E. W. McCleskey (1984). The nonselective conductance in calcium channels of frog muscle: calcium selectivity in a single file pore. J. Phsiol. *353*, 585-608.

J. E. Amoore and R. G. Buttery (1978). Partition coefficients and comparative olfactomery. Chem. Sens. Flavor *3*, 57-71.

R. R. H. Anholt and A. M. Rivers (1990). Olfactory transduction - cross-talk between 2nd-messenger systems. Biochem. *29*, 4409-4054.

H. A. Bakalyar and R. R. Reed (1990). Identification of a specialized adenylyl cyclase that may mediate odorant detection. Science *250*, 1403-1406.

D. J. Benos (1982). Amiloride: a molecular probe of sodium transport in tissues and cells. Amer. J. Physiol. *242*, C131-C145.

M. Berkelaar, D. B. Clarke, Y. C. Wang, G. M. Bray and A. J. Aguayo (1994). Axotomy results in delayed death and apoptosis of retinal ganglion-cells in adult-rats. J. Neurosci. *14*, 4368-4374.

D. R. Bielefeld Hadley, R.W., Vassilev, P.M., Hume, J.R. (1986). Membrane electrical-properties of vesicular na-ca exchange inhibitors in single atrial myocytes. Circul. Res. *59*, 381-389.

I. Boekhoff, E. Tareilus, J. Strotmann and H. Breer (1990). Rapid activation of alternative second messenger pathways in olfactory cilia from rats by different odorants. EMBO *9*, 2453-2458.

J. Bradley, J. Li, N. Davidson, H. A. Lester and K. Zinn (1994). Heteromeric olfactory cyclic nucleotide-gated channels: A subunit that confers increased sensitivity to cAMP. Proc. Natl. Acad. Sci. USA *91*, 8890-8894.

H. Breer, I. Boekhoff and E. Tareilus (1990). Rapid kinetics of second messenger formation in olfactory transduction. Nature *345*, 65-68.

H. Breer, T. Klemm and I. Boekhoff (1992). Nitric oxide mediated formation of cyclic GMP in the olfactory system. NeuroReport *3*, 1030-1032.

L. Buck and R. Axel (1991). A novel multigene family may encode odorant receptors: a molecular basis for odor recognition. Cell *65*, 175-187.

L. B. Buck (1996). Information coding in the vertebrate olfactory system. Ann. Rev. Neurosci. *19*, 517-544.

N. Buonviso and M. A. Chaput (1990). Response similarity to odors in olfactory-bulb output cells presumed to be connected to the same glomerulus: electrophysiological study using simultaneous single-unit recordings. J. Neurophysiol. *63*, 447-454.

M. Caggiano, J. S. Kauer and D. D. Hunter (1994). Globose basal cells are neuronal progenitors in the olfactory epithelium: a lineage analysis using a replication-incompetent retrovirus. Neuron *13*, 339-352.

T.-Y. Chen and K.-W. Yau (1994). Direct modulation by Ca^{2+}-calmodulin of cyclic nucleotide-activated channel of rat olfactory receptor neurons. Nature *368*, 545-548.

A. Chess, I. Simon, H. Cedar and R. Axel (1994). Allelic inactivation regulates olfactory receptor gene-expression. Cell *78*, 823-834.

A. I. Cohen and C. Blazynski (1993). The determination of total cGMP levels in rod outer segments from intact toad photoreceptors in response to light superimposed on background and to consecutive flashes: A 2nd light flash accelerates the dark recovery rate of cGMP levels in control media, but not in Na^{+}-free, lowCa^{2+} medium. Visual Neurosci. *10*, 73-79.

T. M. Dawson and S. H. Snyder (1994). Gases as biological messengers: nitric oxide and carbon monoxide in the brain. J. Neurosci. *14*, 5147-5159.

M. K. Dehamer, J. L. Guevara, K. Hannon, B. B. Olwin and A. L. Calof (1994). Genesis of olfactory receptor neurons *in vitro* : Regulation of progenitor cell divisions by fibroblast growth-factors. Neuron *13*, 1083-1097.

R. S. Dhallan, K.-W. Yau, K. A. Schrader and R. R. Reed (1990). Primary structure and functional expression of a cyclic nucleotide-activated channel from olfactory neurons. Nature *347*, 184-187.

A. M. Dizhoor Lowe, D.G., Olshevskaya, E.V., Laura, R.P., Hurley, J.B. (1994). The human photoreceptor membrane guanylyl cyclase, retGC, is present in outer segments and is regulated by calcium and a soluble activator. Neuron *12*, 1345-1352.

S. L. Drinnan, B. T. Hope, T. P. Snutch and S. R. Vincent (1991). $G_{\alpha olf}$ in the basal ganglia. Mol. Cell Neurosci. *2*, 66-70.

A. Duchamp, M. F. Revial, A. Holley and M. P. (1974). Odor discrimination by frog olfactory receptors. Chem.Senses Flavor *1*, 213-233.

D. A. Fadool and B. W. Ache (1992). Plasma-membrane inositol 1,4,5-trisphosphate-activated channels mediate signal transduction in lobster olfactory receptor neurons. Neuron *9*, 907-918.

E. E. Fesenko, S. S. Koleniskov and A. L. Lyubarsky (1985). Induction by cGMP of cationic conductance in plasma membrane of retinal rod outer segment. Nature *313*, 310-313.

S. Firestein, B. Darrow and G. M. Shepherd (1991b). Activation of the sensory current in salamander olfactory receptor neurons depends on a G protein-mediated cAMP second messenger system. Neuron *6*, 825-835.

S. Firestein, C. Picco and A. Menini (1993). The relation between stimulus and response in olfactory receptor-cells of the tiger salamander. J. Physiol. *468*, 1-10.

S. Firestein and G. M. Shepherd (1991c). A kinetic-model of the odor response in single olfactory receptor neurons. J. Steroid Biochem. *39*, 615-620.

S. Firestein, G. M. Shepherd and F. S. Werblin (1990). Time course of the membrane current underlying sensory transduction in salamander olfactory receptor neurons. J. Physiol. *430*, 135-158.

S. Firestein and F. Werblin (1989). Odor-induced membrane currents in vertebrate-olfactory receptor neurons. Science *244*, 79-82.

S. Firestein, F. Zufall and G. M. Shepherd (1991a). Single odor-sensitive channels in olfactory receptor neurons are also gated by cyclic nucleotides. J. Neurosci. *11*, 3565-3572.

J. Freitag, J. Krieger, J. Strotmann and H. Breer (1995). 2 classes of olfactory receptors in *Xenopus laevis*. Neuron *15*, 760-773.

S. Frings and B. Lindemann (1988). Odorant response of isolated receptor cell is blocked by amiloride. J. Memb. Biol. *105*, 233-243.

S. Frings, J. W. Lynch and B. Lindemann (1992). Properties of cyclic nucleotide-gated channels mediating olfactory transduction: activation, selectivity, and blockage. J. Gen. Physiol. *100*, 45-67.

S. Frings, R. Seifert, M. Godde and U. P. Kaupp (1995). Profoundly different calcium permeation and blockage determine the specific function of distinct cyclic nucleotide-gated channels. Neuron *15*, 169-179.

R. C. Gesteland, J. Y. Lettvin and W. H. Pitts (1965). Chemical transmission in the nose of the frog. J. Physiol. London. *181*, 525-559.

M. L. Getchell and T. V. Getchell (1991). Immunohistochemical localization of components of the immune barrier in the olfactory mucosae of salamanders and rats. Anat. Rec. *231*, 358-374.

T. V. Getchell and G. M. Shepherd (1978). Responses of olfactory receptor cells to step pulses of odor at different concentrations in the salamander. J. Physiol. London *282*, 521-540.

A. G. Gilman (1984). G proteins and duel control of adenylate cyclase. Cell *36*, 577-579.

A. G. Gilman (1987). G-proteins: Transducers of receptor-generated signals. Ann. Rev. Biochem. *56*, 615-649.

G. Gold and G. Lowe (1995). Single odorant molecules? Nature *376*, 27.

M. K. Gordon, J. S. Mumm, R. A. Davis, J. D. Holcomb and A. L. Calof (1995). Dynamics of mash1 expression in-vitro and in-vivo suggest a non-stem cell site of mash1 action in the olfactory receptor neuron lineage. Mol. Cell Neurosci. *6*, 363-379.

P. P. C. Graziadei, R. R. Levine and G. A. Monti Graziadei (1979). Plasticity of connections of the olfactory sensory neuron: regeneration into the forebrain following bulbectomy in the neonatal mouse. Neurosci. *4*, 713-727.

P. P. C. Graziadei and G. A. Monti Graziadei (1979). Neurogenesis and neuron regeneration in the olfactory system of mammals. I. Morphological aspects of differentiation and structural organization of the olfactory sensory neurons. J. Neurocytol. *8*, 1-18.

F. Guillemot, L. C. Lo, J. E. Johnson, A. Auerbach, D. J. Anderson and A. L. Joyner (1993). Mammalian achaete-scute homolog-1 is required for the early development of olfactory and autonomic neurons. Cell *75*, 463-476.

K. M. Guthrie, A. J. Anderson, M. Leon and C. Gall (1993). Odor-induced increases in c-fos messenger-rna expression reveal an anatomical unit for odor processing in olfactory-bulb. Proc. Natl. Acad. Sci. U.S.A. *90*, 3329-3333.

J. Hagman, C. Belanger, A. Travis, C. W. Turck and R. Grosschedl (1993). Cloning and functional-characterization of early b-cell factor, a regulator of lymphocyte-specific gene-expression. Genes Dev. *7*, 760-773.

B. S. Hansson, H. Ljungberg, E. Hallberg and C. Lofstedt (1992). Functional specialization of olfactory glomeruli in a moth. Science *256*, 1313-1315.

L. W. Haynes (1992). Block of the cyclic GMP-gated channel of vertebrate rod and cone photoreceptors by *l-cis*-diltiazem. J. Gen. Physiol. *100*, 783-801.

L. W. Haynes and K. W. Yau (1985). Cyclic GMP-sensitive conductance in outer segment membrane of catfish cones. Nature *317*, 61-64.

D. Herve, M. Levistrauss, I. Mareysemper, C. Verney, J. P. Tassin, J. Glowinski and J. A. Girault (1993). G_{olf} and G_s in rat basal ganglia: Possible involvement of G_{olf} in the coupling of dopamine-D_1 receptor with adenylyl cyclase. J. Neurosci. *13*, 2237-2248.

P. Hess and R. W. Tsien (1984). Mechanism of ion permeation through calcium channels. Nature *309*, 453-456.

J. D. Holcomb, J. S. Mumm and A. L. Calof (1995). Apoptosis in the neuronal lineage of the mouse olfactory epithelium: regulation in-vivo and in-vitro. Develop. Bio. *172*, 307-323.

R. Horn and A. Marty (1988). Muscarinic activation of ionic currents measured by a new whole-cell recording method. J. Gen. Physiol. *94*, 145-159.

Y.-T. Hsu and R. S. Molday (1993). Modulation of the cGMP-gated channel of rod photoreceptor cells by calmodulin. Nature *361*, 76-79.

T. Huque and R. C. Bruch (1986). Odorant and guanine nucleotide-stimulated phosphoinositide turnover in olfactory cilia. Biochem. Biophys. Res. Commun. *137*, 36-42.

R. Hurwitz and V. Holcombe (1991). Affinity purification of the photoreceptor cGMP-gated cation channel. J. Biol. Chem. *226*, 7975-7977.

K. Imamura, N. Mataga and K. Mori (1992). Coding of odor molecules by mitral tufted cells in rabbit olfactory-bulb 1. Aliphatic-compounds. J. Neurophysol. *68*, 1986-2002.

T. Ingi and G. V. Ronnett (1995). Direct demonstration of a physiological-role for carbon-monoxide in olfactory receptor neurons. J. Neurosci. *15*, 8214-8222.

J. E. Johnson, S. J. Birren and D. J. Anderson (1990). 2 rat homologs of drosophila-achaete-scute specifically expressed in neuronal precursors. Nature 858-861.

D. T. Jones, E. Barbosa and R. R. Reed (1988). Expression of G-protein α subunits in rat olfactory neuroepithelium: Candidates for olfactory signal transduction. Cold Spring Harbor Symp. Quan. Bio. *LIII*, 349-353.

D. T. Jones, S. B. Masters, H. R. Bourne and R. R. Reed (1990). Biochemical-characterization of 3 stimulatory GTP binding proteins: The large and small forms of G_s and the olfactory-specific G-protein, G_{olf}. J. Biol. Chem. *265*, 2671-2676.

D. T. Jones and R. R. Reed (1987). Molecular cloning of five G-bindin protein cDNA species form rat olfactory neuroepithelium. J. Biol. Chem. *262*, 14241-14249.

D. T. Jones and R. R. Reed (1989). G_{olf}: an olfactory neuron-specific G-protein involved in odorant signal transduction. Science *244*, 790-795.

U. B. Kaupp, T. Niidome, T. Tanabe, S. Terada, W. Bonigk, W. Stuhmer, W. J. Cook, K. Kangawa, H. Matsuko, T. Hirose, T. Miyata and S. Numa (1989). Primary structure and functional expression from complementary cDNA of the rod photoreceptor cyclic GMP-gated channel. Nature *342*, 762-766.

B. Key and R. A. Akeson (1990). Olfactory neurons express a unique glycosylated form of the neural adhesion molecule (N-CAM). J. Cell Biol. *110*, 1729-1743.

S. Kleene (1992). Basal conductance of frog olfactory cilia. Pflügers Arch. *421*, 374-380.

S. J. Kleene (1993). Origin of the chloride current in olfactory transduction. Neuron *11*, 123-132.

S. J. Kleene and R. C. Gesteland (1991). Calcium-activated chloride conductance in frog olfactory cilia. J. Neurosci. *11*, 3624-3629.

T. R. Kleyman and E. J. Cragoe (1988). Amiloride and its analogs as tools in the study of ion-transport. J. Membr. Bio. *105*, 1-21.

T. Kurahashi and A. Kaneko (1991). High-density camp-gated channels at the ciliary membrane in the olfactory receptor cell. Neuroreport *2*, 5-8.

T. Kurahashi and T. Shibuya (1990). Ca^{2+}-dependent adaptive properties in the solitary olfactory receptor cell of the newt. Brain Res. *515*, 261-268.

T. Kurahashi and K.-W. Yau (1993). Co-existence of cationic and chloride components in odorant-induced current of vertebrate olfactory receptor cells. Nature *363*, 71-74.

D. Lazard, K. Zupko, Y. Poria, P. Nef, J. Lazarovits, S. Horn, M. Kehn and D. Lancet (1991). Odorant signal termination by olfactory UDP-glucuronosyl transferase. Nature *349*, 790-793.

T. Leinders-Zufall, G. M. Shepherd and F. Zufall (1995). Regulation of cyclic nucleotide-gated channels and membrane excitability in olfactory receptor cells by carbon monoxide. J. Neurophys. *74*, 1498-1508.

M. S. Levey, D. M. Chikaraishi and J. S. Kauer (1991). Characterization of potential precursor populations in the mouse olfactory epithelium using immunocytochemistry and autoradiography. J. Neurosci. *11*, 3556-3564.

A. Levitski (1988). From epinephrine to cyclic AMP. Science *241*, 800-806.

E. R. Liman and L. B. Buck (1994). A second subunit of the olfactory cyclic nucleotide-gated channel confers high sensitivity to cAMP. Neuron *13*, 611-621.

H. H. Lin and R. Grosschedl (1995). Failure of B-cell differentiation in mice lacking the transcription factor ebf. Nature *376*, 263-267.

G. Lowe and G. Gold (1993). Nonlinear amplification by calcium-dependent chloride channels in olfactory receptor cells. Nature *366*, 283-286.

M. D. Maines (1988). Heme oxygenase: function, multiplicity, regulatory mechanisms, and clinical applications. FASAB J. 2, 2557-2568.

F. L. Margolis (1972). A brain protein unique to the olfactory bulb. Proc. Natl. Acad. Sci. *69*, 1221-1224.

L. M. Masukawa, B. Hedlund and G. M. Shepherd (1985). Electrophysiologicl properties of identified cells in the *in vitro* olfactory epithelium of the tiger salamander. J. Neurosci. *5*, 128-135.

P. M. B. Menco (1994). Ultrastructural aspects of olfactory transduction and perireceptor events. Seminars Cell Bio. *5*, 11-24.

A. Menini (1990). Currents carried by monovalent cations through cyclic gmp-activated channels in excised patches from salamander rods. J. Physiol. *424*, 167-185.

A. Menini, C. Picco and S. Firestein (1995). Quantal-like fluctuations induced by odorants in olfactory receptor cells. Nature *373*, 435-437.

A. V. Minor and N. L. Sakina (1973). Role of cyclic adenosine-3',5' -monophosphate in olfactory reception. Neurofysiologiya *5*, 415-422.

R. S. Molday, L. L. Molday, A. Dosé, I. Clark-Lewis, M. Illing, N. J. Cook, E. Eismann and U. B. Kaupp (1991). The cGMP-gated channel of the rod photoreceptor cell characterization and orientation of the amino terminus. J. of Biol. Chem. *266*, 21917-21922.

K. Mori, N. Mataga and K. Imamura (1992a). Differential specificities of single mitral cells in rabbit olfactory bulb for a homologous series of fatty acid odor molecules. J. Neurophysiol. *67*, 786-789.

K. Mori, N. Mataga and K. Imamura (1992b). Differential specificities of single mitral cells in rabbit olfactory-bulb for a homologous series of fatty-acid odor molecules. J. Neurophisl. *67*, 786-789.

M. Mousli, J. L. Bueb, C. Bronner, B. Rouot and Y. Landry (1990). G-protein activation - a receptor-independent mode of action for cationic amphiphilic neuropeptides and venom peptides. Trends. in Pharm. *11*, 358-362.

T. Nakamura and G. H. Gold (1987). A cyclic nucleotide-gated conductance in olfactory receptor cilia. Nature *325*, 342-344.

P. Nef, J. Heldman, D. Lazard, T. Margalit, M. Jaye, I. Hanukoglu and D. Lancet (1989). Olfactory-specific cytochrome-p-450: cDNA cloning of a novel neuroepithelial enzyme possibly involved in chemoreception. J. Biol. Chem. *264*, 6780-6785.

G. D. Nicol, P. P. M. Schnetkamp, Y. Saimi, E. J. Cragoe and M. D. Bownds (1987). A derivative of amiloride blocks both the light-regulated and cyclic GMP-regulated conductances in rod photoreceptors. J. Gen. Physiol. *90*, 651-669.

M. Okano Tagaki, S.F. (1974). Secreation and electrogenesis of the supporting cell in the olfactory epithelium. J. Physiol. Lond. *242*, 353-370.

D. Ophir Lancet, D. (1988). Expression of intermediate filaments and desmoplakin in vertebrate olfactory mucosa. Anat. Rec. *221*, 754-760.

D. Ottoson (1956). Analysis of the electrical activity of the olfactory epithelium. Acta Physiol. Scand. *122*, 1-83.

U. Pace, E. Hanski, Y. Salomon and D. Lancet (1985). Odorant-sensitive adenylate cyclase may mediate olfactory reception. Nature *316*, 255-258.

U. Pace and D. Lancet (1986). Olfactory GTP-binding protein: Signal-transducing polypepide of vertebrate chemosensory neurons. Proc. Natl. Acad. Sci. USA *83*, 4947-4951.

K. J. Ressler, S. L. Sullivan and L. B. Buck (1994a). Information coding in the olfactory system - evidence for a stereotyped and highly organized epitope map in the olfactory-bulb. Cell *79*, 1245-1255.

K. J. Ressler, S. L. Sullivan and L. B. Buck (1994b). A molecular dissection of spatial patterning in the olfactory system. Curr. Op. Neurobio. *4*, 588-596.

L. D. Rhein and R. H. Cagan (1980). Biochemical studies of olfaction: isolation, characterization, and odorant binding activity of cilia from rainbow trout olfactory rosettes. Proc. Natl. Acad. Sci. USA *77*, 4412-4416.

G. A. Robison, R. W. Butcher and E. W. Sutherland (1971). cAMP (Orlando, FL: Academic Press).

G. V. Ronnett, C. H., L. D. Hester, Wood-SF and S. H. Snyder (1993). Odorants differentially enhance phosphoinositide turnover and adenylyl cyclase in olfactory receptor neuronal cultures. J. Neurosci. *13*, 1751-1758.

A. J. Roskams, D. S. Bredt, T. M. Dawson and G. V. Ronnett (1994). Nitric-oxide mediates the formation of synaptic connections in developing and regenerating olfactory receptor neurons. Neuron *13*, 289-299.

J. E. Schwob, N. B. Farber and D. I. Gottlieb (1986). Neurons of the olfactory epithelium in adult-rats contain vimentin. J. Neurosci. *6*, 208-217.

G. M. Shepherd (1994). Discrimination of molecular signals by the olfactory receptor neuron. Neuron *13*, 771-790.

A. W. Shyjan, F. J. Desauvage, N. A. Gillett, D. V. Goeddel and D. G. Lowe (1992). Molecular-cloning of a retina-specific membrane guanylyl cyclase. Neuron *9*, 727-737.

G. Sicard and A. Holey (1984). Receptor cell responses to odorants: similarities and differences among odorants. Brain Res. *292*, 283-296.

M. S. Singer, G. M. Shepherd and C. A. Greer (1995). Olfactory receptors guide axons. Nature *377*, 19-20.

P. B. Sklar, R. R. H. Anholt and S. H. Snyder (1986). The odorant-sensitive adenylate cyclase of olfactory receptor cells: differential stimulation by different classes of odorants. J. Biol. Chem. *261*, 15538-15543.

W. D. Snider, J. L. Elliott and Q. Yan (1992). Axotomy-induced neuronal death during development. J. Neurobiol. *23*, 1231-1246.

S. P. Soltoff and L. J. Mandel (1983). Amiloride directly inhibits the Na,K-atpase activity of rabbit kidney proximal tubules. Science *220*, 957-959.

J. H. Stern, U. B. Kaupp and P. R. Macleish (1986). Control of the light-regulated current in rod photoreceptors by cyclic-gmp, calcium, and l-cis-diltiazem. Proc. Natl. Acad. Sci. *83*, 1163-1167.

S. L. Sullivan, M. C. Adamson, K. J. Ressler, C. A. Kozak and L. B. Buck (1996). The chromosomal distribution of mouse odorant receptor genes. Proc. Natl. Acad. Sci. U.S.A. *93*, 884-888.

C. M. Tang Presser, F., Morad, M. (1988). Amiloride selectively blocks the low threshold (T) calcium-channel. Science *240*, 213-215.

R. Vassar, S. K. Chao, R. Sitcheran, J. M. Nunez, L. B. Vosshall and R. Axel (1994). Topographic organization of sensory projections to the olfactory-bulb. Cell *79*, 981-991.

C. Viereck, R. P. Tucker and A. Matus (1989). The adult-rat olfactory system expresses microtubule-associated proteins found in the developing brain. J. Neurosci. *9*, 3547-3557.

M. M. Wang and R. R. Reed (1993). Molecular-cloning of the olfactory neuronal transcription factor olf-1 by genetic selection in yeast. Nature *364*, 121-126.

S. Yoshikami and W. A. Hagins (1985). Cytoplasmic pH in rod outer segments and high energy phosphate metabolism during phototransduction. Bio. Phys. J. *47*, 101a (Abstr).

Y. X. Zhuang Cragoe, E.J., Shaikewitz, T., Glaser, L., Cassel, D. (1984). Characterization of potent Na/H exchange inhibitors from the amiloride series in a431 cells. Biochem. *23*, 4481-4488.

F. Zufall and S. Firestein (1993b). Divalent-cations block the cyclic nucleotide-gated channel of olfactory receptor neurons. J. Neurophysiol. *69*, 1758-1768.

F. Zufall, S. Firestein and G. M. Shepherd (1991a). Analysis of single cyclic nucleotide-gated channels in olfactory receptor cells. J. Neurosci. *11*, 3573-3580.

F. Zufall, G. M. Shepherd and S. Firestein (1991b). Inhibition of the olfactory cyclic nucleotide-gated ion channel by intracellular calcium. Proc. R. Soc. Bio. *246*, 225-230.

Figure legends

Fig1.1 Schematic diagram of the olfactory epithelium

Illustration of the three basic cell type in the olfactory epithelium. Basal cells are located along the basment membrane. The olfactory sensory neuron is located in the central portion of the epithelium and has a bipolar morphology with a single dendrite extending to the luman and an axon extending to the olfactory bulb. The tip of the dendrite forms a knob from which eminate the olfactory cilia. Supporting cells constitute the third type of cell in the epithelium

Fig 1.2 Schematic drawing of an olfactory receptor neuron

See caption to figure for legend

Fig 1.3 Whole cell recording of odorant response by an olfactory receptor neuron

See caption to figure for legend

Fig 1.4 Effects of GTP-γ-S and GTP-β-S on the whole cell odorant response by an olfactory receptor neuron

See caption to figure for legend

Fig 1.5 Schematic diagram of the olfactory signal transduction pathway

Odorant interacts with a seven helix receptor (7HR) activating a G protein (G) which stimulates adenylyl cyclase (AC) to produce cAMP. cAMP opens the cng channel allowing Ca^{2+} influx. Ca^{2+} down regulates the cng channels sensitivity to cAMP by interaction with calmodulin (CaM) and gates a Cl^- channel amplifying the depolarization.

Fig 1.6 Whole mount staining for β-galactosidase expressed in the axons of olfactory receptor neurons.

Mice were generated such that the β-galactosidase-tau fusion gene would be expressed under control of a olfactory receptor gene promoter. The blue stain reveals the expression and localization of the β-galactosidase-tau fusion protein. Axons can be seen leaving the olfactory epithelium and converging on a single glomerulus.

From The molecular logic of smell, by Richard Axel, in *Scientific American*, October 1995.

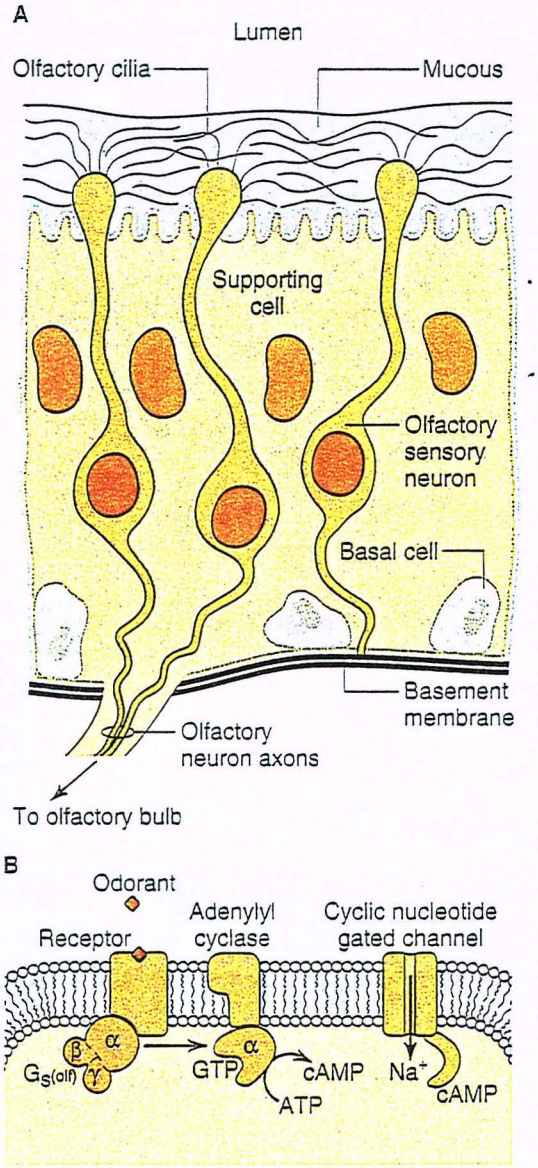

FIG. 1. A schematic diagram of the olfactory epithelium. The initial events in odor perception occur in the olfactory epithelium of the nasal cavity. Odorants interact with specific odorant receptors on the lumenal cilia of olfactory sensory neurons. The signals generated by these initial binding events are transmitted along olfactory neuron axons to the olfactory bulb of the brain.

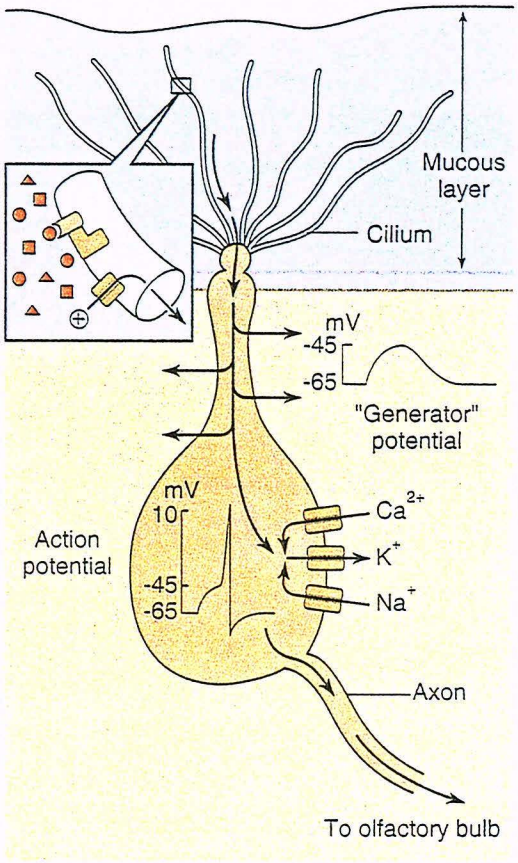

FIG. 5. Schematic drawing of an olfactory neuron showing the single bipolar morphology, with a single thick dendrite ending in a knob-like swelling and an unbranched axon projecting from the proximal soma centrally to the olfactory bulb. The cell is highly compartmentalized into transduction and signaling regions. Transduction occurs in the cilia which extend from the distal dendritic knob into the mucous layer. A receptor-coupled second messenger system (see Fig. 6) results in the opening of a cation selective channel in the ciliary membrane. The influx of cations depolarizes the cell membrane from its resting level near −65 mV to −45 mV in a graded manner. This depolarization spreads by passive current flow through the dendrite to the soma. A depolarization that reaches −45 mV is sufficient to activate voltage-gated Na^+ channels and initiate impulse generation. This Na^+ current, along with several varieties of voltage-dependent K^+ currents and a small Ca^{2+} current act to produce one or more action potentials that are propagated down the axon to the brain.

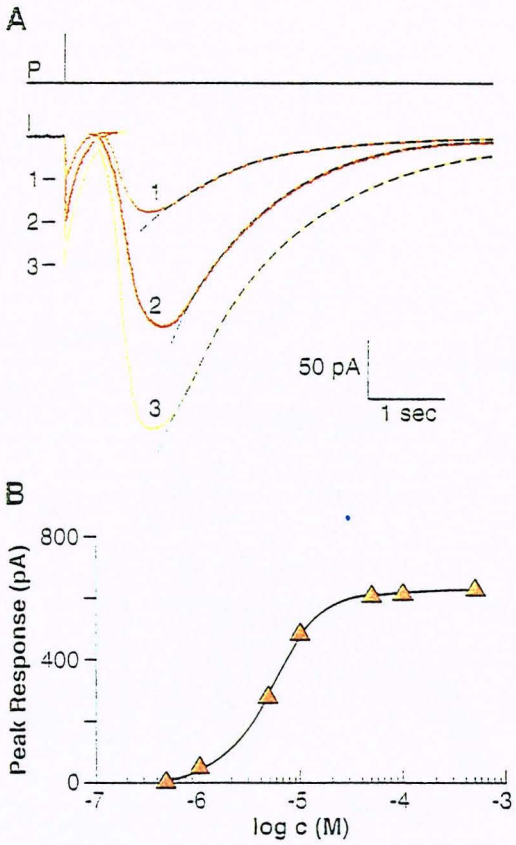

FIG. 7A: Three responses to 50 msec pulses of odor stimuli of low, intermediate, and saturating concentration. The initial fast, downward deflections are responses to KCl and provide a record of the time course and relative strength of the stimuli. The slower and larger downward deflections are the currents that flow in response to the odor pulses. Downward deflections of the current traces denote positive current flowing into the cell (i.e., a depolarizing current). Note the 100–200 msec latency between the arrival of the stimulus and the initiation of the current and also the continued activation of the current even after the stimulus has disappeared. These features are indicative of a second messenger process. The decay of the current is reasonably well fit by a single exponential time course *(dashed lines)*. B: Dose-response curve for a cell that responded to the odorant, cineole. The *solid line* is a fit of the Hill equation with a $K_{1/2}$ of 3×10^{-5} M and a Hill coefficient equal to 2. This curve shows the narrow operating range of the olfactory neuron.

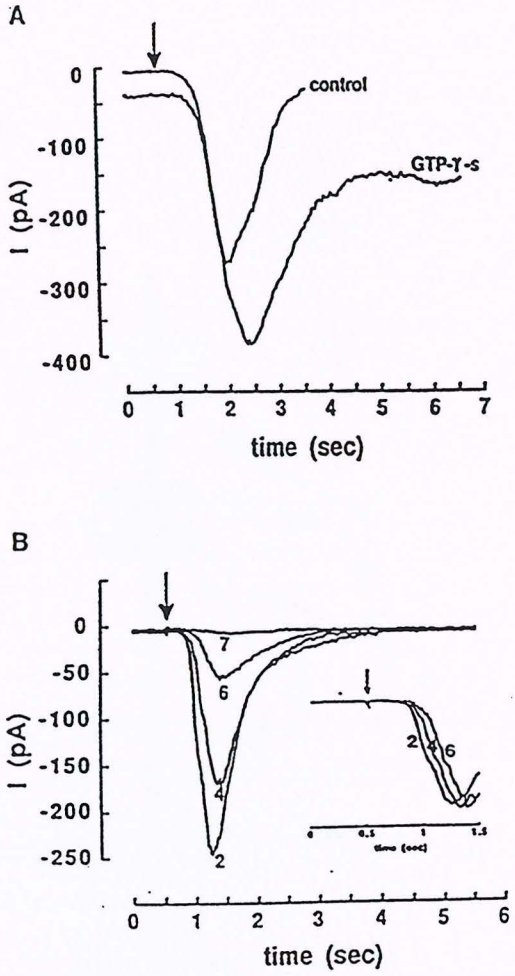

Figure 5. Nonhydrolyzable Nucleotide Analogs Alter the Odor-Sensitive Current

(A) GTP-γ-s prolongs the response to a 50 ms pulse of odor stimulus (arrow). Note that there is a shift in the baseline of some 40 pA and that the decay is clearly biphasic. GTP-γ-s (50 μM) was included in the patch pipette solution. The first (control) response was obtained within 30 s of patch rupture. The second trace was obtained after 3 min and two prior stimulations (including the control).

(B) GDP-β-s blocks the response to 50 ms pulses of odor stimulus (arrow). GDP-β-s (50 μM) was included in the patch pipette. Stimuli were delivered once per minute after patch rupture until the response was negligible. Numbers near the traces refer to the number of minutes after patch rupture that the record was obtained. The inset shows the same four records scaled to equal amplitudes so that the onset kinetics can be compared.

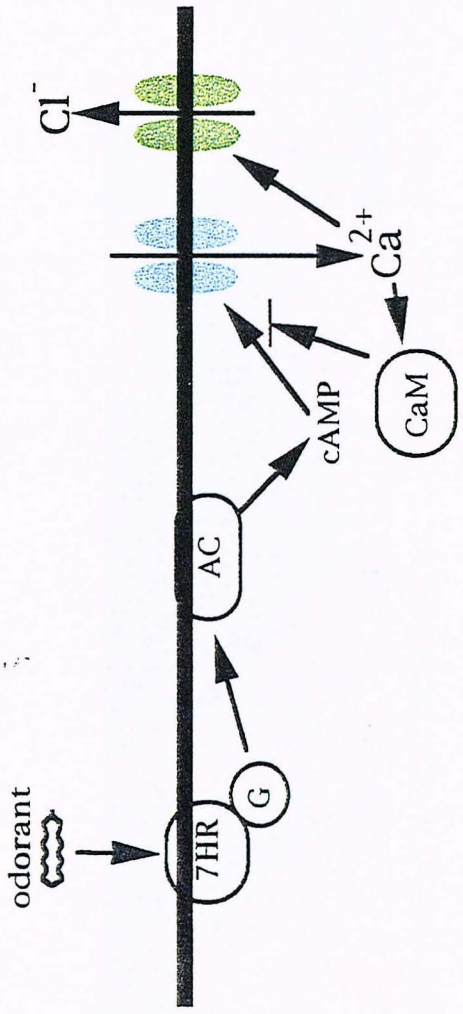
odorant
7HR
G
AC
cAMP
CaM
Ca^{2+}
Cl^-

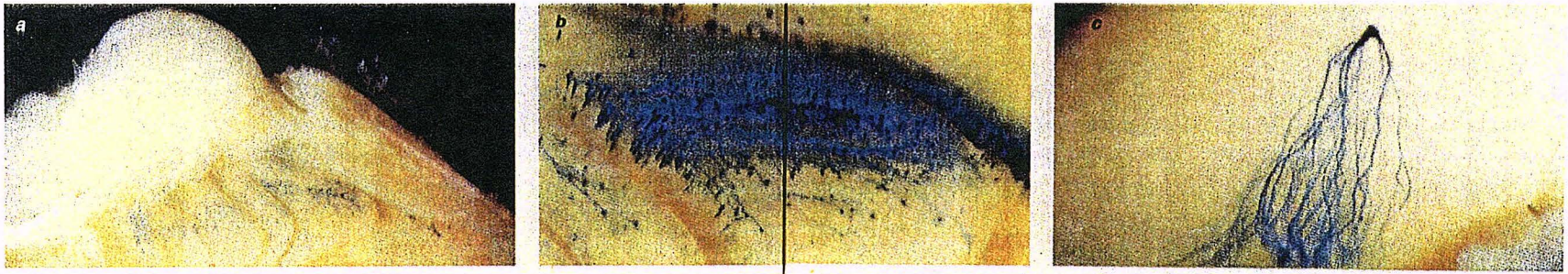

BLUE NEURONS reveal the pathway of sensory information from the olfactory epithelium in the nose to the olfactory bulb in the brain (*a*). By genetically modifying the odor receptor genes in mice, the author and his colleagues dyed deep blue the neurons that bear a particular type of receptor—and are therefore sensitive to a limited number of odors. Randomly positioned neurons on the olfactory epithelium (*b*) converge at one location in the olfactory bulb (*c*).

Chapter 2. Heteromeric olfactory cyclic nucleotide-gated channels: a new subunit that confers increased sensitivity to cAMP

Published as an article in Proc. Natl.Acad. Sci. U.S.A. *91* 8890-8894 (1994).

Classification: Neurobiology

Heteromeric olfactory cyclic nucleotide-gated channels: a new subunit that confers increased sensitivity to cAMP

(cyclic nucleotide-gated channel/olfaction/cAMP/cGMP)

Jonathan Bradley, Jun Li, Norman Davidson,

Henry A. Lester, and Kai Zinn*

Division of Biology,

California Institute of Technology,

Pasadena, CA 91125

* To whom reprint requests should be addressed.

Abbreviations: cng, cyclic nucleotide-gated; rOCNC1 and rOCNC2, rat olfactory cyclic nucleotide-gated channel subunits; G protein, guanine nucleotide binding protein; PCR, polymerase chain reaction; CN, cyclic nucleotide-binding; EC_{50}, agonist concentration at which a half-maximal current response is observed; hRCNC1 and hRCNC2, human retinal cyclic nucleotide-gated channel subunits.

ABSTRACT **Olfactory receptor neurons respond to odorant stimulation with a rapid increase in intracellular cAMP that opens cyclic nucleotide-gated (cng) cation channels. Cng channels in rat olfactory neurons are activated by cAMP in the low micromolar range and are outwardly rectifying. The cloned rat olfactory cng channel (rOCNC1), however, is much less sensitive to cAMP and exhibits very weak rectification. Here we describe the cloning and characterization of a novel rat cng channel subunit, denoted rOCNC2. rOCNC2 does not form functional channels when expressed alone. When rOCNC1 and rOCNC2 are coexpressed, however, an outwardly rectifying cation conductance with cAMP sensitivity near that of the native channel is observed. *In situ* hybridization with probes specific for the two subunits shows that they are coexpressed in olfactory receptor neurons. These data indicate that the native olfactory cng channel is likely to be a hetero-oligomer of the rOCNC1 and rOCNC2 subunits.**

One mechanism of olfactory signal transduction involves a rapid and transient increase of intracellular cAMP concentraton, in response to the binding of odorants to guanine nucleotide binding protein (G protein)-coupled receptors. Receptor binding activates a Gs-like G protein which increases the enzymatic activity of adenylyl cyclase [reviewed in (Lancet and Ben-Arie, 1993; Reed, 1992)]. cAMP opens cyclic nucleotide-gated (cng) cation channels that are localized to the cilia and dendrites of olfactory neurons (Firestein et al., 1991; Frings et al., 1992; Kurahashi, 1990; Nakamura and Gold, 1987; Zufall et al., 1991). The cng channels are permeable to both monovalent and divalent cations. The influx of Ca^{2+} activates a Cl^- conductance (Kleene, 1993; Kurahashi and Yau, 1993; Lowe and Gold, 1993) which amplifies the initial depolarization. The depolarization triggers sensory nerve impulses.

Each of the components of this transduction pathway has been cloned and characterized. A very large family of G protein-coupled receptors is expressed in olfactory receptor neurons (Buck and Axel, 1991). These receptors could interact with Golf, a G protein expressed in olfactory neurons that is very similar in sequence to Gs (Jones and Reed, 1989) An olfactory adenylyl cyclase (Bakalyar and Reed, 1990) and olfactory cng channels (Dhallan et al., 1990; Goulding et al., 1992; Ludwig et al., 1990) have also been cloned and characterized.

The rat olfactory cng channel clone (rOCNC1) forms cyclic AMP-activated channels when heterologously expressed in mammalian cells. The conductance is characterized by a half-maximal concentration (EC_{50}) for cAMP of 68 μM, and very weak rectification in the absence of divalent cations (Dhallan, et al., 1990). In contrast, the native conductance in rat olfactory neurons is much more sensitive to cAMP (EC_{50}=2.5 μM) and is outwardly rectifying (Frings, et al., 1992). There are several possible explanations for these functional differences. A second olfactory channel might exist that would display the cAMP sensitivity and rectification behavior of the native

channel when heterologously expressed. Alternatively, another channel subunit might modulate the properties of rOCNC1 by forming hetero-oligomeric channels with it.

Materials and methods

Isolation and characterization of rOCNC2 cDNA clones. Primers CN2 (5' AA(A/G)(C/T)TIGCIGTIGTNGCNGA, corresponding to rOCNC1 residues 500-506 (KLAVVAD)) and CN1 (5' AT(A/G)TTIGCIGTIC(G/T)IC(G/T)(A/G)TTNCC, corresponding to residues 535-542 (GNRRTANI)) were used for polymerase chain reaction (PCR) (19) experiments, with oligo-dT primed first-strand cDNA synthesized from rat nasal epithelial RNA as a template. The annealing temperature was 42°C, and 35 amplification cycles were performed. Restriction analysis of the PCR product revealed that it contained two sequence classes, and one of these corresponded to the rOCNC2 sequence (see Appendix I). To obtain an rOCNC2-specific hybridization probe an rOCNC2-specific PCR primer was designed from amino acids 417-426, and used in combination with vector primers flanking the polylinker of λZAPII (Stratagene Cloning Systems) to PCR amplify sequences from a rat nasal epithelial λZAPII cDNA library (K.Z., unpublished results). The ends of the 1090 bp fragment thus isolated were sequenced, and new rOCNC2-specific PCR primers were designed and used to amplify a non-crosshybridizing fragment of 820 bp. This was used to screen 1.8 x 10^6 phage from the library, and 8 full-length rOCNC2 clones were isolated; two of these were sequenced. We sequenced the 5' ends of all 8 clones in order to determine whether a second form of rOCNC2 with a longer N terminus might exist, but found no evidence for such a form.

Measurement of channel mRNA levels. cDNA was quantitated by amplifying with β-actin primers (15 and 20 cycles), and the amounts of cDNA in each channel primer amplification were adjusted based on these results. Primer sequences are available on request. For the channel mRNA amplifications, 25, 30, and 35 PCR cycles were used, and approximately 1 ng of cDNA was amplified. The 30 cycle amplification is shown in

Fig. 2.2. In 35 cycle amplifications, both PCR products can be detected when cDNA from brain, cortex, cerebellum, and olfactory bulb is used, but not with cDNA from any of the other tissues (J.B., unpublished results). The amplification reactions were subjected to electrophoresis on 1.5% agarose gels, which were then stained with ethidium bromide and photographed. Fig. 2.2 is a negative image.

***In situ* hybridization.** Digoxigenin antisense RNA probes were synthesized using an *in vitro* transcription kit (Ambion) in the presence of digoxigenin-UTP (at a ratio of 1:3 relative to UTP). The Golf probe template was a full-length cDNA clone of 3 kb. The I7 receptor probe template was the entire coding sequence (984 bp). rOCNC1 and rOCNC2 probe templates were generated from pBluescript (Stratagene Cloning Systems) clones of rOCNC1 and rOCNC2 by PCR using primers 1849 (rOCNC1; corresponding to amino acids 624-630) and 1666 (rOCNC2; amino acids 518-524), in combination with vector primers flanking the transcription promoters at the 3' ends of these genes. These probes were shown to be incapable of cross-hybridization to the other channel sequence by Northern blot analysis using full-length sense-strand *in vitro* transcripts of rOCNC1 and rOCNC2 cDNA clones (J.B., unpublished results). *In situ* hybridization was performed as described (Schaeren-Wiemers and Gerfin-Moser, 1993). Sections were mounted in glycerol and photographed under coverslips with a Zeiss Axioplan microscope.

Electrophysiology. The pCIS expression vector was used, and transfections into 293 cells were performed as described (Chen et al., 1993). Patch-clamp recordings were made 1-3 days after transfection. Electrodes were fabricated from borosilicate glass and had resistances of 1-3 MΩ. Cyclic nucleotides were applied using a fast microperfusion system that allowed solution changes within 100 msec. Divalent-free solution: 140 mM NaCl, 5 mM KCl, 10 mM Na-HEPES, 0.5 mM Na-EDTA, 0.5 mM Na-EGTA, pH 7.6. Solution with divalents: 140 mM NaCl, 5 mM KCl, 10 mM Na-HEPES, 2 mM $CaCl_2$, 1 mM $MgCl_2$, pH 7.6. Single-channel recordings were made from excised inside-out patches with symmetrical divalent cation-free solutions. Data were filtered at 2kHz,

digitized at 16-bit resolution and 22kHz frequency for storage on magnetic tape, and redigitized and analyzed at 4kHz using Axotape 2.0/Fetchan 6.0 (Axon Instruments).

Results

We used PCR to amplify cng channel-related sequences from primary olfactory epithelial cDNA. We identified a novel amplification product whose sequence is closely related to rOCNC1. This product was used to isolate a full-length cDNA clone, denoted rOCNC2. The predicted amino acid sequence of rOCNC2 comprises 575 residues, and is 51% identical to rOCNC1 (Fig. 2.1). Hydropathy plots of the two sequences are almost superimposable, indicating similar transmembrane topology. Each protein contains six putative transmembrane regions (S1-S6), and a pore region (P) homologous to the pore region of voltage-gated channels.

The cyclic nucleotide binding (CN) domain is highly conserved (77% identity). The threonine that influences selectivity for cGMP over cAMP (Altenhofen et al., 1991) is present in both sequences (residue 539 in rOCNC1). However, there are three adjacent nonconservative differences (serine-lysine-methionine (residues 532-534) in rOCNC1 vs. asparagine-methionine-serine (residues 424-426) in rOCNC2) within the most conserved part of the CN domain (Kaupp, 1991; Shabb and Corbin, 1992). The S4 region (corresponding to the putative voltage sensor of voltage-gated channels) of rOCNC2 is likely to bear 1-2 more positive charges than the corresponding sequence from rOCNC1 (2 if histidine 254 of rOCNC1 is uncharged). The two sequences also differ at a position in the P region (glutamic acid 342 in rOCNC1, aspartic acid 234 in rOCNC2) that influences interactions between divalent cations and the channel pore (Eismann et al., 1994; Heginbotham et al., 1992; Root and MacKinnon, 1993). Finally, rOCNC2 is 109 residues shorter than rOCNC1 at its N terminus.

We used quantitative reverse transcription-PCR (RT-PCR) to assay the tissue-specific expression patterns of the rOCNC1 and rOCNC2 mRNAs. Both mRNAs are

highly enriched in the olfactory epithelium, although low-level expression can be detected in brain and olfactory bulb (Fig. 2.2). To examine the cell-specific expression patterns of the mRNAs, we performed *in situ* hybridization with digoxigenin-labeled rOCNC1 and rOCNC2 probes on sections of rat olfactory epithelium. We also used probes recognizing mRNAs encoding Golf (Jones and Reed, 1989) and the I7 olfactory receptor(Buck and Axel, 1991) to visualize olfactory neurons and to provide controls for nonspecific background hybridization. Golf mRNA is expressed at high levels throughout the neuronal layer (Fig. 2.3*B*), while I7 mRNA, like other olfactory receptor mRNAs (Ressler et al., 1993; Vassar et al., 1993), is expressed only in a small subset of neurons (Fig. 2.3*A*). Both rOCNC1 (Fig. 2.3*C*) and rOCNC2 (Fig. 2.3*D*) mRNAs are expressed in the olfactory neuronal layer. There is significant heterogeneity in rOCNC2 expression between individual neurons, while rOCNC1 is more homogenously expressed. These patterns suggest that some olfactory neurons may express only the rOCNC1 channel. This could explain earlier observations that for a subpopulation of neurons the cng conductance exhibits a lower sensitivity to cAMP (Nakamura and Gold, 1987). *In situ* hybridization to brain sections shows that both channel subunit mRNAs are also expressed in subsets of neurons in the olfactory bulb, cerebellum, and cortex (J.B., unpublished results).

To determine whether rOCNC2 could function as a cng channel, we transiently transfected HEK 293 cells with an rOCNC2 expression vector. 10-40% of the transfected cells exhibited bright surface staining with an rOCNC2-specific antiserum (J.B., unpublished results), but we could not detect any cyclic nucleotide-activated conductances in excised inside-out patches from these cells.

In order to evaluate whether rOCNC2 could alter the properties of the rOCNC1 channel, we transfected HEK 293 cells with an rOCNC1 expression vector or with a 1:1 mixture of the rOCNC1 and rOCNC2 plasmids. At a membrane potential (V_m) of +60 mV, an inside-out patch from an rOCNC1-expressing cell displayed a cyclic nucleotide-

activated conductance with an EC_{50} for cAMP of 64 μM. A cell expressing both subunits, in contrast, had an EC_{50} for cAMP of 6.3 μM at +60 mV (Fig. 2.4*A*, left panel; macroscopic current traces from these two patches are shown in Fig. 2.4*B*). While expression of rOCNC2 increased the apparent affinity of the channel for cAMP, it had the opposite effect for cGMP. The EC_{50} for cGMP was 1.5 μM for a cell expressing only rOCNC1, but was 2.8 μM for a cell expressing both subunits (Fig. 2.4*A*, right panel). The data obtained from 34 different patches are summarized in Table 1.

Table 1 also shows that the Hill coefficients for the rOCNC1/rOCNC2 channel are significantly lower than for the rOCNC1 channel, and approximate those observed for the native channel (Frings, et al., 1992). We do not know whether the lower Hill coefficients of the rOCNC1/rOCNC2 channel are due to a reduced cooperativity at the molecular level or to the presence of a heterogeneous population of channels in the patch that have different subunit stoichiometries. In cells cotransfected with rOCNC2 and rOCNC1 plasmids at ratios of 3:1 or 6:1, the average EC_{50} for cAMP was 6.9 ±0.8 at +60 mV (n=8). Thus, increasing the relative proportion of rOCNC2 does not increase the sensitivity to cAMP beyond the values observed with a 1:1 ratio. The EC_{50}s for both cAMP and cGMP that we measured for the rOCNC1/rOCNC2 channel in HEK 293 cells are approximately 3-fold higher than those observed for the native rat channel (Frings, et al., 1992)(Table 1). This may be due to differences in experimental conditions, in post-translational modification, or in interactions with cell-specific modulatory factors. A recent study demonstrated that the cyclic nucleotide sensitivity of the rOCNC1 and native rat channels can be dramatically altered by direct interaction with Ca^{2+}-calmodulin (Chen and Yau, 1994).

The differences in apparent agonist affinity between the hetero-oligomeric and homo-oligomeric channels may be partially due to the three adjacent nonconservative amino acid substitutions within the highly conserved CN domain (Fig. 2.1). In the determined three-dimensional structures of CN domains from another protein (Shabb and

Corbin, 1992), these three positions are within a loop that forms part of the cyclic nucleotide binding pocket.

The rOCNC1/rOCNC2 channel shows outward rectification in symmetrical divalent-free solutions. The kinetic basis for this rectification is a current relaxation (time constant=30-50 msec) to smaller or larger amplitudes following a step from zero to negative or positive membrane potentials, respectively (Fig. 2.4*B*, right panel). The relaxation was not observed for cells transfected with rOCNC1 alone (Fig. 2.4*B*, left panel). The increased voltage dependence of the hetero-oligomeric channel could be due to the larger number of positive charges in the S4 domain of rOCNC2 relative to rOCNC1.

In the presence of extracellular divalent cations, both the homo-oligomeric and hetero-oligomeric channels are outwardly rectifying, but the divalents have a smaller effect on the hetero-oligomeric channel. In the absence of divalent cations, the ratio of current amplitudes at -60 and +60 mV (I^{-60}/I^{+60}) was 0.84 for rOCNC1 (see Fig. 2.4*B*); and this ratio decreased by 8-fold, to 0.11, with the inclusion of 2 mM Ca^{2+} and 1 mM Mg^{2+} in the extracellular solution (Fig. 2.4*C*). Divalent cations had a smaller effect on the rOCNC1/rOCNC2 channel, decreasing I^{-60}/I^{+60} by only a factor of 3 (from 0.62 to 0.2). These data suggest that the two channels could have different Ca^{2+} permeabilities. Permeability to Ca^{2+} is likely to be functionally important in light of recent observations that a major component of the depolarizing current in olfactory neurons is carried by Ca^{2+}-activated Cl^- channels (Kleene, 1993; Kurahashi and Yau, 1993; Lowe and Gold, 1993).

The rOCNC1/rOCNC2 channel also differs from the rOCNC1 channel in its single-channel properties. The openings of the rOCNC1 channel are stable, last for tens of msec, and have a maximal conductance of ~48 pS at +60 mV (Fig. 2.5, left panel). The rOCNC1/rOCNC2 channel is flickery at +60 mV, making it difficult to accurately measure single-channel conductances. At -60 mV, the flickering is further accentuated

(Fig. 2.5, right panel). This reduces the effective single-channel conductance and contributes to outward rectification. Flickery opening behavior has also been observed for the native channel (Frings, et al., 1992).

Discussion

In this paper, we describe the identification of a novel subunit of the rat olfactory cyclic nucleotide-gated channel, rOCNC2. This subunit does not form a functional channel by itself, but hetero-oligomerizes with the previously identified olfactory channel, rOCNC1, to produce a channel whose electrophysiological behavior differs from that of the homo-oligomeric rOCNC1 channel.

These data reveal a parallelism between the native cng channels in olfactory neurons and those in retinal rods. A second subunit of the human rod channel, hRCNC2, has been recently described (Chen, et al., 1993). This subunit lacks channel activity when expressed alone, but can form functional hetero-oligomers with the previously characterized rod cng channel, hRCNC1. Compared to the hRCNC1 channel, the hRCNC1/hRCNC2 channel is more similar to the native photoreceptor channel in its sensitivity to drug blockade and its single channel properties. The openings of both olfactory and retinal hetero-oligomeric channels are flickery, while the openings of both homo-oligomeric channels are stable. Like rOCNC2, hRCNC2 is shorter at its N terminus than the first rod channel subunit. An evolutionary tree of these cng channel sequences (Fig. 2.6) suggests that the rOCNC2 and hRCNC2 subunits arose from a common ancestral protein after the rOCNC1 and hRCNC1 subunits diverged. Thus, the olfactory and retinal channels may have once shared a common modulatory subunit.

The rOCNC2 subunit confers several properties that are characteristic of the native channel from olfactory neurons, but differ from those of the homo-oligomeric rOCNC1 channel. These include agonist sensitivity, rectification, and single-channel behavior. The ratio of the EC_{50}s for cAMP versus cGMP is 34 for the homo-oligomeric

rOCNC1 channel, and 2.5 for the hetero-oligomeric rOCNC1/rOCNC2 channel (Table 1). The value of 2.5 is equal to that observed for the native rat channel from olfactory neurons. Our results, together with the studies on the retinal channel (Chen, et al., 1993), provide molecular and functional evidence for the presence of hetero-oligomeric cng channels *in vivo*. The existence of additional subunits that modulate channel properties has also been described for K^+ channels and for various ligand-gated channels.

We thank T-Y. Chen and K-W. Yau for helpful discussions, HEK 293 cells, and an rOCNC1 clone; W. Zagotta for providing the sequences of the CN1 and CN2 primers; Genentech, Inc. for the pCIS plasmid; M. Quick and Y. Uezono of Caltech for experimental contributions to the early phase of this project; and L. Buck and E. Liman for communicating data before publication. J.B. was supported by an NIH graduate training grant and by the ARCS Foundation. This work was supported by grants from the National Institute of Mental Health and the National Institutes of Health to K.Z., H.A.L., and N.D.

References

W. Altenhofen, J. Ludwig, E. Eismann, W. Kraus, W. Bonigk and U. B. Kaupp (1991). Control of ligand specificity in cyclic nucleotide-gated channels from rod photoreceptors and olfactory epithelium. Proc. Natl. Acad. Sci. USA *88*, 9868-9872.

H. A. Bakalyar and R. R. Reed (1990). Identification of a specialized adanylylcycalse that may mediate odorant detection. Science *250*, 1403-1406.

L. Buck and R. Axel (1991). A novel multigene family may encode odorant receptors: a molecular basis for odor recognition. Cell *65*, 175-187.

T.-Y. Chen, Y.-W. Peng, R. S. Dhallan, B. Ahamed, R. R. Reed and K.-W. Yau (1993). A new subunit of the cyclic nucleotide-gated cation channel in retinal rods. Nature *362*, 764-767.

T.-Y. Chen and K.-W. Yau (1994). Direct modulation by Ca^{2+}-calmodulin of cyclic nucleotide-activated channel of rat olfactory receptor neurons. Nature *368*, 545-548.

R. S. Dhallan, K.-W. Yau, K. A. Schrader and R. R. Reed (1990). Primary structure and functional expression of a cyclic nucleotide-activated channel from olfactory neurons. Nature *347*, 184-187.

E. Eismann, F. Muller, S. H. Heinemann and U. B. Kaupp (1994). A single negative charge within the pore region of a cGMP-gated channel controls rectification, Ca2+ blockage, and ionic selectivity. Proc. Natl. Acad. Sci. USA *91*, 1109-1113.

S. Firestein, B. Darrow and G. M. Shepherd (1991). Activation of the sensory current in salamander olfactory receptor neurons depends on a G protein-mediated cAMP second messenger system. Neuron *6*, 825-835.

S. Frings, J. W. Lynch and B. Lindemann (1992). Properties of cyclic nucleotide-gated channels mediating olfactory transduction: activation, selectivity, and blockage. J. Gen. Physiol. *100*, 45-67.

E. H. Goulding, J. Ngai, R. H. Kramer, S. Colicos, R. Axel, S. A. Siegelbaum and A. Chess (1992). Molecular cloning and single-channel properties of the cyclic nucleotide-gated channel from catfish olfactory neurons. Neuron *8*, 45-58.

L. Heginbotham, T. Abramson and R. MacKinnon (1992). A functional connection between the pores of distantly related ion channels as revealed by mutant K+ channels. Science *258*, 1152-1155.

D. T. Jones and R. R. Reed (1989). G_{olf}: an olfactory neuron-specific G-protein involved in odorant signal transduction. Science *244*, 790-795.

U. B. Kaupp (1991). The cyclic nucleotide-gated channels of vertebrate photoreceptors and olfactory epithelium. Trends Neurosci. *14*, 150-157.

S. J. Kleene (1993). Origin of the chloride current in olfactory transduction. Neuron *11*, 123-132.

T. Kurahashi (1990). J. Physiol., Lond. *430*, 355-371.

T. Kurahashi and K.-W. Yau (1993). Co-existence of cationic and chloride components in odorant-induced current of vertebrate olfactory receptor cells. Nature *363*, 71-74.

D. Lancet and N. Ben-Arie (1993). Olfactory receptors. Current Biology *3*, 668-674.

G. Lowe and G. Gold (1993). Nonlinear amplification by calcium-dependent chloride channels in olfactory receptor cells. Nature *366*, 283-286.

J. Ludwig, T. Margalit, E. Eismann, D. Lancet and U. B. Kaupp (1990). Primary structure of cAMP-gated channel from bovine olfactory epithelium. FEBS Lett. *270*, 24-29.

T. Nakamura and G. H. Gold (1987). A cyclic nucleotide-gated conductance in olfactory receptor cilia. Nature *325*, 342-344.

R. R. Reed (1992). Signaling pathways in odorant detection. Neuron *8*, 205-209.

K. J. Ressler, S. L. Sullivan and L. B. Buck (1993). A zonal organization of odorant receptor gene expression in the olfactory epithelium. Cell *73*, 597-610.

M. J. Root and R. MacKinnon (1993). Identification of an external divalent cation-binding site in the pore of a cGMP-activated channel. Neuron *11*, 459-466.

N. Schaeren-Wiemers and A. Gerfin-Moser (1993). A single protocol to detect transcripts of various types and expression levels in neural tissues and cultured cells; in situ hybridization using digoxigenin-labeled cRNA probes. Histochemistry *100*, 431-440.

J. B. Shabb and J. D. Corbin (1992). Cyclic nucleotide-binding domains in proteins having diverse functions. J. Biol. Chem. *267*, 5723-5726.

R. Vassar, J. Ngai and R. Axel (1993). Spatial segregation of odorant receptor expression in the mammalian olfactory epithelium. Cell *74*, 309-318.

F. Zufall, S. Firestein and G. M. Shepherd (1991). Analysis of single cyclic nucleotide-gated channels in olfactory receptor cells. J. Neurosci. *11*, 3573-3580.

Figure legends

Fig. 2.1. Aligned amino acid sequences of rOCNC1 and rOCNC2 proteins. In the alignment, dashes indicate the absence of an amino acid, and dots in the consensus line indicate amino acids that are not conserved between the sequences. S1 to S6 are putative transmembrane domains, and P is the putative pore region. The cyclic nucleotide binding domain is defined by homology to the sequences of other proteins that bind cAMP and cGMP (Kaupp, 1991; Shabb and Corbin, 1992).

Fig. 2.2. Expression pattern of rOCNC1 (left panel) and rOCNC2 (right panel) mRNAs, as determined by quantitative RT-PCR. Primers specific for the 3' untranslated regions of the two mRNAs were used to amplify oligo-dT primed cDNA made from RNA isolated from various rat tissues. The tissue source is indicated at the top of the figure. Total RNA was used except where indicated. The rOCNC1 PCR product is 159 bp, and the rOCNC2 product is 122 bp. M, markers (sizes in bp indicated at the right), NepA, nasal epithelium (polyA+ RNA); BrpA, brain (excluding olfactory bulb; polyA+ mRNA); Lu, lung; Ov, ovary; Ne1, Ne2, nasal epithelium (2 isolates); Co, cortex; Ce, cerebellum; He, heart; OB1, OB2, olfactory bulb (2 isolates); +, positive control (rOCNC1 or rOCNC2 plasmid clone); -, negative control (no DNA).

Fig. 2.3. Expression of rOCNC1 and rOCNC2 mRNAs within the neuronal layer of the olfactory epithelium. We performed *in situ* hybridization to 20 μm horizontal sections of rat olfactory epithelium, using digoxigenin-labeled antisense RNAs as probes. Panels *A-D* are high-magnification photographs (788x), using Nomarski optics, of the same region of the epithelium. The olfactory cilia are at the top, and below them are the supporting cell layer (**S**), the neuronal layers (**N**), and the basal cell layer (**B**), as indicated in panel **B**. Cells expressing a particular mRNA are visualized as dark disks. (*A*) I7 olfactory receptor probe. One I7-expressing neuron is observed in this photograph. The I7 probe,

which is about twofold larger than the channel probes, also serves as a control for nonspecific hybridization. (*B*) G_{olf} probe. Note the uniform hybridization within the neuronal layers. (*C*) rOCNC1 probe. (*D*) rOCNC2 probe. Widespread hybridization in the neuronal layers is observed with these two probes. Note the heterogeneity in rOCNC2 mRNA expression. A cell expressing rOCNC2 mRNA at high levels is indicated by a black arrowhead, and a cell lacking the mRNA or expressing it at low levels by a white arrowhead. Scale bar: 5μM. Panels *C* and *D* are adjacent sections, and panels *A* and *B* are sections within 50 μM of *C* and *D*. Examination of the epithelial sections at low magnification shows that rOCNC1 and rOCNC2 mRNAs are present in all regions of the epithelium that contain G_{olf} mRNA.

Fig. 2.4. Comparisons between cng conductances produced by expression of rOCNC1 alone and by coexpression of rOCNC1 and rOCNC2. Recordings were obtained from inside-out patches excised from HEK 293 cells transfected either with rOCNC1 plasmid, or with a 1:1 mixture of rOCNC1 and rOCNC2 plasmids. (*A*) Normalized dose-response relations for cAMP (left panel) and cGMP (right panel), at V_m=+60 mV. The left panel is derived from macroscopic current data for the two cells shown in (*B*). The right panel displays cGMP results from two other cells. Currents were measured at the end of the 800 msec voltage pulse. The symbols represent the average responses, while the smooth lines are described by the Hill equations with best-fitting values. (*B*) Macroscopic currents recorded from two patches (left panel, rOCNC1; right panel, rOCNC1/rOCNC2). The membrane potential (V_m) was stepped from 0 mV to +60 mV or to -60 mV for 800 msec. The patches were maintained in symmetrical divalent-free solutions, and the bath contained cAMP at various concentrations (indicated adjacent to the traces). Top traces show the voltage commands for each episode in a trial. Episodes shown are averaged from 3-6 trials, each taken during a separate series of cAMP applications at ascending concentrations. Leak currents have been subtracted. Filter corner frequency, 2kHz. (*C*)

Current-voltage relation in the presence of extracellular divalent cations. Currents were activated with cAMP at 50 μM for rOCNC1/rOCNC2 patches (1:1 plasmid ratio; n=3), and at 200 μM for rOCNC1 patches (n=4). Both were normalized to current amplitudes at V_m=+60 mV. Leak currents were subtracted. The error bars indicate s.e.m. values.

Fig. 2.5. Single-channel properties of homo-oligomeric and hetero-oligomeric olfactory channels. Left panels, rOCNC1 channel (the patch contained hundreds of channels, thus 0.1 μM cAMP was used); right panels, rOCNC1/rOCNC2 channel (the patch contained one channel, 2 μM cAMP was used). Top panels, V_m=+60 mV; bottom panels, -60 mV. O1, O2 represent the conductance from the openings of one, and two channels within the rOCNC1 patch, respectively. C represents the closed state. The dotted line represents the current amplitude corresponding to a single-channel conductance of ~48 pS. Consecutive sweeps are shown.

Fig. 2.6. One unrooted parsimonious tree of cng channel coding region DNA sequences, calculated using the PHYLIP program. h, human; r, rat; m, mouse; b, bovine; f, catfish.

Table 2.1 Summary of properties of cyclic nucleotide-activated conductances observed in 293 cells expressing the rOCNC1 and rOCNC1/rOCNC2 channels*. These properties are compared to those previously measured for the rat native olfactory cng channels (Frings, et al., 1992).

```
rOCNC1      MMTEKSNGVK SSPANNHNHH PPPSIKANGK DDHRAGSRPQ SVAADDDTSP    50

rOCNC1      ELQRLAEMDT PRRGRGGFQR IVRLVGVIRD WANKNFREEE PRPDSFLERF   100

rOCNC2             MS QDGKVKTTES TPPAPTKARK WLPVLDPSGD YYYWWLNTMV    42
rOCNC1      RGPELQTVTT HQGDDKGGKD GEGKGTKKKF ELFVLDPAGD WYYRWLFVIA   150
Consensus   .......... ..G..K.... .....TK... .L.VLDP.GD .YY.WL....   150
                 S1                           S2
rOCNC2      FPIMYNLIIV VCRACFPDLQ HSYLVAWFVL DYTSDLLYLL DIGVRFHTGF    92
rOCNC1      MPVLYNWCLL VARACFSDLQ RNYFVVWLVL DYFSDTVYIA DLIIRLRTGF   200
Consensus   .P..YN.... V.RACF.DLQ ..Y.V.W.VL DY.SD..Y.. D...R..TGF   200
                                          S3
rOCNC2      LEQGILVVDK GMIASRYVRT WSFLLDLASL VPTDAAYVQL GPHIPTLRLN   142
rOCNC1      LEQGLLVKDP KKLRDNYIHT LQFKLDVASI IPTDLIYFAV GIHSPEVRFN   250
Consensus   LEQG.LV.D. ......Y..T ..F.LD.AS. .PTD..Y... G.H.P..R.N   250
                 S4                              S5
rOCNC2      RFLRVPRLFE AFDRTETRTA YPNAFRIAKL MLYIFVVIHW NSCLYFALSR   192
rOCNC1      RLLHFARMFE FFDRTETRTS YPNIFRISNL VLYILVIIHW NACIYYVISK   300
Consensus   R.L...R.FE .FDRTETRT. YPN.FRI..L .LYI.V.IHW N.C.Y...S.   300
                                                      P
rOCNC2      YLGFGRDAWV YPDPAQPGFE RLRRQYLYSF YFSTLILTTV GDTPLPDREE   242
rOCNC1      SIGFGVDTWV YPNITDPEYG YLAREYIYCL YWSTLTLTTI GETPPPVKDE   350
Consensus   ..GFG.D.WV YP....P... .L.R.Y.Y.. Y.STL.LTT. G.TP.P...E   350
                            S6
rOCNC2      EYLFMVGDFL LAVMGFATIM GSMSSVIYNM NTADAAFYPD HALVKKYMKL   292
rOCNC1      EYLFVIFDFL IGVLIFATIV GNVGSMISNM NATRAEFQAK IDAVKHYMQF   400
Consensus   EYLF...DFL ..V..FATI. G...S.I.NM N...A.F... ...VK.YM..   400

rOCNC2      QHVNKRLERR VIDWYQHLQI NKKMTNEVAI LQHLPERLRA EVAVSVHLST   342
rOCNC1      RKVSKDMEAK VIKWFDYLWT NKKTVDEREV LKNLPAKLRA EIAINVHLST   450
Consensus   ..V.K..E.. VI.W...L.. NKK...E... L..LP..LRA E.A..VHLST   450
                              Cyclic Nucleotide Binding Domain
rOCNC2      LSRVQIFQNC EASLLEELVL KLQPQTYSPG EYVCRKGDIG REMYIIREGQ   392
rOCNC1      LKKVRIFQDC EAGLLVELVL KLRPQVFSPG DYICRKGDIG KEMYIIKEGK   500
Consensus   L..V.IFQ.C EA.LL.ELVL KL.PQ..SPG .Y.CRKGDIG .EMYII.EG.   500

rOCNC2      LAVVADDGVT QYAVLGAGLY FGEISIINIK GNMSGNRRTA NIKSLGYSDL   442
rOCNC1      LAVVADDGVT QYALLSAGSC FGEISILNIK GSKMGNRRTA NIRSLGYSDL   550
Consensus   LAVVADDGVT QYA.L.AG.. FGEISI.NIK G...GNRRTA NI.SLGYSDL   550

rOCNC2      FCLSKEDLRE VLSEYPQAQA VMEEKGREIL LKMNKLDVNA EAAEIALQEA   492
rOCNC1      FCLSKDDLME AVTEYPDAKK VLEERGREIL MKEGLLDENE VAASMEVD--   598
Consensus   FCLSK.DL.E ...EYP.A.. V.EE.GREIL .K...LD.N. .AA.......   600

rOCNC2      TESRLKGLDQ QLDDLQTKFA RLLAELESSA LKIAYRIERL EWQTREWPMP   542
rOCNC1      VQEKLEQLET NMDTLYTRFA RLLAEYTGAQ QKLKQRITVL E--TK-----   641
Consensus   ....L..L.. ..D.L.T.FA RLLAE..... .K...RI..L E..T......   650

rOCNC2      EDMGEADDEA EPGEGTSKDG EGKAGQAGPS GIE                     575
rOCNC1      --MKQNHEDD YLSDGINT-- ------PEPT AAE                     664
Consensus   ..M....... ....G..... ........P. ..E                     683
```

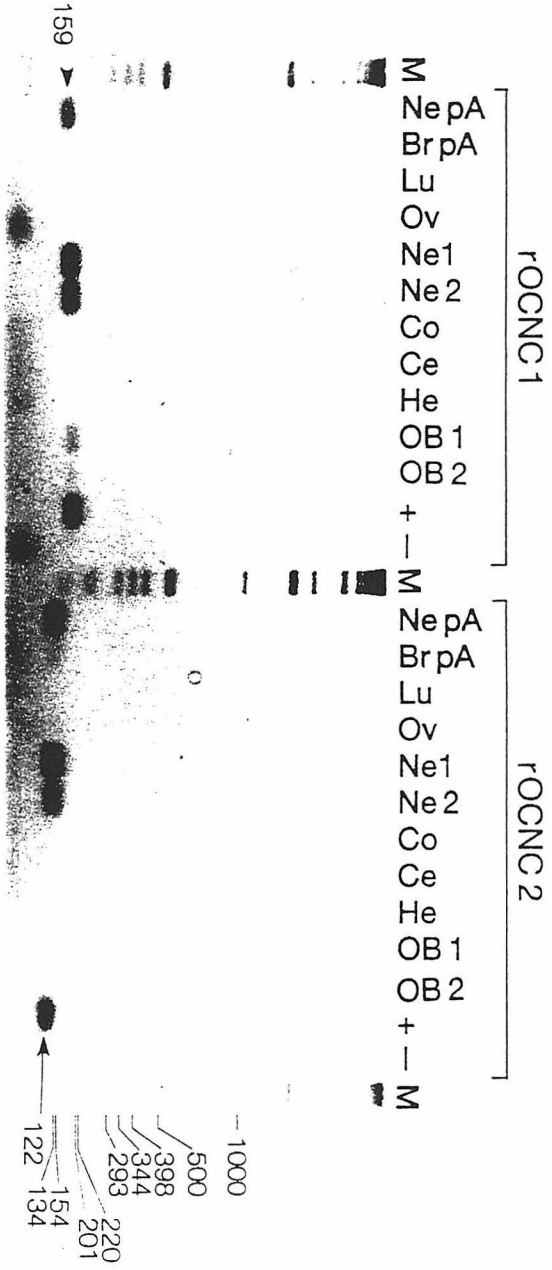
M
Ne pA
Br pA
Lu
Ov
Ne1
Ne 2
Co
Ce
He
OB 1
OB 2
+
–
M
rOCNC 1
M
Ne pA
Br pA
Lu
Ov
Ne1
Ne 2
Co
Ce
He
OB 1
OB 2
+
–
M
rOCNC 2
159
1000
500
398
344
293
220
201
154
134
122

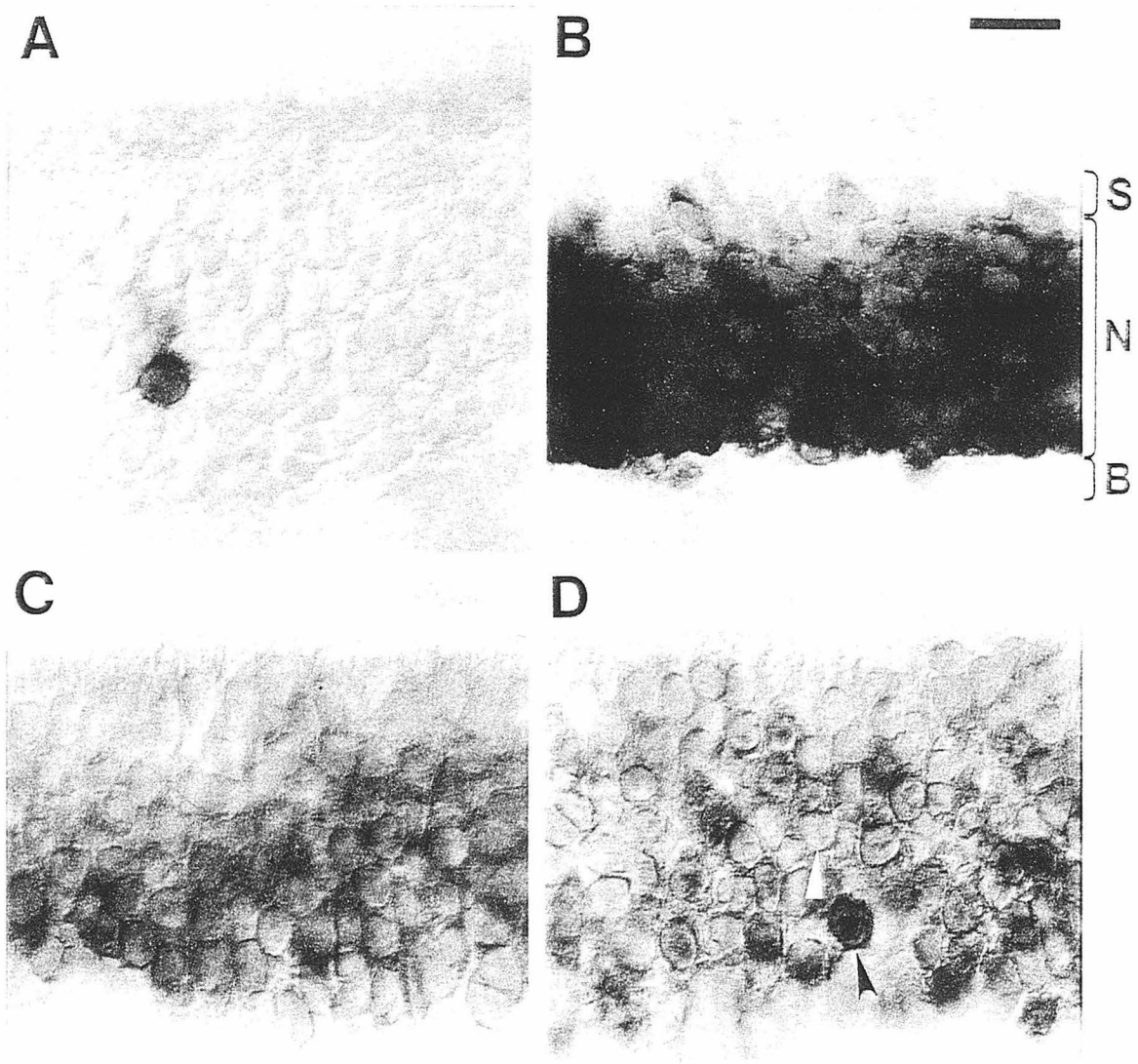
A
B
S
N
B
C
D

A

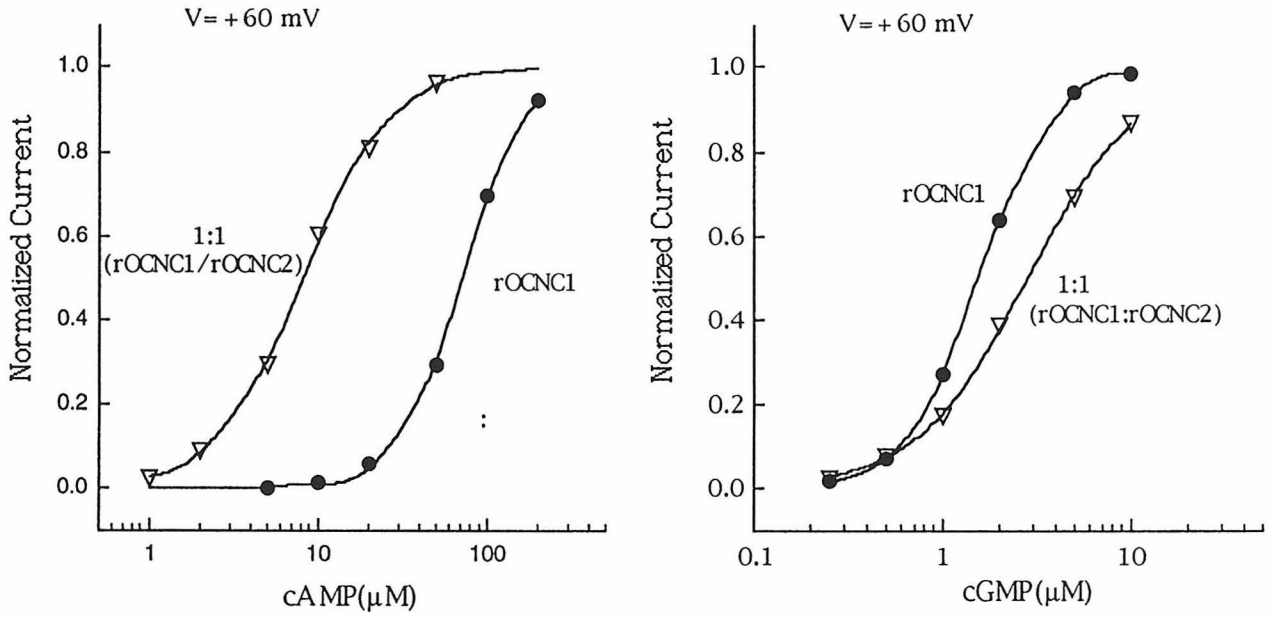
V= + 60 mV
Normalized Current
1.0
0.8
0.6
0.4
0.2
0.0
1:1
(rOCNC1/rOCNC2)
rOCNC1
1
10
100
cAMP(μM)
V= + 60 mV
Normalized Current
rOCNC1
1:1
(rOCNC1:rOCNC2)
0.1
1
10
cGMP(μM)

B

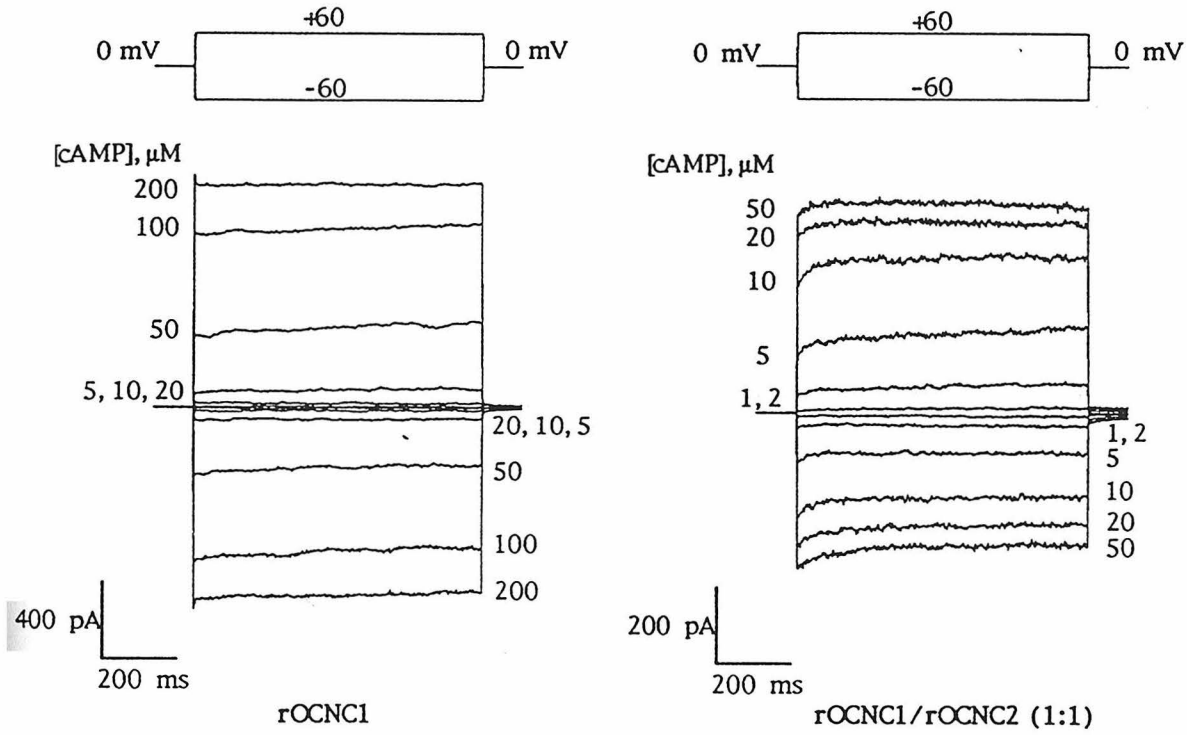
+60
0 mV
0 mV
-60
[cAMP], µM
200
100
50
5, 10, 20
20, 10, 5
50
100
200
400 pA
200 ms
rOCNC1
+60
0 mV
0 mV
-60
[cAMP], µM
50
20
10
5
1, 2
1, 2
5
10
20
50
200 pA
200 ms
rOCNC1/rOCNC2 (1:1)

C

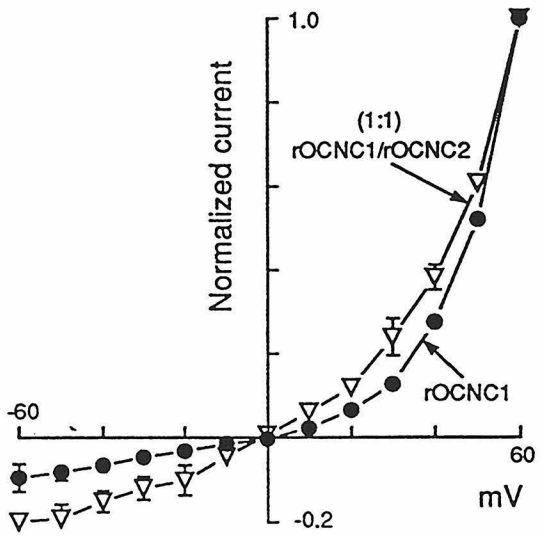

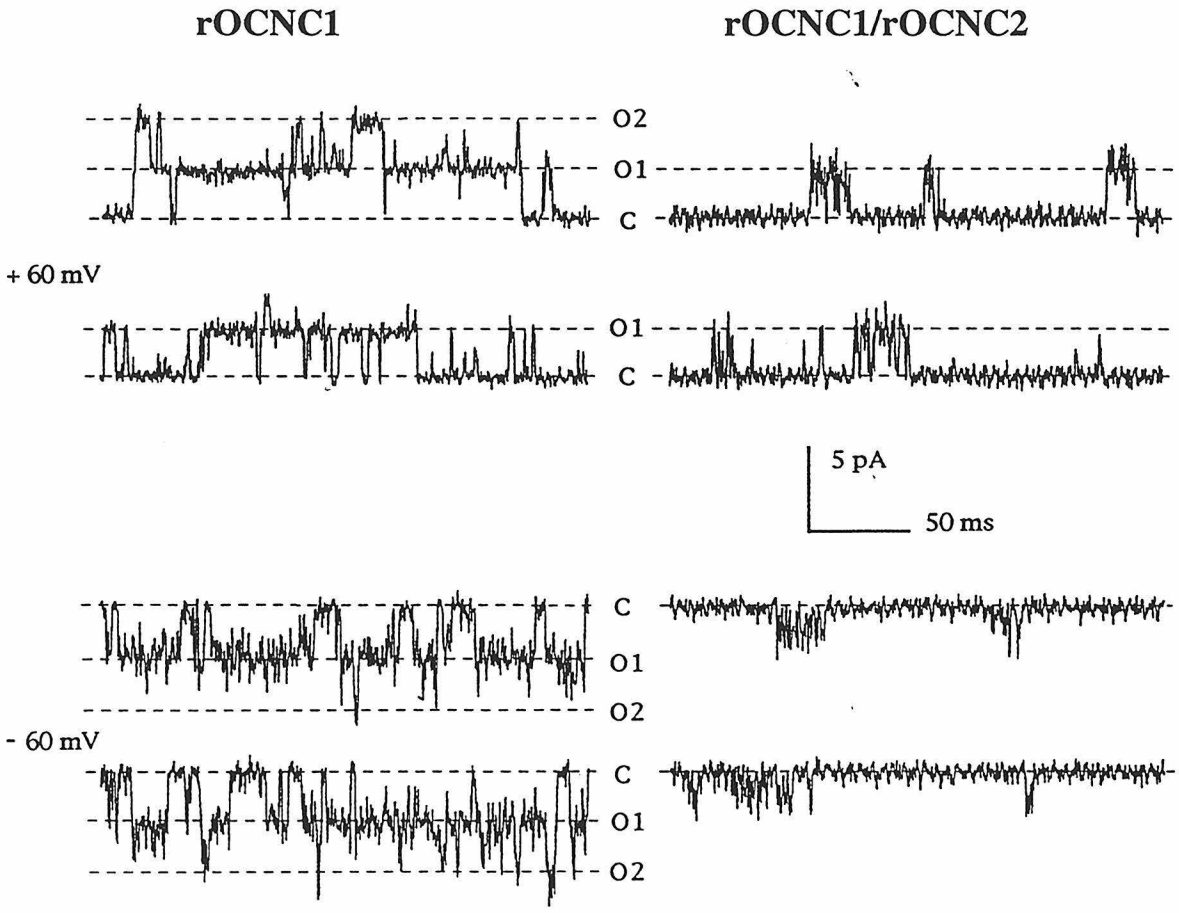
rOCNC1
rOCNC1/rOCNC2
O2
O1
C
+ 60 mV
O1
C
5 pA
50 ms
C
O1
O2
- 60 mV
C
O1
O2

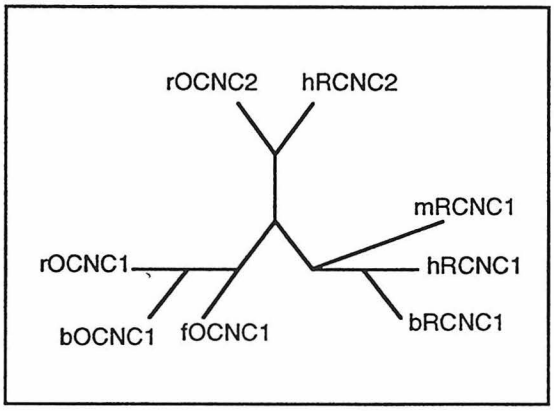
rOCNC2
hRCNC2
mRCNC1
rOCNC1
hRCNC1
bOCNC1
fOCNC1
bRCNC1

Table 2.1

Channel type	V_m§	cAMP		cGMP		EC_{50}(cAMP) /EC_{50}(cGMP)
		EC_{50}(μM)‡	H†	EC_{50}(μM)‡	H†	
rOCNC1	-60 mV	48 ±4.6(n=11)	2.8 ±0.3(n=11)	1.6 ±0.2(n=7)	2.1 ±0.2(n=7)	30
	+60 mV	47 ±3.5(n=11)	2.6 ±0.3(n=11)	1.4 ±0.1(n=7)	2.4 ±0.4(n=7)	34
rOCNC1/rOCNC2	-60 mV	10.8 ± 1.7(n=8)	1.8 ±0.2(n=8)	2.7 ±0.5(n=8)	1.8 ±0.1(n=8)	4.0
	+60 mV	7.3 ±0.8(n=8)	1.9 ±0.1(n=8)	2.9 ±0.4(n=8)	1.6 ±0.1(n=8)	2.5
native channel	+50 mV	2.5	1.8	1.0	1.3	2.5

* All results are given in mean ± s.e.m.
† Hill coefficient (H).
‡ Concentration for half-maximal activation (EC_{50}).
§ Membrane potential (Vm).

Chapter 3. Olfactory cyclic nucleotide-gated channels are expressed in non sensory neurons.

Some of this chapter (cerebellum) was written together with Philippe Ascher at the École Normale Supérieure, Paris France.

Immunohistochemistry and Western blotting was done in collaboration with Gabriele Ronnett, Johns Hopkins University, Dept. of Neuroscience, Baltimore MD

Electrophysiology on hippocampal neurons in culture was done in collaboration with Yinong Zhang, Caltech, Division of Biology, Pasadena CA

Abstract

Our RT-PCR and in situ hybridization studies show that rOCNC1 and rOCNC2 olfactory cng channel mRNAs are expressed in the olfactory bulb, cerebellum, cortex and hippocampus. We have used subunit specific antibodies to show localization of the channel proteins in sections from rat brain and in cultured hippocampal neurons. In addition, we have recorded cng channels with high sensitivity to cAMP and cGMP in excised inside out patches from these cultures. This is of interest for hippocampal physiology, because cAMP elevation has been implicated in one mechanism of long-term potentiation (LTP) . Nitric oxide (NO) is thought to be involved in another mechanism of LTP, and cGMP can be elevated in response to the binding of NO to its effector guanylyl cyclase. Thus, the "olfactory" cng channel may be an electrophysiological sensor for cAMP or cGMP elevation, and Ca^{2+} flow through this channel could be a component of synaptic plasticity in the hippocampus.

The identification of the cells in which cGMP is raised during synaptic activity appears particularly important in cerebellum. Here a link appears to exist between NO, cGMP and the process of "long-term depression" (LTD) in which the temporal association of two inputs to the Purkinje neurons (the climbing fibre and the parallel fibre) can lead to a prolonged reduction of the parallel fibre synaptic potential. Cerebellar LTD *in vitro* has been found to be blocked by perfusing the preparation with inhibitors of NOS or with hemoglobin. Daniel *et al.*, Ito and Karachot, and,Shibuki and Okadahave have shown that endogenous NO is released by climbing fiber stimulation, and that exogenous NO paired with parallel fiber activation can produce LTD.

Relevant properties of neuronal cyclic nucleotide-gated channels (cng)

Cng channels were first described in the vertebrate retina, where they mediate visual transduction. In rod photoreceptors a cation conductance activated by guanosine 3',5'-cyclic monophosphate (cGMP) was identified in 1985(Fesenko et al., 1985; Yau and Nakatani, 1985). The "dark current" flows through this cng channel. A similar cGMP gated channel was found in cone photoreceptors (Cobbs et al., 1985; Haynes and Yau, 1985). In rods and cones, light activates a G protein-mediated signaling cascade that leads to activation of a cGMP phosphodiesterase (PDE). The reduced concentration of cGMP resulting from PDE activity closes the cng channels and thereby hyperpolarizes the cell.

The third cng channel expressed in olfactory receptor neurons, responds equally well to two cyclic nucleotides, cGMP (with a much lower EC_{50} than the retinal channel) and adenosine 3',5'-cyclic monophosphate (cAMP)(Nakamura and Gold, 1987). As in the visual system the olfactory cng channel mediates sensory transduction. In the case of olfaction, however, some odorants activate a G protein signaling cascade which stimulates adenylyl cyclase (AC) to produce an increase in cAMP. The rise in cAMP opens the cng channels and initiates depolarization, reviewed in (Reed, 1992). The importance of the olfactory cng channel's high sensitivity to cGMP and the role of cGMP in olfaction are unclear.

cDNA clones encoding the subunits of the three channels have been isolated(Dhallan et al., 1990; Kaupp et al., 1989; Weyand et al., 1994). Analysis of the deduced amino acid sequence indicates that the subunits resemble voltage gated channels with six transmembrane domains, one being a S4 like voltage sensor and a K^+ channel like pore region(Goulding et al., 1993; Heginbotham et al., 1992). An intracellular region with homology to the cyclic nucleotide binding domains of cGMP and cAMP-dependent protein kinases (PKG, PKA) has been identified(Goulding et al., 1995).

The native rod and olfactory cng channels consist of at least two subunits, 1 and 2 (or alpha and beta)(Bradley et al., 1994; Chen et al., 1993; Liman and Buck, 1994). Alpha

subunits can form homooligomeric cng channels. The beta subunits cannot form functional homooligomeric channels, but modify the properties of the alpha subunits. For example, single channel openings become flickery with beta subunit expression. Two alternatively spliced forms of the rod beta exist (Chen, et al., 1993)with the larger of the two, beta-b, mediating a calmodulin effect(Chen et al., 1994). In the case of the olfactory channels it is the alpha subunit that interacts with calmodulin (Chen and Yau, 1994)(see below for discussion of calmodulin). In contrast to the rod beta subunits the olfactory beta has a profound effect on cyclic nucleotide sensitivity, decreasing the EC_{50} for cAMP about 10 fold(Bradley, et al., 1994; Liman and Buck, 1994).

Electrophysiological characterization indicates that the channels do not discriminate between Na^+ and K^+. They are permeant to, but also blocked, by divalent cations. In this respect cng channels resemble both Ca^{2+} channels (which are nonselectively permeable to monovalent cations in the absence of divalent cations, but whose monovalent cation conductance is blocked by divalent cations) and NMDA channels, which are permeable to monovalent cations and Ca^{2+}, but blocked in a voltage dependent manner by Mg^{2+}. In the presence of physiological levels of extracellular monovalent and divalent cations, Ca^{2+} is the preferred ion of olfactory cng channels and carries 70-80% of the inward current, giving these channels a relatively high permeability to calcium (Frings et al., 1995). The permeability to Ca^{2+} is also significant in the visual channels(Frings, et al., 1995).

In both the visual and olfactory receptors the Ca^{2+} component of the inward current functions not to regulate membrane potential per se but as an intracellular second messenger. In the photoreceptors light produces a reduction in cytoplasmic Ca^{2+} concentration which leads to activation of G-CAP, a calcium binding protein that is a positive regulator of guyanylyl cyclase (GC)(Palczewski et al., 1994). Reduced Ca^{2+} also causes deactivation of S-modulin, a Ca^{2+} binding protein that is a positive regulator of cGMP phosphodiesterase (Kawamura and Murakami, 1991).

Light adaptation of the channel itself is also regulated by Ca^{2+}. In this process, the channels' sensitivity to cGMP is regulated by its interaction with Ca^{2+}-calmodulin which, binds the channel and lowers the sensitivity to cGMP by about two fold(Hsu and Molday, 1993). Thus, when the channel closes in response to light the reduced Ca^{2+} concentration will increase sensitivity to cGMP due to a decrease in Ca^{2+}-calmodulin binding to the channel. In the olfactory system, similarly, the olfactory channels sensitivity to cAMP is reduced about two fold in the presence of Ca^{2+} through the action of calmodulin. This effect could be involved in odorant adaptation(Chen and Yau, 1994). Another role for Ca^{2+}, unique to olfactory signal transduction, is to gate an inward Cl^- conductance (Kurahashi and Yau, 1993)which constitutes 80% of the depolarizing current(Lowe and Gold, 1993).

Methods

***In situ* hybridization**

Before acetylation, the sections were digested with proteinase K (50µg/ml) for 5min followed by fixation in 4% paraformaldehyde. Prehybridization was as described (Schaeren-Wiemers and Gerfin-Moser, 1993)except for the addition of 0.1% Triton X-100. Hybridization was at a probe concentration of 600ng/ml in prehybridization solution without Triton at 70°C for 12-15 hours. After hybridization, the sections were equilibrated in 2x SSC and incubated with RNase A (1ng/ml) for 20 min at 37°C, then washed extensively in 2x SSC before a high stringency wash in 0.2x SSC at 70°C. Probes were detected with an antidigoxygenin antibody conjugated to alkaline phosphatase. All solutions used together with antibody contained 0.1% Tween -20. A positive signal is indicated a by colored (purple) enzymatic reaction product of the alkaline phosphatase.

Immunohistochemistry

Immunocytochemistry with olfactory channel antibodies was essentially as described (Dawson et al., 1993). Detection was with an avidin-biotin-peroxidase system (Vector Laboratories) with diaminobenzidine as a chromogen. Immunofluorescence was indirect

epifluorescence. Antibodies were generated against carboxyterminal channel sequences expressed in *E. coli.* as GST fusion proteins.

Hippocampal culture

Embryos were removed from pregnant Wistar rats by standard cesarean section after asphyxiation with CO_2. Hippocampi were dissected out immediately from the embryos and chopped into ~1mm pieces. Following digestion for 15 min at 37°C with 0.25% trypsin and 2μg/ml DNase I the cells were dispersed with gentle trituration and plated on poly-D-lysine/laminin coated coverslips. Cells were cultured in Neurobasal medium at 37°C under 5% CO_2 for between 3 and 10 days. Fixation of the cells with paraformaldehyde was found to greatly reduce morphology while 0°C methanol proved to maintain morphology. Unfortunately methanol fixation is incompatible with the anti-rOCNC1 rabbit antisera and therefore accurate immuno-detection of rOCNC1 was not possible on these cultured neurons. Attempts to use *in situ* hybridization to detect rOCNC1, or rOCNC2 expression in these cultures also failed.

Electrophysiology

For whole-cell patch recordings the pipettes were filled with 140mM CsCl, 5mM EGTA, 0.5mM $CaCl_2$, and 10mM HEPES pH7.2. For the inside-out patch recordings the pipettes were filed with 140mM NaCl , 5mM KCl, 5mM EGTA, and 20mM HEPES. The bath solutions contained 167mM NaCl, 2.4mM KCl, 10mM HEPES, 10 mM glucose, and 1 mM $CaCl_2$, pH 7.2.

Results

The expression of cng channels in the nervous system is not restricted to sensory neurons. Cng channels appear to modulate excitability in vertebrate retinal bipolar(Nawy and Jahr, 1991)and ganglion cells(Ahmad et al., 1994)and in molluscan neurons(Kehoe, 1990; Sudlow and Gillette, 1995).

Expression analysis by RT-PCR

The expression pattern of several cng channel subunits was surveyed using semi-quantitative RT-PCR essentially as described (Bradley, et al., 1994). First strand cDNA was synthesized from various neuronal and non-neuronal rat tissues. The cDNA samples were quantitated for actin content using non-saturating (15 and 20) cycles of PCR with β actin primers. Fig 3.1 shows the result of 30 cycles of PCR using cng channel specific primers directed against sequences in the 3' untranslated regions of rOCNC1 (A), rOCNC2 (B)and, rRCNC1 (D) mRNAs. The reactions in C were amplified with a pair of primers in which one primer corresponds to a sequence located in an intron of rOCNC2 and the other primer is located in a downstream exon. This pair of primers serves as a control for the presence of contaminating genomic DNA and indicates that the products seen by PCR in A, B, and D were amplified from cDNA template. The results show that both rOCNC1 and rOCNC2 channel subunit mRNAs are expressed in the olfactory bulb, cortex, embronic and adult hippocampus, and cerebellum. The retinal rod channel does not appear to be expressed in any tissues other than the eye.

Expression analysis by *in situ* hybridization

To look at channel mRNA expression at the cellular level cryostat sections (20μM thick) from various brain regions of 2-3 month old rats were analyzed by *in situ* hybridization with digoxigenin-UTP labeled antisense riboprobes by modification of the protocol of (Schaeren-Wiemers and Gerfin-Moser, 1993) .

As control for these experiments sections of OE and retina were also hybridized to the same probes. The results confirm the RT-PCR analysis, which indicated that the olfactory cng channels are expressed in the OE (Fig 3.2 A and B) but not in the eye (Fig 3.2 F and G) and vice versa for the retinal rod channel. Interestingly, while the mRNA for the olfactory channels is abundant in the receptor cell bodies but not in the cilia, the opposite is seen for the rod channel mRNA. In this case high levels of rod channel mRNA are seen in

the cilium-like inner segment of the photoreceptors , but not in the cell body in the outer nuclear layer of the retina (Fig 3.2 H).

In the OE, the signal seen with the olfactory channel probes is not non-specific, as shown by the cessation of staining at the border between the sensory and respiratory epithelia (arrow head in A-D). A probe for the olfactory receptor I7 was also used, and showed expression only in a restricted ventral zone of the OE (Fig 3.2 E). As a positive control a probe for mRNA encoding the abundant neuronal protein SCG10 was used in both OE and retina. In the OE, SCG10 mRNA is expressed in the primary sensory neurons (Fig 3.2 D). In contrast, SCG10 mRNA in the retina is not localized to photoreceptors, but is seen in amacrine cells (weakly) and ganglion cells (strongly) (Fig 3.2 I).
When we examined the brain sections, we also observed expression of the olfactory channels, but not the retinal rod channel mRNAs.

In the hippocampus, CA1 and CA3 pyramidal cells and dentate gyral granule cells all express the two subunits of the olfactory channel (Fig 3.3 A and B) but not the rod channel (Fig 3.3 C). Figure 3.4 shows higher power DIC photographs of the expression in the dentate gyrus (left) and at the boundary of the CA1 and CA3 pyramidal cell regions of the hippocampus (right). As judged relative to the SCG10 expression, the olfactory cng channel mRNAs are not expressed in all CA3 pyramidal cells (Fig 3.4 F and G). In the olfactory bulb (Fig 3.5, right) the inhibitory granule cells (g), and periglomerular cells (pg), the excitatory mitral (m) and tufted (t) output cells of the bulb express both olfactory channel subunit mRNAs (Fig 3.5 F and G). Again, mRNA for the rod channel is not detected in the olfactory bulb (Fig 3.5 H,). In the cerebellum, olfactory cng channel mRNA expression (Fig 3.5 A and B) is in Purkinje (p, and arrow head), granule (g), and some interneurons of the molecular layer (in). No signal is observed with the rod channel probe (Fig 3.5 C). The I7 olfactory receptor probe was negative in all brain regions.

Expression analysis by immunocytochemistry

To examine olfactory channel protein expression, we used two antibodies raised against bacterially expressed fusion protein.

The fusion protein for rOCNC1, generated in Gabriele Ronnett's laboratory, spanned from amino acid residues 556-664 (see Figure 2.1) of the channel and was used to raise polyclonal antisera in rabbits. Crude serum was affinity purified against the fusion protein. This antisera reacts strongly to methanol treated and permeablized rOCNC1 transfected 293 cells (Fig 3.6 C and D)

The fusion protein for rOCNC2, generated in our laboratory, spanned from residues 392-575 (see figure 2.1) of the channel and was used to generate monoclonal antibodies (MAbs) in mice. Hybridoma supernatants were screened by dot blot against the GST fusion protein (positively) and against GST protein (negatively). In the dot blot screen no hybridomas were found to react against a rOCNC1 GST fusion protein spanning residues 500-664. Of ~800 hybridomas, 17/18 (1C9, 1H10, 2H11, 3E1, 4B12, 4F8, 4G12, 5A2, 6A4, 6H2, 7B11, 7D5, 7F7, 7G1, 7H2, 7H3, and 8F6) were positive by the above criteria. 8D1 reacted just as well to the GST as to the GST channel fusion and might be against a GST epitope. Five of the 18 positives (2D6, 6H2, 7B11, 7H2, and 8D1) were also strong in a Westen blot against channel fusion protein. Four of these five (2D6, 6H2, 7B11, and 7H2), plus 7D5, were tested by immunofluorescence against 293 cells transiently expressing either rOCNC1 or rOCNC2. Two of the five (7H2 and (7B11, fig 3.6 A and B)) showed very strong reactivity, 6H2 was weak, and, 2D6 and 7H5 didn't react at all with the methanol and permeablized rOCNC2 transfected cells. None of the five reacted with the rOCNC1 transfected cells and all were isotyped to IgG_1. All 18 clones were saved and two (7B11 and 7H2) were subcloned. All subsequent anti rOCNC2 data is with antibody 7B11/2B8. An interesting observation of rOCNC2 expressing 293 cell is that these cells are easily identified because they appear slightly rounded-up or raised relative to untransfected cells.

Gabriele Ronnett's lab used immunoprecipitation (IP) and Western blot analysis to show that the olfactory cng channels are associated with each other in vivo, and, the channel antibodies do not crossreact. Fig 3.7 A shows the results of Western blots of olfactory cilia membranes using the cng channel antibodies (left four panels). rOCNC1 is ~78 kDa (lane 1) and rOCNC2 is ~67 kDa (lane 3), and neither of the antibodies crossreact with a band the size of the other channel. Preincubation of the antisera (+) with cognate fusion protein removes activity (lanes 2 and 3). rOCNC1 antisera was also used to detect the proteins immunoprecipitated with either rOCNC1 or rOCNC2 antisera from the cilia membranes (fig 3.7 A center two panels). rOCNC1 immunoprecipitates itself (lane 5) and that reactivity is competed with rOCNC1 GST-fusion protein (lane 7). rOCNC1 antisera detects a 78kDa protein immunoprecipitated with rOCNC2 antisera (lane 6) that was not detected with the rOCNC2 antisera on the gel (lane3). This implies that rOCNC1 is associated with rOCNC2 and coimmunoprecipitates with rOCNC2. Lane 8 shows that preabsorbtion of rOCNC2 antisera with rOCNC2 GST fusion protein reduces the amount coprecipitated (lane 6). The large band (lanes 5, 6, 7, 8) labeled IgG is heavy chain of the antibody used in the IP detected with the secondary antibody (anti rabbit) used in the western blot. When OCNC2 antisera is used to detect the immunoprecipitated proteins (lanes 9, 10, 11, 12), rOCNC2 is coimmunoprecipitated with OCNC1 antisera (lane 9). As for lanes 7 and 8, preabsorbtion of the immunoprecipitating antisera removes the reactivity of the OCNC2 antisera (lanes 11 and 12).

Both olfactory channels subunits can be immunoprecipated from lysates of adult hippocampi (100μg) (Fig 3.7 B).

The channel protein expression pattern as revealed by antibody staining of brain sections (Fig 3.8) correlates with the mRNA expression pattern seen by *in situ* hybridization. Under our fixation conditions (4% paraformaldehyde) the two subunits of the olfactory cng channel show an overlapping pattern of localization, but each has distinct features. rOCNC2 localization is most prominent on cell bodies with little signal on the

processes of the neurons (see Fig 3.8, higher power photographs of the cortex and cerebellum). In contrast, rOCNC1 is localized both to the cell bodies and the neuronal processes. In particular rOCNC1 appears to be localized to the dendrites of the pyramidal cells located in the CA3 and CA1 regions of the hippocampus (Fig 3.8, C and E respectively). In the cerebellum, channel protein is most abundant in the Purkinje cells, (arrow head). Lower levels of the olfactory cng channels are seen in the granule cells and in some isolated cells in the molecular layer.

Hippocampal cell culture

Expression analysis, immunofluorescence

In order to develop a system in which functional channel expression in brain neurons could be studied, cultured embryonic (E17) hippocampal neurons were examined by immunofluorescence with the anti-rOCNC2 MAb. Staining with the 7B11/2B8 anti-rOCNC2 MAb is observed in methanol fixed neurons (Fig 3.9 A and B). rOCNC2 protein is localized to the processes of a limited number of cells. There was a window of time after plating in which the strongest signal could be obtained. This was usually between one and three days after plating. In general the longer the cells were in culture the fewer processes expressed rOCNC2.

To phenotypically characterize the cells and processes that express rOCNC2, several other MAbs were also used for immunofluorescence. These were, HM-2 (Sigma) which recognizes the dendritic protein MAP-2 (Fig 3.10 A and B), SDL.3D10 (Sigma) that recognizes the more general microtubule associated protein, β tubulin type III (Fig 3.10 C and D), and G-A-5 (Sigma) against the glial marker, glial acidic fibrillary protein (GFAP). The GFAP antibody was used on coverslips that had been first developed for SCG10 mRNA expression by *in situ* hybridization (Fig 3.9 C and D). Comparison of the rOCNC2, tubulin III, and MAP2 localization indicates that rOCNC2 is expressed on the smallest subset of processes in the culture. MAP-2 is expressed on a larger subset of processes, and tubulin III on the largest set. The arrow heads in the MAP-2 figure indicate processes that

fail to stain with this marker. In the tubulin III figure the arrowheads indicate the abundance of staining with this marker. The thicker morphology of the of the rOCNC2 positive processes proximal to the cell body is consistent with the appearance of the processes stained for the dendritic marker MAP-2. The tubulin III positive processes show less of a bias and are both thick and thin, consistent with this microtubule associated protein being expressed more generally. Double labeling with the two antibodies, rOCNC2 and MAP-2, was not done for technical reasons. Fig 3.9 C and D illustrates morphologically that the processes that have MAP-2 and rOCNC2 are from cells that are like those which express the neuronal marker SCG10 mRNA, and that those same cells do not express the glial marker GFAP. The arrow head in this figure indicates the flat morphology of the GFAP positive cell. This is consistent with the idea that rOCNC2 is on neuronal processes. I haven't tested this yet by doing the same experiment with the 7B11/2B8 antibody in place of the GFAP. Several preparations of embryonic hippocampal cells were tested with a monoclonal antibody (PMc 1D1) (Molday et al., 1991)that recognizes the rat retinal rod cng channel, but no signal was ever seen.

The observation that rOCNC2 is localized to processes in culture is at odds with the immunohistochemistry shown in Fig 3.8 D and F. This could be explained by the difference between the embryonic origin (E17) of the cultured cells and the "adult" (P60-90) origin of the sections used for the immunohistochemistry. This could suggest for some sort of dynamic or developmental role for rOCNC2 which could directly be examined by using embryonic tissue for immunohistochemistry. In fact, when the olfactory epithelium of the adult rat is lesioned, inducing dramatic new receptor cell growth, there is a concomitant up regulation of rOCNC2 expression as visualized immunohistochemically consistent with a dynamic role for the rOCNC2 subunit (Gabriele Ronnett, personal communication).

Hippocampal cell culture

Expression analysis, electrophysiology (Yinong Zhang)

Having established that the cultured hippocampal neurons expressed a channel protein, we examined functional expression of the cng channels by electrophysiology. Neuronal expression of the channel was examined after 24-36 hours in culture by recording either in whole-cell configuration or from excised inside-out patches. Figure 3.11 A shows whole cell recording using a pipette backfilled with 100μM cAMP (left) from one cell or cGMP (right) from another cell. The voltage was ramped from -120mV to +40mV in 20mV steps lasting 150ms. The upper set of traces is the current immediately after rupture of the patch. The lower trace was taken four minutes after patch rupture and diffusion of the cyclic nucleotide into the cell. Both cells respond to cyclic nucleotide and the whole cell currents show slight outward rectification. The difference in amplitude of the current likely reflects differences in the number of channels on the surface of these two cells. The whole cell current response to cyclic nucleotide was recorded from greater than 90% of the neurons, and was blocked by 10mM Mg^{2+}.

Figure 3.11 B shows an example of single channel openings of cng gated channels in an excised inside-out patch from a cultured hippocampal neuron that was first perfused with 10μM cAMP followed by 10μM cGMP. These recording were also done in divalent cation free solutions. In contrast to the whole cell recording the frequency of obtaining a patch with analyzable cng channel activity was very low. Of 632 successful patches 17 showed long lasting cng channel activity with no "run down". About 10% of the total patches had cng currents that showed quick "run down", generally within seconds. The fact that the channels can be opened by micromolar concentrations cAMP suggests that these channels resemble olfactory cng channels. The hippocampal cng channel is sensitive to 10μM cAMP, suggesting that this channel could be a heterooligomer of the two olfactory cng channel subunits (Bradley, et al., 1994; Liman and Buck, 1994). Because the density

of open channels in the patch was so low attempts to construct dose-response profiles for cGMP and cAMP were unsuccessful.

The single channel records resemble those of the native olfactory cng channels in several other ways. Figure 3.11 C summarizes the single channel properties of the hippocampal cng channels. Their flickery open behavior (Fig. 3.11 C expanded trace) at both positive and negative membrane potentials is a characteristic of the cng channels and in particular of heterooligomeric cng channels composed of two homologous subunits thought to represent the native channels in vertebrate retinal photoreceptors (Chen, et al., 1993) and vertebrate ORNs (Bradley, et al., 1994; Liman and Buck, 1994). Retinal rod and cone cng channels are refractory to 1mM cAMP(Kaupp, et al., 1989; Weyand, et al., 1994). Analysis of single channel activity by amplitude histogram (Fig. 3.11 C) indicates that the hippocampal cng channel is outwardly rectifying under these conditions. This is consistent with what is observed for the native olfactory cng channel(Nakamura and Gold, 1987) and the heterologously coexpressed rOCNC1 and rOCNC2 subunits(Bradley, et al., 1994; Liman and Buck, 1994). At +80mV the estimated single channel conductance is 31±3.2pS, and at -80mV the single channel conductance drops to 15.2±2.7pS. There are no published reports of the single channel conductance of the native rat olfactory cng channel.

Ni^{2+}, which has a differential effect on olfactory and rod cng channels was used to further characterize the cng channels in the hippocampal neurons. Addition of Ni^{2+} ions to either cGMP or cAMP increases the open probability of the native rod cng channel from vesicles of bovine rod outer segment membranes incorporated into planar lipid bilayers, effectively increasing the channels' affinity for cyclic nucleotide(Ildefonse et al., 1992). When bRCNC1 is expressed in *Xenopus* oocytes the apparent affinity for cyclic nucleotide increases by ~10 fold for cGMP and ~3 fold for cAMP. A histidine (H420) residue likely mediating the potentiating effect of Ni^{2+} on the bovine rod channel has been identified. This residue is absent from the olfactory channel sequence.

Ni^{2+} has a completely different effect on the olfactory channel. Instead of the potentiating effect seen with the rod channel, Ni^{2+} produces a small reduction in the olfactory (rOCNC1) channels' response, decreasing both the maximum current and the apparent affinity for cyclic nucleotides. This effect is most pronounced at low concentrations (<20μM) of cGMP. The apparent shift in $K_{1/2}$ for cGMP was from 2.3 ± 0.8μM (n=13) to 6.0 ±1.5μM (n=7). Ni^{2+} exerts its effect by binding preferentially to the closed configuration of the channel, thereby destabilizing the opening conformational change. This inhibition has been localized to a single histidine (H396) in rOCNC1 following the last transmembrane segment, suggesting a role for this region in channel gating(Gordon and Zagotta, 1995a). One caveat to keep in mind for our use of Ni^{2+} is: At the corresponding position rOCNC2 has a lysine residue (K288), suggesting that it might not bind at this site. Thus Ni^{2+} might not block the heterooligomeric olfactory channel.

Figure 3.11 D shows the results of testing Ni^{2+} on the hippocampal cng channels and heteromeric olfactory cng channels expressed in a HEK293 cell line. On the left is one example (n=3) of the single channel record during perfusion of 10μM cAMP or 10μM cAMP plus 10μM Ni^{2+} onto the hippocampal cng channel. Time constants of the open time distributions with or without Ni^{2+} are about the same. Indicating that Ni^{2+} has almost no effect on the open probability of the hippocampal cng channel. A very slight effect is seen on the heteromeric olfactory channel expressed in 293 cells. The effective $K_{1/2}$ values for cAMP were 8.96±1.10μM without Ni^{2+} and 14.49±2.21μM with Ni^{2+}. The change in effective $K_{1/2}$ values for cGMP were less, 3.31±0.36μM without Ni^{2+} and 4.19±0.21μM with Ni^{2+}. Together these data argue in favor of the presence of heteromeric olfactory cng channels in the hippocampus and against the presence of the rod cng channel which would have shown an increase in sensitivity to cyclic nucleotide.

Interestingly, the bovine cone cng channel (bCCNC1) (Weyand, et al., 1994)would be predicted not to be blocked by Ni^{2+} (bCCNG1 has Q441 at the blocking site, equivalent to H396 in rOCNC1). The bCCNC1 would also be predicted not to be potentiated by Ni^{2+}

either, as it has a Q at position 444, which is equivalent to the H420 in bRCNC1. It is thus possible that cone channel could be a component of the hippocampal cng channel. This is unlikely, however, given its high sensitivity to cAMP.

Searching for new cng channels in the CNS

To examine whether novel cng channels are expressed in the hippocampus, PCR was done using the degenerate primers against the cyclic nucleotide binding domain described in chapter 2 and with hippocampal cDNA. The expected size product (123bp) was cloned and sequenced. Of the 15 clones sequenced, two were rOCNC1, one was rOCNC2 and a fourth (#14) was much like a cng channel that is expressed in bovine retinal cone photoreceptors and sperm(Weyand, et al., 1994). There were some differences between the rat hippocampal sequence and the bovine sperm/cone sequence (11/78 nucleotides and two amino acids, not including the primer sequence) but these could just be species specific differences in the same gene in a region already known to be very homologous between different cng channels. In the absence of a long enough specific sequence for generation of a probe for *in situ* hybridization, further investigation to validate the expression of the cone channel in the hippocampus could take advantage of the anti cone channel antibody(Weyand, et al., 1994). The expression of the cone channel would be significant because of the three cng channels examined for Ca^{2+} permeability and fractional Ca^{2+} current ($[Ca2+]_o$ of 0.3mM) the cone channel was 1.5 fold greater than the olfactory channel in both categories. In this assay the olfactory channel was 3 fold more permeable to Ca^{2+} than the rod and had 15 fold more fractional Ca^{2+} conductance than the rod channel(Frings, et al., 1995). On the other hand the cone channel is less sensitive to Mg^{2+} block, complete block of the cng current with 10 μM $[Mg^{2+}]_o$ could not be accomplished with the cone channel.

Discussion

Possible functional significance of cng channel expression in nonsensory neurons.

The function of cng channels in nonsensory neurons would be to control ionic fluxes in response to a synaptic stimulation capable of producing variations in the intracellular level of cyclic nucleotides. This appears well established in the case of bipolar retinal cells, in which glutamate released by the presynaptic cell is assumed to activate a receptor coupled to cGMP hydrolysis(Nawy and Jahr, 1991; Shiells and Falk, 1992). In the case of Aplysia neurons, Kehoe(Kehoe, 1990) has found a presynaptic neuron which appears capable of producing a slow depolarizing synaptic potential by raising cAMP in the post-synaptic cell. A last example is that of the retinal ganglion cells, in which there is evidence that nitric oxide (NO) can activate a cGMP sensitive conductance, probably by raising the cGMP level(Ahmad, et al., 1994). In order to establish the functional significance of cng channels in the brain, one will need to identify the pathways which are capable of modifying the intracellular concentration of either cAMP or cGMP in these cells.

Two of the brain regions (hippocampus and cerebellum) that show cng channel expression are extensively studied by electrophysiology as slices. This area of research is far from my training but one I plan to pursue in postgraduate work. The following is a basic outline of the studies conducted in these two brain regions and my plans to further examine the significance of cng channel expression in the CNS, in particular in the cerebellum.

Hippocampus

Long term potentiation (LTP) is a ubiquitous form of use-dependent synaptic plasticity that occurs at most excitatory synapses in the central nervous system (CNS). In the mammalian hippocampus, LTP is studied as a model of use-dependent synaptic strengthening that is assumed to be a physiological mechanism of information storage. Synaptic strengthening means that on average the size of the excitatory post synaptic current (EPSC) increases. LTP can persist from hours to weeks.

At the synaptic level, there are two well studied pathways in the hippocampus. The first involves the axons of the CA3 pyramidal cells (Schaffer collaterals) which synapse on dendrites of the pyramidal cells in the CA1 region. The second well studied pathway is between axons of the granule cells in the dentate gyrus (mossy fibers) and the dendrites of pyramidal cells in the CA3 region. Both synaptic pathways undergo LTP which is recorded as an increase in excitatory PSPs (EPSPs). LTP in postsynaptic CA3 or CA1 cells is induced by a brief, high frequency field stimulation (tetanus) of the afferents, mossy fibers or Schaffer collaterals respectively. Although both synapses can undergo LTP they have different properties and likely occur by different mechanisms.

The model for the induction of LTP in CA1 requires the coincident occurrence of activation of postsynaptic *N*-methyl-D-aspartate (NMDA) type glutamate receptor channels by presynaptically released glutamate and postsynaptic depolarization. Studies have shown that hyperpolarization of the postsynaptic cell blocks the induction of LTP. Further, depolarization of the of the postsynaptic cell by injection of current induces LTP when paired with weak presynaptic input.

In CA1 the initial depolarization is produced by current flow through nonNMDA type glutamate receptors known as AMPA type receptors. Depolarization is required to relieve an extracellular voltage dependent block by Mg^{2+} of the NMDA receptor channel and allow Ca^{2+} entry. Ca^{2+} appears to act as a trigger for LTP. LTP is blocked by postsynaptic Ca^{2+} chelators or by the selective NMDA receptor antagonist D-2-amino-5-phosphonovalerate (APV). Perfusion of APV during the tetanus blocks LTP, but APV has no effect after LTP has been established. Therefore APV blocks the induction of LTP, which requires Ca^{2+} influx, not the expression of LTP, for review see (Siegelbaum and Kandel, 1991).

The mechanism of action of postsynaptic Ca^{2+} in triggering LTP is poorly understood. Mechanistically the two basic questions being asked are 1) is the EPSC larger because the postsynaptic cell has become more responsive to transmitter release (a

postsynaptic change) and/or 2) has the presynaptic cell been influenced to release more transmitter.

Evidence exists for postsynaptic Ca^{2+} having many effects in CA1 pyramidal cells. These include activation of Ca^{2+}/calmodulin-dependent protein kinase II (CaMKII) which itself has many effects including activation of adenylyl cyclase types 1 and 8 (ACI, AC8) and, most recently, a role in recruitment of new postsynaptic AMPA receptors . A clear role has been established for an increase in cAMP leading to activation of protein kinase A (PKA) during LTP in CA1. It is generally thought that PKA in turn influences gene expression through the activation of transcription factors promoting what is termed the late phase of LTP that is sensitive to protein synthesis inhibitors (for review see (Bilss and Collingridge, 1993)).

The activation of adenylyl cyclase during LTP has obvious implications for a cng channel like the olfactory channel, if it is localized postsynaptically. The cng channel could behave as a postsynaptic Ca^{2+} channel sensitive to extracellular Mg^{2+} block and therefore sensitive to the membrane potential of the cell. Coincident with its sensitivity to membrane potential the channel requires an intracellular increase in cAMP to open (Fig 3.12 A).

A mechanism of LTP with presynaptic expression involves some sort of retrogade message from the postsynaptic cell to the presynaptic cell. One example proposes that the signal is the short lived, diffusible gas, nitric oxide (NO). In this scenario, Ca^{2+} entering through the NMDA receptor activates postsynaptically localized nitric oxide synthetase (NOS). NO diffuses to the presynaptic cell and activates heme containing enzymes. In the context of the cng channels, the heme containing enzyme soluble guanylyl cyclase which could be an effector of NO. Presynaptic cng channels, if present, might open in response to increased cGMP concentration, providing an inducible Ca^{2+} conductance that is blocked by extracellular block by Mg^{2+} (Fig 3.12 B).

A mechanism such as this could explain the lack of an effect seen on paired pulse facilitation (PPF) by LTP. PPF occurs when two presynaptic stimuli are delivered within

50-200ms and is seen as an increase in the postsynaptic signal from the second pulse relative to the first. This is thought to result from residual Ca2+ from the first stimulus enhancing the release during the second stimulus. Manipulations known to increase transmitter release cause a decrease in PPF. This could be because release during the first stimulus was close to saturation, so that the second stimulus cannot efficiently produce vesicle fusion.

LTP in CA1 doesn't effect PPF, and this has been used as evidence against a presynaptic change during LTP. Arguments against this conclusion are that release by facilitation and release by LTP are two differently regulated exocytotic pathways. Or that they act on two different types of synapses, one responsive to PPF types of stimulation and the other responsive to influences of LTP. Both of these arguments have been used to support the hypothesis of "silent synapses", which has been invoked to explain the results from quantal analysis that support a presynaptic site of expression for LTP. Quantal analysis measures a coefficient of variation of the postsynaptic signal, or end plate potentials (EPPs) due to spontaneous presynaptic release of transmitter. These spontaneous releases are so small and quantized that they are considered to be a result of individual vesicle releases from the presynaptic cell and are recorded as mini EPPs (mEPPs). Because mEPPs are a result of spontaneous release their analysis is based on probabilistic models. Therefore a change in the baseline state of mEPPs, quantitated by amplitude histogram, is considered a change in release probability and would argue for a presynaptic change. This is what is observed after LTP by quantal analysis.

To reconcile these two conflicting observations, a model has been proposed in which LTP occurs because the postsynaptic cell changes the configuration of the glutamate receptors such that synapses that were refractile to glutamate before LTP become sensitive to glutamate by insertion of AMPA receptors into the membrane. This is the unmasking of "silent synapses". This explanation would account for the lack of change in PPF, the decrease in failures, and increase in quantal content during LTP (Edwards, 1995).

Activation of CaMKII has been implicated in this step of unmasking of "silent synapses". The hippocampal cng channels could function here to potentiate Ca^{2+} influx via cAMP production known to occur for postsynaptic PKA activation.

LTP at Schaffer collateral synapses in CA1 has Hebbian characteristics, requiring coincident activity in the dendrite of the postsynaptic pyramidal neuron and the presynaptic axon. A second feature of CA1 LTP related to its Hebbian character is that when a weak stimulus, insufficient on its own to induce LTP, is paired temporally with a separate strong stimulus capable of inducing LTP the weak pathway becomes potentiated. This property is referred to as associativity. The NO pathway described above could be invoked to explain the associativity seen in CA1. Here NO would diffuse not only to the presynaptic cell but to neighboring cells and potentiate their weak response. This could be through the production of cGMP and activation of the hippocampal cng channels in the weakly activated cell.

LTP in the CA3/mossy fiber pathway is different from LTP in the CA1/Schaffer collateral pathway in several fundamental ways. Mossy fiber LTP is NMDA receptor independent, there is no effect of APV on mossy fiber LTP . There also appears to be no role for postsynaptic Ca^{2+} as determined by intracellular application of BAPTA to the postsynaptic CA3 cell. Zalutsky and Nicoll (Zalutsky and Nicoll, 1990) show that paired pulse-facilitation during mossy fiber LTP is reduced. This suggests that there is an increase in release probability during mossy fiber LTP(Weisskopf and Nicoll, 1995). It has also been shown that intracellular manipulation of postsynaptic membrane potential fails to reveal any postsynaptic dependence of LTP induction in the mossy fiber pathway. These results suggest a presynaptic site for increased expression of synaptic strength in mossy fiber LTP and argue that mossy fiber LTP is a presynaptic phenomenon(Zalutsky and Nicoll, 1990).

How is it that high frequency stimulation of the mossy fibers leads to a persistent increase in the strength of synaptic transmission? Mossy fiber LTP is blocked by removal

of extracellular Ca^{2+}, preventing Ca2+ influx into the presynaptic cell. Activators of adenylyl cyclase like forskolin, or membrane permeable analogues of cAMP cause presynaptic enhancement of mossy fiber responses and occlude mossy fiber LTP. The action of forskolin is also reduced after LTP induction, and forskolin reduces PPF. This argues that forskolin (cAMP) and mossy fiber LTP interact with one another and suggest they share a common process that is expressed presynaptically. Using membrane permeable blockers of the catalytic site of PKA (H-89 and KT 5720) to block mossy fiber LTP, it was argued that cascades to produce cAMP and LTP converge at PKA activation.

A direct model has been proposed to account for these observations. Adenylyl cyclase type I (AC I), a form of AC that has been implicated in learning and memory and is activated by Ca2+/calmodulin, is highly expressed in dentate granule cells. The model relies on a tetanus-induced rise in Ca^{2+} concentration leading to stimulation of AC I by Ca2+/calmodulin to promote activation of PKA. It is unknown how PKA activation causes an enhancement of transmitter release. An alternative model, incorporating presynaptic cng channels, would be that the presynaptic increase in cAMP could open the cng channel, potentiating Ca2+ influx and enhancing transmitter release.

Cerebellum

Among the pathways which may induce changes in cAMP levels in the cerebellum, the two most obvious are the noradrenergic and the serotoninergic projections to the cerebellar cortex.

The noradrenergic innervation arises from the locus coeruleus (see (Olson, 1971; Ungerstedt, 1971) (Pickel, 1972) . It is a "diffuse" pathway distributing its axons very widely in the cerebellar cortex. Application of norepinephrine (NE) onto cerebellar neurons produces mainly inhibitory effects, through a potentiation of GABA-A currents in isolated Purkinje cells (Cheun, 1992) and in slices through an increase of the frequency of the inhibitory synaptic potentials (mediated by GABA) in the Purkinje cells as well as in

stellate and basket cells (see (Llano and Gerschenfeld, 1993). There is evidence that both effects involve β-receptors (Sessler et al., 1989) (Cheun, 1992) (Llano and Gerschenfeld, 1993). Activation of these receptors is classically coupled to an increase of cAMP synthesis, and indeed the effects of norepinephrine are mimicked by 8-bromo-cAMP and by forskolin (Cheun, 1992) (Hoffer et al., 1971) (Llano and Gerschenfeld, 1993). Since there is no evidence that the activation of β receptors and the resulting increase in cAMP are followed by an activation of PKA, the possibility exists that cAMP would act directly on cng channels.

The serotoninergic innervation of the cerebellar cortex appears to originate mainly in the raphe nucleus (Hökfelt and Fuxe, 1969). As in the case of the noradrenergic pathway, it leads to a "diffuse" innervation. The 5HT receptors appear to be of multiple types (see (Lucas and Hen, 1995). The functional effects of serotonin in the cerebellum have not been characterized in great detail at the single cell level. Strahlendorf *et al.* (1987)(Strahlendorf et al., 1987) among others, have described complex effects, both inhibitory and excitatory, both pre and postsynaptic. In the Laboratoire de Neurobiologie at the École Normale Supérieure, Stéphane Dieudonné (unpublished) has observed that serotonin increases the frequency of inhibitory synaptic currents recorded in Golgi cells, suggesting that, to a first approximation, the effect of 5HT is inverse from the effects of noradrenaline mentioned above.

Other possible inputs which could modulate intracellular levels of cAMP include a dopaminergic innervation (Simon et al., 1979), peptidergic inputs (Bishop and Kerr, 1992), and finally the glutamatergic fibers of the cerebellum. Glutamate, through metabotropic receptors coupled to G proteins, has been found to inhibit cAMP production in a certain number of cases, and in particular in cerebellum granule cells (Prézeau, 1994). In other cells the same metabotropic receptors have been found to potentiate the cAMP production triggered by norepinephrine (Winder and Conn, 1995). Vranesic *et al.* (Vranesic, 1993) have reported that activation of metabotropic glutamate receptors in rat Purkinje cells

produces an outward current which is potentiated by inhibitors of phosphodiesterases, and which seems to be generated by the inhibition of an inward current tonically active at rest.

In contrast to cAMP, for which there is only suggestive evidence of functional changes, cGMP levels are known to be dramatically increased by a variety of manipulations in which an increase of intracellular Ca^{2+} activates nitric oxide synthase (NOS) to produce NO which in turn activates guanylyl cyclase. This pattern can be triggered by a number of depolarizing stimuli, among which the most prominent, and the most effective, are those which produce the opening of NMDA channels (Garthwaite, 1991; Garthwaite and Boulton, 1995).

If one attempts to identify the cells in which the increase in cGMP occurs, one encounters the caveat which has often been underlined by the group of John Garthwaite, namely that the cells in which NO is produced are not necessarily the cells in which the rise of cGMP occurs. Thus, in the case of stimulation of NMDA receptors by glutamate, it is known that NMDA receptors are present in granule cells and in inhibitory interneurons; granule cells are also the cells in which one finds the largest amount of NO synthase. In contrast, both NMDA receptors and NOS seem absent (at least in the adult) in Purkinje neurons and in glial cells (astrocytes of the granular layer; Bergmann glial cells), in which major rises in cGMP have been detected(DeVente, 1990).

The identification of the cells in which cGMP is raised during synaptic activity appears particularly important in view of the link which appears to exist between NO, cGMP and the process of "long-term depression" (LTD) in which the temporal association of two inputs to the Purkinje neurons (the climbing fibre and the parallel fibre) can lead to a prolonged reduction of the parallel fibre synaptic potential. Cerebellar LTD *in vitro* has been found to be blocked by perfusing the preparation with inhibitors of NOS or with hemoglobin (Crepel, 1990). Daniel *et al.*(Daniel, 1993); Ito and Karachot,(Ito and Karachot, 1990) and, Shibuki and Okada(Shibuki and Okada, 1991) have shown that

endogenous NO is released by climbing fiber stimulation, and that exogenous NO, paired with parallel fiber activation, can produce LTD.

In conclusion, there exist in the brain a number of cells in which synaptic inputs can be expected to modulate the intracellular levels of cAMP and/or cGMP, and therefore the opening of cng channels, if these are present. It is worth mentioning that in the facial motorneurons, where olfactory cng channel expression has been detected by immunocytochemistry and *in situ* hybridization (Bradley, manuscript in preparation) , the group of M. Raggenbass has observed a current induced by vasopressin which has the expected properties of a cng induced current in its voltage dependence and sensitivity to divalent cations(Alberi, 1993; Widmer et al., 1992).

The cng channels gating by ligands, Ca^{2+} permeability, voltage dependent divalent block, and heterooligomeric-nature are similar to those of another well studied channel implicated in synaptic plasticity, the NMDA receptor channel. The main difference is the site of agonist binding, cng channels being gated by an intracellular second messenger and the NMDA receptor gated by an extracellular neurotransmitter. It is tempting to consider that the analogy between the two channels could correspond to a functional analogy, and that, in particular, the cng channel would open when activation by cyclic nucleotides is associated with depolarization to increase intracellular Ca^{2+} concentration. One could then consider a next step, which would be to probe the functional role of the cng channels and the possibility that, like NMDA, they could behave as coincidence detectors, opening only when agonist binding and depolarization occur synchronously.

References

I. Ahmad, T. Leinders-Zufall, J. D. Kocsis, G. M. Shepherd, F. Zufall and C. J. Barnstable (1994). Retinal ganglion cells express a cGMP-gated cation conductance activatable by nitric oxide donors. Neuron *12*, 155-165.

S. Alberi Dubois-Dauphin ,M., Dreifuss, J.J., Raggenbass, M. (1993). Modulation by divalent cations of the current generated by vasopressin in facial motoneurons. Brain Research *624*, 326-330.

T. T. P. Bilss and G. L. Collingridge (1993). A synaptic model of memory: Long-term potentiation in the hippocampus. Nature *361*, 31-38.

G. A. Bishop and C. W. Kerr (1992). The physiological effects of peptides and serotonin on Purkinje cell activity. Progress in Neurobiology *39*, 475-492.

J. Bradley Zhang, Y., Bakin R., Matsuzaki O., Ronnett G., and Zinn, K. (manuscript in preparation). Expression and functional identification of "olfactory" cyclic nucleotide-gated channels in the brain.

J. Bradley, J. Li, N. Davidson, H. A. Lester and K. Zinn (1994). Heteromeric olfactory cyclic nucleotide-gated channels: A subunit that confers increased sensitivity to cAMP. Proc. Natl. Acad. Sci. USA *91*, 8890-8894.

T.-Y. Chen, M. Illing, L. L. Molday, Y.-T. Hsu, K.-Y. Yau and R. S. Molday (1994). Subunit 2 (or beta) of retinal rod cGMP-gated cation channel is a component of the 240-kDa channel-associated protein and mediates Ca^{2+}- calmodulin modulation. PNAS *91*, 11757-11761.

T.-Y. Chen, Y.-W. Peng, R. S. Dhallan, B. Ahamed, R. R. Reed and K.-W. Yau (1993). A new subunit of the cyclic nucleotide-gated cation channel in retinal rods. Nature *362*, 764-767.

T.-Y. Chen and K.-W. Yau (1994). Direct modulation by Ca^{2+}-calmodulin of cyclic nucleotide-activated channel of rat olfactory receptor neurons. Nature *368*, 545-548.

J. E. Cheun Yeh, H.H. (1992). Modulation of $GABA_A$ receptor-activated current by norepinephrine in cerebellar Purkinje cells. Neuroscience *51*, 951-960.

W. H. Cobbs, A. E. Barkdoll and E. N. Pugh (1985). Cyclic-GMP increases photocurrent and light sensitivity of retinal cones. Nature *317*, 64-66.

F. Crepel Jaillard, D. (1990). Protein kinases, nitric oxide and long-term depression of synapses in the cerebellum. NeuroReport *1*, 133-136.

H. Daniel Hemart, N., Jaillard, D., Crepel, F. (1993). Long -term depression requires nitric oxide and guanosine 3',5' cyclic monophosphate in rat cerebellar Purkinje cells. Eur. J. Neurosci. *5*, 1079-1082.

T. M. Dawson, J. L. Arriza, D. E. Jaworsky, F. F. Borisy, H. Attramadal, R. J. Lefkowitz and G. V. Ronnet (1993). Beta-adrenergic-receptor kinase-2 and beta-arrestin-2 as mediators of odorant-induced desensitization. Science *259*, 825-829.

J. DeVente Bol, J. G. J. M., Berkelmans, J., Schipper, J., Steinbusch, H. M. W. (1990). Immunocytochemistry of cGMP in the cerebellum of the immature, adult, and aged rat:

the involvement of nitric oxide. A micropharmacological study. Eur. J. of Neurosci. *2*, 845-862.

R. S. Dhallan, K.-W. Yau, K. A. Schrader and R. R. Reed (1990). Primary structure and functional expression of a cyclic nucleotide-activated channel from olfactory neurons. Nature *347*, 184-187.

F. Edwards (1995). LTP: A structural model to explain the inconsistances. Trends Neurosci. *18*, 250-255.

E. E. Fesenko, S. S. Koleniskov and A. L. Lyubarsky (1985). Induction by cGMP of cationic conductance in plasma membrane of retinal rod outer segment. Nature *313*, 310-313.

S. Frings, R. Seifert, M. Godde and U. P. Kaupp (1995). Profoundly different calcium permeation and blockage determine the specific function of distinct cyclic nucleotide-gated channels. Neuron *15*, 169-179.

J. Garthwaite (1991). Glutamate, nitric oxide and cell-cell signalling in the nervous system. TINS *14*, 60-67.

J. Garthwaite and C. L. Boulton (1995). Nitric oxide signaling in the central nervous system. Annu. Rev. Physiol *57*, 683-706.

S. E. Gordon and W. N. Zagotta (1995a). A histidine residue associated with the gate of the cyclic nucleotide-activated channels in rod photoreceptors. Neuron *14*, 177-183.

E. H. Goulding, G. R. Tibbs, D. Liu and S. A. Siegelbaum (1993). Role of H5 domain in determining pore diameter and ion permeation through cyclic nucleotide-gated channels. Nature *364*, 61-64.

E. H. Goulding, G. R. Tibbs and S. S.A. (1995). Molecular mechanism of cyclic-nucleotide-gated channel activation. Nature *372*, 369-374.

L. W. Haynes and K. W. Yau (1985). Cyclic GMP-sensitive conductance in outer segment membrane of catfish cones. Nature *317*, 61-64.

L. Heginbotham, T. Abramson and R. MacKinnon (1992). A functional connection between the pores of distantly related ion channels as revealed by mutant K+ channels. Science *258*, 1152-1155.

B. J. Hoffer, G. E. Siggins and F. E. Bloom (1971). Studies on norepinephrine-containing afferents to Purkinje cells of rat cerebellum. II. Sensitivity of Purkinje cells to norepinephrine and related substances administered by iontophoresis. Brain Research *25*, 523-534.

T. Hökfelt and K. Fuxe (1969). Cerebellar monoamine nerve terminals, a new type of afferent fibers to the cortex cerebelli. Exp. Brain Res. *9*, 63-72.

Y.-T. Hsu and R. S. Molday (1993). Modulation of the cGMP-gated channel of rod photoreceptor cells by calmodulin. Nature *361*, 76-79.

M. Ildefonse, S. Crouzy and N. Bennett (1992). Gating of retinal rod cation channel by different nucleotides: comparative-study of unitary currents. J. Membr. Bio. *130*, 91-104.

M. Ito and L. Karachot (1990). Messenger mediating long-term densensitization in cerebellar Purkinje cells. NeuroReport *1*, 129-132.

U. B. Kaupp, T. Niidome, T. Tanabe, S. Terada, W. Bonigk, W. Stuhmer, W. J. Cook, K. Kangawa, H. Matsuko, T. Hirose, T. Miyata and S. Numa (1989). Primary structure and functional expression from complementary cDNA of the rod photoreceptor cyclic GMP-gated channel. Nature *342*, 762-766.

S. Kawamura and M. Murakami (1991). Calcium-dependent regulation of cyclic GMP phosphodiesterase by a protein from frog retinal rods. Nature *349*, 420-423.

J.-S. Kehoe (1990). Cyclic AMP-induced slow inward current: Its synaptic manifestation in *Aplysia* neurons. J. Neurosci. *10*, 3208-3218.

T. Kurahashi and K.-W. Yau (1993). Co-existence of cationic and chloride components in odorant-induced current of vertebrate olfactory receptor cells. Nature *363*, 71-74.

E. R. Liman and L. B. Buck (1994). A second subunit of the olfactory cyclic nucleotide-gated channel confers high sensitivity to cAMP. Neuron *13*, 611-621.

I. Llano and H. M. Gerschenfeld (1993). β-adrenergic enhancement of inhibitory synaptic activity in rat cerebellar stellate and Purkinje cells. J. Physiol. *468*, 201-224.

G. Lowe and G. Gold (1993). Nonlinear amplification by calcium-dependent chloride channels in olfactory receptor cells. Nature *366*, 283-286.

J. J. Lucas and R. Hen (1995). New players in the 5-HT receptor field: genes and knockouts. TIPS *26*, 246-252.

R. S. Molday, L. L. Molday, A. Dosé, I. Clark-Lewis, M. Illing, N. J. Cook, E. Eismann and U. B. Kaupp (1991). The cGMP-gated channel of the rod photoreceptor cell characterization and orientation of the amino terminus. J. of Biol. Chem. *266*, 21917-21922.

T. Nakamura and G. H. Gold (1987). A cyclic nucleotide-gated conductance in olfactory receptor cilia. Nature *325*, 342-344.

S. Nawy and C. E. Jahr (1991). cGMP-gated conductance in retinal bipolar cells is suppressed by the photo receptor transmitter. Neuron *7*, 677-683.

L. Olson Fuxe, K. (1971). On the projections from locus coeruleus norepinephrine neurons: the cerebellar projections. Brain Research *28*, 165-171.

K. Palczewski, I. Subbaraya, W. A. Gorczyca, B. S. Helekar, C. C. Ruiz, H. Ohguro, J. Huang, X. Y. Zhao, J. W. Crabb, R. S. Johnson , K. A. Walsh, M. K. Gray-Keller, P. B. Dwiler and W. Baher (1994). Molecular-cloning and characterization of retinal photoreceptor guanylyl cyclase-activating protein. Neuron *13*, 395-404.

V. M. Pickel Segal, M., Bloom, F.E. (1972). A radioautographic study of the afferent pathways of the nucleus locus coeruleus. Journal of Comparative Neurology *155*, 15-42.

L. Prézeau Carette, J., Helpap, B., Curry, K., Pin, J-P, Bockaert, J. (1994). Pharmacological characterization of metabotropic glutamate receptors in several types of brain cells in primary cultures. Mol. Pharmacol. *45*, 570-577.

R. R. Reed (1992). Signaling pathways in odorant detection. Neuron *8*, 205-209.

N. Schaeren-Wiemers and A. Gerfin-Moser (1993). A single protocol to detect transcripts of various types and expression levels in neural tissues and cultured cells; in situ hybridization using digoxigenin-labeled cRNA probes. Histochemistry *100*, 431-440.

F. M. Sessler, R. D. Mouradian, J.-T. Cheng, H. H. Yeh, W. Liu and B. Waterhouse (1989). Noradrenergic potentiation of cerebellar Purkinje cell responses to GABA: evidence for mediation through the β-adrenoreceptor-coupled cyclic AMP system. Brain Research *499*, 27-38.

K. Shibuki and D. Okada (1991). Endogenous nitric oxide release required for long-term synaptic depression in the cerebellum. Nature *349*, 326-328.

R. A. Shiells and G. Falk (1992). The glutamate-receptor linked cGMP cascade of retinal ON-bipolar cells is pertusis and cholera toxin-sensitive. Proc. R. Soc. Lond. *247*, 17-20.

S. Siegelbaum and E. R. Kandel (1991). Learning related synaptic plasticity: LTP and LTD. Curr. Op. Neurobio. *1*, 113-120.

H. Simon, M. L. Moal and A. Calas (1979). Efferents and afferents of the ventral tegmental-A 10 region studied after local injection of (^{3}H)leucine and horseradish peroxidase. Brain Res. *175*, 1-23.

J. C. Strahlendorf, H. K. Strahlendorf and M. Lee (1987). Electrophysiological effects of serotonin on cerebellar Purkinje cells. (New York: Alan R. Liss).

L. Sudlow and R. Gillette (1995). Cyclic AMP-gated sodium current in neurons of the pedal ganglion of *Pleurobranchaea californica* is activated by serotonin. J. Neurosci. *73*, 2230-2236.

U. Ungerstedt (1971). Stereotaxic mapping of the monoamine pathways in the rat brain. Acta Physiologica Scandinavica Supplementum *367*, 1-48.

I. Vranesic Staub, C., Knöpfel, T. (1993). Activation of metabotropic glutamate receptors induces an outward current which is potentiated by methylxanthines in rat cerebellar Purkinje cells. Neuroscience Research *16*, 209-215.

M. G. Weisskopf and R. A. Nicoll (1995). Presynaptic changes during mossy fiber ltp revealed by nmda receptor-mediated synaptic responses. Nature *376*, 256-559.

I. Weyand, M. Godde, S. Frings, J. Weiner, F. Muller, W. Alenhofen, H. Hatt and U. B. Kaupp (1994). Cloning and functional expression of a cyclicnucleotide-gated channel from mammalian sperm. Nature *368*, 859-863.

H. Widmer, D. Jacques and M. Raggenbass (1992). *N*-methyl-D-aspartate and vasopressin activate distinct voltage-dependent inward currents in facial motorneurons. Brain Research *593*, 215-220.

D. G. Winder and P. J. Conn (1995). Metabotropic glutamate receptor (mGluR)-mediated potentiation of cyclic AMP responses does not require phosphoinositide hydrolysis: mediation by a group II-like mGluR. J. Neurochem. *64*, 592-599.

K.-W. Yau and K. Nakatani (1985). Light-suppressible, cyclic GMP-sensitive conductance in the plasma membrane of a truncated outer rod segment. Nature *317*, 252-255.

R. A. Zalutsky and R. A. Nicoll (1990). Comparison of two forms of LTP in single hippocampal neurons. Science *248*, 1619-1624.

Figure legends

Figure 3.1 Expression pattern of rOCNC1 (A), rOCNC2 (B), rRCNC1 (D) mRNAs, as determined by quantitative RT-PCR.

Primers specific for the 3' untranslated regions of the three mRNAs were used to amplify oligo-dT primed cDNA made from RNA isolated from various rat tissues. The tissue source is indicated at the top of the figure. Total RNA was used for cDNA synthesis. The reactions in C were amplified with a primer set in which one primer is located in an intron and one in a down stream exon of rOCNC2 and serves as a control for the presence of genomic DNA in the cDNA samples. The rOCNC1 PCR product is 159 bp, the rOCNC2 product is 122 bp (B) 363 bp (C), and the rRCNC1 product is 202 bp. Marker sizes in bp are indicated at the left, Hi, hippocampus; Co, cortex; eye, eye; No, nasal epithelium; OB, olfactory bulb; BrSt, brain stem; Ce, cerebellum; EHi, embryonic hippocampus; He, heart; Lu, lung; gen, genomic DNA; 0, negative control (no DNA).

Figure 3.2 Characterization of probes used for *in situ* hybridizations.

Expression of rOCNC1 (A and F), rOCNC2 (B and G), rRCNC1 (C and H), SCG10 (D and I), and olfactory receptor I7 (E and J) mRNAs in the olfactory epithelium (A-E) and the retina (F-J). We performed *in situ* hybridization to 20 μm horizontal sections of rat olfactory epithelium or retina using digoxigenin-labeled antisense RNA probes. Panels (A-J) are at a magnification of 250x using Nomarski optics. In A-E the olfactory cilia are at the top, and below them are the supporting cell layer (**S**), the neuronal layers (**ORN**), and the basal cell layer (**B**), as indicated in panel **A**. The arrow head in (A-D) delineates the border between the olfactory epithelium (right) and the respiratory epithelium (left). In F-J the outer segements (**OS**) of the photoreceptors are on top, and below them are the inner segments (**IS**), the outer nuclear layer (**ONL**), outer plexiform layer (**OPL**), inner nuclear layer (**INL**), inner plexiform layer (**IPL**), and ganglion cell layer (**GC**).

Figure 3.3 Cng channel expression in the hippocampus, low power magnification.
Expression of rOCNC1 (A), rOCNC2 (B), rRCNC1 (C), SCG10 (D), and olfactory receptor I7 (E) mRNAs in the hippocampus by *in situ* hybridization to 20 μm sections using digoxigenin-labeled antisense RNA probes. Panels (A-E) are at a magnification of 31.25x using bright field optics. The SCG10 and I7 probes serve as positive and negative controls respectively.

Figure 3.4 Cng channel expression in the hippocampus, high power magnification of the sections in Figure 3.3.
Expression of rOCNC1 (A and F), rOCNC2 (B and G), rRCNC1 (C and H), SCG10 (D and I), and olfactory receptor I7 (E and J) mRNAs in the hippocampus by *in situ* hybridization to 20 μm sections using digoxigenin-labeled antisense RNA probes. Panels (A-E) show a portion of the dentate gyrus, and panels (F-J) shows the transition zone of pyramidal cell regions CA1 (upper left) to CA3 (lower right). Panels (A-J) are at a magnification of 125x using Nomarski optics.

Figurre 3.5 Cng channel expression in the cerebellum and olfactory bulb.
Expression of rOCNC1 (A and F), rOCNC2 (B and G), rRCNC1 (C and H), SCG10 (D and I), and olfactory receptor I7 (E and J) mRNAs in the cerebellum (A-E) and the olfactory bulb (A-J) by *in situ* hybridization to 20 μm sections using digoxigenin-labeled antisense RNA probes. Panels (A-E) show a portion of the cerebellum, and panels (F-J) show a region of the olfactory bulb. In A-E the molecular layer of the cerebellum is at the top (A and B) or right side (C-E)of the photograph. The granule cells (**g**), Purkinje cells (**p**), and interneurons of the molecular layer (**in**), are as indicated in panel **A**. The arrow head in A-E indicates a Purkinje cell. In F-J the granule cells (**g**) of the olfactory bulb are to the lower right, and to the upper left of them are the mitral cells (**m**), the tufted cells (**t**), and the periglomerular cells (**pg**) as indicated in panel **F**. Panels (A-E) are at a

magnification of 250x, and panels (F-J) are at a magnification of 125x using Nomarski optics.

Figure 3.6 Channel antibodies recognize the channel in transfected 293 cells.
rOCNC2 (A and B) and rOCNC1 (C and D) were expressed using the vector pCIS in HEK293 cells by transfection and detected by immunofluorescence. rOCNC2 staining was with the MAb 7B11/2B8. rOCNC1 staining was with the affinity purified rabbit antiserum. Note, rOCNC2 transfected cells can be distinguished from non transfected cells by a rounded morphology.

Figure 3.7 A. The olfactory channel subunits are associated in vivo and the antichannel antibodies do not cross react by immunoprecipitation or Western blot.
Western blot of olfactory cilia membranes (lanes 1-4) probed with anti rOCNC1 (lanes 1 and 2) or anti-rOCNC2 (lanes 3 and 4). Antiserum for the Western blot was (+) or was not (-) preabsorbed against specific antigen produced in bacteria. Western blot of immunoprecipitations from olfactory cilia membranes (lanes 5-12). Antiserum used for immunopecipitation was (+) or was not (-) preabsorbed against specific antigen produced in bacteria. The immunoprecipitating antibody is along the top. The antibody used in the Western blot is along the bottom, rOCNC1 (lanes 5-8), and rOCNC2 (lanes 9-12). The band labeled IgG is detection of the heavy chain polypeptide from the immunoprecipitating antibody by the secondary antibody used in the Western.

Figure 3.7 B. rOCNC1 and rOCNC2 protein is expressed in the hippocampus.
Western blot of immunoprecipitations from hippocampal lysates, 100μg of proten/lane. Lanes 2 and 4 are Western blots with preabsorbed antibody.

Figure 3.8. Expression of rOCNC1 and rOCNC2 by immunohistochemistry.

In the upper left, staining of sections of cerebellum at low magnification (31.25x)(A and B). Below (C and D) higher magnification (250x), molecular layer above and granule cell layer below, arrow head is the Purkinje cell layer. Upper right staining of sections of cortex with successive increase in magnification (31.25x, 125x, 250x). Arrows indicate punctate areas of intense staining in 250x photographs. Lower left, low power magnification of hippocampus (31.25x). Lower right, low power magnification of hippocampus with successive increase in magnification. CA3 region of pyramidal cells at 125x magnification (C and D), CA1 region of pyramidal cells at 125x magnification (E and F), CA3 region of pyramidal cells at 250x magnification (G and H). Arrows

Figure 3.9. rOCNC2 is expressed on neuronal processes of embryonic hippocampal cell cultures.

A and B, the rOCNC2 MAb stains processes of fixed and permeabilized cultured embryonic hippocampal cells . C and D, *in situ* hybridization for the mRNA of the neuronal marker SCG10 (blue cell bodies) counter stained for the glial marker GFAP (flat cell body and green processes).

Figure 3.10. Morphological comparison of the processes of cultured embryonic hippocampal cells.

A and B, the HM-2 anti-MAP2 MAb stains a subset of the neuronal processes, arrows indicate processes not stained with this dendritic marker. C and D, the SDL.3D10 anti-tubulin III MAb stains most processes, arrows indicate the variety of processes stained by this more general microtubule marker.

Figure 3.11. Electrophysiology: recording of cng channels from cultured embryonic hippocampal cells.

A Whole cell recording. Currents activated in a cell by diffusion from the patch pipette of cAMP at 100μM (left), or in a different cell, by cGMP at 100μM (right). Middle two panels currents immediately after patch rupture during applied voltage protocol (shown in the upper right). Bottom two panels, currents four minutes after patch rupture during applied voltage protocol.

B Excised inside-out patch recording. Channel openings in a patch from a cultured embryonic hippocampal neuron with Vm=-60mV in response to perfusion of 10μM cAMP followed by perfusion of 10μM cGMP in symmetrical divalent free solution.

C Single channel analysis. The upper left is a portion of an expanded trace from an excised inside-out patch perfused with 10μM cAMP. Lower left is the amplitude histogram analysis at -60mV (left) and +60mV (right). Right, the I-V relation for this patch.

D Analysis of the effect of Ni^{2+} ions on the hippocampal cng channels. (A), recording from an inside-out patch excised from a hippocampal in culture perfused with 10μM cAMP or 10μM cAMP+10μM Ni^{2+}. Below, the open time distribution under each condition. (B), recording from an inside-out patch excised from a HEK293 cell having stabile expression of rOCNC1 and rOCNC2 (see Appendix III) perfused with 10μM cAMP, followed by 10μM cGMP, then 10μM cAMP+10μM Ni^{2+}, and finally 10μM cGMP+10μM Ni^{2+}. The effective change in $K_{1/2}$ is plotted below, closed symbols are without Ni^{2+} open symbols are in the presence of Ni^{2+}.

Figure 3.11. Pathways by which cyclic nucleotide concentration could be increased in a nerve terminal to open the "olfactory" cng channel. On the left adenylyl cyclase (AC) can be stimulated through the conventional seven helix receptor (7HR) G protein (G) coupled pathway, or, by Ca^{2+}-calmodulin (CaM). The "red" channel is a Ca^{2+} channel not acted on by cyclic nucleotide and can be voltage activated or ligand gated depending

on the synaptic localization. The "blue" channel is the cng channel. On the right, soluble guanylyl cyclase (GC) acts as an effector of nitric oxide (NO) and generates cGMP to open the cng channel.

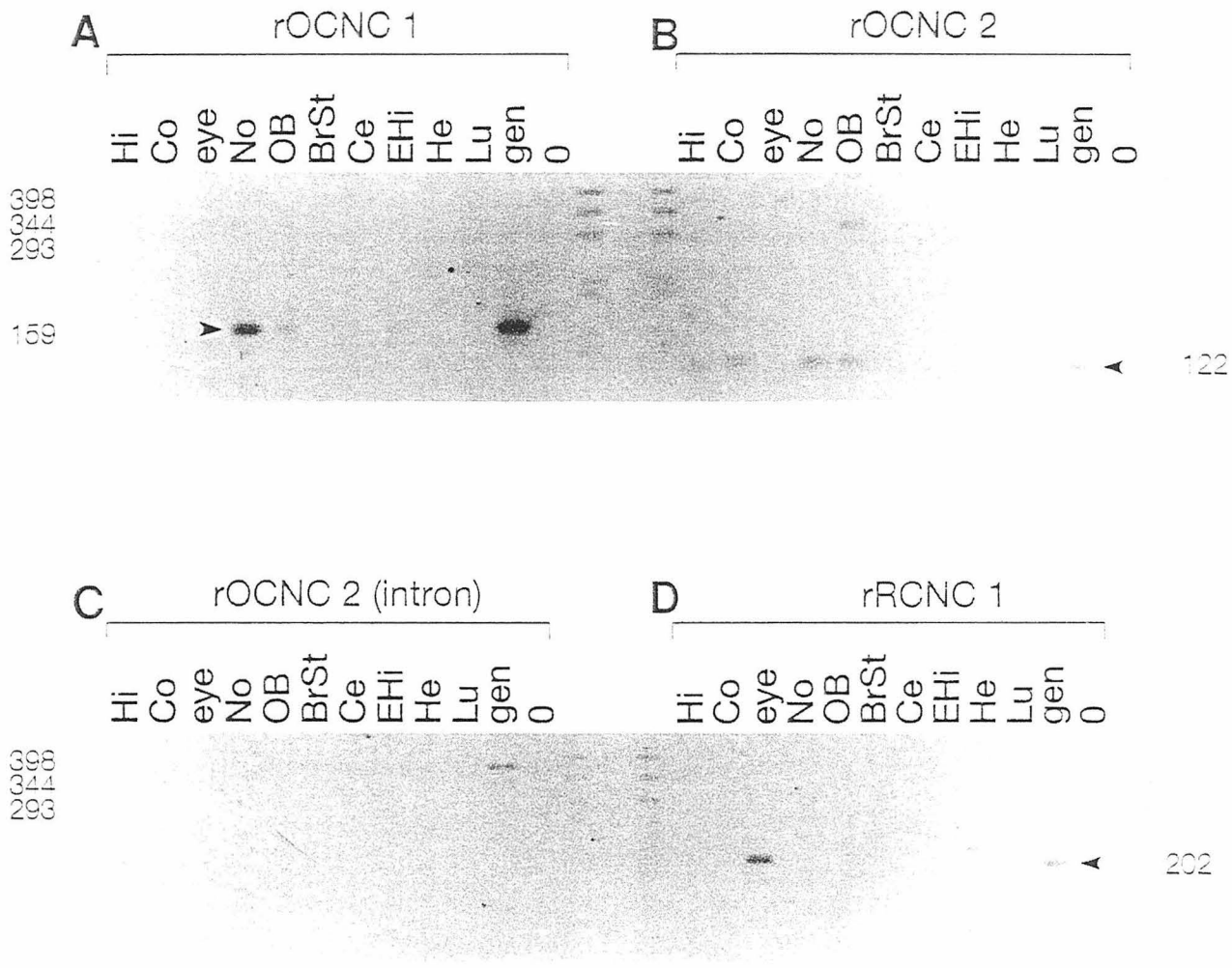
A
rOCNC 1
Hi
Co
eye
No
OB
BrSt
Ce
EHi
He
Lu
gen
0
398
344
293
159
B
rOCNC 2
122
C
rOCNC 2 (intron)
D
rRCNC 1
202

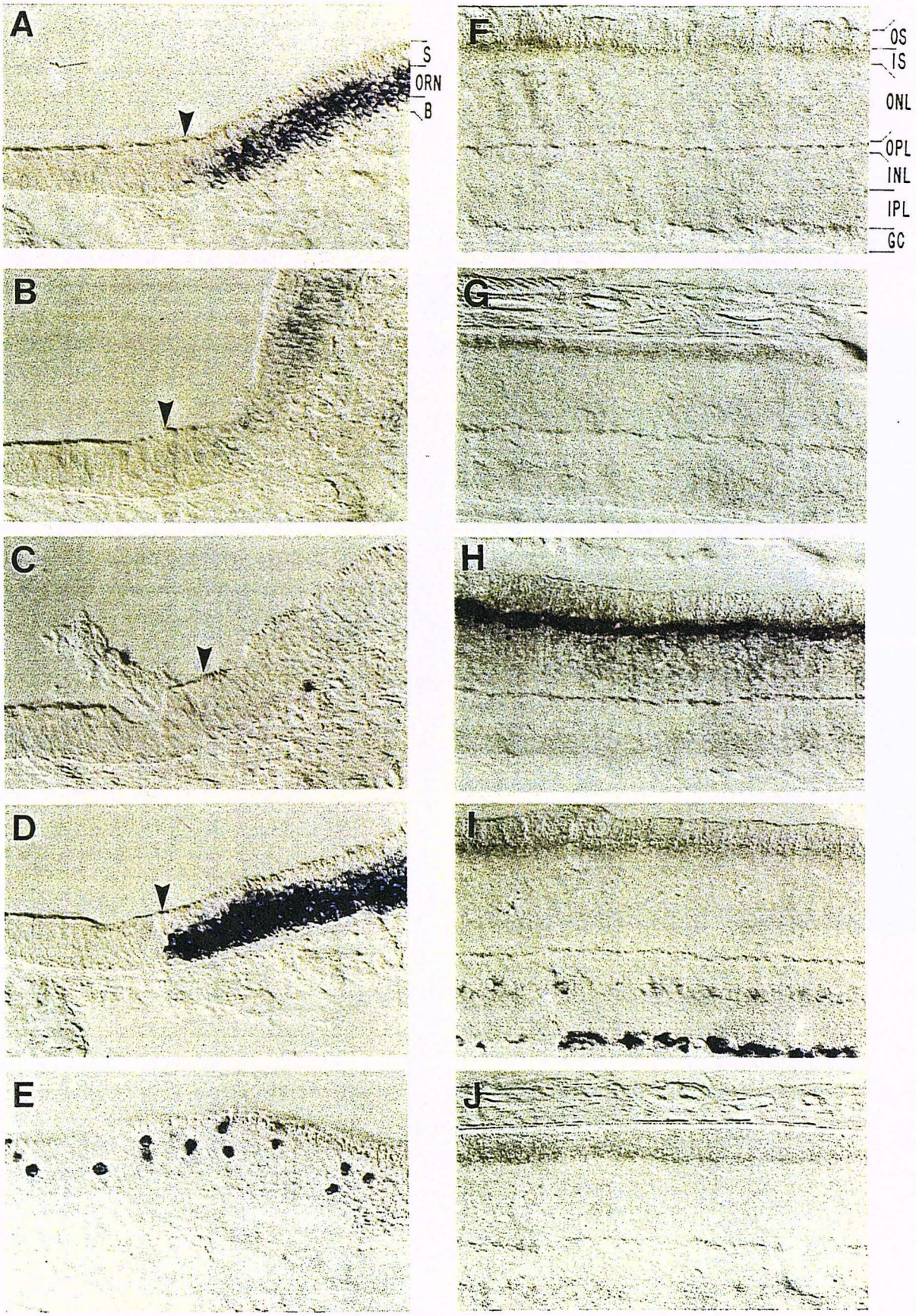
A
S
ORN
B
F
OS
IS
ONL
OPL
INL
IPL
GC
B
G
C
H
D
I
E
J

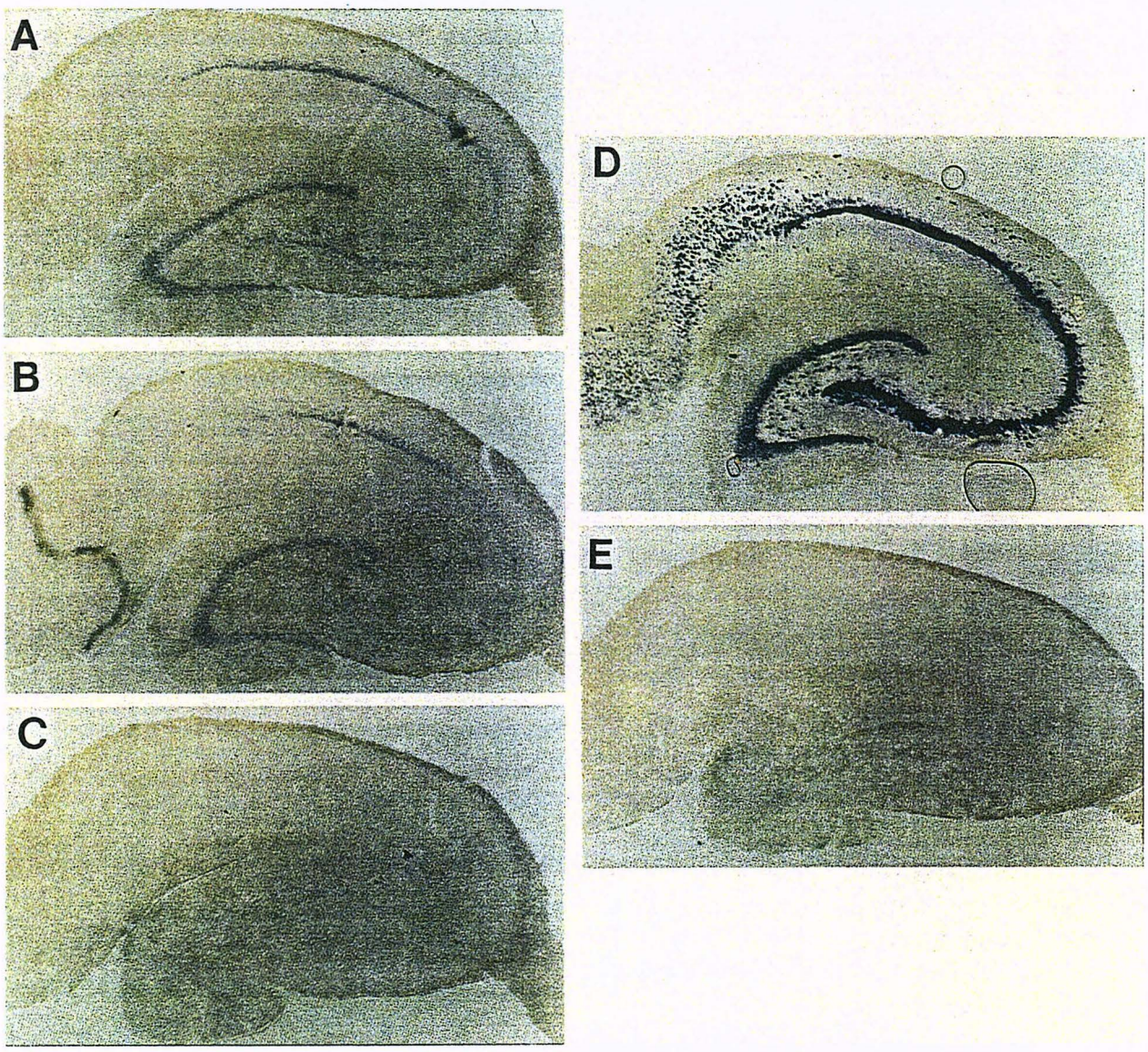
A
B
C
D
E

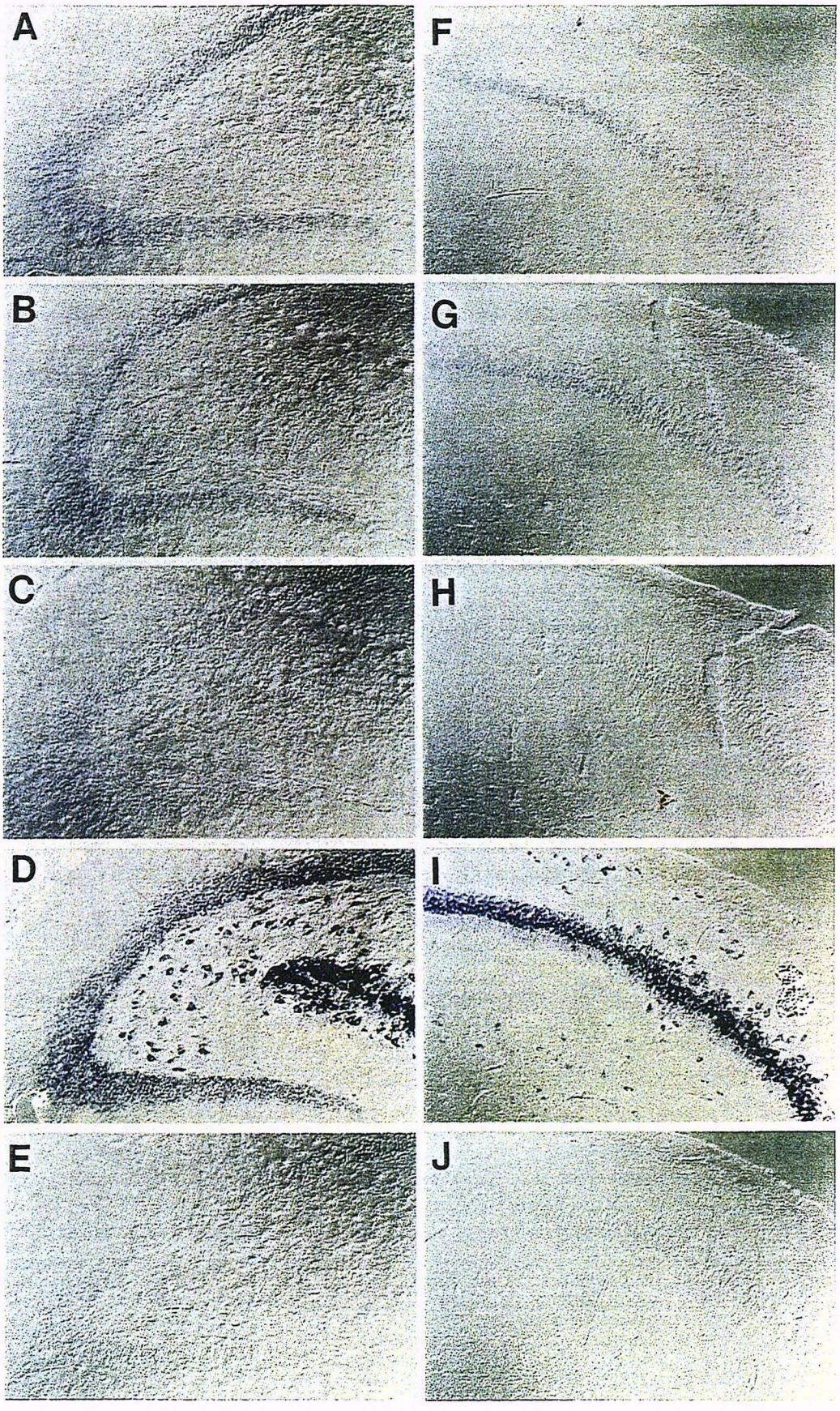
A
F
B
G
C
H
D
I
E
J

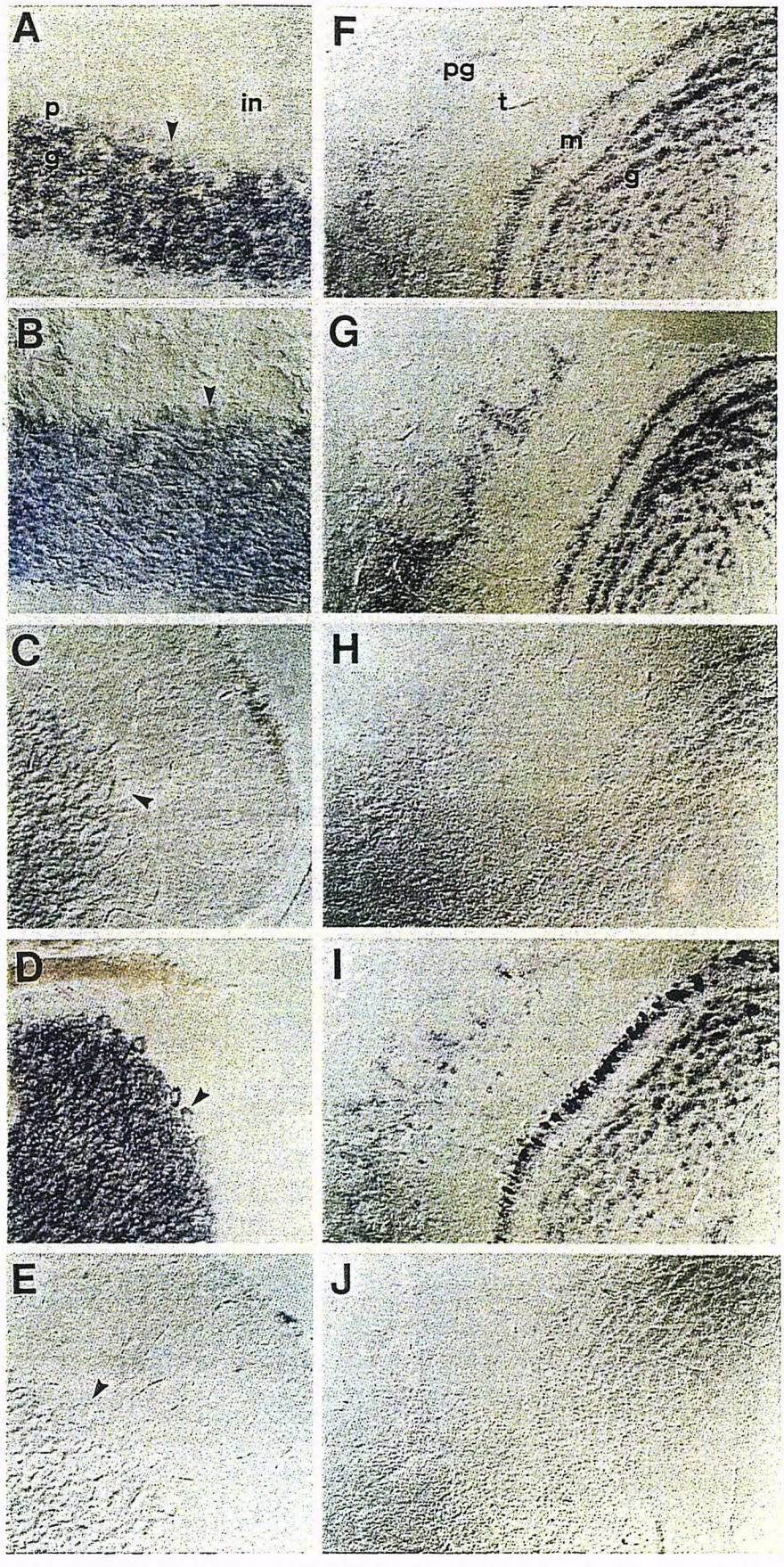
A
p
in
g
F
pg
t
m
g
B
G
C
H
D
I
E
J

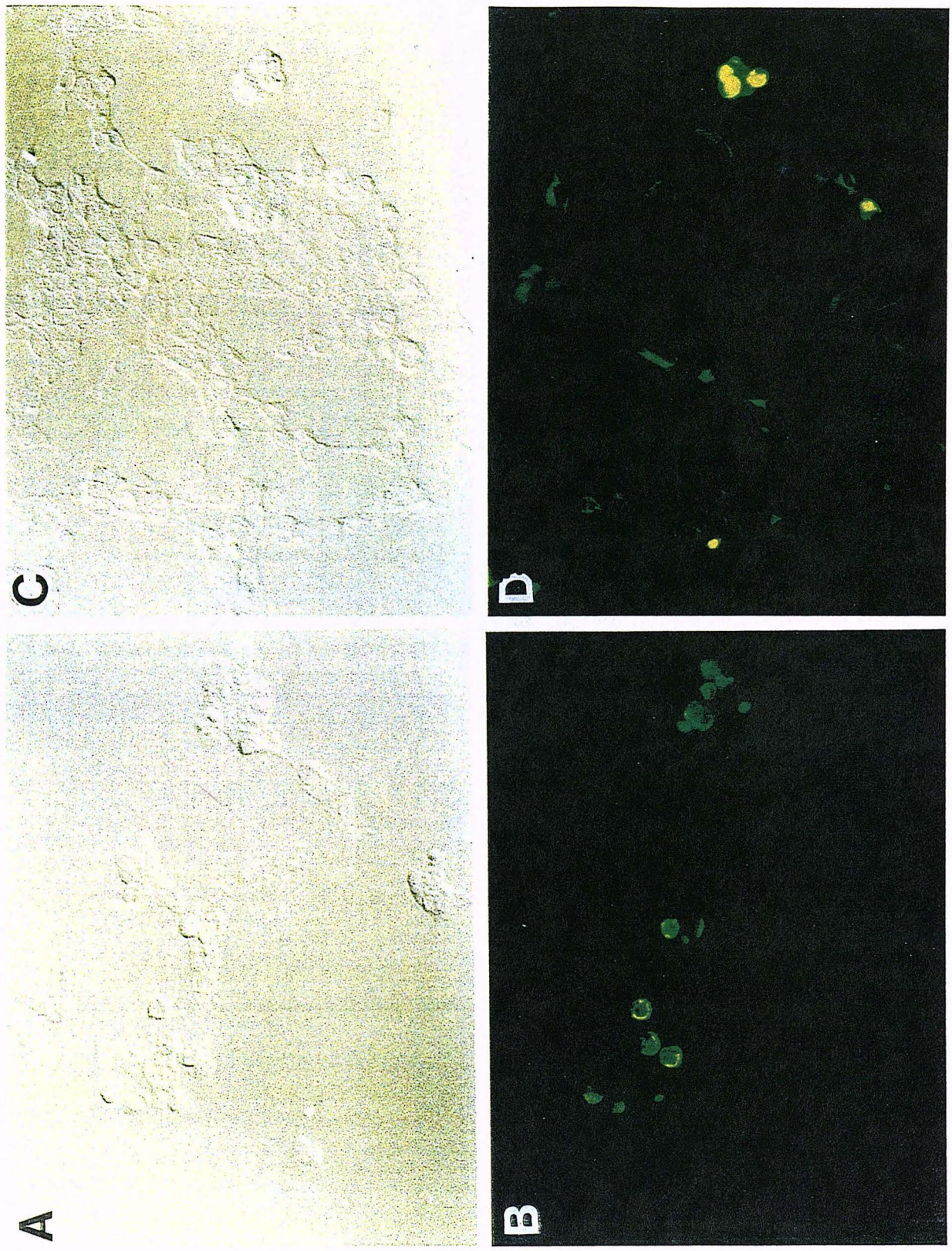
A
B
C
D

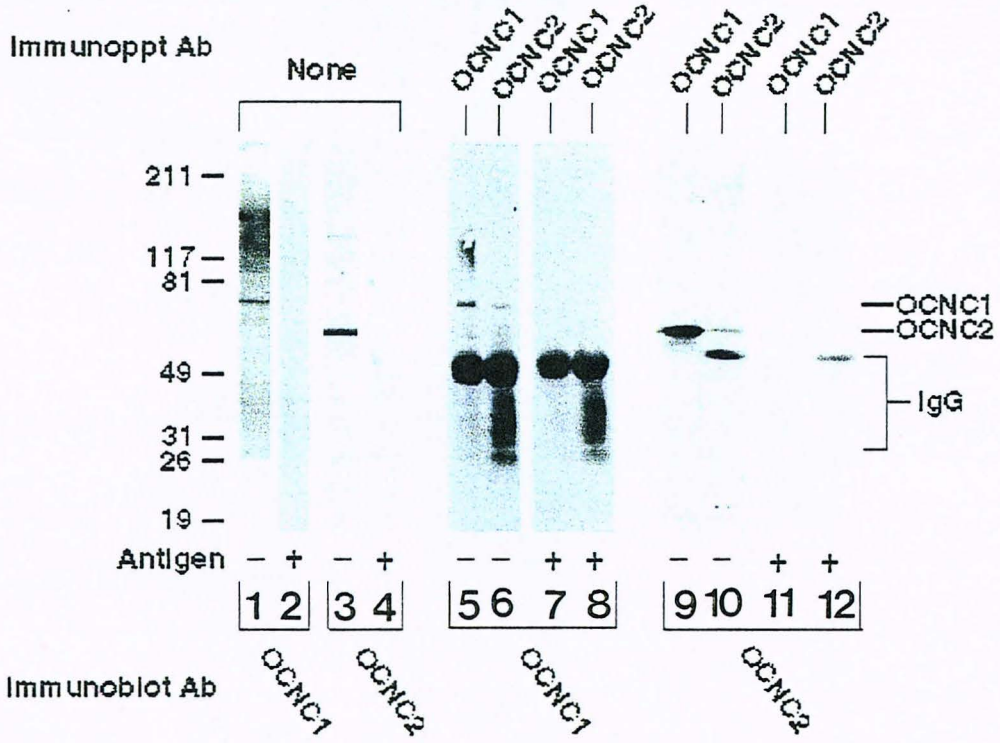
Immunoppt Ab
None
OCNC1
OCNC2
OCNC1
OCNC2
OCNC1
OCNC2
OCNC1
OCNC2
211
117
81
49
31
26
19
OCNC1
OCNC2
IgG
Antigen
1 2 3 4 5 6 7 8 9 10 11 12
Immunoblot Ab
OCNC1
OCNC2
OCNC1
OCNC2

Hippocampus

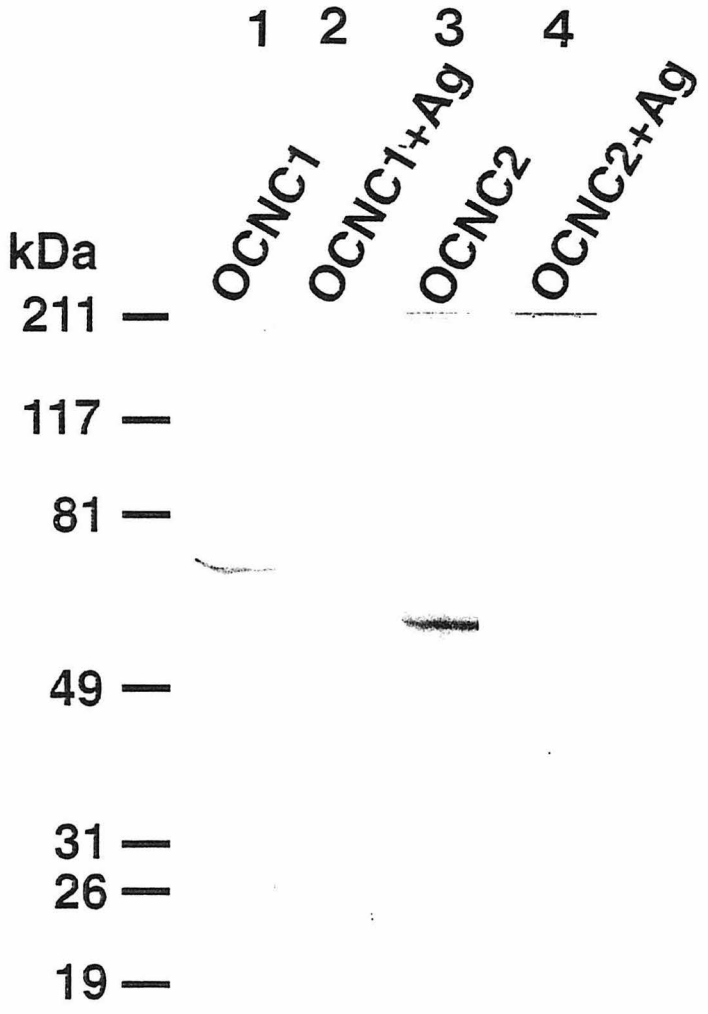

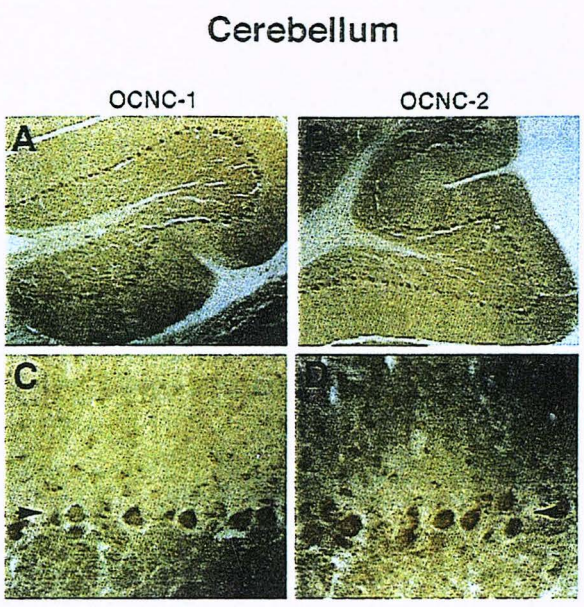
Cerebellum
OCNC-1
OCNC-2
A
C

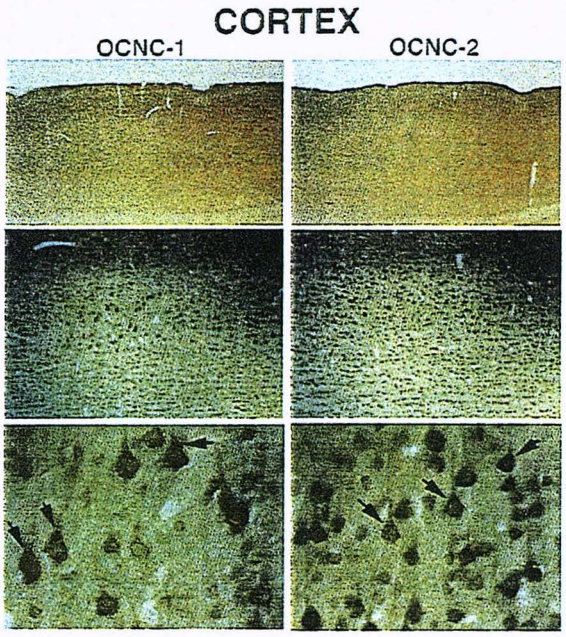
CORTEX
OCNC-1
OCNC-2

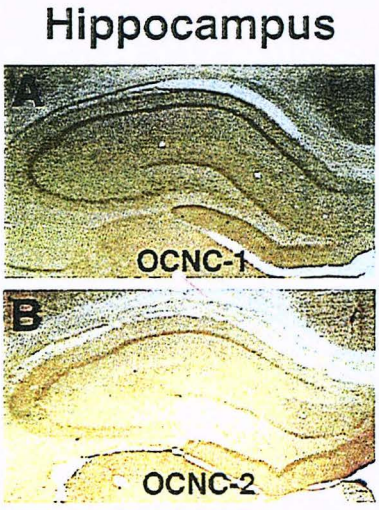
Hippocampus
A
OCNC-1
B
OCNC-2

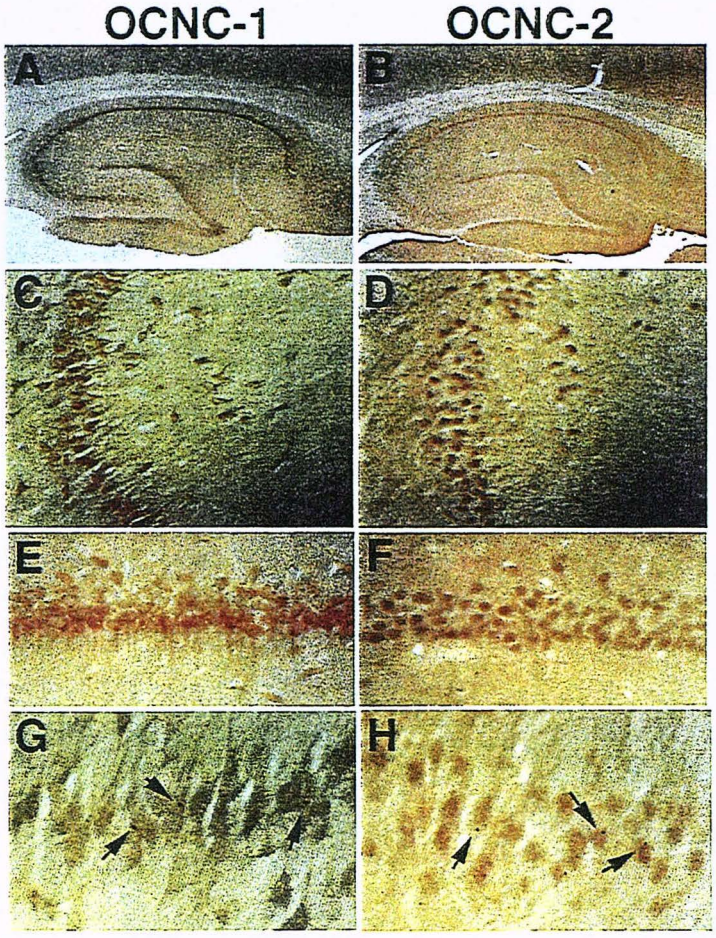
OCNC-1
OCNC-2
A
B
C
D
E
F
G
H

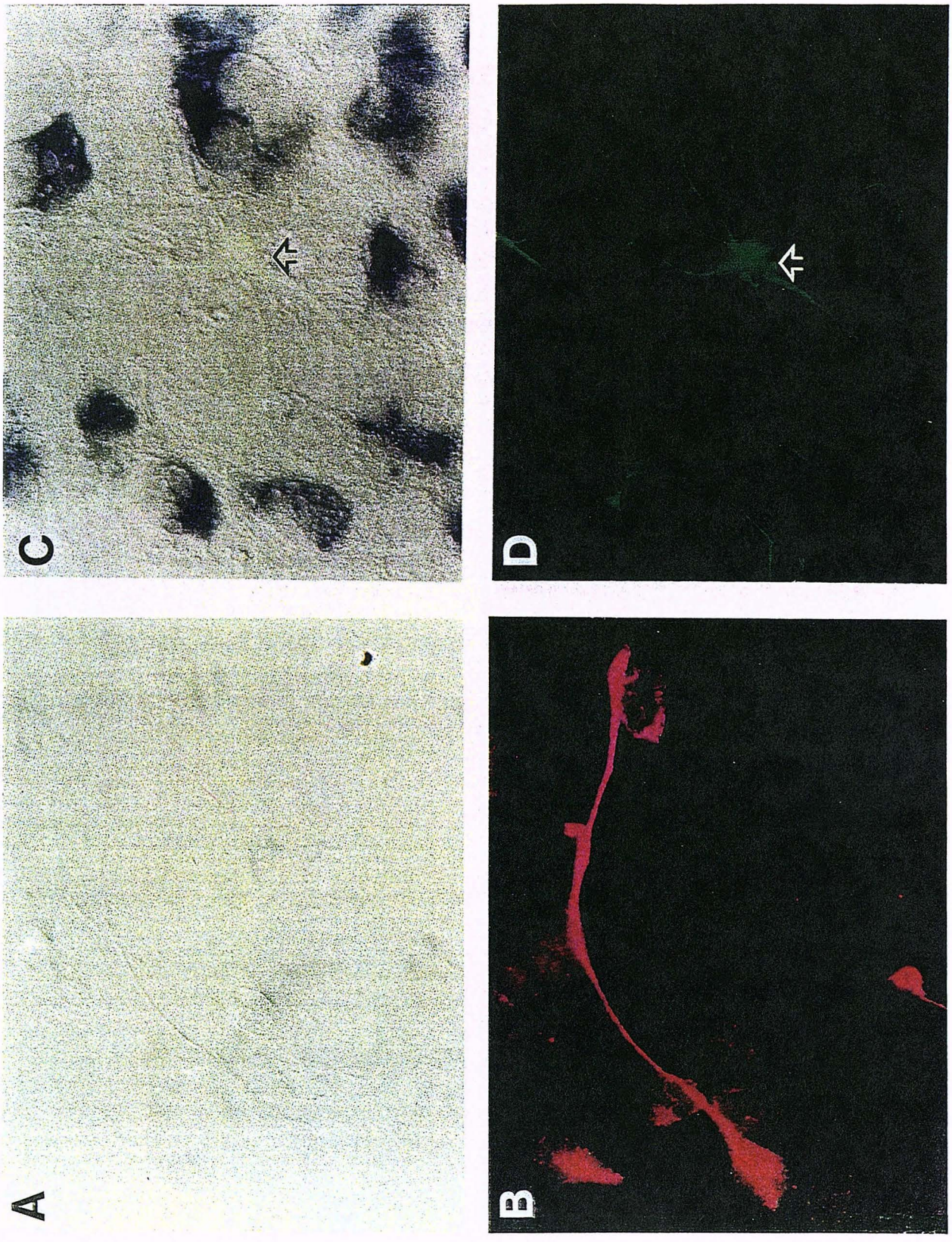
A
B
C
D

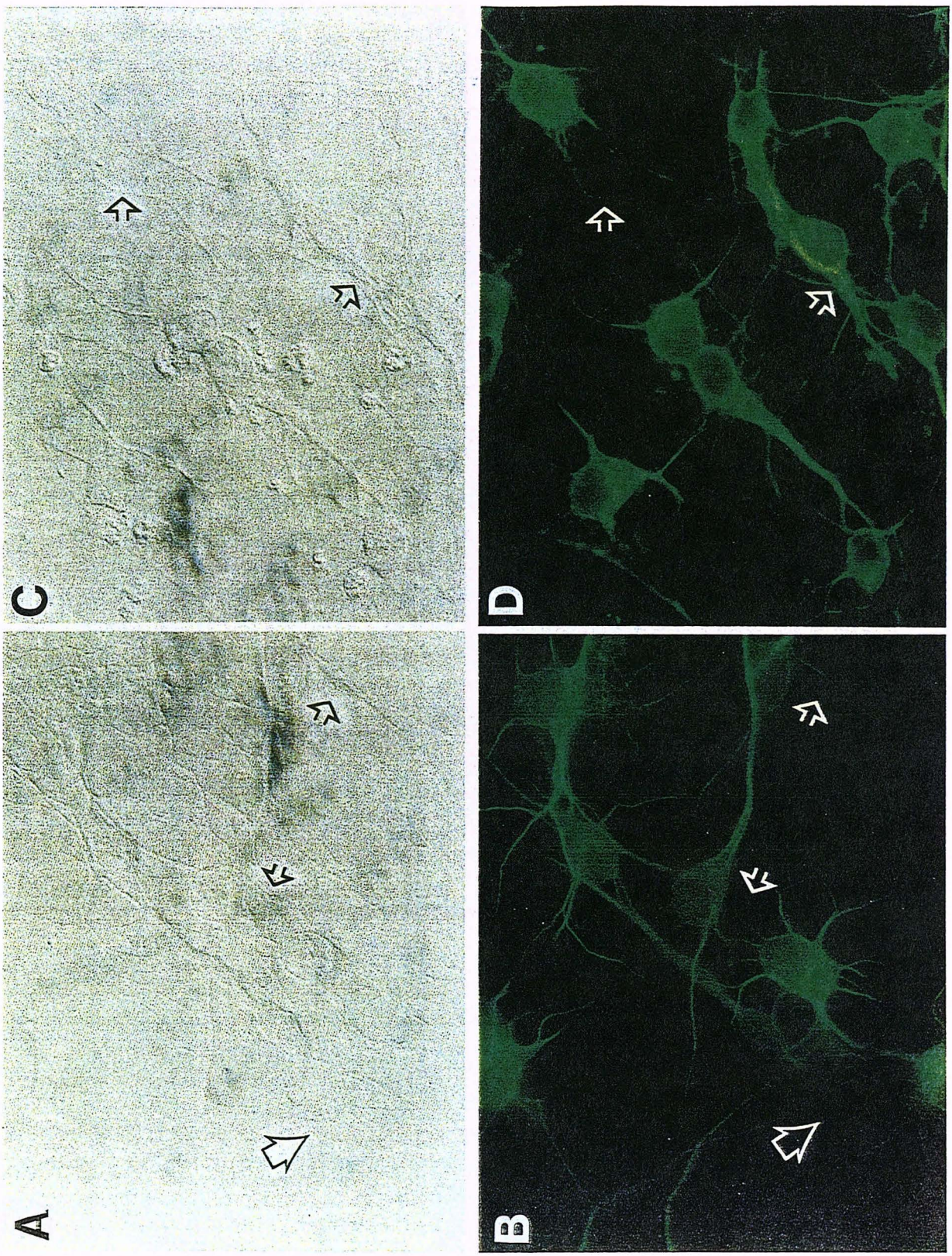
A
B
C
D

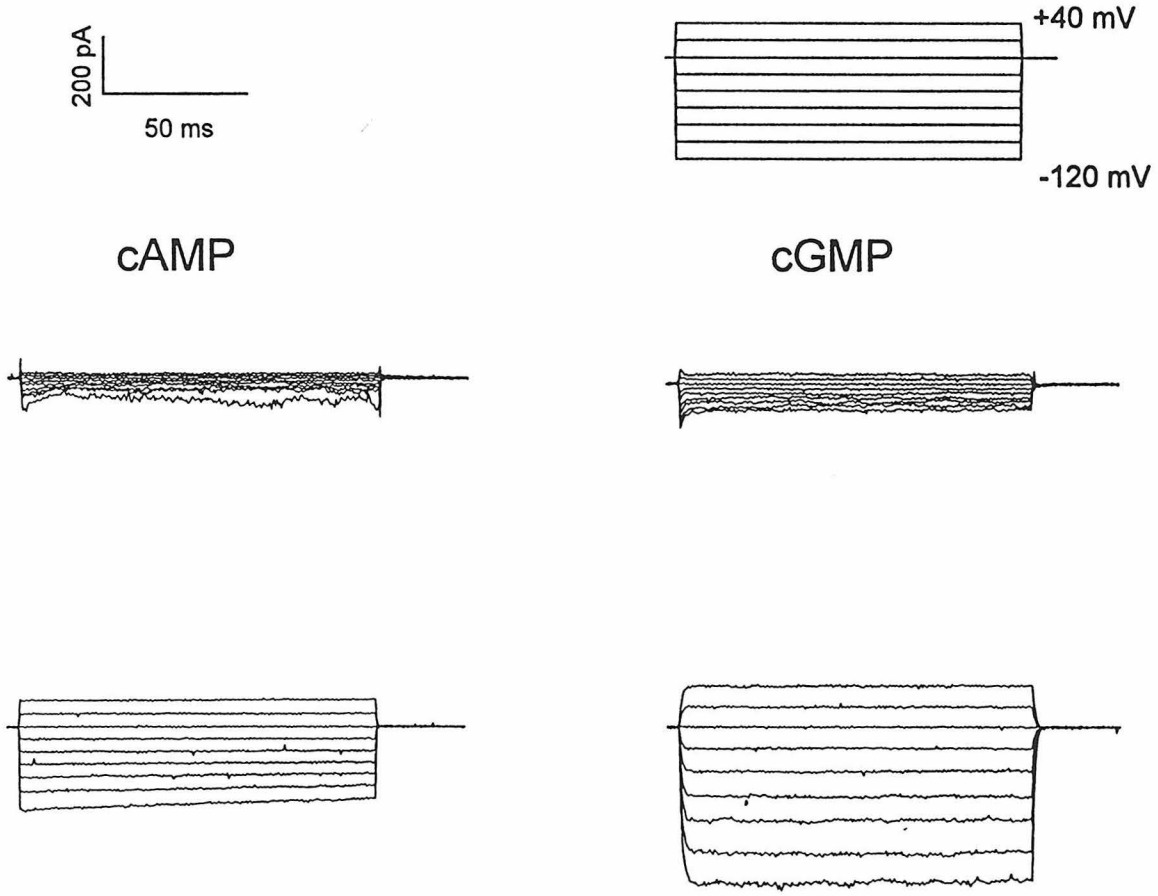
200 pA
50 ms
+40 mV
-120 mV
cAMP
cGMP

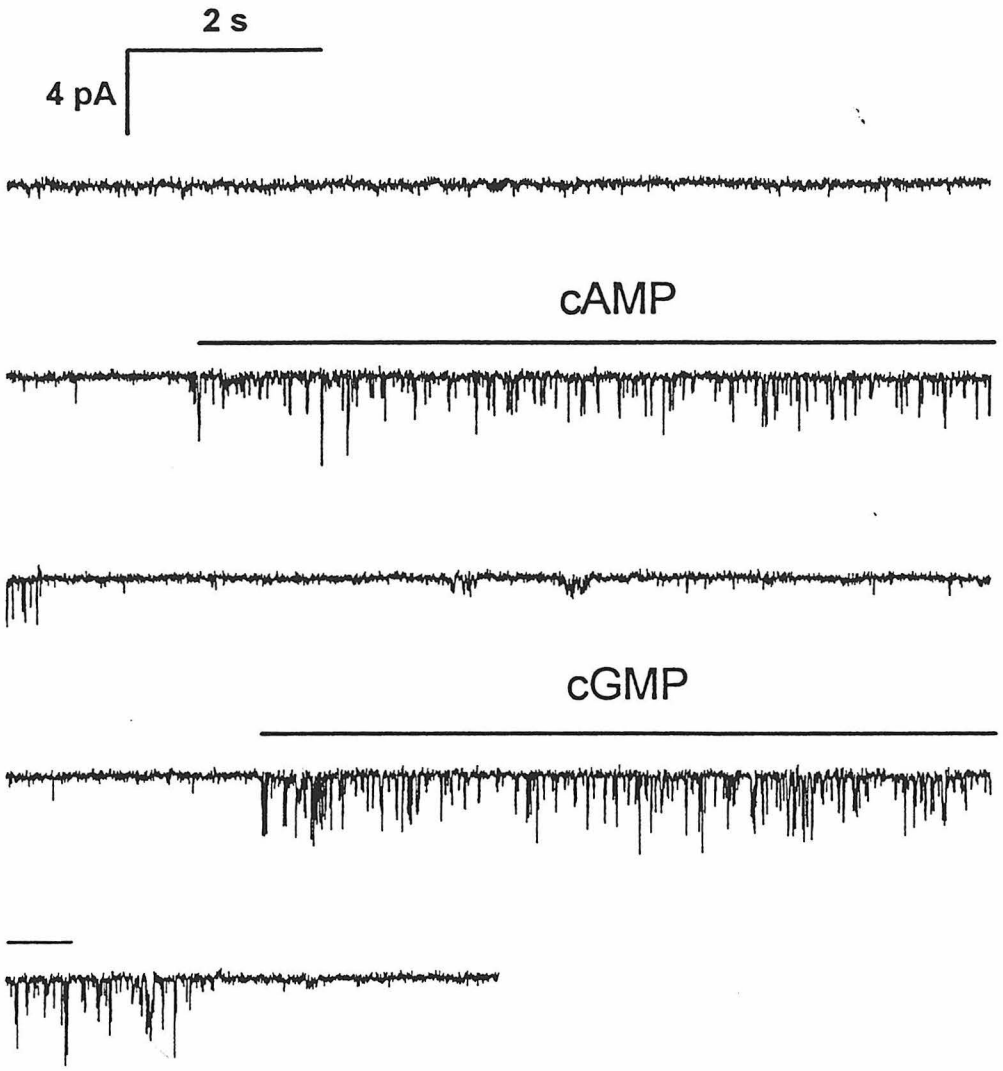
2 s
4 pA
cAMP
cGMP

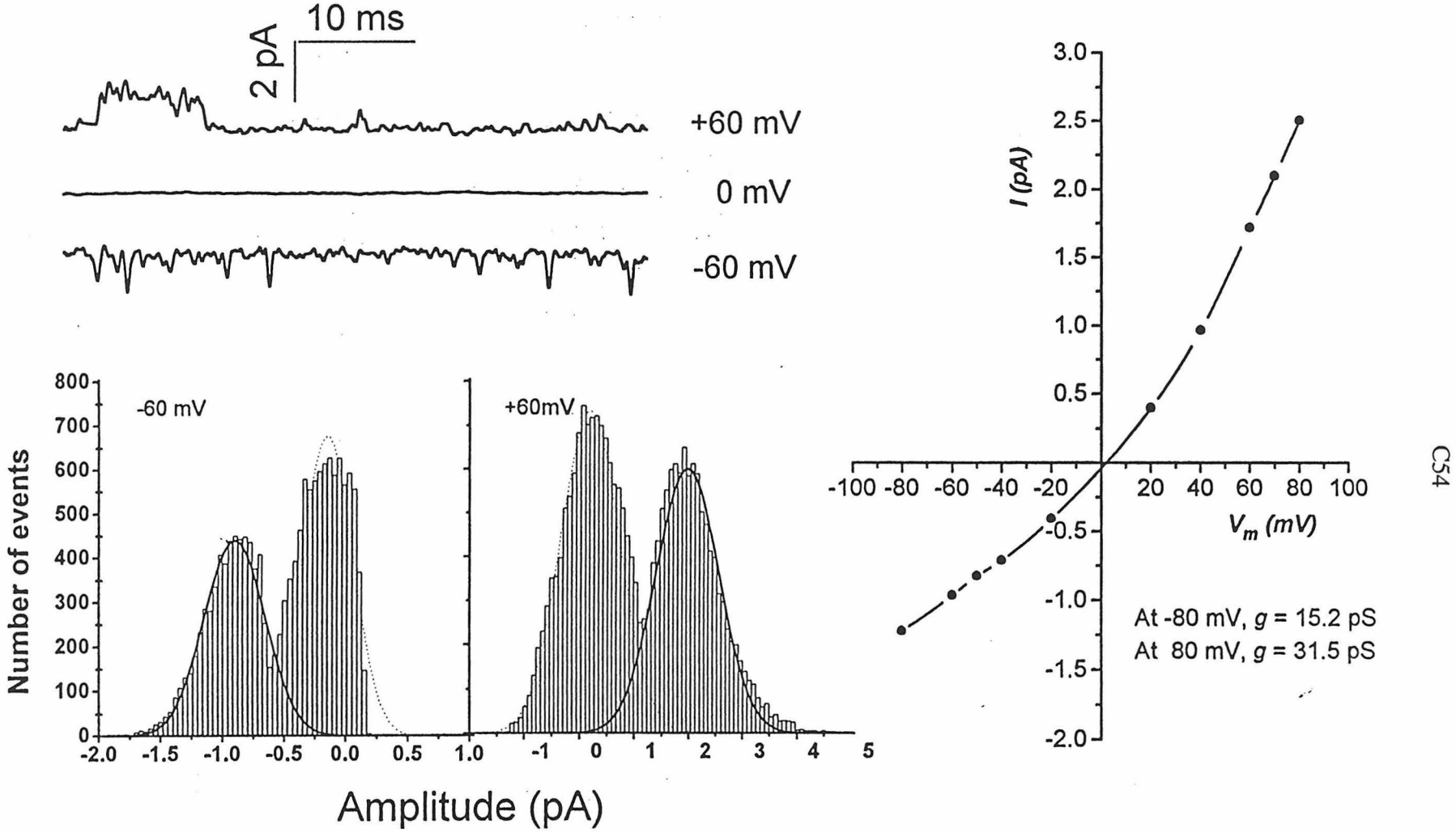
10 ms
2 pA
+60 mV
0 mV
-60 mV
-60 mV
+60mV
Number of events
Amplitude (pA)
I (pA)
V_m (mV)
At -80 mV, g = 15.2 pS
At 80 mV, g = 31.5 pS

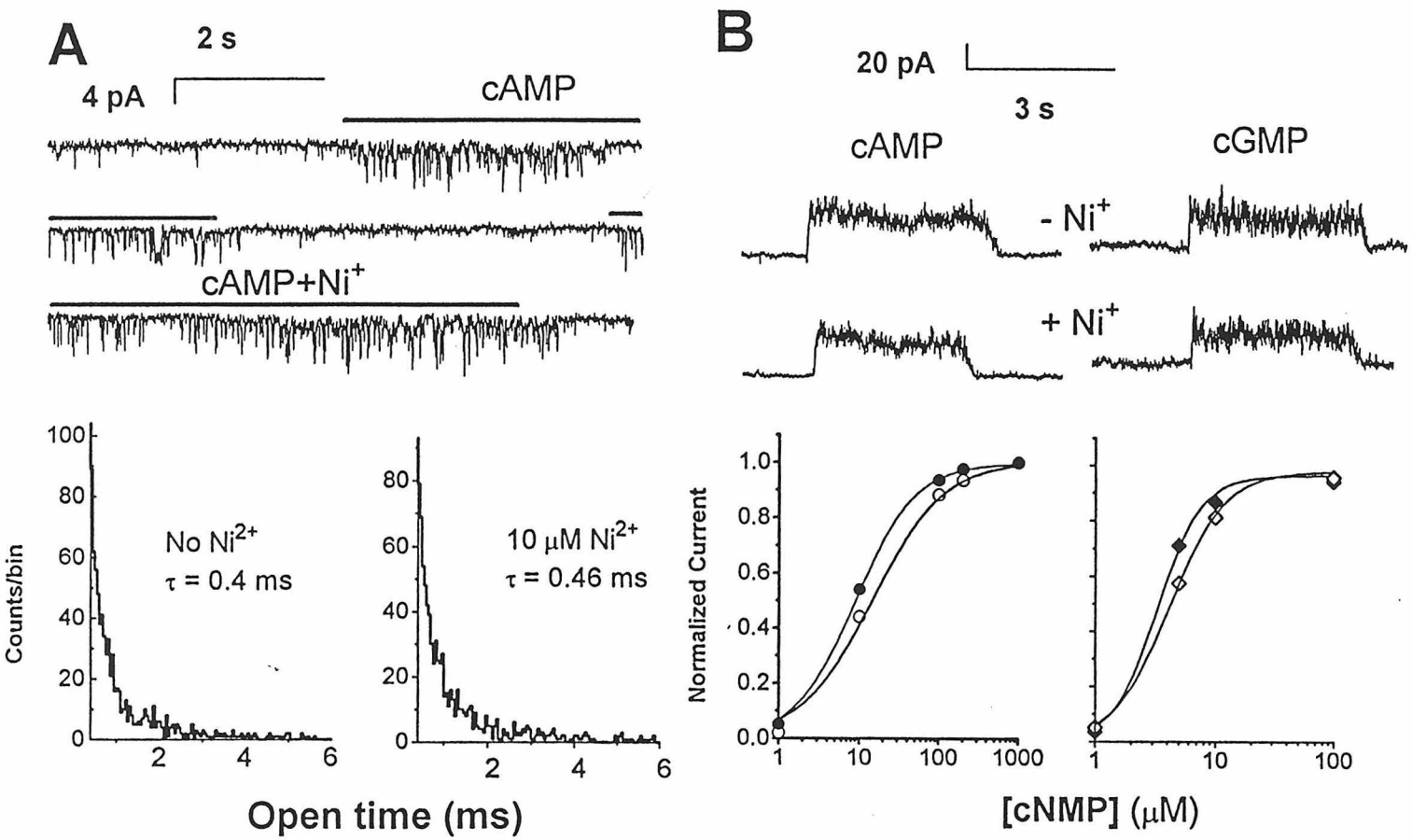
A
2 s
4 pA
cAMP
cAMP+Ni+
Counts/bin
No Ni2+
τ = 0.4 ms
10 μM Ni2+
τ = 0.46 ms
Open time (ms)
B
20 pA
3 s
cAMP
cGMP
- Ni+
+ Ni+
Normalized Current
[cNMP] (μM)

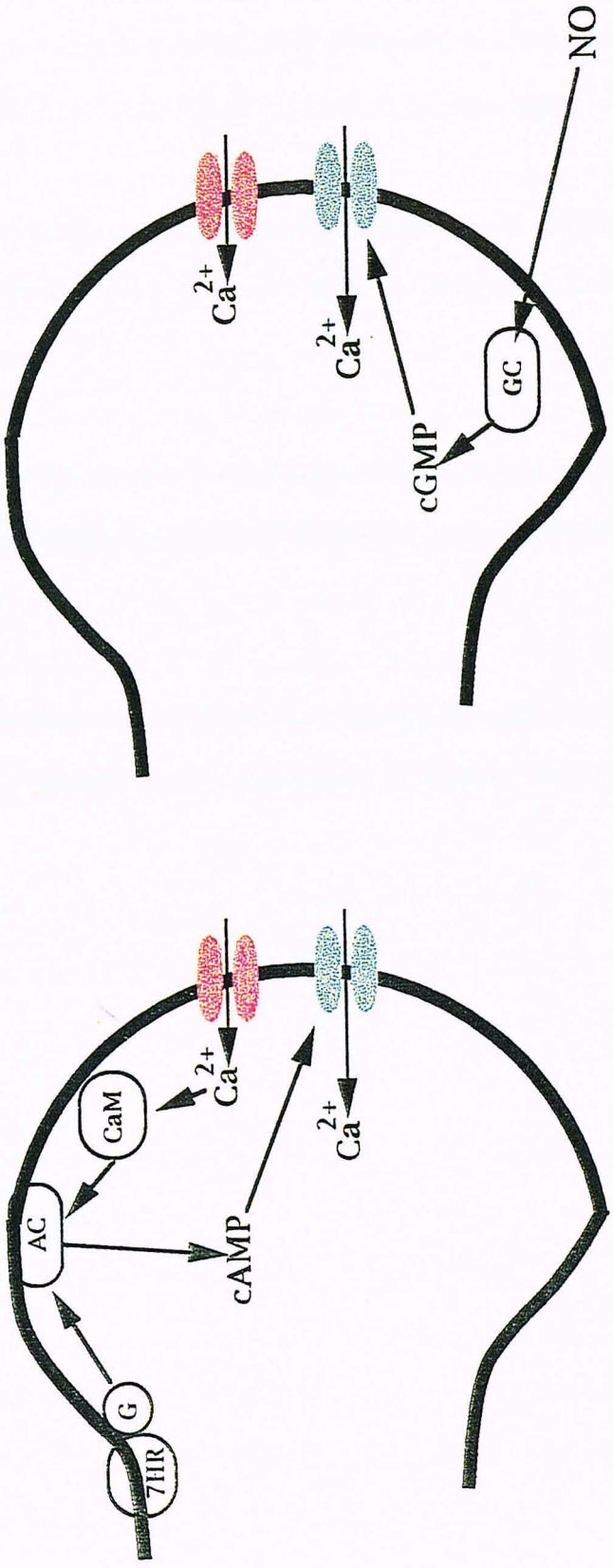
NO
GC
cGMP
Ca2+
Ca2+
CaM
AC
cAMP
Ca2+
Ca2+
G
7HR

Chapter 4. Expression and analysis of putative olfactory receptors. Although this was the first project I started working on progress has been very slow despite the efforts of the below mentioned collaborators. Much of the data presented in this chapter is preliminary.

Functional analysis in *Xenopus* oocytes was done in collaboration with Yasuhito Uezono in the Lester/Davidson group and Yinong Zhang in the Zinn group, Division of Biology, Caltech

Biochemical analysis of receptor expressing *Xenopus* oocytes was done in collaboration with Mike Quick, Neurobiology Research Center, University of Alabama, Birmingham, AL

Immunofluorescence of receptor expressing *Xenopus* oocytes was done in collaboration with Jost Vielmetter in the Zinn group, Division of Biology, Caltech

Introduction and background

It has been shown electrophysiologically and by direct biochemical techniques that vertebrate olfactory receptor neurons (ORNs) respond to odorant with an increase in the second messengers cAMP and/or inositol trisphosphate (IP_3). Substantial molecular evidence for a signal transduction pathway that leads to the production of cAMP has accumulated over the past 5-10 years. A cation channel that is sensitive to changes in intracellular cAMP concentration is expressed in ORNs and has been cloned from the olfactory epithelium (OE) . An adenylyl cyclase and a stimulatory G protein have also been cloned from the OE and shown to be expressed in ORNs. Completing the picture, a very large family of seven-helix receptors expressed in ORNs has been characterized at the level of mRNA expression. These expression studies have lead credence to a proposed signal transduction pathway in which odorant receptors of the seven helix class interact with a G protein which stimulates an adenylyl cyclase (AC) to produce cAMP. cAMP then gates a cation channel initiating depolarization, reviewed in (Reed, 1992)(fig. 4.0). Some receptors could also couple to a G protein pathway leading to IP_3 production, but whether such pathways are involved in vertebrate olfaction is still unclear. Although the receptor sequences were identified in early 1991, the participation of any of these cloned genes in olfaction or in this proposed pathway remain circumstantial and unproven.

There has been one report of a cloned olfactory receptor (OR) mediating an increase in IP_3 production in insect (Sf9) cells when expressed using baculovirus(Raming et al., 1993). In their report these authors show production of IP_3 in the cell lysate of receptor (OR5) transfected cells in response to the two aldehydes lyral (fruity) and lilial (floral). Their are, however, a few problems with this piece of work. No evidence of receptor RNA or protein expression is given for either OR5, the receptor giving the positive signal, or equally important, the one used as a negative control (OR12). Equally disturbing, the change in IP_3 concentration (119±21 pmol/mg protein) is only 2.22 fold

over background (53.44±18 pmol/mg protein) when a mixture of both odorants is used. This is in contrast to the 25 fold pmole increase in IP_3 concentration/mg protein with lyral reported by these authors using olfactory cilia membrane preparations(Boekhoff and Breer, 1990; Breer, 1991). These preparations would be expected to contain far less of the OR5 receptor/mg of lysate. An explanation for this discrepancy could be that several receptors in the cilia lysate can mediate a response to lyral. It would therefore be interesting to know if any other receptors in addition to OR12 were tested in this assay. In the three years since this report no new related data has been published and several independent groups have tried to repeat these results without success (Randall Reed, Johns Hopkins University, Gabriele Ronnett, Johns Hopkins University, Barry Ache, University of Florida St. Augustine, Tim McClintock, University of Kentucky; personal communications). Therefore, although intriguing, this result has yet to be repeated and remains suspect. Lastly, the baculovirus based expression assay involved direct measurement of the second messenger and therefore did not implicate any other transduction molecules in an odorant response.

Heterologous expression of olfactory receptors in *Xenopus* oocytes

In order to assay odorant receptor function we chose expression in *Xenopus* oocytes. *Xenopus* oocytes constitute a highly sensitive system for the cloning and expression of seven helix receptors that couple to the turnover of phosphatidylinositol. This takes advantage of an endogenous signaling pathway that mediates the fast block to polyspermy(Dascal, 1987). The putative sperm receptor couples to a G protein mediated cascade that activates phospholipase C (PLC) to produce IP_3. The IP_3 releases Ca^{2+} from intracellular IP_3 sensitive Ca^{2+} stores resulting in opening of a Ca^{2+} sensitive Cl^- channel in the plasma membrane. To assay receptors that couple to activation of adenylyl cyclase, we expressed the cystic fibrosis transmembrane conductance regulator (CFTR) in the oocytes (see Appendix II). CFTR is a Cl^- channel activated by phosphorylation by

protein kinase A. Thus in the one cell we have a system to functionally assay receptors that couple to stimulation of AC, and PLC (fig 4.1).

Production of receptor sequences and functional odorant assay in *Xenopus* oocytes

A panel of 130 odorants separated into 12 chemical groups was first prescreened against CFTR alone injected oocytes giving a subpanel of 80 odorants that did not give a response at a concentration of 10μM. The mechanism of this "background" CFTR mediated response to the 50 odorants is not clear and was not pursued. To try to generate an assay system for intracellular increases in cAMP levels that didn't rely on CFTR we have also investigated two systems based on the cng channels (see Appendix III).

Primers were designed to amplify by PCR ten full length olfactory receptor cDNAs (Buck and Axel, 1991), and one isolated in our lab by library screen (J.B. unpublished; see Appendix IV). Template for the PCR reactions was cDNA synthesized from rat OE RNA or genomic DNA. It is possible to use genomic DNA as template for the PCR because these receptor genes are encoded in one exon. The 5' and 3' primers consisted of 7 codons of receptor sequence flanked by regulatory sequences for enhancement of translation (Jobling and Gehrke, 1987) and message stability respectively (see fig. 4.2). A second round of PCR was done using the product of the first as template. In this case the primers added a SP6 RNA polymerase promoter at the 5' end and 50 adenosine bases at the 3' end. This secondary PCR product was used as template for *in vitro* transcription.

Transcripts were synthesized in vitro and injected into the oocytes together with CFTR cRNA. cRNA of the G protein G_{olf} and the olfactory adenylyl cyclase (type III) were also tested. One pool of receptor RNAs gave a small (20-60nA) response to a pool of macrocyclic lactones. Subdivision of the odorants and the receptor pools indicated that clone I7 could generate a response to the compound ω-pentadecalactone at a concentration of 10μM. None of the other 10 receptors gave responses to ω-

pentadecalactone. This response could be quite strong but was not consistently of the same magnitude for a given concentration of ω-pentadecalactone. Because of this a dose response relationship was hard to generate. Also no response could be generated with 1μM odorant. Perhaps this was due to solubility problems of these highly hydrophobic compounds. An alternative explanation could be the rather steep dose response relationships that many of the odorants have as determined electrophysiologically with dissociated ORNs (Firestein and Werblin, 1989) (see Fig 1.3).

Interestingly, the odorant response was dependent on coexpression of G_{olf}, and did not work with G_s. Related macrocyclic lactones were tested and it was found that I7 could also respond to 10μM cyclopentadecanone (Exaltone®) (Fig 4.3). With more experiments the response of I7 injected oocytes to ω-pentadecalactone and cyclopentadecanone showed more variability. In some batches of I7 injected oocytes there were never any responses. This batch to batch variability of the I7 receptor response to the ω-pentadecalactone and cyclopentadecanone was further confounded when some oocyte batches, when injected with CFTR alone, could respond to these odorants (Fig 4.4). The variability of response as well as a lack of a consistent response could be explained by inefficiencies in protein expression. Of course, this could also invalidate the negative results with the other receptors, which we considered to be good controls for the I7 ω-pentadecalactone and cyclopentadecanone responses.

Another explanation for variability could be inefficiency in activation of the transduction cascade at steps downstream of the receptor odorant interaction. We are relying on the faithful expression of several proteins (receptor, G protein, cyclase and CFTR) involved in this transduction cascade and changes in expression of any could be a source of response variability. Two ways we have attempted to short circuit the receptor G protein interaction are outlined in Appendix V.

Analysis of olfactory receptor expression in heterologous cells.

Epitope "tagging" of receptors

To examine subcellular distribution of the expressed odorant receptors several were cloned into the multipurpose expression vector pCS2+MT (Rupp et al., 1994; Turner and Weintraub, 1994). pCS2+MT has six copies of a 13 amino acid epitope from the *myc* oncogene against which there is a very good monoclonal antibody (Oncogene science). This vector can be used for either *in vitro* transcription of RNA for injection into oocytes or transient expression in tissue culture cells by transfection. Receptor PCR products from the primary amplification were cloned, sequenced and shuttled into pCS2+MT down stream of the *myc* epitopes such that expression would produce a receptor with the *myc* "tag" fused to the amino terminus. This region of the receptor is believed to reside extracellulary and therefore should also allow detection of surface protein on unpermeabilized cells. As a control we used a construct of the β 2 adrenergic receptor (β2AdR) with an N-terminal 12CA5 (hemagglutinin) epitope fusion (β2AdRHA)(kind gift of Marc Caron, Duke University).

Fractionation of oocytes (Mike Quick)

One way we looked at subcellular localization of receptor protein in the oocytes was by fractionation of oocyte lysates on discontinuous sucrose gradients. Sixty injected oocytes were lysed, fractionated, and analyzed by Western blot as described (Corey et al., 1994). Figure 4.5 shows the results of two such experiments. In A, the fractions from oocytes injected with mRNAs encoding olfactory receptors I7myc (the epitope-tagged version described above) and I9myc were analyzed in parallel with β2AdRHA mRNA injected oocytes. Each oocyte in this case was injected with 10ng of receptor cRNA. The predicted molecular weight of the receptors is 30kDa. This is what is observed in the I7myc injected oocytes. It appears that the I7myc receptor protein can be found in the plasma membrane fraction and in the Golgi fraction. Receptor protein for either I9myc or β2AdRHA could not be detected, although the β2AdRHA-injected oocytes were expressing functional levels of receptor when assayed electrophysiologically. Figure 4.5

B shows a cleaner localization of I7myc receptor to the plasma membrane. These data suggest that the I7myc receptor protein is expressed in the oocytes and is associated with the plasma membrane and Golgi fractions. The I9myc receptor may not be translated efficiently in oocytes.

Antibody staining of oocytes (Jost Vielmetter)

In order to look at subcellular localization in the oocyte at higher resolution we examined expression by direct immunofluorescence of oocyte sections. Figure 4.6 shows cryostat sections of receptor injected oocytes (I7myc or β2AdRHA) that were first stripped of the vitelline membrane and then incubated with the primary and secondary (FITC conjugated) antibodies without permeabilization. The anti-*myc* antibody was used as primary in the case of I7myc and the anti-12CA5 antibody (BMB) in the case of the β2AdRHA receptor. Bright surface staining is detected with the 12CA5 antibody indicating robust surface expression of the β2AdRHA receptor, top two panels.

The staining for the I7myc olfactory receptor shows a very different pattern of localization. The middle two panels show no staining in a region of intact plasma membrane in the I7 injected oocytes. The bottom two panels illustrate that I7 and β 2 appear to be expressed equally well but that I7myc is localized to the inner surface of the plasma membrane. The region shown of the oocyte plasma membrane was damaged, as indicated by the interruption in the pigment. Because this damage occurred before staining with the antibodies, and the rest of the oocyte is intact, the damage site allows limited access to the inside of the oocyte . It is only under this region of damage that expression of I7myc can be seen with this technique, indicating that most if not all of the I7myc olfactory receptor protein is not on the surface of these oocytes. This result clearly shows there is an inefficiency in trafficking. One caveat to keep in mind when considering these results is that in order to detect the β2AdRHA receptor 1000 fold more RNA (100ng) had to be injected than is required to detect expression by an electrophysiological response to agonist (isoproterenol). Thus, a negative result by

immunofluorescence staining doesn't prove necessarily that there is no protein on the surface of the cell, only that the amount of protein is insufficient to visualize over background using immunofluorescence.

An attempt to provide olfactory specific accessory proteins in trans by coinjection of poly A RNA from rat OE failed to change the localization of the I7myc receptor (data not shown).

Transient expression in transfected 293 cells-antibody staining

Expression of five myc tagged odorant receptors (F3, F6, I3, I9, and I7) was analyzed by transfection into 293 cells. Three other receptors (M3, M50, and K18) (Ressler et al., 1993) were analyzed as 12CA5 fusions. About 36 hours after transfection, the cells were fixed and permeabilized with ice-cold methanol and stained with the appropriate antibodies using standard procedures. The expression efficiency varied quite a bit between the eight clones with some showing <1% expression as assayed by immunofluorescence. Only F6 and I7 consistently showed expression in > 10% of the cells. Figure 4.7 shows the results of transfection into 293 cells of the β2AdRHA receptor (A, B) and olfactory receptors F6 (C, D)and I7 (E, F). Figure 4.8 shows representative cells from the same transfections at higher magnification. The red signal is detection of a nuclear localized β-galactosidase protein. The β2AdRHA receptor (A, B) has a very distinctive plasma membrane staining pattern. In contrast, the olfactory receptors I7 (C, D, E, F) and F6 (G) show an intracellular ER or Golgi pattern. Again, this suggests that most of the epitope tagged receptor is sequestered inside the cell.

A similar trafficking problem has been assigned to one class of human autosomal dominant retinitis pigmentosa (ADRP) mutants. These are rhodopsin mutants that are expressed to lower levels, regenerate variably or not at all with 11-*cis*-retinal, and are transported inefficiently to the plasma membrane accumulating in the ER (Fig 4.9)(Sung et al., 1991). Although these mutants have a clear intracellular trafficking problem they

do function, albeit poorly. Therefore the possibility exists that some of the olfactory receptor is also on the surface.

Transient expression in transfected HEK293 cells-FACS analysis

In order to determine if the olfactory receptors were on the surface at a low level when expressed in the HEK293 cells we used fluorescence activated cell sorting (FACS). This takes advantage of the extracellular location of the *myc* epitope tag on the olfactory receptors, and the 12CA5 epitope on the β2AdRHA. As a control for "leaky" cells that might allow intracellular access to antibody we cotransfected cells with a plasmid that expressed a cytoplasmic form of β-galactosidase and sorted with an anti-β-galactosidase monoclonal antibody (Promega). 36 hours after transfection the cells were removed from the plates without trypsin and incubated with the antibodies, each for 15 min with two washes in between. The results of the sorting I7myc (A and B) or β2AdRHA (C and D) transfected 293 cells are shown in figure 4.10. The boxes represent the cut-off for positive cells. In A the background of cells sorted with the anti-β-galactosidase antibody is 0.1%. When the myc antibody is used there are 0.8% positive cells (B). C is the negative control for the β2AdRHA transfected cells (0.3%), and with the 12CA5 antibody close to 10% of the cells show surface expression of the β2AdR. Both populations of transfected cells had equal numbers of cells expressing β-galactosidase as assayed by x-gal staining (data not shown). These data suggest that some cells have I7 receptor on the surface. Calculating from the number of cell sorted as positive, a typical 10cm plate of transfected HEK293 cell would yield ~3000 cells with I7 receptor on the surface. These cells could then be analyzed for odorant response with the FURA based Ca^{2+} immaging assay outlined in Appendix III.

One mechanism of seven helix receptor trafficking control has been worked out with the aid of *Drosophila* genetics. In the *Drosophila* eye the cyclophilin (CyP) homologue NinaA functions as a chaperone, forming a stable complex *in vivo* with its protein target NinaE, rhodopsin I (Rh1) (Baker et al., 1994) reviewed in (Stamnes et al.,

1992). CyPs are a highly conserved family of proteins that have peptidyl-prolyl *cis-trans* isomerase (PPIase) activity implicating them in catalyzing protein folding. In the fly NinaA is a photoreceptor specific CyP required for proper surface expression of the visual pigment RhI. RhI is synthesized in the ER and transported via the secratory pathway to the rhabdomeres (micro-villar light-transducing organelles) where it functions in phototransduction. In the absence of NinaA opsin accumulates in the ER and is not transported to the rhabdomeres, resulting in expansion of the ER network and decreased levels of rhodopsin.

A second relevant example of CyP mediated regulation of protein trafficking was demonstrated in *Xenopus* oocytes(Helekar et al., 1994). In this case it was shown that cyclosporin A, a potent antagonist of cyclophinin, reduced the surface expression of the homooligomeric nicotinic acetylcholine receptor subunit $\alpha 7$ without blocking protein synthesis. These authors demonstrated that the effect of cyclosporin A was reversed by overexpression of rat brain cyclophinin in the oocytes. It would therefore be of interest to see if cotransfection of cyclophinin with the olfactory receptors could increase the positive fraction above 1% in the FACS analysis.

References

E. K. Baker, N. J. Colley and C. S. Zuker (1994). The cyclophilin homolog NinaA functions as a chaperone, forming a stable complex *in vivo* with its protein target rhodopsin. EMBO *13*, 4895-4895.

I. Boekhoff and H. Breer (1990). Differential stimulation of second messenger pathways by distinct classes of odorants. Neurochem. Int. *17*, 553-557.

H. Breer (1991). Molecular reaction cascades in olfactory signal transduction. J. Steroid Biochem. Molec. Bio. *39*, 621-625.

L. Buck and R. Axel (1991). A novel multigene family may encode odorant receptors: a molecular basis for odor recognition. Cell *65*, 175-187.

J. L. Corey, N. Davidson, H. A. Lester, N. Brecha and M. W. Quick (1994). Protein-kinase-c modulates the activity of a cloned gamma-aminobutyric-acid transporter expressed in xenopus-oocytes via regulated subcellular redistribution of the transporter. J. Biol. Chem. *269*, 14759-14767.

N. Dascal (1987). The use of xenopus oocytes for the study of ion channels. CRC Crit. Rev. Biochem. *22*, 317-387.

S. Firestein and F. Werblin (1989). Odor-induced membrane currents in vertebrate-olfactory receptor neurons. Science *244*, 79-82.

S. A. Helekar, D. Char, S. Neff and J. Patrick (1994). Prolyl isomerase requirement for the expression of functional homooligomeric ligand-gated ion channels. Neuron *12*, 179-189.

S. A. Jobling and L. Gehrke (1987). Enhanced translation of chimaeric messenger RNAs containing a plant viral untranslated leader sequence. Nature *325*, 622-625.

K. Raming, J. Krieger, J. Strotmann, I. Boekhoff, S. Kubick, C. Baumstark and H. Breer (1993). Cloning and expression of odorant receptors. Nature 353-356.

R. R. Reed (1992). Signaling pathways in odorant detection. Neuron *8*, 205-209.

K. J. Ressler, S. L. Sullivan and L. B. Buck (1993). A zonal organization of odorant receptor gene expression in the olfactory epithelium. Cell *73*, 597-610.

R. A. W. Rupp, L. Snider and H. Weintraub (1994). *Xenopus*-embryos regulate the nuclear-localization of XMyoD. Gene Dev. *8*, 1311-1323.

M. A. Stamnes, S. L. Rutherford and C. S. Zuker (1992). Cyclophilins: a new family of proteins involved in intracellular folding. Trend. Cell Bio. *2*, 272-276.

C. H. Sung, B. G. Schneider, N. Agarwal, D. S. Papermaster and J. Nathans (1991). Functional-heterogeneity of mutant rhodopsins responsible for autosomal retinitis-pigmentosa. Proc. Natl. Acad. Sci. *88*, 8840-8844.

D. L. Turner and H. Weintraub (1994). Expression of achaete-scute homolog-3 in xenopus-embryos converts ectodermal cells to a neural fate. Gene Dev. *8*, 1434-1447.

Figure Legends

Fig 4.0 Schematic diagram of olfactory signal transduction.

Odorant interacts with a seven helix receptor (7HR) activating a G protein (G) which stimulates adenylyl cyclase (AC) to produce cAMP. cAMP opens the cng channel allowing Ca^{2+} influx. Ca^{2+} down regulates the cng channels sensitivity to cAMP and gates a Cl^- channel amplifying the depolarization.

Fig 4.1 Functional assay for receptors that couple to the production of cAMP or IP_3.

Schematic representation of the pathways for assay of receptors that couple to the production of the second messenger IP3 (blue) or cAMP (red). Representative currents are displayed below. It is noted that the CFTR current shows slower onset and longer duration than the endogenous Ca^{2+} activated Cl^-curent.

Fig 4.2 DNA primers used to amplify the olfactory receptors

Shown is the sequence of the primer used for primary PCR of the F3 receptor. Each receptor was then reamplified with the same secondary primers. The 5' primer was designed to incorporate the SP6 transcription promoter and a translation enhancer from alfalfa mosaic virus (AMV)(Jobling and Gehrke, 1987). The 3' primer incorporated a portion of the 3' untranslated sequence from Xenopus beta-globin and 50 adenosine bases. A tail.

Fig 4.3 CFTR current responses to odorant of an I7 (cRNA) injected oocyte (10ng), Golf (5ng), ACIII (5ng), CFTR (1ng) injected (cRNA) oocyte under voltage clamp (-80mV). 1). mixture of 5 heterocycles at 5μM each, 2). mixture of 5 non-aromatic ketones at 5μM each, 3). mixture of 5 aliphatic aldehydes at 5μM each, 4). 10μM ω-pentadecalactone, 5). 10μM cyclopentadecanone

Fig 4.4 CFTR current responses to odorant of an oocyte without receptor injected with Golf (5ng), ACIII (5ng), CFTR (1ng) injected (cRNA) oocyte under voltage clamp (-80mV).
1). ω-pentadecalactone (10μM), 2). cyclopentadecanone (10μM), 3). ω-pentadecalactone (100μM),4). a mixture of 6 macrocyclic lactones (ω-pentadecalactone, ω-tetradecalactone, ω-hexadecalactone, 11-oxahexadecalactone, 12-oxaheacecalactone and ethylene brassylate), 5). A mixture of 5 heterocycles (3-acetyl- pyridine, cyclacet, iso butyl guinoline, indole and coumarin)

Fig 4.5 Western blot of receptor (cRNA) injected oocytes. Approximatly 20 μg of protein was loaded per lane. A), plasma membrane (PM), Golgi (G), and endoplasmic reticulum (ER) fractions from discontinuous sucrose gradients blotted against both the anti-myc and anti-12CA5 mouse monoclonal antibodies. B), same as in A but a different batch of oocytes

Fig 4.6 Sections of oocytes after staining with anti-epitope tag antibodies. Top two panels), β2AdRHA expressing oocytes, middle two panels), intact region of I7myc expressing oocyte, bottom two panels), region of damaged plasma membrane of I7myc-expressing oocyte

Fig 4.7 Staining of receptor transfected HEK293 cells, low magnificationA, B) β2AdRHA; C, D) F6myc; E, F) I7myc, at a magnification of 250x

Fig 4.8 Staining of receptor transfected HEK293 cells-high magnification. A, B) β2AdRHA; C-F) I7myc; G) F6myc, at a magnification of 788x

Fig 4.9 Rhodopsin mutants, Sung, C.H., *et al.* Proc. Natl. Acad. Sci. 88 p8840-8844 1991

Fig 4.10 FACS analysis of beta-galactosidase (β-gal) and I7myc receptor cotransfected HEK293 cells. A and B) I7myc+β-gal transfected, C and D) β2AdRHA +beta-gal transfected. A and C) sorted with anti-beta-gal monoclonal, B) sorted with anti-myc monoclonal, D) sorted with anti-12CA5 monoclonal. Sorting of I7myc+betagal transfected cells with the 12CA5 monoclonal, 0.1% (data not shown). Sorting of β2AdRHA +beta-gal transfected cells with the anti-myc monoclonal, 0.3%.(data not shown).

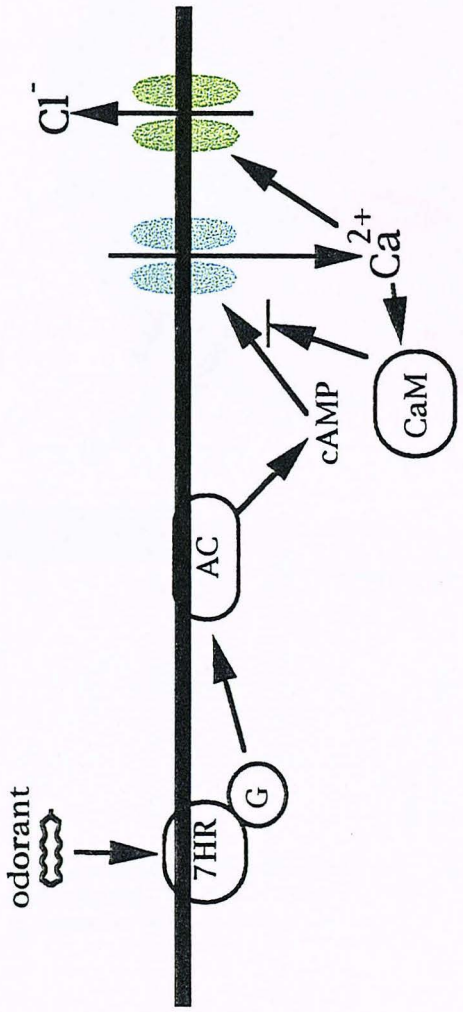
odorant
7HR
G
AC
cAMP
CaM
Ca^{2+}
Cl^-

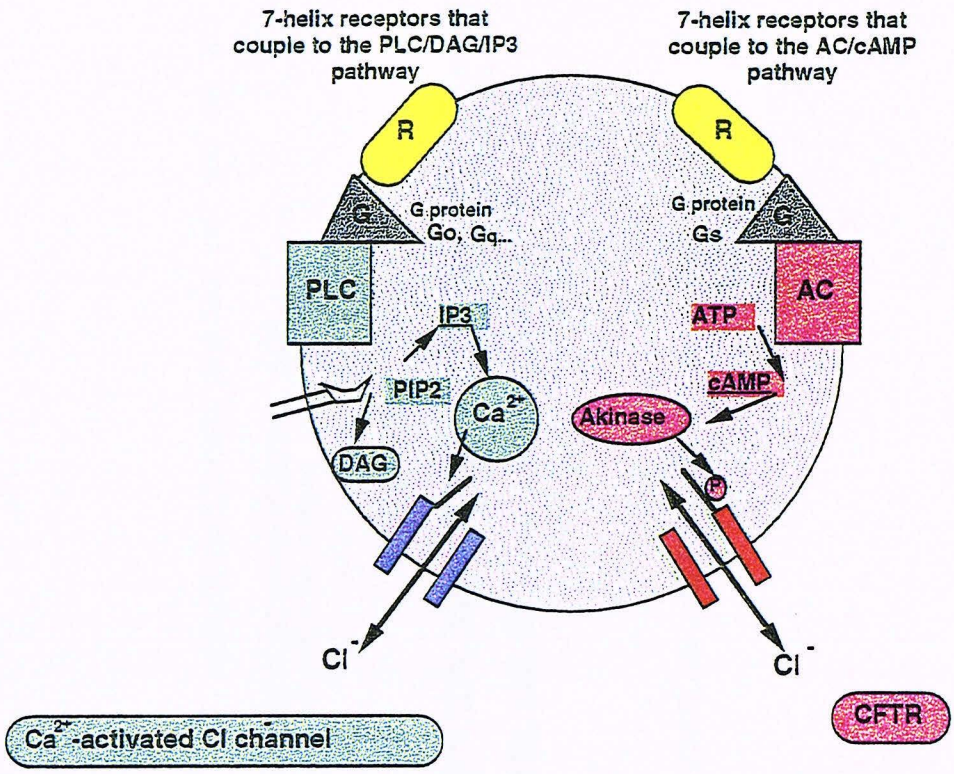

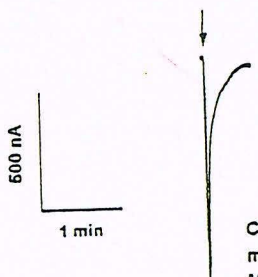

Ca^{2+} activated Cl^- current by 50 μM ACh
mRNA injected:
M_3 muscarinic receptor: 10 ng

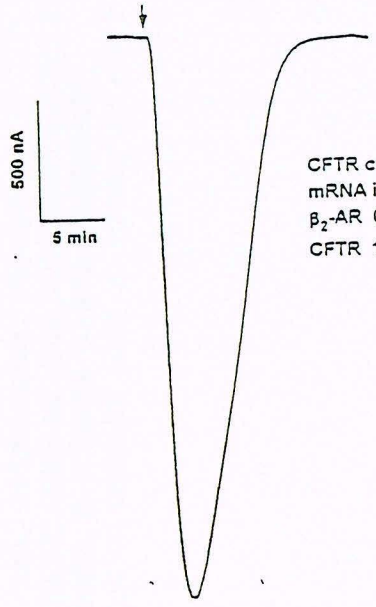

CFTR current induced by 10 μM Is
mRNA injected:
β_2-AR 0.5 ng
CFTR 1 ng

5' primers

F3-5' primer TTTCAAATACTTCCACC *ATG* GAC *TCA AGC AAC AGG ACA*

SP6-ATG primer 5'GAC{A/AGCTT}**ATTTAGGTGACACTATAGAATC**TTTCTTTCAAATACTTCCACC *ATG*

⇒ start of transcription

3' primers

F3-3'primer 5'**TTC GGGTG TTC TTG AGG CTG GT** *TTA ATA ACA AAA AAT AAA ACA AGG*

Xen 3'βglob pA $(T)_{48}$ 5'**TTC GGGTG TTC TTG AGG CTG GT**

D18

A SP6 RNA POLYMERASE PROMOTOR

A REGION OF OVERLAP USED TO DIRTCT 2°PCR (5' SEQUENCE IS AMV TRANSLATION ENHANCER)

A **XENOPUS ß-GLOBIN 3'NTR SEQUENCE**

A REGION OF OVERLAP USED TO DIRECT 1° PCR

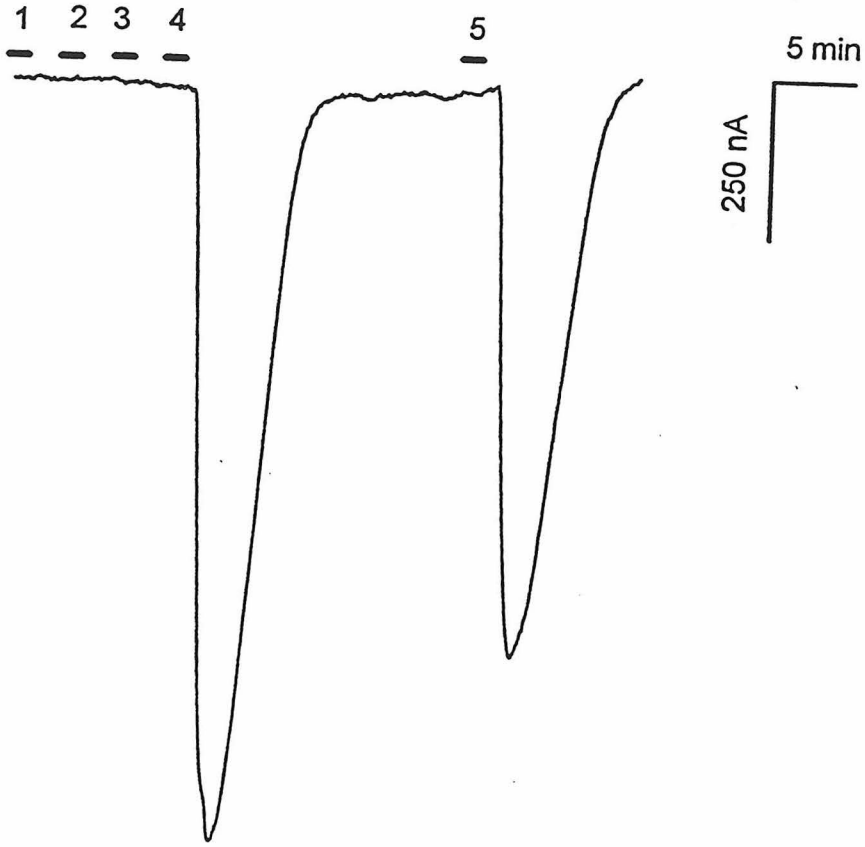
1
2
3
4
5
5 min
250 nA

D20

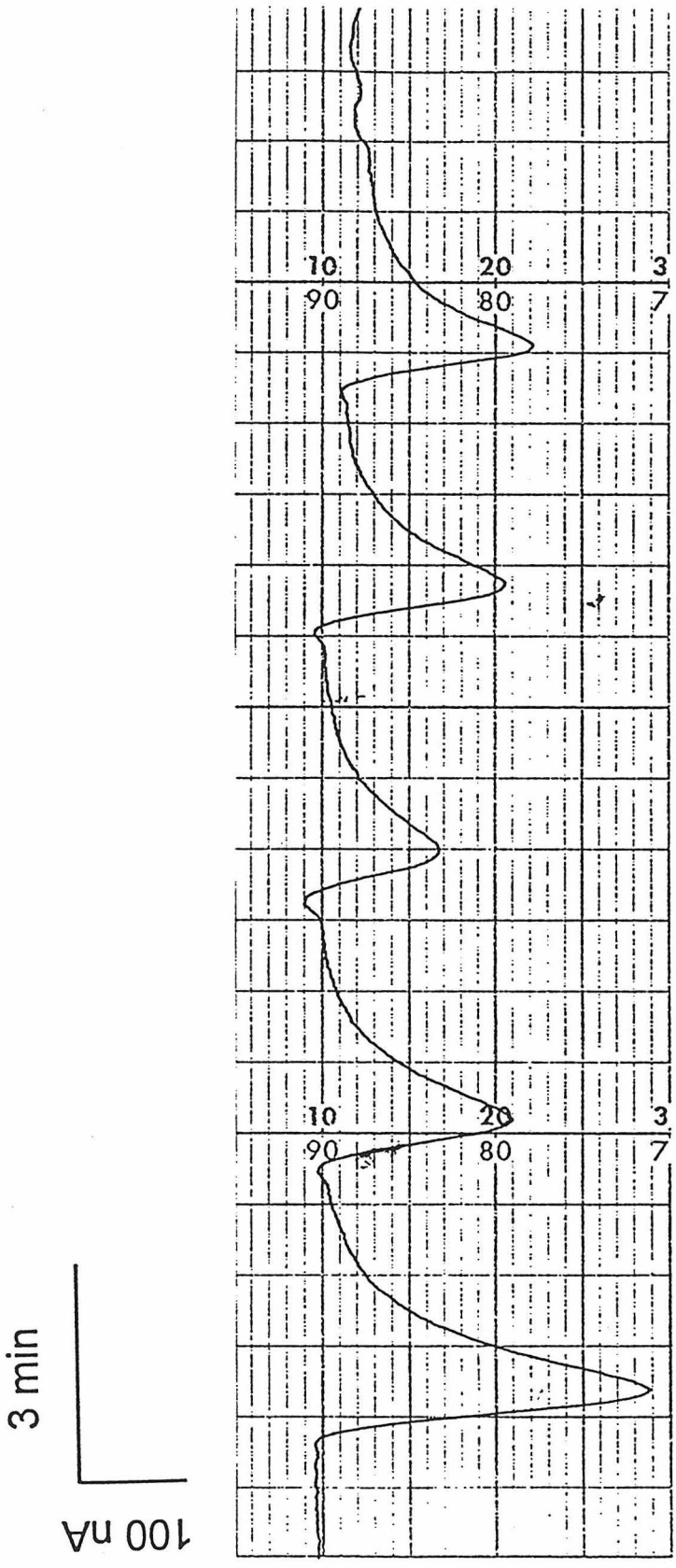

A

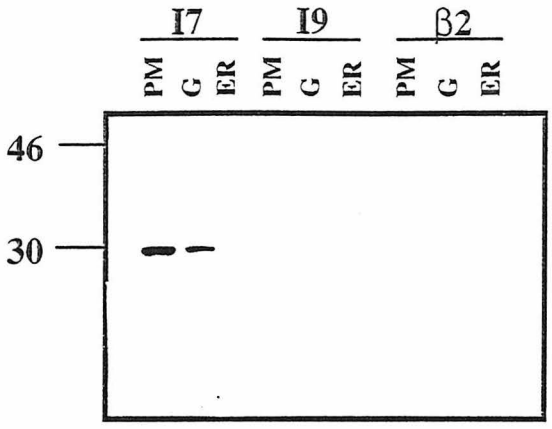

B

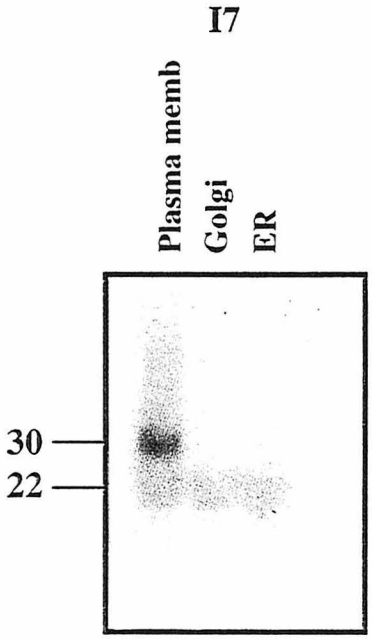

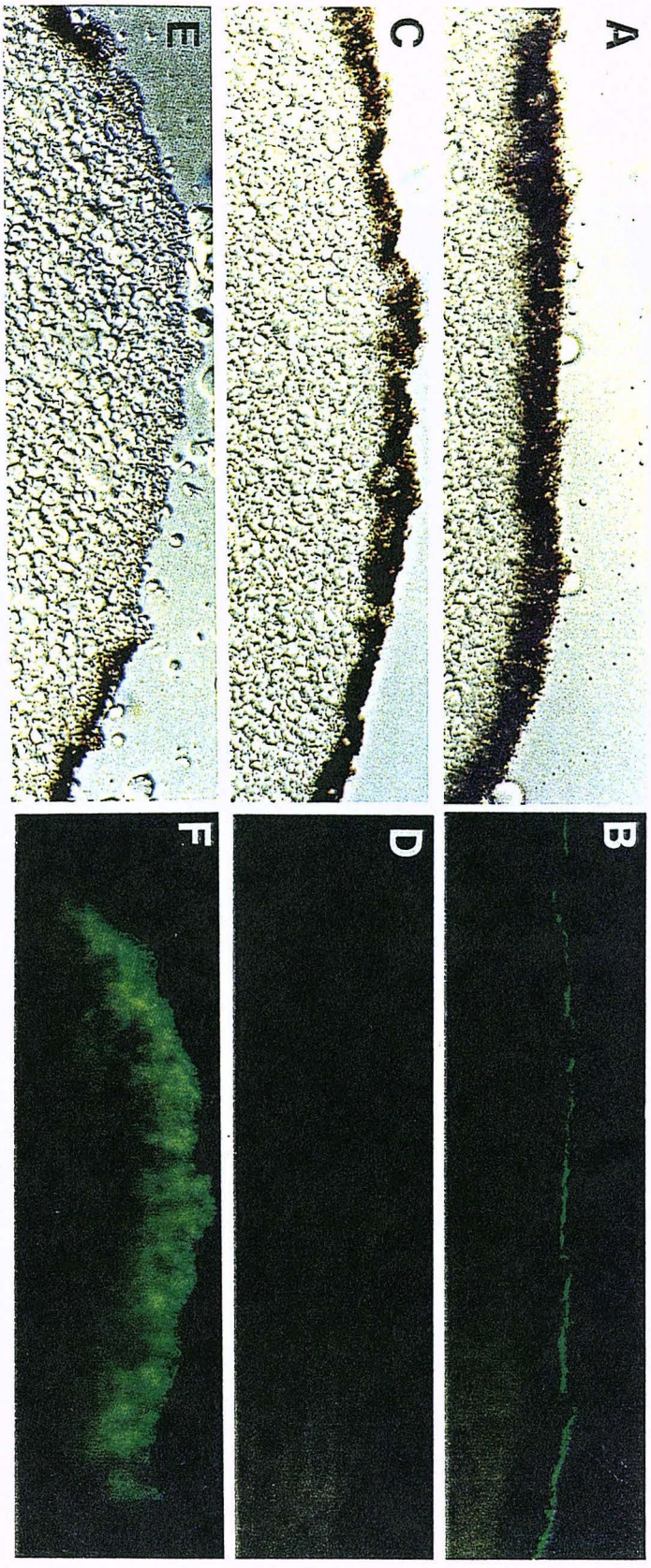
A
B
C
D
E
F

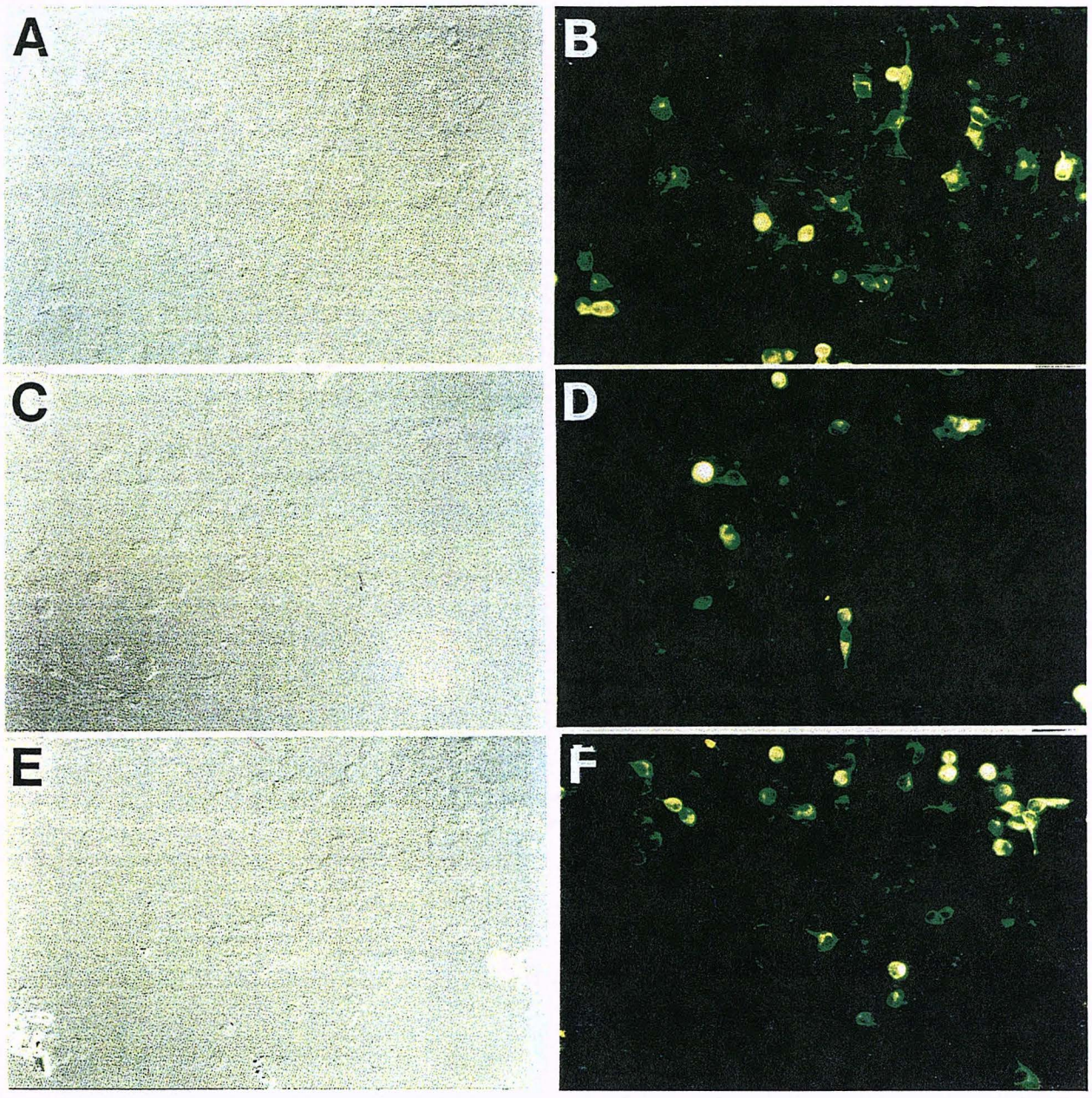
A
B
C
D
E
F

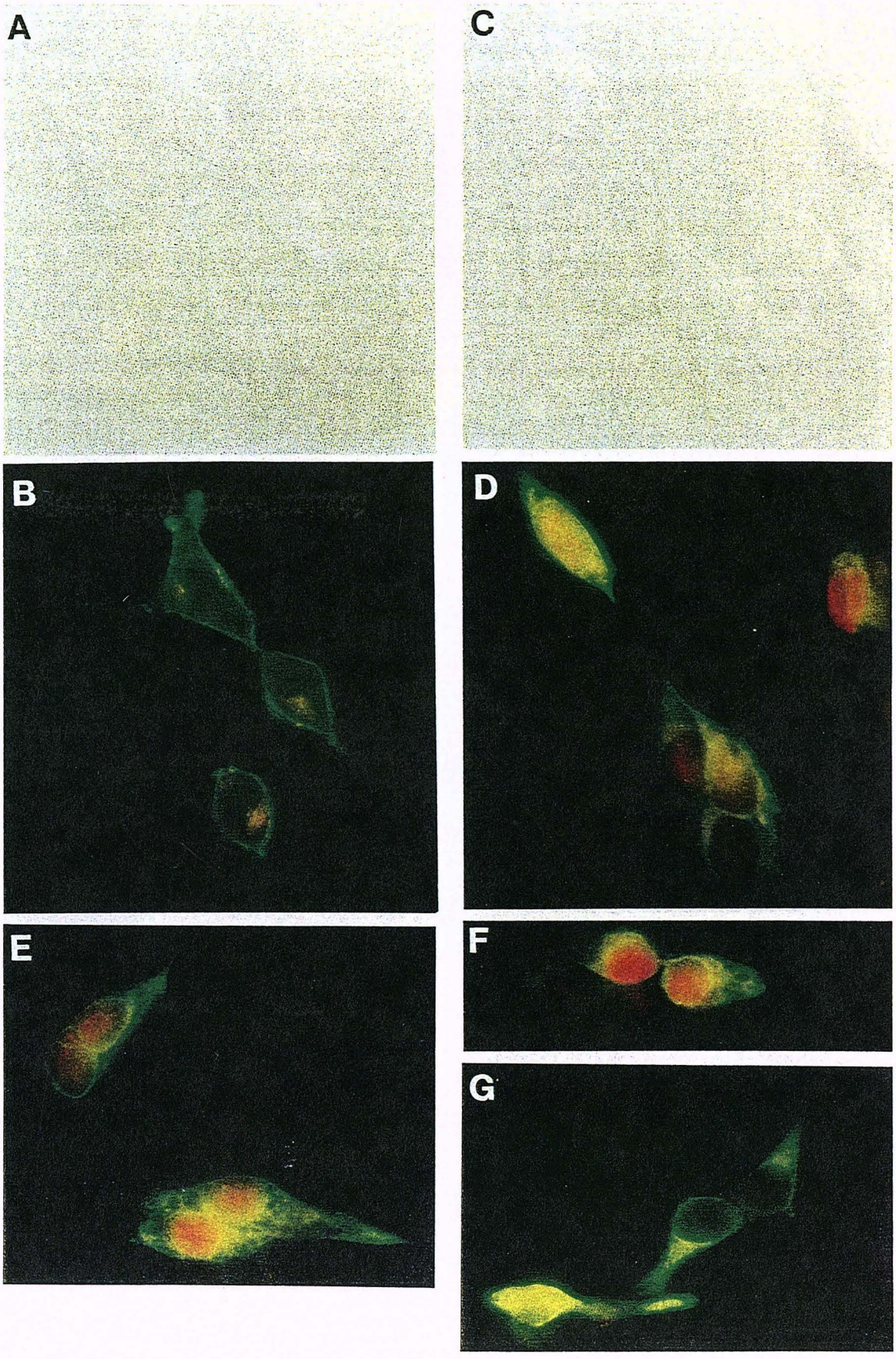
A
C
B
D
E
F
G

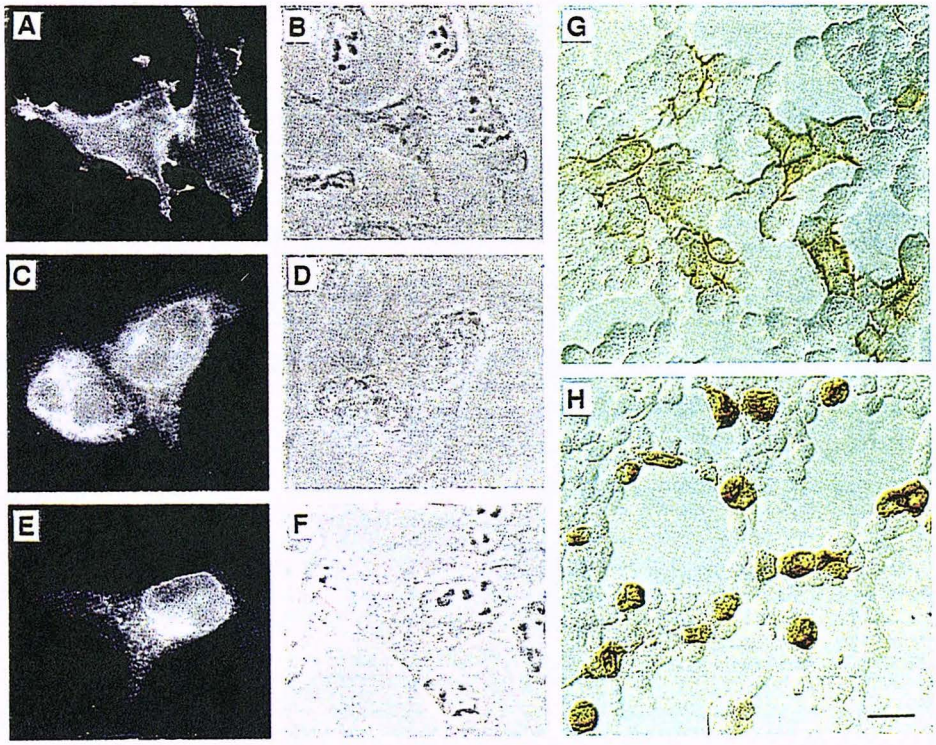

FIG. 4. Immunolocalization of wt opsin (*A*, *B*, and *G*) and mutants P23H (*C*, *D*, and *H*), and Y178C (*E* and *F*) in transiently transfected 293S cells. Cells were fixed 24 hr after transfection and stained with mAb 1D4 followed by a fluorescent second antibody (*A–F*) or horseradish peroxidase-coupled avidin–biotin complex (*G* and *H*). *B*, *D*, and *F* are the phase-contrast counterparts of *A*, *C*, and *E*, respectively. [Bar = 10 μm (*A–F*) and 25 μm (*G* and *H*)].

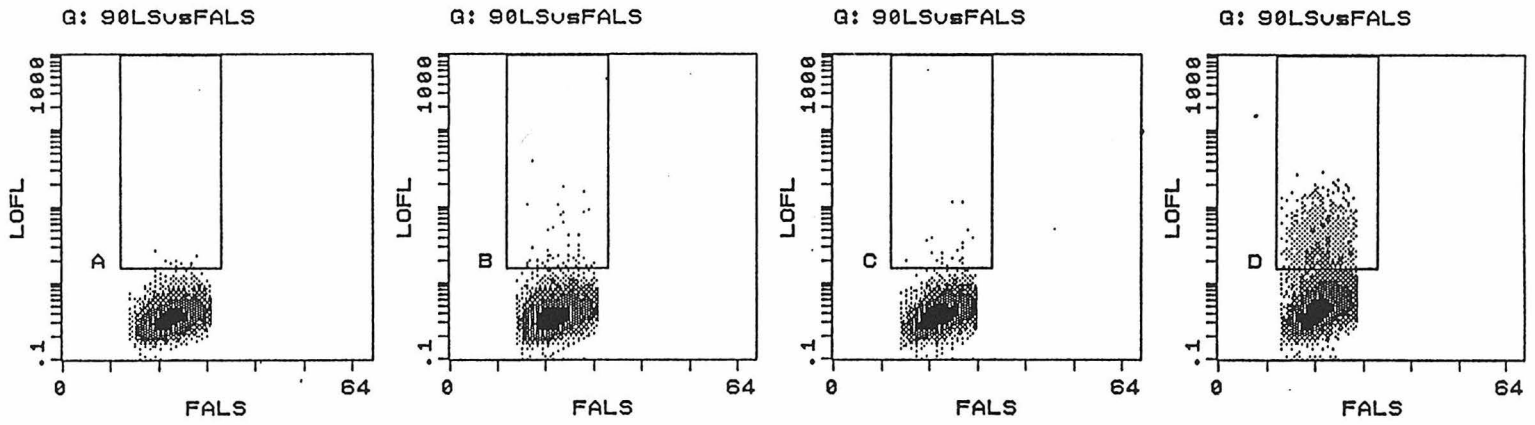

STATISTICS

DUAL PARAMETER STATISTICS

			.....Peak.....		....X Channel....			....Y Channel....		
ID	Pcnt	Area	Position	Height	Mean	SD	CV	Mean	SD	CV
A	0.1	12	15, 2.8	1	22.5	3.6	16.2	1.98	0.443	22.4
B	0.8	81	28, 1.6	5	23.5	4.0	16.8	2.55	1,77	69.6
C	0.3	30	26, 1.8	3	23.8	3.1	12.9	2.46	1.29	52.5
D	9.7	969	20, 3.2	15	21.1	3.6	16.8	3.56	2.26	63.7

Appendix I

Restriction analysis of PCR products generated with the CN1 (BZ2) and CN2 (BZ1) primers.

I used restriction analysis to determine if the 125bp PCR product generated from the nasal epithelial cDNA was unique or a mixture of products all the same size. This approach had been used previously to determine the heterogeneous character of a PCR product(Buck and Axel, 1991).

PCR was done using cDNA synthesized from rat olfactory epithelial RNA (NE), or plasmid DNA of the rOCNC1 clone(Dhallan et al., 1990). Between the primers used for the PCR there are restriction sites for several enzymes (Hinf I, DdeI, and Pvu II) in the rOCNC1 sequence (see top of Fig. AI 1). These restriction enzymes were used to diagnostically characterize the PCR products generated either from the NE cDNA or the rOCNC1 clone. The results are shown in Figure AI 1 and indicate that the product from PCR with rOCNC1 digests completely to bands of the expected size (Hinf I, 26bp, 99bp; Pvu II, 46bp, 79bp; DdeI, 28bp, 16bp, 81bp). In contrast the product from PCR with the NE cDNA digests only partially with the same restriction enzymes as indicated by the residual 125bp band.

To determine if the residual DNA was indeed new sequence and not DNA with the rOCNC1 sequence that was unrestrictable for some reason I tested for restriction with several enzymes (Hae III, Mbo I, Msp I) not having sites in rOCNC1 or bRCNC1 (bovine rod cng channel) (Kaupp et al., 1989)in this region. The results are shown in Figure AI 2. In this case the rOCNC1 PCR product is resistant to digestion as expected. The NE cDNA PCR product, on the other hand, does have a species that restricts with Mbo I indicating a heterogeneity in the NE PCR product with a novel restriction pattern. To examine this novel sequence I cloned and sequenced the Pvu II resistant fraction of the

NE cDNA PCR product. This new sequence (with an Mbo I site) was used to clone rOCNC2.

References

L. Buck and R. Axel (1991). A novel multigene family may encode odorant receptors: a molecular basis for odor recognition. Cell *65*, 175-187.

R. S. Dhallan, K.-W. Yau, K. A. Schrader and R. R. Reed (1990). Primary structure and functional expression of a cyclic nucleotide-activated channel from olfactory neurons. Nature *347*, 184-187.

U. B. Kaupp, T. Niidome, T. Tanabe, S. Terada, W. Bonigk, W. Stuhmer, W. J. Cook, K. Kangawa, H. Matsuko, T. Hirose, T. Miyata and S. Numa (1989). Primary structure and functional expression from complementary cDNA of the rod photoreceptor cyclic GMP-gated channel. Nature *342*, 762-766.

Figures

Fig AI 1. Restriction analysis with Hinf I, DdeI, and Pvu II

Fig AI 2. Restriction analysis with Hae III, Mbo I, and Msp I

HinfI
DdeI
PvuII
DdeI

primer BZ2

AAATTGGCAGTGGTAGCTGATGATGGCGTGACTCAGTATGCCTTGCTCTCAGCTGGGAGCTGC
K L A V V A D D G V T Q Y A L L S A G S C

primer BZ1

TTTGGTGAGATTAGTATCCTTAACATTAAGGGTAGCAAAATGGGCAATCGACGTACTGCTAATAT
F G E I S I L N I K G S K M G N R R T A N I

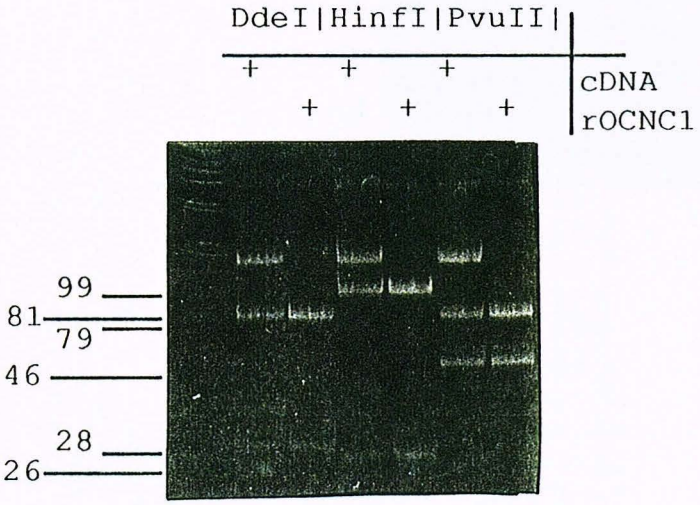

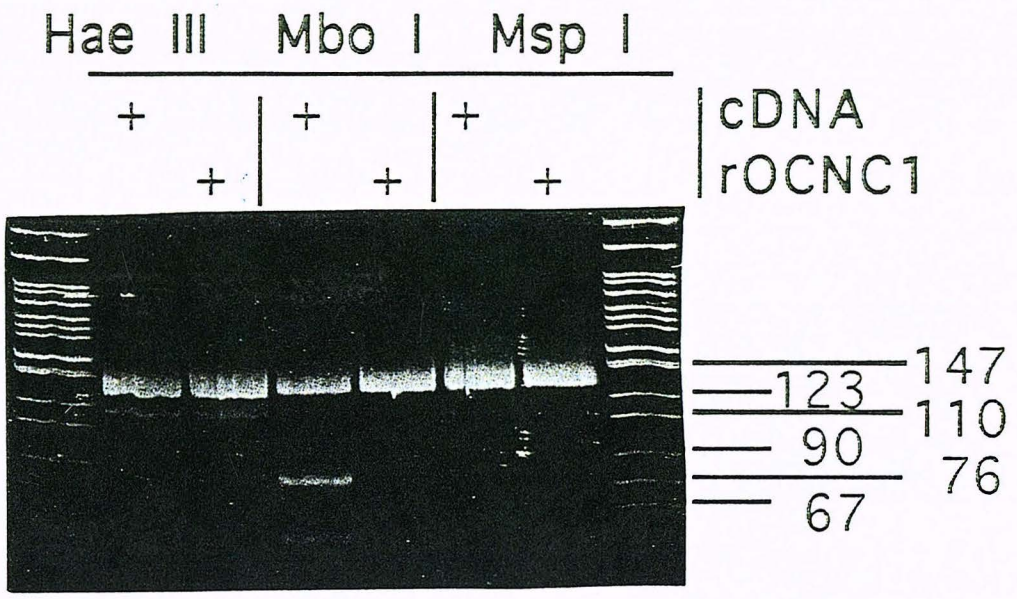
Hae III
Mbo I
Msp I
+
+
+
+
+
+
cDNA
rOCNC1
147
123
110
90
76
67

Appendix II Receptors that couple to 2 classes of G-proteins increase cAMP and activate CFTR expressed in *Xenopus*-oocytes

Published as an article in Receptors and Channels *1* 223-241 (1993)

Receptors and Channels, Vol. 1, pp. 233–241
Reprints available directly from the publisher
Photocopying permitted by license only

AII2

Receptors that Couple to 2 Classes of G Proteins Increase cAMP and Activate CFTR Expressed in *Xenopus* Oocytes

Y. UEZONO, J. BRADLEY, C. MIN, N. A. McCARTY, M. QUICK, J. R. RIORDAN[1], C. CHAVKIN[2], K. ZINN, H. A. LESTER*, and N. DAVIDSON

Division of Biology, California Institute of Technology, Pasadena CA 91125. [1]The Hospital for Sick Children, 555 University Avenue, Toronto, Ontario, Canada M5G 1X8. [2]Department of Pharmacology SJ-30, University of Washington, Seattle WA 98125

(Received March 15, 1993, Revised May 15, 1993)

The cystic fibrosis transmembrane conductance regulator (CFTR), a Cl^- channel activated by phosphorylation, was expressed in *Xenopus* ooctyes along with various combinations of several other components of the cAMP signalling pathway. Activation of the coexpressed β2 adrenergic receptor increased cAMP and led to CFTR activation. The activation of CFTR (1) requires only short (15 s) exposure to isoproterenol, (2) occurs for agonist concentrations 100–1000 fold lower than those that produce cAMP increases detectable by a radioimmunoassay, (3) requires injection of only 5 pg of receptor cRNA per oocyte, and (4) can be increased further by coexpression of cRNA for adenylyl cyclase type II or III or for Gsα. In addition, CFTR activation and cAMP increases by β2 activation were enhanced by activation of the coexpressed 5HT1A receptor, which is thought to couple to Gi. The additional activation by the 5HT1A receptor was enhanced by coexpression of adenylyl cyclase type II but not with type III and may proceed via the $\beta\gamma$ subunits of a G protein. The sensitivity of the assay system is also demonstrated by responses to vasoactive intestinal peptide and to pituitary adenylate cyclase-activating polypeptide in oocytes injected with cerebral cortex mRNA.

KEY WORDS: Gs Gi cystic fibrosis β2 receptor serotonin receptors

INTRODUCTION

Cystic fibrosis is the most common inherited recessive disease in Caucasian societies. Most pathophysiological aspects of cystic fibrosis can be explained by a defect in regulated Cl^- transport. The single gene responsible for this disease encodes a protein termed the cystic fibrosis transmembrane conductance regulator (CFTR; Riordan *et al.*, 1989). CFTR is a Cl^- channel activated via phosphorylation by A kinase and perhaps by other kinases as well (Anderson *et al.*, 1991; Kartner *et al.*, 1991; Welsh *et al.*, 1992).

Xenopus oocytes are a convenient system for the heterologous expression of (a) 7-helix receptors coupled to G proteins, (b) intracellular messenger systems activated by G proteins, and (c) ion channels. It therefore seemed to us that oocyte reconstitution of the entire pathway, leading from activation of a 7-helix receptor to activation of CFTR, might allow quantitative measurements that in turn could afford new insights into such signalling mechanisms. We report experiments showing that such reconstitution does reveal the expected activation of CFTR by receptors that couple to Gs. Furthermore, we describe an unexpected further activation by receptors that couple to Gi.

Xenopus oocytes also constitute a highly sensitive system for the cloning, by functional expression, of 7-helix receptors that activate phosphatidyl inositol

turnover. This sensitivity derives from the presence of an endogenous signalling pathway that underlies the fast block to polyspermy in mature oocytes (Dascal, 1987; Lester, 1988). The pathway is presumably coupled to the putative sperm receptor and comprises G protein(s), phospholipase C, inositol trisphosphate (IP_3)-sensitive internal Ca^{2+} stores, and Ca^{2+}-activated Cl^- channels in the plasma membrane. There has been no comparably sensitive method for the detection of receptors that couple to the cAMP pathway. The reconstituted $\beta 2$ receptor/CFTR system was expected to include several stages of enzymatic amplification: activation of G proteins by receptors, activation of adenylyl cyclases by G proteins, activation of A-kinase by cAMP, and activation of CFTR by A-kinase phosphorylation. We therefore hoped that this system might have comparable sensitivity to the phospholipase system. We report here that expression of CFTR in ooctyes does provide an assay system for receptors that activate Gs and that this method is more sensitive than radioimmunoassay (RIA), a commonly used assay for cAMP.

RESULTS

Activation by cAMP cocktail

Noninjected defolliculated oocytes do not respond with detectable conductance changes or other electrophysiological signals to agents that increase cAMP. Oocytes injected with CFTR cRNA respond to such agents with a conductance increase to Cl^- (Figure 1), as reported in detail earlier (McCarty *et al.*, 1992; McDonough *et al.*, 1993; McCarty *et al.*, 1993) and independently by others (Bear *et al.*, 1991; Drumm *et al.*, 1991).

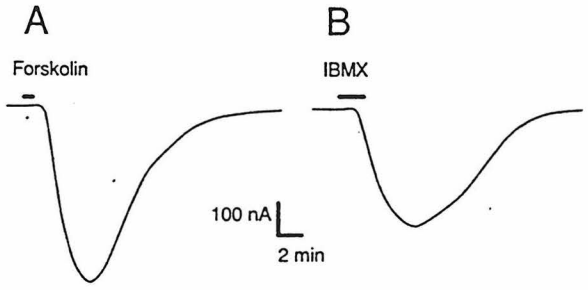

Figure 1 Agents that increase cAMP cause inward currents in oocytes expressing CFTR. Oocytes injected with 1 ng CFTR cRNA were voltage clamped at a holding potential of −80 mV. Drugs were present in the bathing solution during the times indicated by the bars. (A) Response to a 30-s application of forskolin (100 μM). (B) Response to a 120-s application of isobutyl methylxanthine (100 μM) in a different oocyte. Inward currents are shown by downward deflections of the trace in this and subsequent illustrations.

Activation by β2-adrenergic receptors

There are no endogenous responses to β-adrenergic agonists in noninjected, defolliculated oocytes. In addition, receptors thought to couple primarily to Gs produce little or no electrophysiological signals when expressed in defolliculated oocytes. For instance, oocytes injected with cRNA for the human $\beta 2$ adrenergic receptor (Kobilka *et al.*, 1987) showed <10 nA responses in all of >10 batches (Figure 2A, left panel). There were also no responses to isoproterenol, a typical β-adrenergic

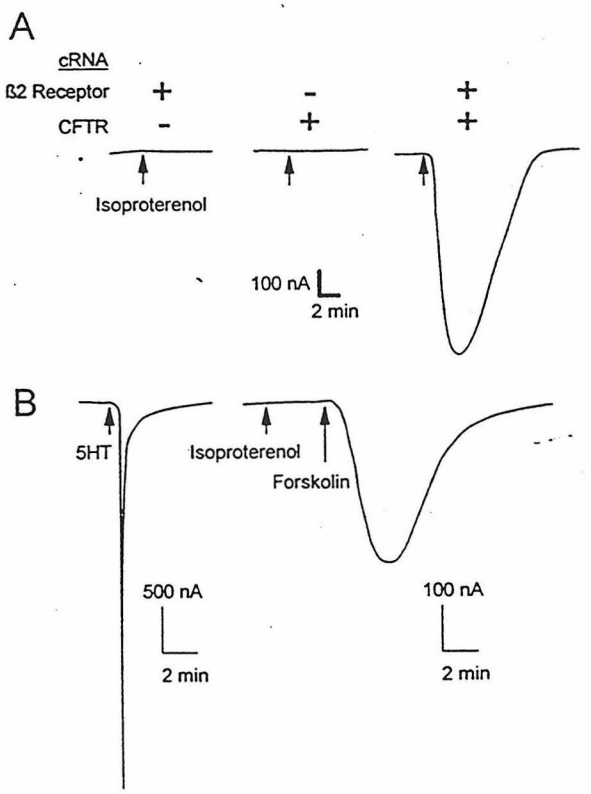

Figure 2 Specificity of the isoproterenol-induced conductance. (A) Tracings of voltage-clamp currents in 3 oocytes from the same batch. Left panel, oocyte injected with 0.1 ng $\beta 2$ receptor cRNA. Middle panel, oocyte injected with 1 ng CFTR cRNA. Right panel, oocyte coinjected with 0.1 ng $\beta 2$ receptor cRNA and 1 ng CFTR cRNA. Isoproterenol 10^{-8} M was applied to each oocyte. (B) An oocyte coinjected with 10 pg serotonin 5HT1C receptor cRNA and 1 ng CFTR cRNA. 5HT (10^{-7} M) evoked a typical Ca^{2+}-activated Cl^- current but no CFTR current as seen with application of forskolin (10^{-4} M). Isoproterenol (1 μM) evoked no current. Isoproterenol or 5HT were applied for 15 s in each case at the time indicated by the arrow; forskolin was applied for 30 s.

agonist, in oocytes injected with CFTR cRNA alone (Figure 2A, middle panel). However, oocytes coinjected with cRNA for the β2 receptor and CFTR showed robust currents in each of >30 batches assayed (Figure 2A, right panel).

These responses were specific to the β2-adrenergic receptor, as shown by the following results. (1) Serotonin (5HT) produced no CFTR responses in oocytes coinjected with the 5HT1C receptor and CFTR, although 5HT did produce a much more rapid response via a different pathway (Figure 2B, left panel; this response is distinguished from the CFTR response in the next section). In these oocytes injected with the 5HT1C receptor and CFTR, responses to forskolin showed that cAMP activation could still lead to CFTR activation with the expected waveform (Figure 2B, right panel). (2) 5HT also produced no effects in oocytes coinjected with cRNA for the 5HT1A receptor and CFTR (data not shown). (3) 5HT produced no responses in oocytes coinjected with cRNA for the β2 adrenergic receptor and CFTR (data not shown).

Characterization of Cl^- conductance The cAMP-dependent responses displayed a reversal potential between -20 and -30 mV (Figure 3A, B). When the external Cl^- concentration was decreased by 10-fold, this reversal potential changed by ~ +55 mV, close to the 58 mV expected for a pure Cl^- conductance (Figure 3C).

A large number of 7-helix receptors that activate phosphatidyl inositol turnover, for instance the serotonin 5HT1C receptor, liberate Ca^{2+} from intracellular stores and activate endogenous Ca^{2+}-activated Cl^- channels. Both the CFTR and these endogenous Ca^{2+}-activated Cl^- channels would be expected to display the dependence on $[Cl^-]$ shown in Figure 3C. However, the β2/CFTR response differs from the endogenous Ca^{2+}-activated Cl^- channel pathway in several ways. (1) All known responses due to phosphatidyl inositol turnover are transient, peaking within 15 s of agonist application and decaying with a half-time of <30 s (Figure 2B, left-hand panel). In contrast, the β2/CFTR response peaks ~3 min after agonist application and has a half-decay time of ~2 min (Figure 2B, right-hand panel). (2) The I-V relation for the CFTR response displays only slight outward rectification in 100 mM external Cl^-; in contrast, the Ca^{2+}-activated Cl^- conductance shows pronounced outward rectification (Figure 3A) as reported previously (Takahashi *et al.*, 1987). (3) The CFTR response shows little hysteresis during the 500 ms ramps; in contrast, the Ca^{2+}-activated Cl^- conductance shows substantial hysteresis (Figure 3A). (4) The CFTR response is blocked in a voltage-dependent fashion by 200 μM diphenyl-2-carboxylate (DPC) in agreement with previous results on DPC blockade of CFTR (Figure 3B); in

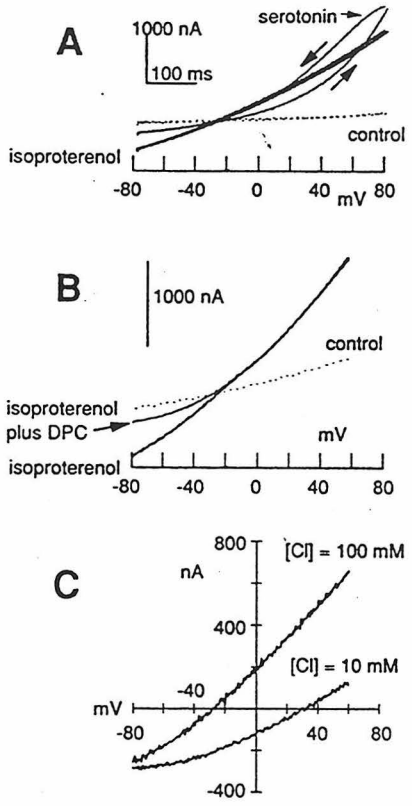

Figure 3 (A) Comparison of current-voltage relations for the Ca^{2+}-activated Cl^- conductance, activated by serotonin 5HT1C receptors, and the β2/CFTR response in an oocyte coinjected with 10 pg 5HT1C receptor cRNA, 0.1 ng β2 receptor cRNA, and 1 ng CFTR cRNA. Ramp responses to 10^{-7} M 5HT, 10^{-8} M isoproterenol, and no added drugs (control). The membrane voltage was ramped under voltage-clamp control from -80 mV to +80 mV, then back to -80 mV; each ramp lasted 500 ms. Arrows give the direction of voltage sweep for the 5HT trial. (B) Blockade by DPC. Currents during a unidirectional voltage ramp from -80 to +60 mV in an oocyte coinjected with cRNA for the β2-adrenergic receptor and for CFTR. Trials were taken before stimulation by isoproterenol (control trace) and at the peak of the current caused by 15 s stimulation by 1 μM isoproterenol. After washing, 200 μM DPC was applied for 10 min and was present during a second 15 s application of isoproterenol. The isoproterenol-induced current reversed at ~-23 mV and was inhibited at hyperpolarizing potentials by 200 μM DPC. (C) Isoproterenol-induced currents revealed by subtracting ramp-clamp currents (isoproterenol minus control) in 100 mM Cl^- and 10 mM Cl^- (methanesulfonate substitution). The reversal potential shifted from -23 mV in 100 mM Cl^- to +32 mV in 10 mM Cl^-.

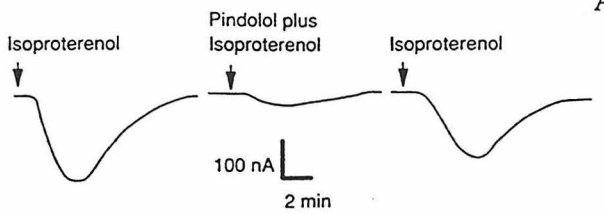

Figure 4. Inhibition of the β2-receptor/CFTR response by pindolol. Oocytes coinjected with 0.1 ng β2-adrenergic receptor cRNA and 1 ng CFTR cRNA were voltage clamped at −80 mV. Isoproterenol (10^{-7} M) was applied for 15 s; 10 min later, the β2-adrenergic antagonist pindolol (10^{-6} M) was applied for 45 s followed by stimulation with isoproterenol plus pindolol for 15 s. Pindolol suppressed the isoproterenol-induced CFTR currents; the blockade was reversed by a 10-min wash, as shown by the last application.

contrast, DPC blockade of the endogenous channels is much weaker and voltage-independent (McCarty *et al.*, 1992; McDonough *et al.*, 1993; McCarty *et al.*, 1993).

Characterization of β2 receptor pharmacology and involvement of cAMP The isoproterenol-induced current in β2/CFTR injected oocytes bears the pharmacological hallmarks of a β2-adrenergic response. Figure 4 demonstrates blockade by the β2-adrenergic antagonist, pindolol. Figure 5A presents dose-response relations and shows that the EC50 for the isoproterenol-induced current was $\sim 2 \times 10^{-7}$ M. For comparison, the response to 100 μM forskolin is also plotted in the y-axis of Figure 5A; this is smaller than the maximal response to isoproterenol itself, as found with many other adenylyl cyclase-dependent systems (the difference was roughly 10-fold in the experiment of Figure 5A). Direct measurements of cAMP over a 30 min time period showed that isoproterenol also increased the cAMP content of the oocytes injected with the β2 receptor cRNA (Figure 5B); the EC50 for this increase was $\sim 10^{-6}$ M. The ~5-fold smaller EC50 for the electrophysiological measurements suggests that the electrophysiological measurements may have saturated due to the presence of spare receptors. Interestingly, the inset to Figure 5A shows that clear current responses (40 ± 6 nA) were obtained at 10^{-9} M isoproterenol, some 100-fold less than the concentration required for a detectable elevation of cAMP as measured by RIA and 1000-fold less than the concentration required for a statistically significant 2-fold elevation of cAMP in the latter assay. Furthermore, the current measurements utilized a 15 s application, while the RIA measurements were performed on oocytes that were exposed to agonist for 30 min. Thus the

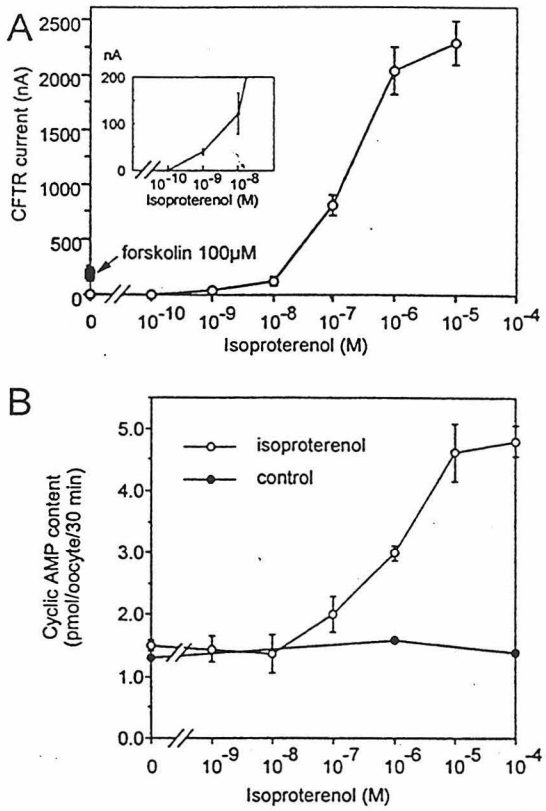

Figure 5 Dose-response relations for the isoproterenol-induced currents (A) and cAMP content measured by RIA (B) in β2/CFTR injected oocytes. Oocytes were coinjected with 0.1 ng β2 receptor cRNA and 1 ng CFTR cRNA. (A) oocytes were voltage clamped at a holding potential of −80 mV and exposed to varying concentrations of isoproterenol for 15 s. For comparison, currents produced by forskolin (100 μM) are shown on the ordinate. *Inset* shows the start of the dose-response relation on a magnified vertical scale. (B) Oocytes from the same batch were exposed to varying concentrations of isoproterenol for 30 min and assayed as in Methods. Control oocytes were not injected with receptor.

electrophysiological measurements are much more sensitive than the RIA measurements from the viewpoints of agonist concentration and of exposure time.

We also studied the effects of varying the amount of injected β2 cRNA (Figure 6). The current measurements showed an approximately linear dependence on the amount of β2 cRNA, with roughly a 10-fold increase in current when the RNA was increased from 0.01 to 0.1 ng/oocyte (Figure 6A). The β2 response became larger than the forskolin response, which did not vary with the amount of receptor injected, for β2 cRNA levels greater than ~5 pg. The direct cAMP assays were insufficiently precise for reliable estimates of the dependence on amount of β2-receptor cRNA but

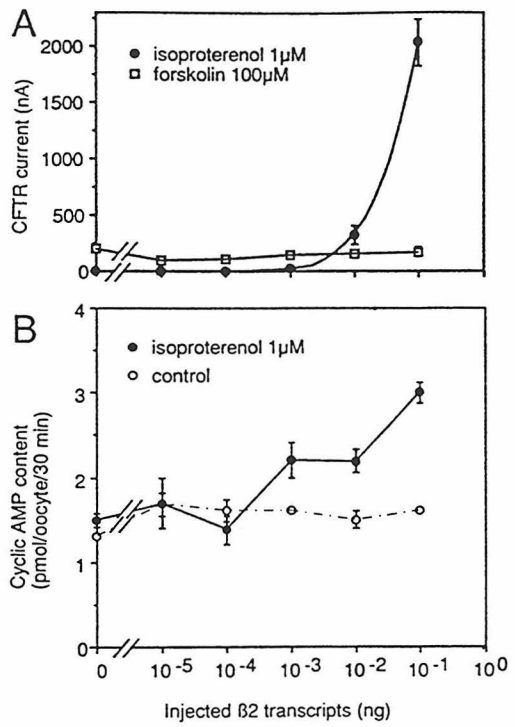

Figure 6 Dependence on amount of $\beta 2$ receptor cRNA injected. All oocytes were coinjected with 1 ng CFTR cRNA and tested 3–4 days later. (A) current measurements in response to a 15-s exposure to 10^{-6} M isoproterenol. Ten minutes after recovery from isoproterenol, forskolin (10^{-4} M) was applied for 30 s. (B) The same oocyte batch as in (A) was subject to cAMP measurements with RIA after a 30-min exposure to 10^{-6} M isoproterenol.

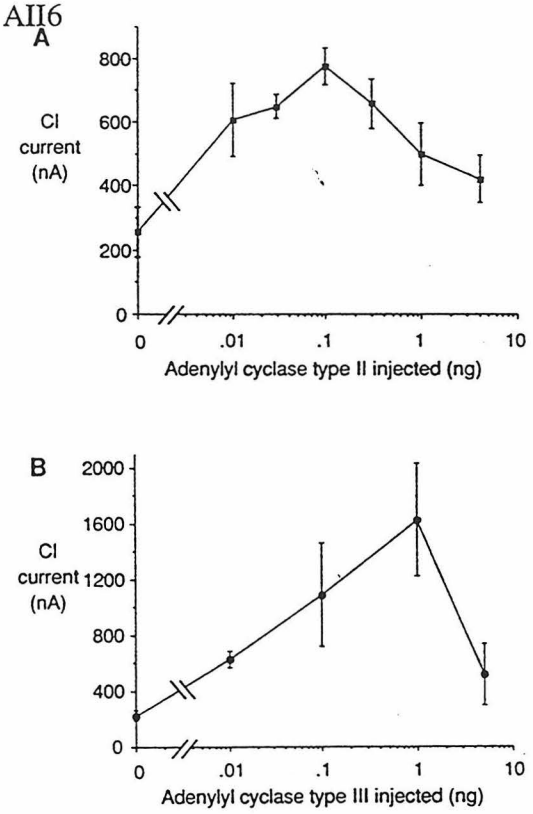

Figure 7 Effects of adenylyl cyclase coinjection. Oocytes received 1 ng of CFTR message and variable amounts of adenylyl cyclase type II (A) or type III (B). The assay consisted of measuring the response to 100 μM forskolin applied for 30 s. Points show mean ±S.E.M. for 5 or 6 oocytes.

showed a less steep dependence on cRNA injection than did the current measurements (Figure 6B). Interestingly, we found significant oocyte death, even in the absence of agonist, after 1–2 days for oocytes coinjected with >1 ng $\beta 2$ receptor cRNA and CFTR cRNA (data not shown). Injection of $\beta 2$-receptor cRNA alone at these levels did not damage oocytes. We suggest that a small amount of basal receptor activation led to enough cAMP generation, and to enough CFTR activation, to depolarize the oocyte to E_{Cl}, leading to a heavy metabolic burden and eventual death.

Injection of cRNA for adenylyl cyclase and G proteins The sensitivity of the transduction system was increased further by coexpressing adenylyl cyclase type II (Feinstein *et al.*, 1991) or type III (Reed *et al.*, 1990) in the oocytes (Figure 7). The peak enhancement of the response to forskolin occurred with 0.1 ng of type II cRNA (Figure 7A) or with 1 ng of type III cRNA (Figure 7B) and amounted to a factor of ~3 or ~6 increase in the CFTR currents for type II and III, respectively. We have not explored the causes for decreased responses with higher levels of cyclase injections.

We also found that the sensitivity of the transduction system was enhanced by coinjection of G protein α subunit cRNA. With coinjection of 2 ng Gs cRNA, 0.1 ng $\beta 2$ cRNA, and 1 ng of CFTR cRNA, the CFTR response to 0.1 μM isoproterenol was increased to 350% ± 23% (mean ± S.D., n = 3 or 4) of the response for injection of $\beta 2$ and CFTR cRNA only. A similar enhancement was observed with direct cAMP measurements on oocytes exposed to 1 μM isoproterenol for 30 min: 4 ± 0.5 pmol with injection of only $\beta 2$ cRNA, increasing to 13 ± 2 pmol (mean ± S.D., n = 4) with coinjection of Gs cRNA. Smaller enhancements were observed with similar coinjections of Golf cRNA (data not shown). Slight decreases in the response were observed with injection of Goα CRNA, allowing us to rule out the hypothesis that a nonspecific effect of Gα expression enhances CFTR activation.

Enhanced activation by 5HT1A receptors

Receptors thought to couple primarily to Gi produce little or no electrophysiological responses in oocytes, although weak signals have been reported under some circumstances (Fukuda *et al.*, 1987; Lechleiter *et al.*, 1990). We performed experiments with the serotonin 5HT1A receptor, typical of many receptors thought to couple to Gi.

When cRNA for serotonin 5HT1A receptors was injected into oocytes, either alone or with coinjected CFTR cRNA, we observed little or no response (<10 nA) to 5HT. However, in another series of experiments, we coinjected cRNA for the 5HT1A receptor with cRNA for the β2 receptor and for CFTR. In these oocytes, isoproterenol produced increases in Cl^- conductance identical to those described above. Surprisingly, these responses were augmented during simultaneous exposure to 5HT (Figure 8). As noted above, 5HT produced little or no consistent CFTR response (<30 nA) in oocytes injected with cRNA for the β2 receptor and CFTR but without the 5HT1A receptor.

This augmentation was observed in each of 7 different batches of oocytes. Under the conditions of Figure 8A (isoproterenol 3×10^{-8} M, 5HT 10^{-8} M), the response in 5HT plus isoproterenol was $153 \pm 48\%$ of the response in isoproterenol alone. This augmentation did not vary consistently with the concentration of isoproterenol tested; for instance, in another experiment, the enhancement was 86% at 10^{-8} M, 68% at 10^{-7} M, and 66% at 10^{-6} M isoproterenol (3 to 5 cells were tested in each case). The augmentation depended on the 5HT concentration, as shown in the dose-response relation of Figure 8B. The EC50 for 5HT was ~10^{-8} M, consistent with action at a 5HT1 receptor.

We found that the augmentation differs for oocytes injected with cRNA encoding the two forms of adenylyl cyclase (Type II and Type III). Figure 9 shows that the effect of serotonin 5HT1A receptor activation was larger (a 3-fold enhancement in CFTR current) in oocytes coinjected with cRNAs for the β2 receptor, the 5HT1A receptor, and adenylyl cyclase type II. When cRNA for adenylyl cyclase type III was used instead, the enhancement of the CFTR response to isoproterenol was roughly 1.5-fold, the same as in control

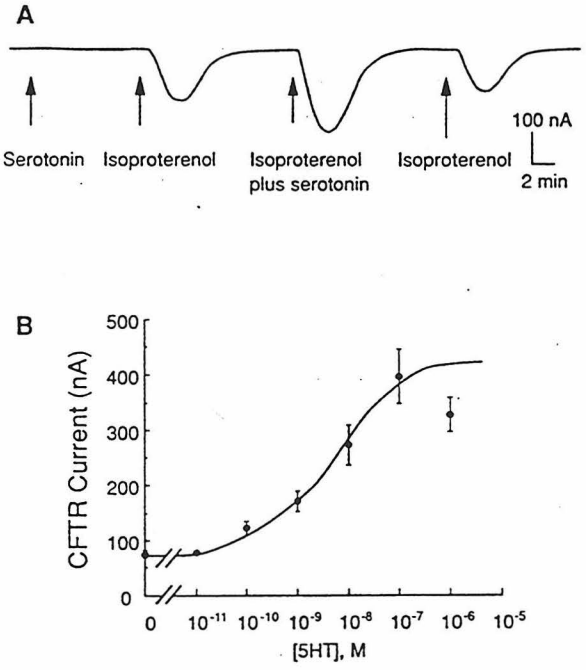

Figure 8 CFTR responses with simultaneous activation of β2 and 5HT1A receptors. (A), tracings from an oocyte coinjected with 3 cRNAs: 0.1 ng β2 receptor, 5 ng 5HT1A receptor, and 1 ng CFTR. Holding potential, −60 mV. Serotonin (10^{-8} M) or isoproterenol (3×10^{-8} M) or both drugs were added for 15 s at the vertical arrows. (B), dose-response relations for 5HT augmentation of CFTR response due to activation of the β2 receptor. Oocytes were coinjected with cRNAs for the 5HT1A receptor (5 ng), the β2 receptor (0.1 ng), and CFTR (1 ng). In this series, isoproterenol was applied for 5 s, followed by 5HT for 10 s; this protocol gave maximal augmentation. Data represent the average response to 10^{-8} M isoproterenol ± SEM (5 oocytes), 5 days after injection.

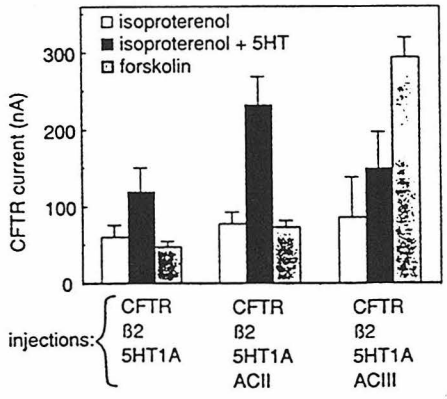

Figure 9 Augmentation of the β2 response in oocytes also expressing adenylyl cyclase type II and type III. Oocytes were injected with the following cRNAs: 0.1 ng β2 receptor, 5 ng serotonin 5HT1A receptor, 1 ng CFTR, 0.2 ng adenylyl cyclase type II or type III (labeled as ACII or ACIII). Test solutions consisted of 10^{-8} M isoproterenol (applied for 15 s, shown as empty bars), 10^{-8} M isoproterenol plus 10^{-7} M 5HT (applied for 15 s, shown as solid bars), or 10^{-4} M forskolin (applied for 30 s, shown as shaded bars). Data are shown as mean ± SEM (n = 5 to 9 oocytes).

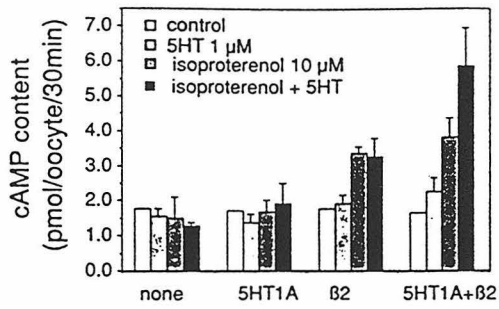

Figure 10 Increases in cAMP, measured by the RIA, with simultaneous activation of $\beta 2$ and 5HT1A receptors. Oocytes were coinjected with 3 cRNAs: 0.1 ng $\beta 2$ receptor, 5 ng 5HT1A receptor, and 1 ng CFTR. Data are mean ± SD for 3–5 oocytes.

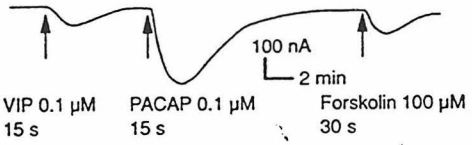

Figure 11 Responses with tissue-derived RNA. The oocyte was injected with rat brain mRNA and tested with VIP, PACAP(1–38), and forskolin at the vertical arrows. Holding potential, −60 mV.

oocytes for this experiment, even though the response to forskolin was greatly enhanced. This experiment, along with that of Figure 7B, shows that the type III cyclase was indeed functional but could not be stimulated by the 5HT1A receptor. Thus, the augmentation seems to be specific for adenylyl cyclase type II.

To test whether the augmentation was caused by an increase in cAMP or by a subsequent step, we also performed cAMP assays on the oocytes coinjected with cRNA for the 5HT1A receptor, the $\beta 2$-adrenergic receptor, and CFTR (Figure 10). For 10^{-5} M isoproterenol, 10^{-6} M 5HT produced an augmentation of the cAMP content by 94%, roughly comparable to the augmentation of the CFTR signal.

Activation by receptors expressed from tissue-derived mRNA

To test the possibility that the cAMP-activated CFTR response could be evoked by receptors synthesized from tissue-derived RNA, we injected oocytes with poly (A+) RNA from rat cerebral cortex with or without CFTR cRNA. Several days later, we measured the responses to vasoactive intestinal peptide (VIP) and to pituitary adenylate cyclase-activating polypeptide (PACAP[1-38]), two agonists known to increase cAMP in brain. There were no detectable responses to these agonists in oocytes injected with brain mRNA alone (data not shown); but in oocytes that also received cRNA for CFTR, we noted the typical CFTR-mediated responses (Figure 11). This indicates that the system has sufficient sensitivity to detect activation of adenylyl cyclase by receptors encoded in tissue-derived mRNA.

DISCUSSION

A highly sensitive assay for cAMP

The present system, in which CFTR is used as an assay for cAMP, seems to be highly sensitive. For our test system involving the $\beta 2$-adrenergic receptor, CFTR currents are detectable at agonist concentrations 100–1000 fold less than those giving significant cAMP increases in the RIA. The following calculation estimates the smallest detectable change in cAMP concentration. Maximal activation of the $\beta 2$-adrenergic receptor in the experiment of Figure 5 corresponded to a current of 2500 nA (Figure 5A) and to a cAMP increase of 3 pmol per oocyte over a time span of 30 min (Figure 5B). The assay is readily capable of detecting only 25 nA; assuming that the response is linear with [cAMP] in the range of subsaturating [cAMP], then this value would correspond to a 30 fmol increase per oocyte over a time span of 30 min. White & Reisine (1990) found that the cAMP assay is linear with time; therefore we would expect generation of 0·25 fmol caused by the 15-s exposure to agonist. The volume of an oocyte is ~0·5 μl; but one might expect that newly synthesized cAMP would diffuse only ~100 μm from the membrane in 15 s, so that the volume occupied by the bolus of cAMP would be roughly half this value, or ~0·25 μl. Therefore the concentration increase would be 1 nM. We note that the basal cAMP level is ~1 pmol, corresponding to a basal concentration of ~2 μM——some 2000 fold greater than the minimum detectable increase.

These simple estimates do not account for possible additional compartmentalization of the newly synthesized cAMP or for other possible distorting processes and should therefore be considered preliminary. Nonetheless it is important to point out that oocytes expressing CFTR displayed no additional Cl^- conductance as

compared to noninjected oocytes, with or without coexpressed β2-adrenergic receptor, *in the absence of agonist or forskolin.* Therefore these considerations suggest that the CFTR system is responding preferentially to small increases of local cAMP concentration rather than to absolute levels. It will be of interest to describe the mechanisms responsible for this adaptation to the steady level.

Our measurements show that detectable CFTR currents are obtained with β2-adrenergic receptor cRNA amounts of 5 pg per oocyte and CFTR cRNA amounts of 1 ng per oocyte (Figure 5A). It is routinely possible to inject 50 ng of RNA; thus, the β2 receptor would be detectable at a dilution of 1 in 10^4 if injected with other RNAs. Several fold greater sensitivity seems to be possible with coinjection of cRNA for adenylyl cyclase type III and for Gs. The complexity of tissue-derived mRNA implies that the message for most individual proteins constitutes on the order of 1 in 10^4 or less of the total mRNA. To test our estimates of the CFTR assay's sensitivity, it was therefore of interest to determine whether the assay allowed the detection of adenylyl cyclase activation with tissue-derived mRNA. Our experiments employed mRNA isolated from rat brain. We confirmed that either VIP or PACAP(1-38) can yield detectable responses with the CFTR assay system, presumably through activation of adenylyl cyclase by receptors for these hormones. Therefore this system may possess the sensitivity required for expression cloning.

Studies in our laboratory are also investigating the possibility that the CFTR system can be used for expression of the putative cAMP system activated by olfactory receptors. Preliminary encouraging data have been reported (Bradley *et al.*, 1992). In this context, one might also suggest the use of cyclic nucleotide-gated channels as cAMP sensors; but we have found, in experiments with expression of the cyclic nucleotide-gated channel reported by Dhallan *et al.* (1990), that the CFTR assay is much more sensitive.

Molecular mechanism of 5HT1A enhancement

Coexpression of the Gi-coupled 5HT1A receptor, the Gs-coupled β2 adrenergic receptor, and CFTR produced surprising results. The G protein Gi received its name because its first known effect was to inhibit adenylyl cyclase activity; yet in our system, activation of this receptor actually augmented the cAMP increase stimulated by the β2 receptor, both as measured directly with the RIA and as monitored by the CFTR activation which forms the major subject of this paper.

The most likely explanation for this finding is the recent observation that the βγ subunits of G proteins can augment the stimulation of some forms of adenylyl cyclase by Gs (Tang & Gilman, 1991; Gao & Gilman, 1991; Birnbaumer, 1992; Bourne & Nicoll, 1993). We suggest that activation of Gi caused the release of βγ subunits, which then interacted directly with adenylyl cyclase. It should be noted that no effects of 5HT1A stimulation were seen in our experiments without concurrent stimulation by the β2 receptors, in keeping with the suggestion that βγ subunits cannot activate adenylyl cyclase on their own but require Gs stimulation. The suggested mechanism received support from the observation that the 5HT augmentation was greater with coinjection of adenylyl cyclase type II cRNA than with adenylyl cyclase type III, in agreement with the reported data on purified cyclase and βγ subunits (Tang & Gilman, 1991).

An interaction between Gs-coupled and Gi-coupled receptors, leading to an enhanced adenylyl cyclase activity, has been reported by use of a mutationally active Gαs (Federman *et al.*, 1992). A synergistic interaction between Gs-coupled and Gi-coupled receptors, leading to an enhanced blockade of a Ca^{2+}-activated K^+ conductance, has been reported independently for responses in hippocampal pyramidal cells (Andrade, 1993). Such interactions present attractive possibilities for use as molecular coincidence detectors (Bourne & Nicoll, 1993).

MATERIALS AND METHODS

Oocytes from adult female *Xenopus laevis* were prepared, injected with various cRNAs and mRNAs, and incubated as described by Quick & Lester (1993). The cDNA for human CFTR has been described by Bear *et al.* (1991). The cDNA for the human β2-adrenergic receptor (Kobilka *et al.*, 1987) was a gift of Dr. B. Kobilka (Stanford University School of Medicine). The cDNA for the human SHTIA receptor was a gift of Dr. P. Hartig (Synaptic Pharmacuticals, Inc.). The mouse 5HTIC receptor has been described by Walter *et al.* (1991). The cDNA for Gs was a gift of Dr. M. Simon (California Institute of Technology). The cDNA for

rat brain adenylyl cyclase type II (Feinstein *et al.*, 1991) was a gift of Dr. R. Reed (Johns Hopkins Univ.). The cDNA for Golf was amplified directly from first strand rat nasal epithelium cDNA using primers derived from the published sequence (Jones & Reed, 1989). The product was then reamplified with SP6 and poly (A) primers at the 5′ and 3′ ends, respectively (Mager *et al.*, 1993). To isolate the adenylyl cyclase type III cDNA, a nasal epithelial cDNA library was constructed in lambda ZAPII. This was screened with a 5′ probe consisting of a PCR product encoding the N-terminus of the protein, then rescreened with a probe from the proximal 3′ untranslated region. In vivo excision of the full-length clone from the phage produced a pBluescript plasmid. cRNAs were prepared from these cDNAs by in vitro synthesis using the appropriate bacteriophage RNA polymerase (SP6, T7, or T3). For experiments on tissue-derived RNA, oocytes were injected with 50 ng of poly (A+) RNA from rat cerebral cortex and were tested 2 to 5 d later.

PACAP(1-38) was obtained from Calbiochem, DPC from Aldrich, and methanesulfonate from Fluka. All other reagents were obtained from Sigma.

Electrophysiological measurements were conducted using the two-electrode voltage clamp (Quick & Lester, 1993); the membrane potential was held at −60 mV or −80 mV except when ramps were applied as in Figure 2. Experiments were performed at room temperature. In all cases, oocytes were superfused continuously with Ca^{2+}-free ND96 solution and all drugs were applied in this solution. The bath had a volume of 150 μl and the flow rate was 5 ml/min, so that the bathing solution reached new steady-state values with a time constant of ~2 s.

For cAMP assays, oocytes were preincubated with 10 mM theophylline for 30 min followed by another incubation with varying concentrations of isoproterenol containing 10 mM theophylline and 1 mg/ml bovine serum albumin as described (White & Reisine, 1990). The reaction was stopped by the addition of 100 mM HCl, followed by heating to 95°C for 5 min. The cAMP content of individual oocytes was measured with an RIA kit (Dupont).

Acknowledgements We thank Drs. M. Simon and Anna Aragay for advice and for the gift of Gs cDNA, R. Reed for the gift of the adenylyl cyclase type II cDNA, and Dr. B. Kobilka for the gift of the β2 receptor cDNA. We thank Drs. N. Dascal and C. Strader for comments on an earlier version of the manuscript. This work was supported by grants from the National Institutes of Health, the National Institute on Drug Abuse, the Silvio Conte Center for Neuroscience Research of the National Institute of Mental Health, the Cystic Fibrosis Foundation, the California Tobacco-Related Disease Program, the Wiersma Memorial Fund, and the Japanese Foundation for Clinical Pharmacology.

REFERENCES

Anderson M P Gregory R J Thompson S Souza D W Paul S Mulligan R C Smith A E and Welsh M J (1991) *Science* **253** 202–205

Andrade R (1993) *Neuron* **10** 83–88

Bear C E Duguay F Naismith A L Kartner N Hanrahan J W and Riordan J R (1991) *J Biol Chem* **266** 19142–19145

Birnbaumer L (1992) *Cell* **71** 1069–1072

Bourne H R and Nicoll R (1993) *Cell* **72** 65–75

Bradley J Uezono Y Davidson N Lester H and Zinn K (1992) *Soc Neurosci Abstr* **18** 596

Dascal N (1987) *CRC Crit Rev Biochem* **22** 317–387

Dhallan R S Yau K W Schrader K A Reed R R (1990) *Nature* **347** 184–187

Drumm M L Wilkinson D J Smit L S Worrell R T Strong T V Frizzell R A Dawson D C and Collins F S (1991) *Science* **254** 1797–1799

Federman A D Conklin B R Schrader K A Reed R R and Bourne H R (1992) *Nature* **356** 159–161

Feinstein P G Schrader K A Bakalyar H A Tang W-J Krupinski J Gilman A G and Reed R R (1991) *Proc Natl Acad Sci USA* **88** 10173–10177

Fukuda K Kubo T Akiba I Maeda A Mishina M and Numa S (1987) *Nature* **327** 623–625

Gao B and Gilman A G (1991) *Proc Natl Acad Sci USA* **88** 10178–10182

Jones D T and Reed R R (1989) *Science* **244** 790–795

Kartner N Hanrahan J W Jensen T J Naismith A L Sun S Ackerly C A Reyes E F Tsui L-C Rommens J M Bear C E and Riordan J R (1991) *Cell* **64** 681–691

Kobilka B K MacGregor C Daniel K Kobilka T S Caron M G and Lefkowitz R J (1987) *J Biol Chem* **262** 15796-15802

Lechleiter J R Hellmiss K Duerson D Ennulat N David D Clapham and E Peralta (1990) *EMBO J* **9** 4381–4390

Lester H A (1988) *Science* **241** 1057–1058

Mager S Naeve J Quick M Guastella J Davidson N and Lester H A (1993) *Neuron* **10** 177–188

McCarty N A Cohen B N Quick M W Riordan J R Davidson N and Lester H A (1992) *Biophys J* **61** A10

McCarty N A McDonough S Cohen B N Riordan J R Davidson N and Lester H A (1993) *J Gen Physiol* **102** 1–23

McDonough S McCarty N A Riordan J Davidson N and Lester H A (1993) *Biophys J* **64** A99

Takahashi T Neher E Sakmann B (1987) *Proc Natl Acad Sci USA* **84** 5063–5067

Quick M W and Lester H A (1993) *Meth in Neurosci* in press

Riordan J R Rommens J M Kerem B Alon N Rozmahel R Grzelczak Z Zielenski J Lok S Plasvic N Chou J-L Drumm M L Iannuzzi M C Collins F S and Tsui L-C (1989) *Science* **245** 1066–1072

Tang W-J and Gilman A G (1991) *Science* **254** 1500–1503

Walter A E Hoger J H Labarea C Yu L Davidson N and Lester H A *J Geb Physiol* **98** 399–417

Welsh M J Anderson M P Rich D P Berger H A Denning G M Ostedgaard L S Sheppard D N Cheng S H and Gregory R J (1992) *Neuron* **8** 821–829

White M M and Reisine T (1990) *Proc Natl Acad Sci USA* **87** 133–136

Appendix III

Two assay systems for intracellular increases in cAMP levels based on the cng channels

Introduction

This is a description of use of the olfactory cng channels as detectors for intracellular increases in cAMP concentrations. Two applications are described, one using expression in *Xenopus* oocytes and the second using expression in a human embryonic kidney cell line 293 (HEK 293).

Electrophysiological recording of Na^+ influx through the cng channel

We determined that the heteromeric olfactory cng channel can be used as a sensor for intracellular increases in cAMP concentration via receptor activation by coexpressing the cng channels subunits (rOCNC1+rOCNC2) in *Xenopus* oocytes together with the β2 adrenergic receptor (β2AdR). The results are shown in Figure AIII 1. In this case the oocyte is clamped at -80mV in ND-96 + 1mM Mg^{2+}. The basal activity of the expressed proteins (rOCNC1, rOCNC2, β2AdR) leads to some basal current that is partially blocked by the 1mM Mg^{2+}. Switching to 10mM Mg^{2+} (1) blocks more of this current and removal of all external divalents (2) reveals all of the basal current. A 10 sec application of isoproterenol (1μM) activates the β2AdR producing cAMP to open more of the cng channels. This result indicates that the olfactory cng channels can be used as an electrophysiological sensor in *Xenopus* oocytes for receptors that couple to the production of cAMP.

Fura based detection of Ca^{2+} influx through cng channels

Because the olfactory cng channels are highly permeable to Ca^{2+} (Frings et al., 1995)we examined the possibility that these channels could be used as a read-out for changes in intracellular levels of cAMP. The idea being that the cAMP would open the

cng channels and allow Ca^{2+} influx. The resultant intracellular change in Ca^{2+} can be imaged with the fluorescent Ca^{2+} detection dye fura-2-AM.

We tested this by transient expression of the olfactory channels in HEK293 cells by transfection, or in a cell line exhibiting stable expression of either rOCNC1(Dhallan et al., 1990) alone (line #12), or both rOCNC1 and rOCNC2 (Bradley et al., 1994)together(line #9) (fig AIII 2). We made these cell lines because transfection efficiencies of rOCNC1 and rOCNC2 are routinely at best 50%. For a functional assay we would ideally like to have the reporter in every cell that may express olfactory receptor. A second reason for making the stable lines expressing channel was because we often observed a low frequency of olfactory receptor expressing HEK293 cell expressing cotransfected genes. The result of an imaging experiment is shown in Figure AIII 3. The cells were loaded with fura2-AM and incubated in the membrane permeable cyclic nucleotide analog 8-Br cGMP at 3mM. This was done in the presence of 10mM Mg^{2+} to block the channel (top three photographs). After 2 minutes (middle three photographs) in Mg^{2+} free solution, a change in internal Ca^{2+} concentration is observed as the cells change from blue to green to yellow to red with increasing Ca^{2+} concentration. After 4 minutes (lower three photographs) many more cells have an increase in internal Ca^{2+} concentration. We have evidence that a similar change can be observed with expression of the β2AdR and perfusion of isoproterenol (data not shown).

If our data is correct concerning the necessity of the G protein G_{olf} for the odorant response (see chapter 4) we would also need expression of this component of the signal transduction cascade. Toward this end I have selected a derivative of channel line #9 that also expresses stable amounts of G_{olf} mRNA (fig AIII 3). This line is called #35.

References

J. Bradley, J. Li, N. Davidson, H. A. Lester and K. Zinn (1994). Heteromeric olfactory cyclic nucleotide-gated channels: A subunit that confers increased sensitivity to cAMP. Proc. Natl. Acad. Sci. USA *91*, 8890-8894.

R. S. Dhallan, K.-W. Yau, K. A. Schrader and R. R. Reed (1990). Primary structure and functional expression of a cyclic nucleotide-activated channel from olfactory neurons. Nature *347*, 184-187.

S. Frings, R. Seifert, M. Godde and U. P. Kaupp (1995). Profoundly different calcium permeation and blockage determine the specific function of distinct cyclic nucleotide-gated channels. Neuron *15*, 169-179.

D. T. Jones and R. R. Reed (1989). G_{olf}: an olfactory neuron-specific G-protein involved in odorant signal transduction. Science *244*, 790-795.

Figure legends

Fig AIII 1 Whole cell recording of cng channels currents through activation of the β2AdR *Xenopus* oocytes were injected with cRNA for expression of rOCNC1 (3ng), rOCNC2 (3ng), and the β2AdR (0.5ng). Expression was for 2 days at 19°C. See above text for description of experimental protocol.

Fig AIII 2 Selection of a cell line expressing a stable level of rOCNC1 and rOCNC2 Detection of high amounts of cng channel expressed stabily by cell line #9, rOCNC1 (A and B), rOCNC2 (C and D). This line was selected by cotransfection of pCIS/rOCNC1,

pCIS/rOCNC2, and PWL-neo (Stratagene). PWL-neo confers resistance to G418. Selection was in 500μg/ml G418.

Fig AIII 3 Change in internal Ca^{2+} concentration of HEK293 cells expressing the olfactory cng channels in response to 8-Br-cGMP.

Fig AIII 4 Selection of a cell line expressing a stable level of G_{olf} mRNA by *in situ* hybridization

The G_{olf} cDNA (Jones and Reed, 1989) was cloned into the expression plasmid pCEP-4 (Invitrogen) which allows selection for transfection in hygromycin (25μg/ml). A), Detection of transient G_{olf} mRNA expression by *in situ* hybridization in pCEP-4/G_{olf} transfected HEK293 cells. B), Detection of stable G_{olf} mRNA expression by *in situ* hybridization in pCEP-4/G_{olf} transfected HEK293 cells (line #35).

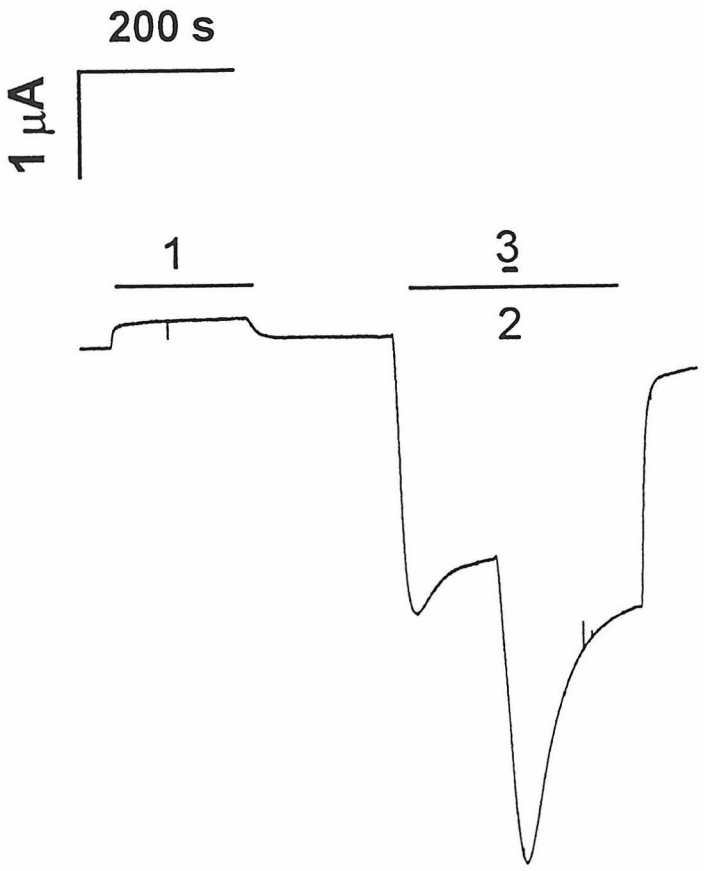
200 s
1 µA
1
3
2

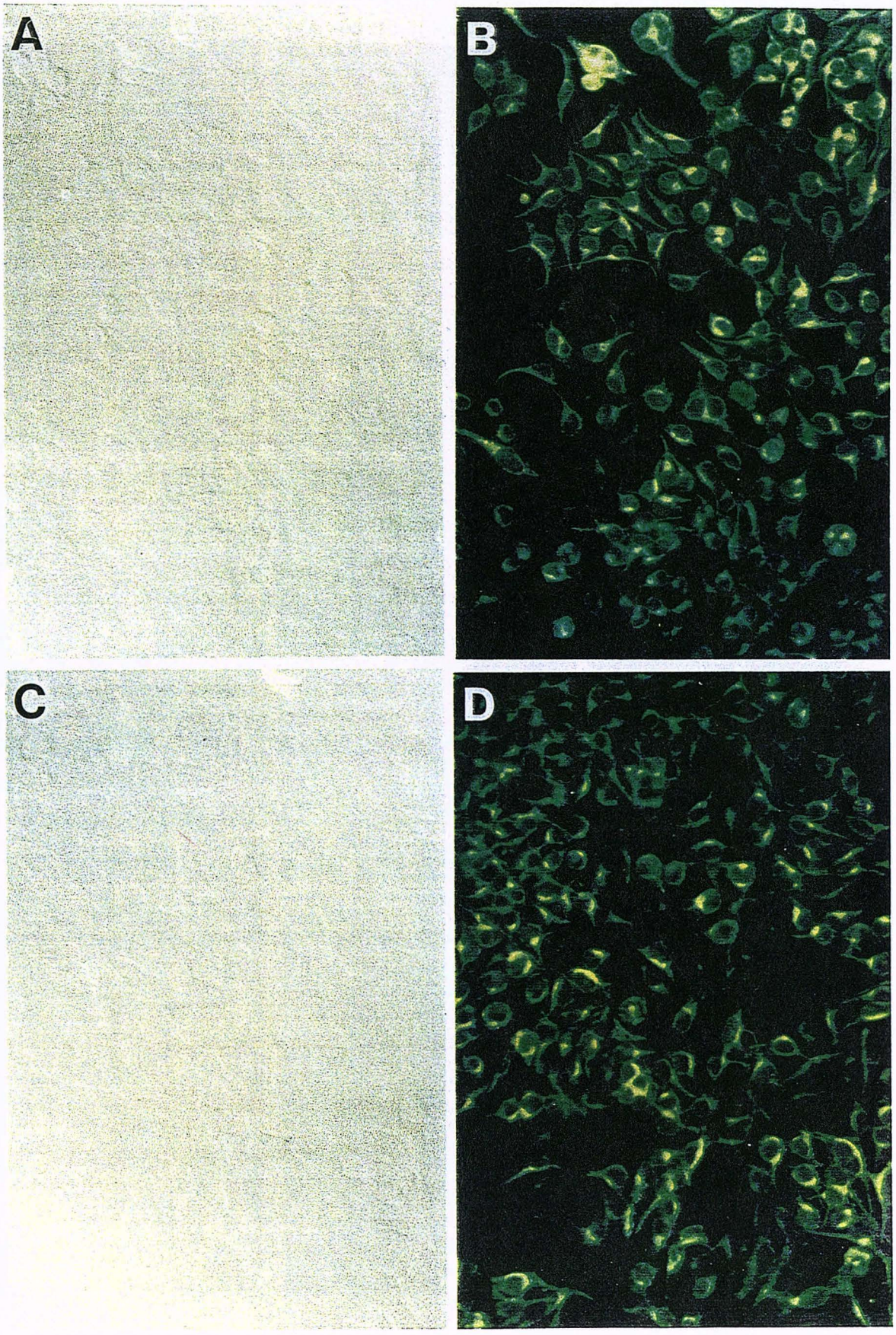
A
B
C
D

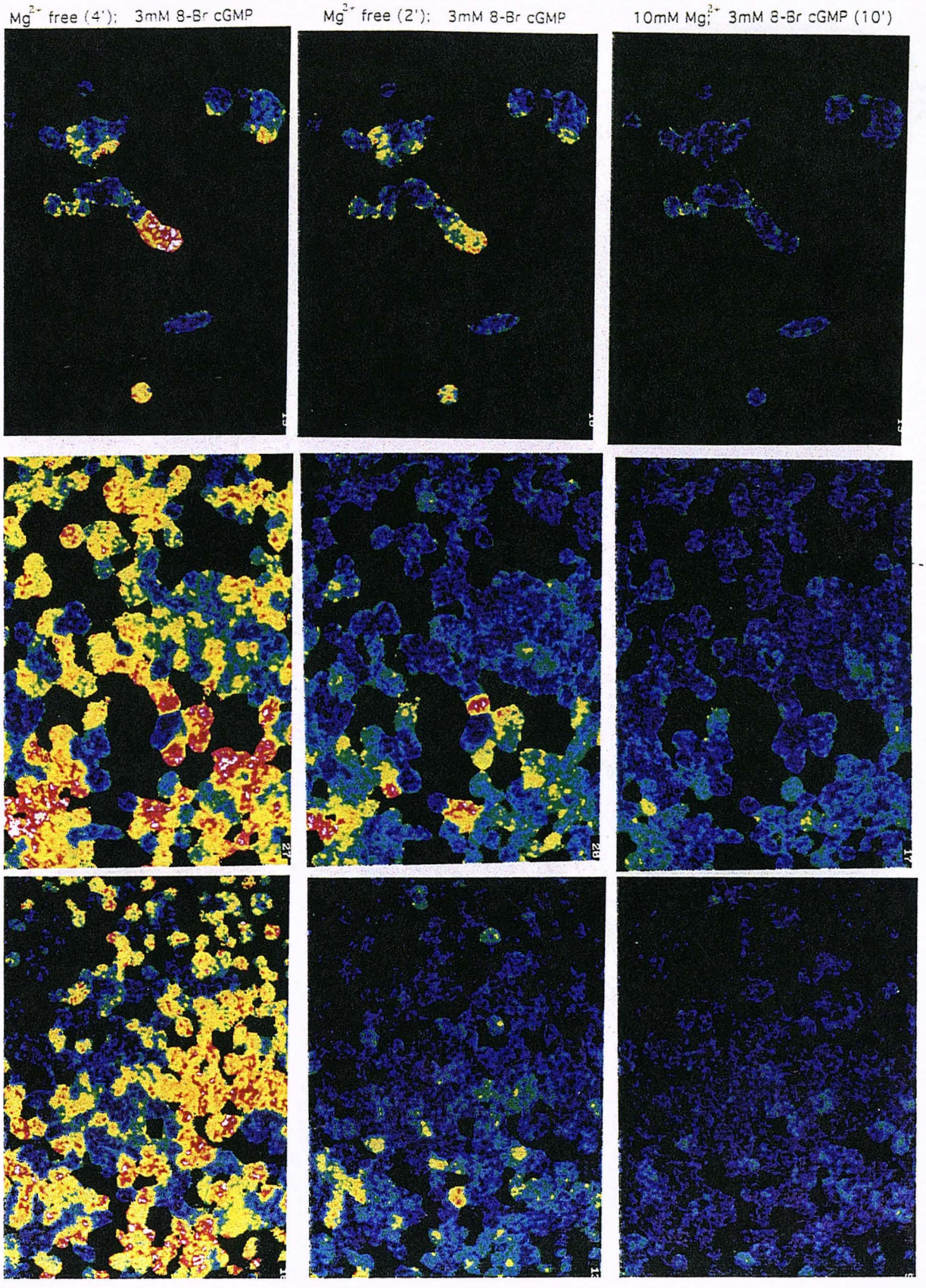
Mg2+ free (4'): 3mM 8-Br cGMP
Mg2+ free (2'): 3mM 8-Br cGMP
10mM Mg2+ 3mM 8-Br cGMP (10')
rOCNC1/rOCNC2 transient
rOCNC1 cell line #12
rOCNC1/rOCNC2 cell line #9

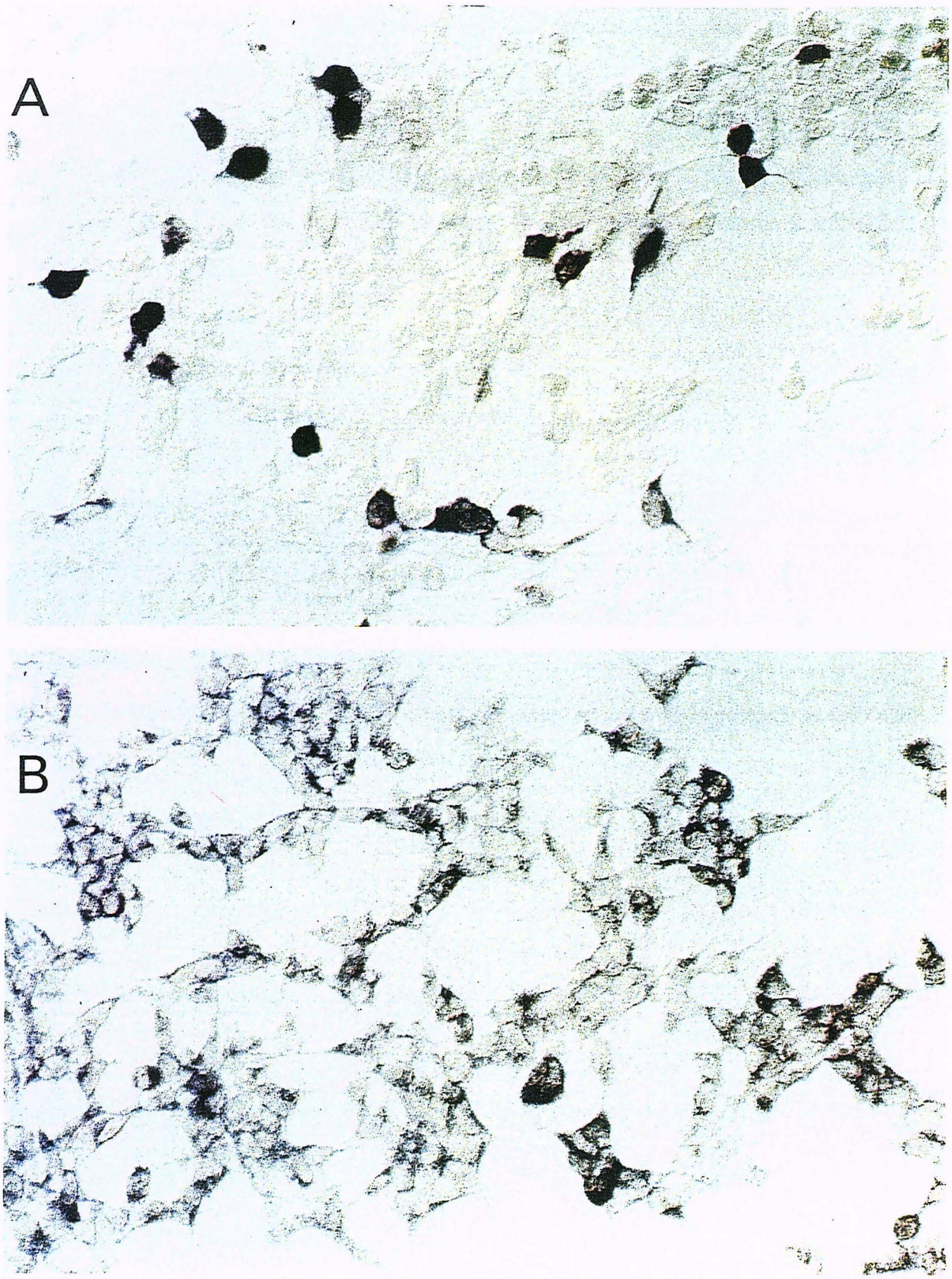
A
B

Appendix IV

Amino acid alignment and identity dendrogram of putative rat olfactory receptors

Fig AIV 1 Amino acid alignment

of 10 published (Buck and Axel, 1991)olfactory receptor sequences and four unpublished (J.B.). The alignment starts at the 5' primer (A4) in transmembrane region II and ends at the 3' primer (B6) in transmembrane region VII.

Fig AIV 2 Identity dendrogram

Dendrogram calculated the Geneworks software from the alignment in Fig AIV 1

Fig AIV 3 Amino acid alignment showing the positions of transmembrane regions and primers

References

L. Buck and R. Axel (1991). A novel multigene family may encode odorant receptors: a molecular basis for odor recognition. Cell *65*, 175-187.

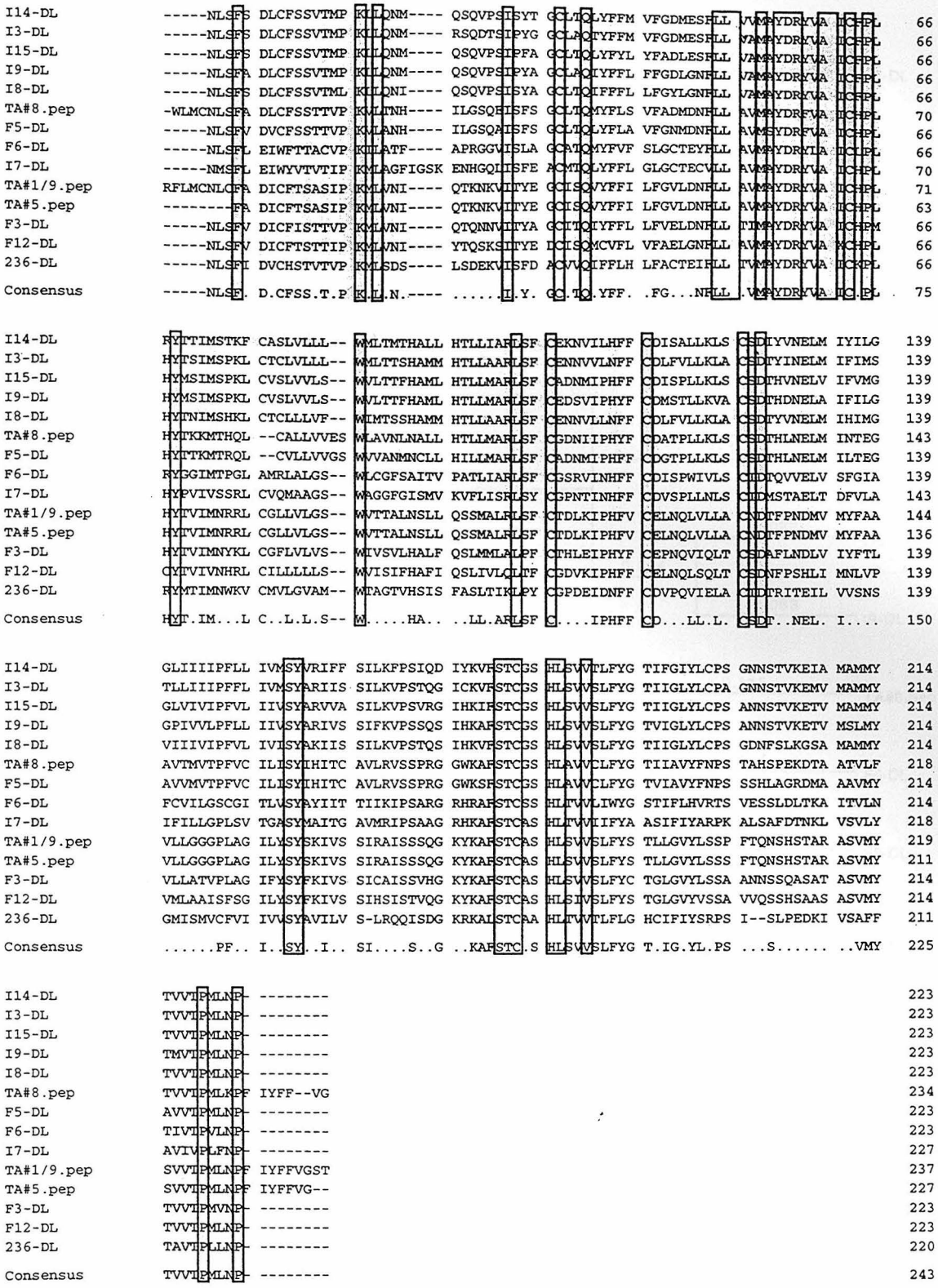

AIV3

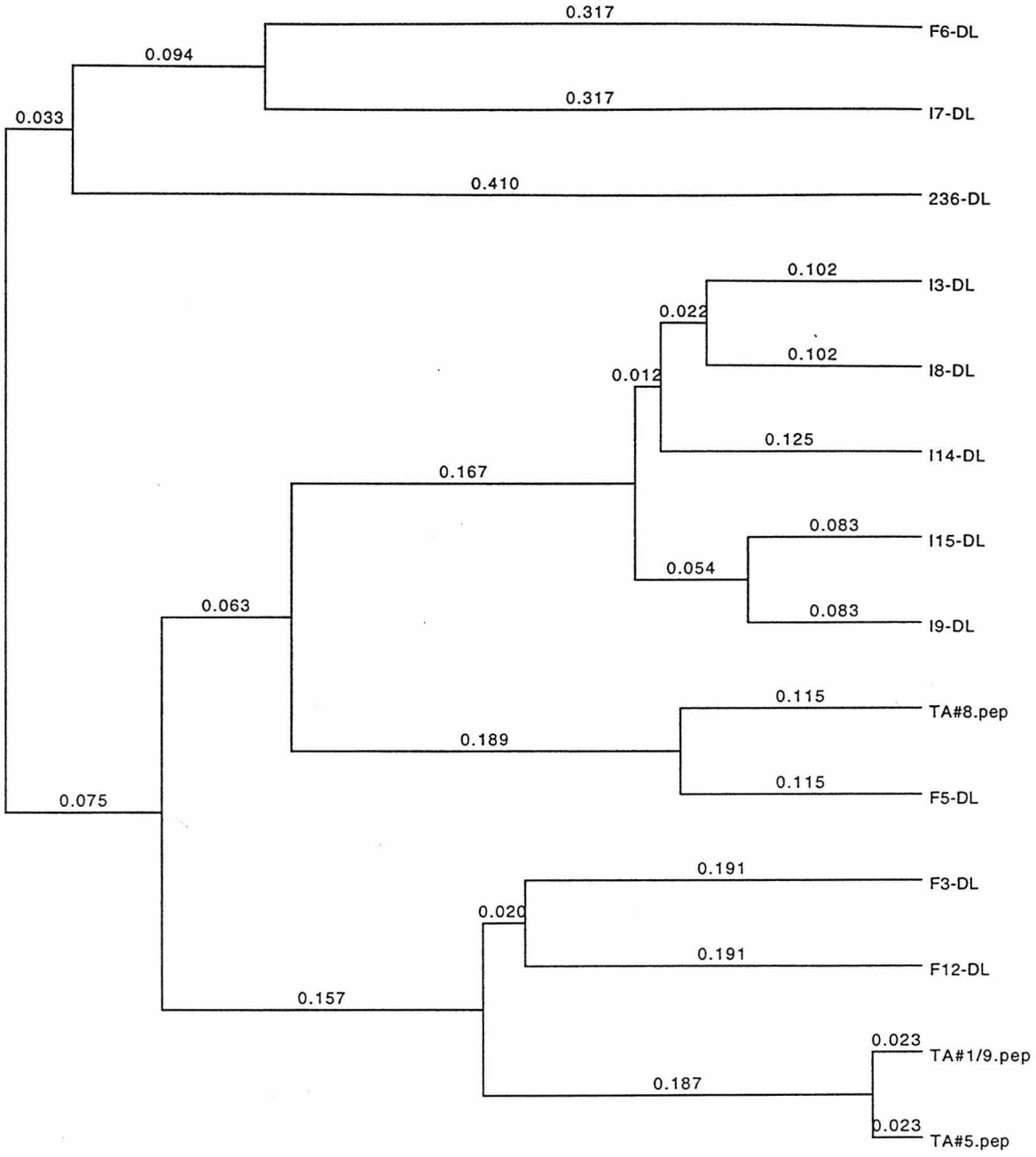
0.317
F6-DL
0.094
0.317
I7-DL
0.033
0.410
236-DL
0.102
I3-DL
0.022
0.102
I8-DL
0.012
0.125
I14-DL
0.167
0.083
I15-DL
0.054
0.063
0.083
I9-DL
0.115
TA#8.pep
0.189
0.115
F5-DL
0.075
0.191
F3-DL
0.020
0.191
F12-DL
0.157
0.023
TA#1/9.pep
0.187
0.023
TA#5.pep

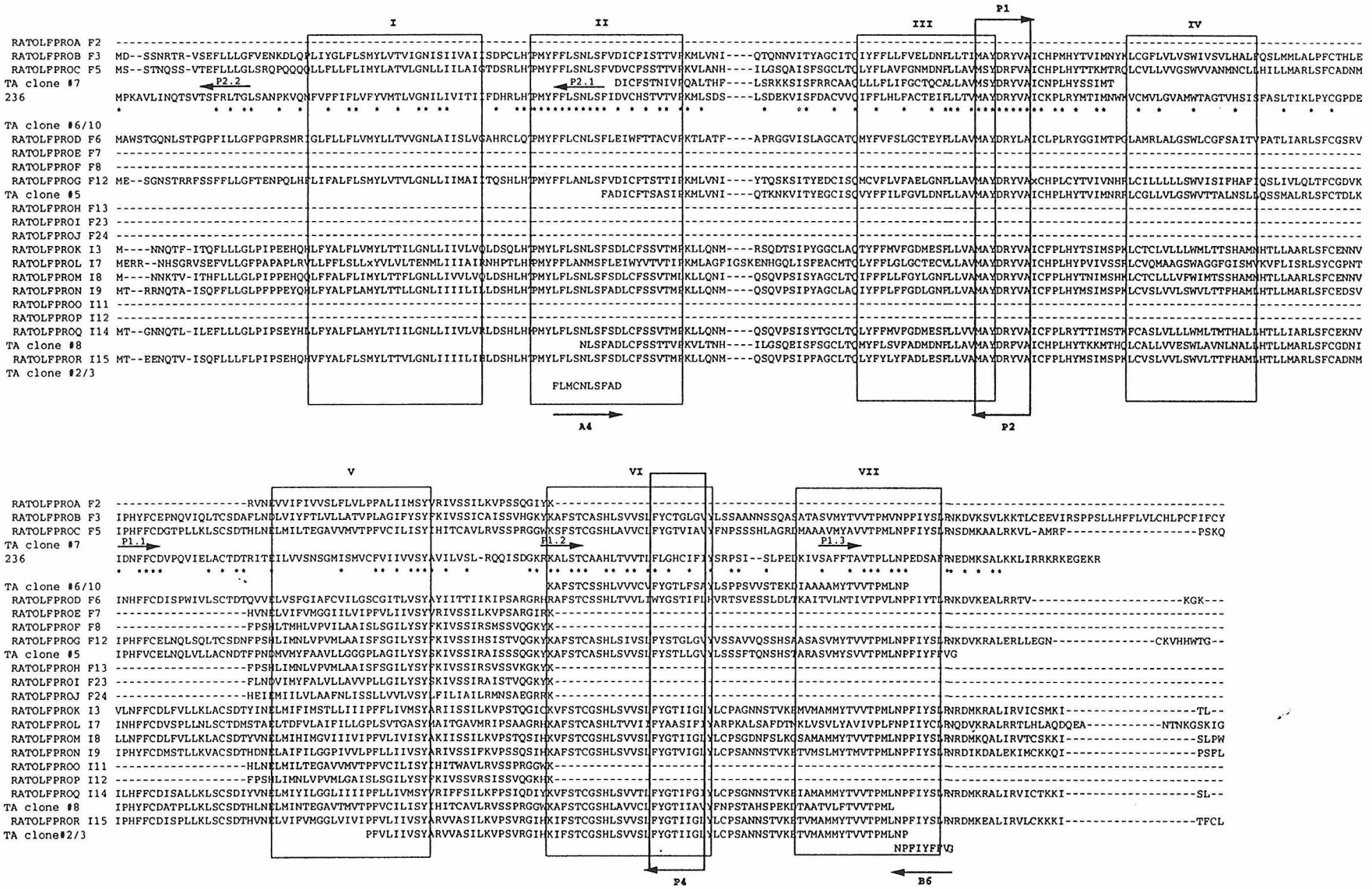

AIV4

Appendix V

Construction of hybrid olfactory receptors to promote G protein interaction.

In method one, I constructed an I7 receptor that had as its putative G protein interaction sequence amino acids from the beta 2 adrenergic receptor shown to confer coupling to the G protein G_S(Takahashi et al., 1993). The strategy I chose was "bridge" PCR and is outlined in Figure AV 1. Preliminary evidence indicates this receptor does express and couple to the G protein as indicated by the presence of a basal current in receptor cRNA injected oocytes.

In method two, I constructed a receptor G protein fusion based on the results of Bertin *et al.* (Bertin et al., 1994) who showed efficient signal of a β2AdR-G_S fusion expressed in S49 cells. This I7-Golf fusion protein has yet to be tested.

References

B. Bertin, M. Freissmuth, R. Jockers, A. D. Strosberg and S. Marullo (1994). Cellular signaling by an agonist-activated receptor G(s)alpha fusion protein. Proc. Natl. Acad. Sci. U.S.A. *91*, 8827-8831.

K. Takahashi, Y. Murayama, T. Okamoto, T. Yokota, T. Ikezu, S. Takahashi, U. Giambarella, E. Ogata and I. Nishimoto (1993). Conversion of G-protein specificity of insulin-like growth factor-II mannose 6-phosphate receptor by exchanging of a short region with beta-adrenergic-receptor. Proc. Natl. Acad. Sci. U.S.A. *90*, 11772-11776.

Figure legend

Fig AV 1 Strategy used to construct the I7/β2 hybrid receptor by bridge PCR

Bridge PCR for construction of hybrid 7-helix receptor I7

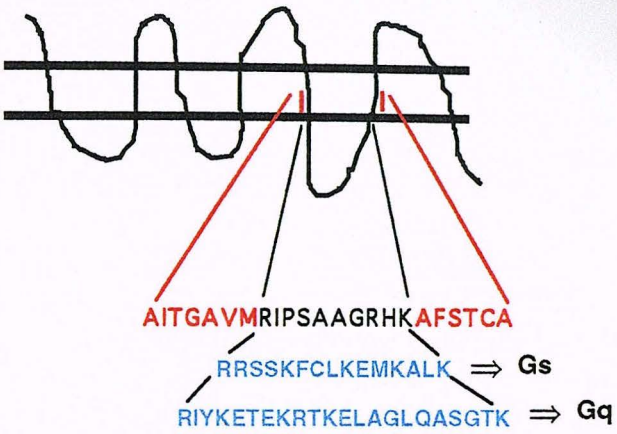

1) Digestion of parent clone I7 in region to be deleted

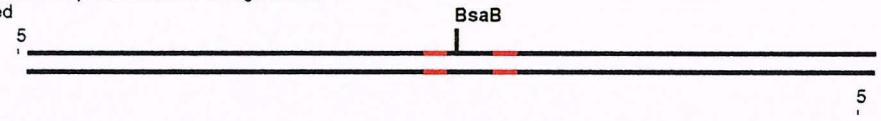

2) Amplification to delete origional sequence and introduce experimental one. "Bridge primers are @[0.1-0.01] of terminal primers and are partially self complementary

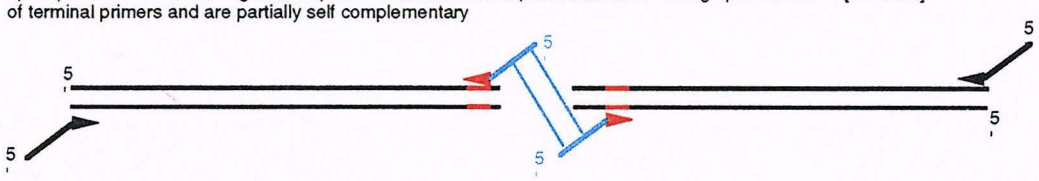

3) "Bridge" primers are depleted after exponentially amplifying the two fragments and incorporating the experimental sequence

4) Complementarity at the 3' end of each fragment act as primers to join fragments and:

the new clone is exponentially amplified with the terminal primers.